The University of Reading

Trends and variability in discharge of the Severnaya Dvina and the Sukhona (north-western Russia), 1882-2004, and their links with climatic variability

Ph.D. Thesis

The University of Reading
School of Human and Environmental Sciences
Department of Geography

Submitted by

Niko Schmitz

January 2007

DECLARATION

I confirm that this is my own work and the use of all material from other sources has been properly and fully acknowledged.

_____

(Niko Schmitz)

ACKNOWLEDGMENTS

The author wishes to thank the following ladies and gentlemen for their assistance:

At the University of Reading

Dr Maria Shahgedanova for providing full-time PhD supervision, guidance, and patience,
Dr Chris Stokes, Dr Paul Whitehead, and Dr Steve Gurney for scientific advice,
Heather Browning for generating a map of my study area,
Judith Fox for providing cartographic materials,
Erika Meller for generating a poster shown at a conference,
Dr Ray Saktreger and Ken Beard for help with computer problems.

Academic community (outside of the University of Reading)

Dr Jürg Luterbacher (University of Bern, Switzerland) for providing reconstructed teleconnection indices of Euro–Atlantic teleconnection patterns;
Dr Michael Rawlins (University of New Hampshire, USA) for providing information on R-ArcticNet database, the main database I used;
Vasilii Shevchenko (SevMeteo UGMS, Arkhangelsk, Russia) for providing information on the meteorological station of Arkhangelsk and recent water abstraction rates;
Dr Alexander Shiklomanov (University of New Hampshire, USA) for providing details on the discharge measurement techniques and errors of the Severnaya Dvina.

In Reading, I also thank Juliana Bittencourt and André Lacerda for various discussions related to PhD work, PhD students' life in general, and friendship.

Being completely self-funded is a very difficult situation. I am largely indebted to my parents, who not only financed my PhD studies in England over the last four years but also provided continuous moral support.

CONTENTS

PHD THESIS ABSTRACT

This thesis investigates the long-term changes and shorter-term variability in monthly, seasonal, and annual discharge between 1882 and 2004 of two rivers, the Severnaya Dvina (SD) and the Sukhona (SU), draining north-western Russia, and links these changes to climatic variability. The Severnaya Dvina is one of the largest rivers of the Arctic Ocean basin and changes in its discharge can potentially affect the Thermohaline Circulation. The SU is a tributary to SD and results have been used to corroborate findings obtained for SD. It has been suggested by previous studies that discharge of the rivers draining the Eurasian sector of the Arctic basin has significantly increased. However, these studies started during one of the warmest and driest periods on record in the 1930s.

Analysis of the discharge records of the SD and the SU has shown that that there has been no long-term, linear change in discharge. Strong interdecadal variability characterises both records and a number of significant shifts from lower to higher discharge occurs. The early part of the records (1882 – the early 1930s) is characterised by high annual discharge with many strong positive anomalies. A period of low discharge started in the dry 1930s and continued until the early 1970s. The last decades were characterised by average annual discharge. The main implication from this study is that freshwater inflow from European Russia into the Arctic Ocean has not changed since 1882.

Oscillations in regional climate and large-scale atmospheric circulation (teleconnection patterns) drive discharge variability. There are close causal links between variability in regional precipitation, air temperature, snow cover, evaporation, and discharge. Variability in teleconnection indices (most importantly North Atlantic Oscillation, Scandinavian and East Atlantic Jet pattern) explains between 13% (summer) and 48% (winter) variance in seasonal discharge. Construction of regression models simulating hydrological variability using climatic variables shows close agreement between modelled and observed values of summer, autumn, and winter discharge of the SD.

LIST OF FIGURES

al. (2000) gridded data set and averaged over the catchment of the SD (58 – 65^{o} N, 40 – 50^{o}E). Linear trends are shown in red (on Arkhangelsk data), Henderson filter in black.

Figure 5.3. Regional seasonal precipitation versus seasonal SD discharge (1901-2000). t = temperature, Q = discharge.

Figure 5.4. Standardised monthly mean air temperature at Arkhangelsk (1881-2003; 64^{o}60'N, 40^{o}50'E) and for the SD catchment (1901-2000). Data have been derived from New *et al*. (2000) gridded data set and averaged over the catchment of the SD (58 – 65^{o} N, 40 – 50^{o}E). Linear trends are shown in red (on Arkhangelsk data), Henderson filter in black.

Figure 5.5. Standardised seasonal temperature at Arkhangelsk (1881-2003; 64^{o}60'N, 40^{o}50'E) and for the SD catchment (1901-2000). Data have been derived from New *et al*. (2000) gridded data set and averaged over the catchment of the SD (58 – 65^{o} N, 40 – 50^{o}E). Linear trends are shown in red (on Arkhangelsk data), Henderson filter in black. Linear trends are shown in red (on Arkhangelsk data), Henderson filters are shown in black.

Figure 5.6. Regional seasonal air temperature versus seasonal SD discharge (1901-2000). t = temperature, Q = discharge.

Figure 5.7. Average snow depth at Arkhangelsk, Koynas and Kotlas for (I) October-May and (II) March (based on Breiling *et al*., 2006).

Figure 5.8. Dates (Julian day) of (a) the onset, (b) complete melt of snow pack and (c) duration of snow cover season at Arkhangelsk (1900-94) and Kotlas (1936-94

Figure 5.9. Monthly P-E (kg m^{2} s^{-1}) at the 850 hPa surface averaged over the SD catchment (58-65^{o}N, 40-50^{o}E) and monthly SD discharge, shown together in order to emphasize the relationship between the two.

Figure 5.10. Seasonal standardised time series of P-E at the 850 hPa surface derived from the NCEP/NCAR reanalysis and averaged over the SD catchment (1948-2000).

Figure 5.11. Seasonal standardised SLP time series averaged over the SD catchment (1900-2004).

Figure 5.12. The 30-year running means of correlation coefficient between the reconstructed teleconnection indices (Luterbacher *et al*., 1999) and AMJ discharge of SD: (a) NAO in January and (b) SCA in May. Correlation coefficients above 0.19 are statistically significant at 0.05 (shown as dashed line).

Figure 6.7. Scree plot (eigenvalues against component numbers) identifying the number of statistically significant components to be retained for the SON season (1901-1995).

Figure 6.8. Modelled versus observed values of SON discharge (m^3 s^{-1}) of SD (1902-1994). The black line shows the long-term average of the observed discharge (2,443 m^3/sec).

Figure 6.9. Time series of statistically signicant PC scores (SON 1901-1995).

Figure 6.10. Scree plot (eigenvalues against component numbers) identifying the number of statistically significant components to be retained for the DJFM season (1901/02 - 1995/96).

Figure 6.11. Modelled versus observed values of DJFM discharge (m^3 s^{-1}) of SD (1901/02-1995/96). The black line shows the long-term average of the observed discharge (975 m^3/sec).

Figure 6.12. Time series of statistically significant PC scores (DJFM 1902-1994).

LIST OF TABLES

arcticnet.sr.unh.edu/v3.0/index.html) and Arctic RIMS (http://rims.unh.edu/data.shtml).

Table 4.2. Statistical significance of assumed changes in seasonal SD discharge. Means and standard deviations of the before- and after-change samples are *m* and σ; the number of years in a sample is *N*.

Table 4.3. Statistical significance of assumed changes in JA discharge of SU. Means and standard deviations of the before- and after-change samples are *m* and σ; the number of years in a sample is *N*.

Table 4.4. Statistical significance of assumed changes in annual discharge of SD and SU. Means and standard deviations of the before- and after-change samples are *m* and σ; the number of years in a sample is *N*.

Table 5.1. Correlation coefficients between monthly precipitation and monthly discharge of SD. (a) Regional precipitation averaged over the SD catchment (65-58^{o}N and 40-50^{o}E; 1901-2000) (New *et al*., 2000). Discharge months are shown in blue and precipitation months in red. Correlation coefficients significant at 0.05 are shown (> 0.20).(b) Precipitation station data for Arkhangelsk (64^{o}60'N, 40^{o}50'E; 1881-2003). Correlation coefficients significant at 0.05 are shown (> 0.18).

Table 5.2. Correlation coefficients between seasonal regional precipitation (65-58^{o}N and 40-50^{o}E; 1901-2000) (New *et al*., 2000) and seasonal SD discharge. Only values significant at 0.05 are shown.

Table 5.3. Correlation coefficients between monthly air temperature and monthly SD discharge. (a) Regional temperature averaged over the SD catchment (65-58^{o}N and 40-50^{o}E) (1901-2000) (New *et al*., 2000). Discharge months are shown in blue and temperature months are shown in red. Correlation coefficients significant at 0.05 are shown (>0.20). (b) Temperature at Arkhangelsk (64^{o}60'N, 40^{o}50'E; 1881-2003). Discharge months are shown in blue and temperature months are shown in red. Correlation coefficients significant at 0.05 are shown (>0.18).

Table 5.4. Correlation coefficients between seasonal temperatures at Arkhangelsk (64^{o}60'N, 40^{o}50'E; 1882-2003) and seasonal SD discharge. Only values significant at 0.05 are shown.

Table 5.5. Correlation coefficients between (a) monthly snow depth at Arkhangelsk, (b) monthly snow depth at Kotlas, (c) end of snow season at Arkhangelsk and Kotlas, and

seasonal discharge of SD (1936-2001). Only coefficients significant at 0.05 (> 0.21) are shown.

Table 5.6. Correlation coefficients between monthly P-E (averaged over the SD catchment, 58-65^{o} N, 40-50^{o} E) and (a) monthly and (b) seasonal SD discharge (1948-2000). Discharge months are shown in blue and P-E months are shown in red. Coefficients significant at 0.05 (> 0.27) are shown.

Table 5.7. Correlation coefficients between SLP over the SD basin and SD discharge (1899-2004). Discharge months/seasons are shown in blue, SLP months/seasons in red. Only values significant at 0.05 are shown.

Table 5.8. Cumulative variance in the seasonal discharge of the SD explained by regional climatic factors (1882-1995). p = precipitation, t = temperature. Total variance explained is highlighted in bold.

Table 5.9. Correlation coefficients between the monthly teleconnection indices and AMJ discharge of SD (1882-1995). Correlation coefficients above 0.19 are statistically significant at 0.05. Only statistically significant correlation coefficients are shown.

Table 5.10. Cumulative variance in the AMJ discharge of SD (1882-1995) explained by the main NH teleconnection patterns. Total variance explained is highlighted in bold.

Table 5.11. Correlation coefficients between the monthly teleconnection indices and JA discharge of SD (1882-1995). Correlation coefficients above 0.19 are statistically significant at 0.05. Only significant values are displayed.

Table 5.12. Cumulative variance in the JA discharge of SD (1882-1995) explained by the main NH teleconnection patterns. Total variance explained is highlighted in bold.

Table 5.13. Correlation coefficients between the monthly teleconnection indices and SON discharge of SD (1882-1995). Correlation coefficients above 0.19 are statistically significant at 0.05. Only statistically significant correlation coefficients are shown.

Table 5.14. Cumulative variance in the SON discharge of SD (1882-1995) explained by the main NH teleconnection patterns. Total variance explained is highlighted in bold.

Table 5.15. Correlation coefficients between the monthly teleconnection indices and DJFM discharge of SD (1882-1995). Correlation coefficients above 0.19 are statistically significant at 0.05. Only statistically significant correlation coefficients are shown.

Table 5.16. Cumulative variance in the DJFM discharge of SD (1882-1995) explained by the main NH teleconnection patterns. Total variance explained is highlighted in bold.

Table 5.17. Correlation coefficients between monthly teleconnection indices and monthly rainfall at Arkhangelsk and over the SD catchment (1936-95). Precipitation months

are shown in blue and teleconnection months in red. Teleconnection patterns are ordered alphabetically. Only statistically significant coefficients (at 0.05) are shown.

Table 5.18. Correlation coefficients between monthly teleconnection indices and monthly temperature at Arkhangelsk over the SD catchment (1936-95). Teleconnection months are shown in red and temperature months are shown in blue. Patterns are ordered alphabetically. Only statistically significant coefficients (at 0.05) are shown.

Table 5.19. Correlation coefficients between monthly teleconnection indices and (a, b) snow depth and (c, d) onset and melt of snow cover (for the overlap period 1936-95). Correlation coefficients significant at 0.05 are shown (> 0.21).

Table 6.1. Variance explained by the five significant components for the AMJ season (1901-1995). Explained total cumulative variance is highlighted in bold.

Table 6.2. PC loadings of the five statistically significant components for the AMJ season (1901-1995). Only the highest component loadings are highlighted in bold to assist with interpretation of PCs.

Table 6.3. Variance explained by the statistically significant PCs and correlation coefficients between the PCs and the original variables for the AMJ season.

Table 6.4. Variance explained by the five significant components for the JA season (1901-1995). Explained total cumulative variance is highlighted in bold.

Table 6.5. PC loadings of the three statistically significant components for the JA season (1901-1995). Only the highest component loadings are highlighted in bold to assist with interpretation of PCs.

Table 6.6. Variance explained by the statistically significant PCs and correlation coefficients between the PCs and the original variables for the JA season.

Table 6.7. Variance explained by the five significant components for the SON season (1901-1995). Explained total cumulative variance is highlighted in bold.

Table 6.8. PC loadings of the five statistically significant components for the SON season (1901-1995). Only the highest component loadings are highlighted in bold to assist with interpretation of PCs.

Table 6.9. Variance explained by the statistically significant PCs and correlation coefficients between the PCs and the original variables for the SON season.

Table 6.10. Variance explained by the five significant components for the DJFM season (1901/02-1995/96). Explained total cumulative variance is highlighted in bold.

Table 6.11. PC loadings of the five statistically significant components for the DJFM season (1901/02 - 1995/96). Only the highest component loadings are highlighted in bold to assist with interpretation of PCs.

Table 6.12. Variance explained by the statistically significant PCs and correlation coefficients between the PCs and the original variables for the DJFM season.

Chapter 1. Introduction.

This PhD thesis investigates the long-term (1882-2004) trends and shorter-term variability in discharge of two rivers - the Severnaya Dvina and its tributary, the Sukhona - draining north-western Russia and flowing into the Arctic Ocean. The investigation is undertaken in the context of establishing links between variability in discharge and regional climatic variability using univariate and multivariate statistical methods. This chapter discusses the rationale and scientific issues to be addressed by the thesis (section 1.1). Research objectives, together with brief information on the catchment of the Severnaya Dvina, are outlined in section 1.2. The thesis structure is outlined in section 1.3.

1.1. Rationale and scientific issues to be addressed.

The simultaneous rise of global surface air temperature and alteration of the chemical composition of the atmosphere by increasing emissions of carbon dioxide and other greenhouse gases have increasingly led to the hypothesis that the two developments are linked. Various research bodies and, most importantly, the Intergovernmental Panel on Climate Change (IPCC) promote the concept of global anthropogenic climate change to emphasize a human fingerprint in the observed climatic alterations due to which temperature changes in the 20^{th} century are assumed to have exceeded historical natural climatic variability (IPCC, 2001). Changes in air temperature on global and regional scales lead to changes in other meteorological and environmental characteristics, such as the components of global and regional water balance, evoking feedbacks which can potentially result in dangerous climate change (IPCC, 2001). One of the main difficulties in the evaluation of impacts of climate change on both natural and human environments lies in the separation of a true climate change signal from the 'noise of natural climatic variability'. While this separation can only be achieved through the use of numerical climatic modelling, analysis of long-term climatic and environmental records can help to distinguish between the long-term trends potentially resulting in significant environmental change and shorter-term fluctuations, which in turn result from natural oscillations in the atmospheric and oceanic circulations (e.g. IPCC, 2001). However, if such records are to be used, their duration should be long enough for the quasi-decadal climatic variability not to be mistaken for a signal of more permanent

climate change (Hulme *et al*., 1999), and they should be complete and reliable (e.g. Esper *et al*., 2005; Moberg *et al*., 2005).

While the debate on the projected anthropogenic climate change and its impacts on natural and human environments is widening, one particular aspect of the problem stands out: a potential impact of the observed and projected climatic warming on the oceanic circulation in the Arctic Ocean and the North Atlantic and associated impacts on the climates of Eurasia (Manabe and Stouffer, 1988; Rahmstorf, 1994; 1995; 1997; 2000; 2003; 2006; Rahmstorf *et al*., 1996; Broecker *et al*., 1999; Rahmstorf and Ganopolski, 1999; Vellinga and Wood, 2002). The high latitudes are regarded as environments that are especially sensitive to climate change, where a change stronger than anywhere else in both air temperature and precipitation is projected with potential impacts on permafrost melt and regional water balance (IPCC, 2001). The latter is expected to result in changes in discharge of the largest Eurasian rivers contributing a bulk of the freshwater discharge into the Arctic Ocean thereby determining the salinity of the Arctic Ocean. The latter through its links with the North Atlantic, drives the Thermohaline Circulation (THC) providing for the currently relatively mild climate of north-western Eurasia (Manabe and Stouffer, 1988; Rahmstorf, 1994; 1995; 1997; 2000; 2003; 2006; Rahmstorf *et al*., 1996; Broecker *et al*., 1999; Rahmstorf and Ganopolski, 1999; Vellinga and Wood, 2002). Although currently there is no reliable estimate of a magnitude of change in oceanic salinity that may result in the significant weakening or a shutdown of THC, there is a concern that increasing freshwater discharge into the Arctic Ocean may provoke weakening of THC and associated cooling of the European climate.

The debate on changes in freshwater discharge into the Arctic Ocean and its potential impacts on ocean water salinity has been initiated by Peterson *et al*. (2002) who calculated that the annual total discharge of the six largest Eurasian rivers into the Arctic has increased by 7% (128 km^3) between 1936 and 1999 and is projected to increase further. This work has brought to attention earlier and inspired further research focusing on regional changes in water balance and river discharge in the Arctic Ocean basin (e.g. Grabs *et al*., 2000; Semiletov *et al*., 2000; Fukutomi *et al*., 2003; Lammers *et al*., 2001; Yang *et al*., 2002; 2004 a; b; Serreze *et al*., 2003 a; Ye *et al*., 2003). The presented results are often controversial with different conclusions being obtained for the same river basins. Larger-scale studies (Shiklomanov *et al*., 2000; McClelland *et al*., 2006 focusing on the Arctic Ocean basin as a whole; Peterson *et al*., 2002, for Northern Eurasia) have also produced different results. Most notably, a study of trends in freshwater discharge into the Arctic Ocean since 1921 by Shiklomanov *et al*. (2000) has

uncovered no significant long-term changes. The lack of agreement on changes in freshwater discharge in the Arctic Ocean basin may be due to a number of factors. Firstly, trends differ between sectors of the Arctic Ocean basin, most importantly between Eurasia and North America (Shiklomanov *et al*., 2000). Secondly, merely few studies (e.g. Shiklomanov *et al*., 2000; Pekarova *et al*., 2003) use the long-term (i.e. centennial) records and most investigations rely on shorter (60-30 year) records instead, whereby shorter-term fluctuations in both climate and discharge can be potentially mistaken for a signal of climate change (Hisdal *et al*., 2001; Lindström and Bergström, 2004). Thirdly, the quality and reliability of investigated discharge records as well as spatial coverage with regard to discharge monitoring vary across the Arctic Ocean basin (Shiklomanov *et al*., 2000) potentially introducing errors to data analysis. Fourthly, many studies do not distinguish between climatic and non-climatic (e.g. river regulation) impacts on discharge and disagree whether the strongest impacts are derived from natural climatic variability or non-climatic factors (e.g. Serreze *et al*., 2003 a; Yang *et al*., 2004 a). In addition, not all sectors of the Arctic Ocean basin have been investigated equally well. To date, a considerable body of research exists on the Siberian sector (e.g. Grabs *et al*., 2000; Semiletov *et al*., 2000; Fukutomi *et al*., 2003; Lammers *et al*., 2001; Serreze *et al*., 2003 a; Yang *et al*., 2002; 2004 a; b; Ye *et al*., 2003) while the North American sector, where the duration of discharge records is shorter, has received less attention (e.g. Zhang *et al*., 2001; Déry and Wood, 2004; Déry and Wood, 2005; Déry *et al*., 2005), and the European Russian sector has been largely been underreported.

Yet, the longest historical records of river discharge in the Arctic Ocean basin, spanning more than a century, are available for the European Russian sector. The regular measurements of discharge began on rivers of the Severnaya Dvina (7^{th} largest river of the Arctic Ocean basin) and the Sukhona in the 1880s, whereas measurements on the Pechora (5^{th} largest river of the Arctic Ocean basin) began only in 1932. The measurements on the Severnaya Dvina continued without interruption and significant changes in observation practices, and are ongoing. Unlike the Siberian sector of the Arctic Ocean basin, the European sector features limited areas of permafrost and the western part of the sector, drained by the Severnaya Dvina, is permafrost free. In contrast to the Siberian rivers, the Severnaya Dvina and its tributaries have not experienced significant regulations and flow alterations, and water abstraction remains low.

These two factors - (i) the lack of information on changes in river discharge at the European Russian sector of the Arctic Ocean and (ii) long historical extent and good quality of the

discharge records - invite an investigation into the trends and variability of freshwater discharge from the East European plain into the Arctic Ocean and their link with climatic oscillations. It is envisaged that the thesis will make two important contributions into the ongoing debate on changes in the components of water balance in the Arctic Ocean basin: (i) provide an analysis of regional changes in discharge and other components of water balance, such as precipitation, P-E, and snow cover, in the area underreported so far using statistical methods; and (ii) place the existing analyses into a longer-term historical context leading to a better understanding of regional climate change and impacts on freshwater systems.

1.2. Research objectives and study area

The Severnaya Dvina (SD) is one of Northern Eurasia's largest rivers and the 7th largest contributor of freshwater into the Arctic Ocean (section 2.1). The river is formed by the confluence of two smaller rivers, the Yug and the Sukhona (SU) (Figure 1.1). SD drains a vast, largely flat catchment with elevations close to the mean sea level, flowing to the White Sea, which is a part of the Arctic Ocean. The catchment belongs largely within the taiga zone (boreal forests) of Russia (Tishkov, 2002) characterised by low mean annual air temperatures and humid conditions due to abundant precipitation and low evaporation (section 2.4.2.2). Administratively, the catchment is located largely within the Arkhangelskaya Oblast (Arkhangelsk Region) of Russia. The total drainage area of SD is about 348,000 km^2, the river's length is about 1,300 km (Table 1.1), and it contributes about 105 km^3 a^{-1} (Peterson *et al*., 2002; McClelland *et al*., 2004) and 112 km^3 a^{-1} of freshwater (Lvovich, 1971) to the Arctic Ocean (Table 3.1). Both the catchment size and annual total discharge of SD are about seven times larger than of SU (Table 1.1).

Table 1.1. Characteristics of SD and SU catchments and their discharge (based on data from Arctic RIMS; http://rims.unh.edu/data.shtml)

River	Catchment area (km^2)	Mean annual discharge (m^3 s^{-1})	Annual total discharge (km^3)
Severnaya Dvina	348,000	3,360	105
Sukhona	49,200	450	15
TOTAL	**397,200**		**120**

Figure 1.1 shows location of the discharge gauging sites and meteorological stations used in this study.

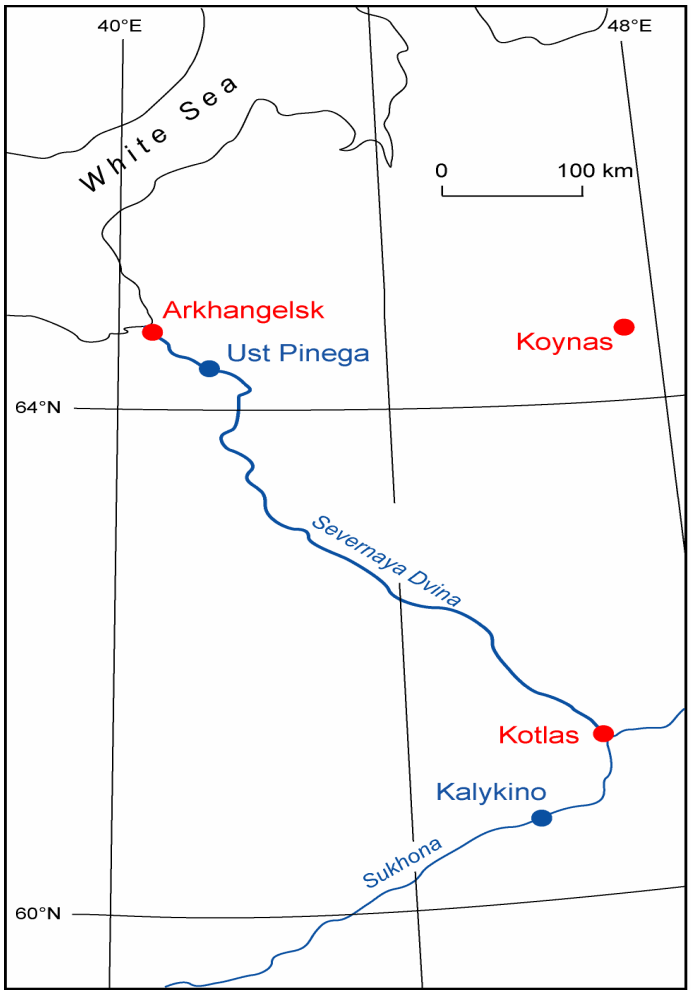

Figure 1.1. Map of the study area. The rectangular line encloses the SD catchment as defined in this thesis (58-65^{o} N, 40-50^{o} E). Discharge gauges are shown in blue, meteorological and snow depth measuring stations are shown in red.

1.3. Thesis structure

The thesis begins with an overview of literature characterising climate and discharge patterns of the Arctic Ocean basin with the emphasis on the Eurasian (particularly European Russian) sector of the basin (Chapter 2). Particular attention is given to the studies of river discharge in the Eurasian sector linking trends and variability in discharge with climatic trends. Controversial results and gaps in existing knowledge are highlighted and research questions to be addressed by the thesis are formulated at the end of Chapter 2. Chapter 3 provides

information on data and methods used in this study. Particular attention is given to the quality of both hydrological and meteorological data. The use of the selected statistical methods is explained and justified and theoretical aspects of the employed statistical methods, their advantages, limitations, and previous use are discussed. Chapter 4 shows and discusses the long-term trends and quasi-decadal oscillations in the monthly, seasonal and annual time discharge series of SD and SU since 1882. Chapter 5 links the uncovered discharge trends with variability in regional climate and the large-scale atmospheric circulation. In Chapter 6, the constructed statistical models linking discharge, regional climatic variables, and atmospheric circulation indices are presented and their performance is tested and discussed. Finally, Chapter 7 brings the obtained results together, provides conclusions from the study, and suggests directions for further research.

Chapter 2. Literature Review.

2.1. Introduction.

Variability in discharge of the rivers of the Arctic Ocean basin has recently received considerable attention because of its potential impact on salinity of the Arctic Ocean and associated changes in the oceanic circulation and climate (e.g. Peterson *et al*., 2002; Anderson *et al*., 2004). Changes in discharge of the Siberian (Grabs *et al*., 2000; Semiletov *et al*., 2000; Fukutomi *et al*., 2003; Lammers *et al*., 2001; Yang *et al*., 2002; 2004 a; 2004 b; Ye *et al*., 2003; Serreze *et al*., 2003 a) and North American rivers (Zhang *et al*., 2001; Déry and Wood, 2004; Déry and Wood, 2005; Déry *et al*., 2005) and their links with climatic variability have been documented. Discharge records from Siberia, dating back to the 1930s, indicate that discharge of the Yenisei, Lena, and Ob – the three largest rivers flowing into the Arctic Ocean – has increased, being attributed to the observed climatic warming and associated increase in winter snow accumulation. The Ob's annual discharge increased by 5% between 1936 and 1990 (Yang *et al*., 2004 a), the Yenisei's discharge by 3% between 1935 and 1999 (Yang *et al*., 2004 b), and the Lena's by 6% between 1936 and 1999 (Yang *et al*., 2002; Ye *et al*., 2003). By contrast, discharge records from the Canadian Arctic, dating back merely to the 1960s, indicate a 15% decrease in annual discharge (Déry and Wood, 2004; Déry *et al*., 2005). As a whole, annual total discharge into the Arctic Ocean increased by 5.6 km^3 in the Northern Eurasian sector and decreased by 2.5 km^3 in the North American sector, yielding a net increase of 3.1 km^3 between 1964 and 2000 (McClelland *et al*., 2006).

Given the importance of the discharge into the Arctic Ocean from the Eurasian sector, the identified trends in discharge of the Siberian rivers, and projections by General Circulation Models (GCMs) of the future warming in the Arctic Ocean basin (IPCC, 2001), concerns have arisen about possible impacts of these changes on the Thermohaline Circulation (THC) in the North Atlantic and associated potential changes on the European climate (Manabe and Stouffer, 1988; Rahmstorf, 1994; 1995; 1997; 2000; 2003; 2006; Rahmstorf *et al*., 1996; Broecker *et al*., 1999; Rahmstorf and Ganopolski, 1999; Vellinga and Wood, 2002), and especially about potential cooling in Europe, which might be associated with a shutdown of the THC (e.g. Rahmstorf, 2006). The strongest impacts of the projected climatic warming on hydrological cycle including river discharge are expected in the Arctic Ocean basin where

annual discharge is projected to increase by 10 to 40% in 2041-2060 in comparison with the 1900-1970 period (Milly *et al*., 2005). Depending on global future surface mean air temperature scenarios (an increase of 1.4 to 5.8^{o} C; IPCC, 2001), the post-1936 linear trend in the annual discharge of the six largest Northern Eurasian rivers has been extrapolated to 2100 yielding a possible increase between 18 % and 70 % over the present values, representing an aggregated total increase in freshwater influx into the Arctic Ocean of 315 – 1,260 km^3 a $^{-1}$ (Peterson *et al*., 2002).

To obtain a reliable answer to the question whether increasing freshwater inflow into the Arctic Ocean, together with the enhanced melt of sea ice, is capable of reducing the salinity of the ocean water to an extent that will reduce the strength of THC, a careful assessment of the observed and projected trends in discharge from all sectors of the Arctic Ocean basin is required. Yet to date, historical discharge records from the European sector of the Arctic Ocean basin have received little attention. Two large rivers, the Severnaya Dvina (SD) and the Pechora, drain northern European Russia contributing on average 112 km^3 a^{-1} (SD)[1] and 130 km^3 a^{-1} (Pechora) of freshwater to the Arctic Ocean (Lvovich, 1971). According to these estimates, the Pechora and SD rank as the 5th and the 7th largest contributors respectively of freshwater into the Arctic Ocean (Table 2.2). While discharge measurements on the Pechora have been intermittent, regular measurements of streamflow at the outlet of the SD began in 1882 and continue at present providing the longest historical river discharge record for the Arctic Ocean basin. Provided that SD has been affected by human interference to a very limited extent (section 3.2), such record is invaluable for detecting long-term linear trends in discharge and making a clear distinction between hydrological changes reflecting climate warming signal and short-term fluctuations in discharge records introduced by natural variability in atmospheric circulation (e.g. Hisdal *et al*., 2001; Lindström and Bergström, 2004).

This chapter reviews the existing knowledge of trends and forcings of river discharge in the Arctic Ocean basin highlighting insufficient knowledge or conflicting findings. It begins with a brief discussion of factors influencing discharge in general (section 2.2) and continues to discuss the main Euro–Atlantic teleconnection patterns in the context of hydrological variability (section 2.3). The climate and hydrology of the European sector of the Arctic

[1] 105 km^3 a^{-1} in the estimation by Peterson *et al*. (2002) and McClelland *et al*. (2004)

Ocean basin and the importance of discharge from the Eurasian sector are discussed in section 2.4. Trends in discharge from different sectors of the Eurasian Arctic Ocean basin and their links with climatic and hydrological variability are discussed in section 2.5. Research questions to be addressed by the thesis are formulated in section 2.6.

2.2. Factors influencing river discharge.

This section briefly discusses the main factors influence river discharge. These are grouped as natural factors and anthropogenic factors and the list is by far not exhaustive. Natural factors (climatic and non-climatic) affecting river discharge behaviour include:

- Sea level pressure (SLP) and geopotential height controlling weather patterns
- Air temperature
- Precipitation
- Evaporation (evapotranspiration)
- Extent of snow cover (lateral extent and snow depth) and its duration
- Ice cover
- Occurrence and extent of permafrost in the catchment
- Geology of a catchment
- Vegetation in a catchment
- Occurrence and extent of wetlands in a catchment
- Natural variations in the river course and channel alterations

SLP and geopotential height control weather patterns and determine temperature and precipitation regimes, which in turn control other climatic and discharge parameters. Both regional and distant SLP and geopotential height are known to control river discharge. For example Fukutomi *et al*. (2003) suggested that atmospheric circulation is a useful predictor determining the behaviour of components of hydrological budget across the three large Siberian watersheds in summer. Sturm *et al*. (2001) and Jacobeit *et al*. (2004) analyzed the occurrence of major floods in Central Europe since 1500 and concluded that these have been initiated by anomalies in large-scale atmospheric circulation.

Precipitation (P) and evaporation (E) are the major components of the regional water balance and difference between the two (known as effective precipitation; P-E) determines water

availability for discharge. Over long periods of time, when changes in a catchment's storage tend towards zero (Jones, 1997; Peel *et al*., 2001), a catchment's discharge can be approximated as the difference between precipitation and evaporation. Air temperature is one of the main factors controlling evaporation (Shaw, 1999). Therefore, precipitation and temperature are the main factors controlling river discharge in the absence of significant changes in basin physiography and water abstraction (Krasovskaia, 1994). There are numerous studies uncovering strong relationships between changes in precipitation and discharge and air temperature and discharge in Eurasia. For example, focusing on Europe, Kiely (1999) linked increasing rainfall to rising river discharge in Ireland in recent decades, while Shorthouse and Arnell (1999) reported that changes in atmospheric circulation patterns over selected European basins have led to higher precipitation and higher discharge. Peterson *et al*. (1999) linked increasing surface air temperatures with rising discharge across Northern Eurasia after 1936. Shiklomanov *et al*. (2000) reported that an increase in surface air temperature has led to higher annual discharge over a large part of European Russian after 1980.

Another important control over evaporation is water availability, which predetermines whether actual evaporation will occur close to its potential rate (e.g. Shaw, 1999). Serreze *et al*. (2003 a) investigated the links between the amount of water available for evaporation in the Siberian catchments and changes in discharge of the Siberian rivers. They have concluded that in the Ob basin, where wetlands are most abundant and evaporation occurs close to its potential rate, effects of an increase in precipitation, attributed to climatic warming, are mitigated by an increase in evaporation producing smaller changes in discharge that could be otherwise expected from rising trends in precipitation alone.

Snow cover insures a cumulative effect of precipitation on discharge and, together with ice cover and permafrost, creates specific river regimes with low winter flow and a sharp peak in spring following ice break-up and snowmelt (Koronkevich, 2002). Changes in temporal and spatial extent of snow cover and their links with discharge have been extensively documented for the Siberian watersheds and are discussed in section 2.5.

The main anthropogenic factors affecting river discharge have been summarised by Newson (1994) and Shiklomanov *et al*. (2000) and include:

- Changes in land use and development of agriculture (through the effects of both water abstraction and changing evapotranspiration)
- Urbanisation and changes in population in the catchment affecting changes in water abstraction for domestic and industrial use, and irrigation
- Reservoir and dam construction
- Inter-basin water diversions

Koronkevich (2002) and McClelland *et al*. (2004) discuss the impacts of these factors on interannual and interseasonal variations in discharge of the large rivers of the Northern Eurasian sector of the Arctic Ocean basin, with a focus on the changed seasonality of discharge patterns due to the above-mentioned anthropogenic (mechanic) interferences.

Climatic characteristics, known to affect river discharge, will be discussed in section 2.4 with emphasis on northern European Russia where the SD catchment is located.

2.3. The major Euro–Atlantic teleconnection patterns affecting climate and hydrology of the study area.

Low-frequency variability in atmospheric circulation is known to control variations in regional climate (Barnston and Livezey, 1987). The main low-frequency modes of atmospheric circulation occurring on the large (global, hemispheric, large regional) scales (Wallace and Gutzler, 1981; Esbensen, 1984; Barnston and Livezey, 1987) and regional climates (through precipitation, temperature, and SLP near the surface) have long been recognised as important controls over anomalous weather events, and the impacts of these forcings on river discharge regimes have been documented (for the most significant studies see section 2.5).

The earliest examples include the pioneering research by Walker and Bliss (1932), who were the first to identify the relationships between the dominant circulation modes and regional temperatures and precipitation anomalies using regression analysis, and Ångström (1935), who termed such links *teleconnections*. There is no unique definition of teleconnections in the contemporary climatological literature. The Climate Prediction Centre (CPC) defines them as "*recurring and persistent, large-scale patterns of pressure and circulation anomalies that*

span vast geographical areas" (www.cpc.ncep.noaa.gov/data/teledoc/telecontents.html). Various teleconnection patterns have been identified by Wallace and Gutzler (1981), Esbensen (1984), Barnston and Livezey (1987), and Thompson and Wallace (1998; 2000 a, b) and used to explain climatic and climate-induced fluctuations and anomalies both in temperature and precipitation (for examples see sections 2.4 and 2.5) as well as to improve short- and medium-range weather forecasts. Panagiotopoulos *et al*. (2002) provide a comprehensive discussion of the major teleconnection patterns and a comparison of methods used to derive them, whereas the CPC provides a shorter summary (www.cpc.ncep.noaa.gov/data/teledoc/telecontents.html).

In this section, the main Northern Hemisphere (NH) teleconnection patterns, affecting the catchment of the SD, and their hydrological importance are briefly discussed. These patterns (in alphabetical order) include the Arctic Oscillation (AO), the East Atlantic pattern (EA), the East Atlantic Jet pattern (EA-JET), the East Atlantic/West Russian pattern (EA/WR), the North Atlantic Oscillation (NAO), the Polar/Eurasian pattern (POL), and the Scandinavian pattern (SCA). The patterns have been derived by different techniques:

- The AO has been defined as the leading Empirical Orthogonal Function (EOF) of the Northern Hemisphere monthly mean sea level pressure (SLP) anomalies polewards of 20^{o} N (Thompson and Wallace, 1998).
- Other teleconnection patterns have been derived from Rotated Principal Component Analysis (RPCA) of monthly mean 700 hPa geopotential height for the period after 1950 by the National Centres for Environmental Prediction (NCEP) and Atmospheric Research (NCAR) of the US-American National Oceanic and Atmospheric Administration (NOAA). Major studies describing these patterns include Wallace and Gutzler (1981), Esbensen (1984), and Barnston and Livezey (1987).

The positive modes of these patterns are displayed in Figure 2.1, and time series of teleconnection indices are shown in Figure 2.2. Calendar months, in which these patterns are active, are given in Table 2.1. In addition to the interseasonal variability, the time series of many teleconnection indices exhibit significant interannual and decadal variability.

Three patterns (AO/NAO, SCA, and EA-JET) are of most hydrological importance for the study area, as demonstrated in Chapter 5. Recent publications have considered the Siberian part of Russia rather than impacts of these three patterns on the hydrology of northern

European Russia. Given that AO/NAO and SCA are the dominating patterns for the SD catchment these patterns will be discussed in greater detail. Few studies investigate the

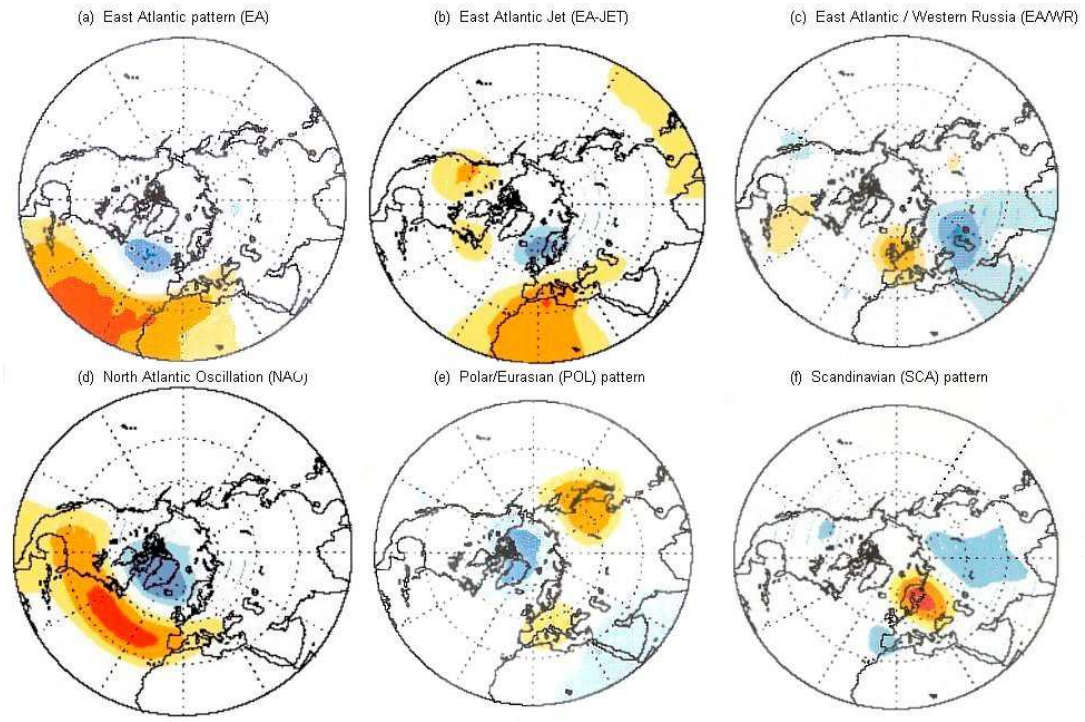

Figure 2.1. Maps of positive phases of the NH teleconnection patterns influencing climate and hydrology of the study area. All maps are for the month of January. The patterns are based on the rotated principal component analysis (RPCA) of monthly mean 700 hPa geopotential height conducted by the CPC. Contours represent loading weights with yellow and red shading corresponding to positive loadings and blue shading corresponding to negative loadings. Patterns are ordered alphabetically. Source: Panagiotopoulos (2004).

Table 2.1. Calendar months, in which teleconnection patterns are active (CPC, www.cpc.ncep.noaa.gov/data/teledoc/teletab.html). See heading of Figure 2.1 for abbreviations.

Pattern	**Jan**	**Feb**	**Mar**	**Apr**	**May**	**Jun**	**Jul**	**Aug**	**Sep**	**Oct**	**Nov**	**Dec**
NAO	x	x	x	x	x	x	x	x	x	x	x	x
EA	x	x	x	x					x	x	x	x
EA-JET				x	x	x	x	x				
EA/WR	x	x	x	x	x					x	x	x
POL	x	x										x
SCA	x	x	x	x	x			x	x	x	x	x

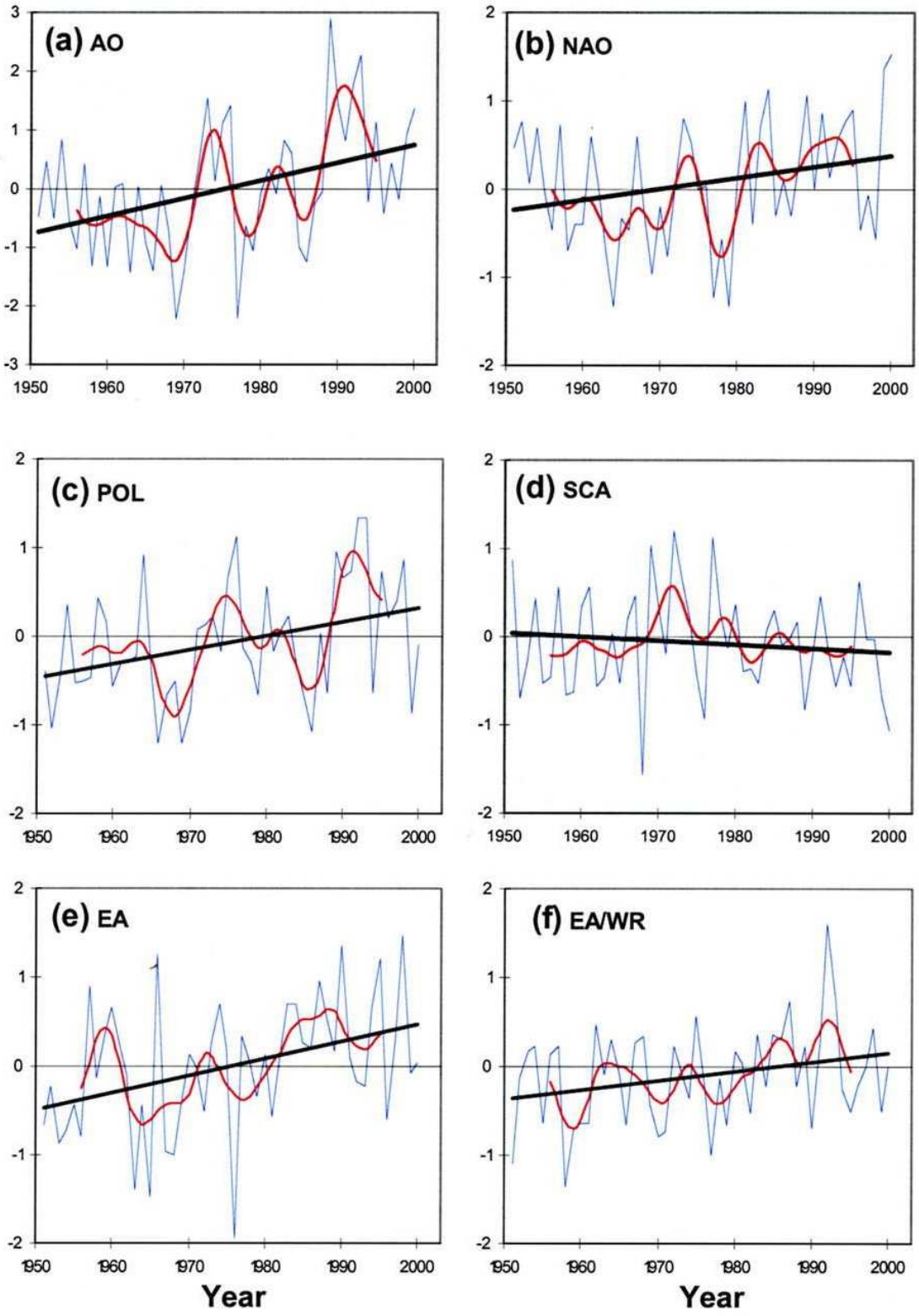

Figure 2.2. Winter (DJF) time series of main NH teleconnection patterns. Data are standardised amplitudes from RPCA performed by CPC (except for AO pattern: Thompson and Wallace, 1998). Linear trends (black line) and 11-point Henderson filters (red line) are also included showing higher and lower frequency variability respectively (Panagiotopoulos, 2004).

hydrological significance of other patterns. The POL pattern (Figure 2.1 e) has been found to control river discharge in the UK (Wedgbrow *et al*., 2002). The EA-JET pattern (Figure 2.1 b) plays an important role in the development of an unusually strong precipitation anomaly in southern Europe, which has resulted in strong flooding events on the River Elbe in August 2002 (Dünkeloh and Jacobeit, 2003).

2.3.1. North Atlantic Oscillation (NAO) and Arctic Oscillation (AO)

The dominant pattern of atmospheric circulation in the Euro–Atlantic region, identified in all studies, is NAO. NAO is defined in the simplest terms as a difference in SLP between the two atmospheric centres of action, the Azores high and the Icelandic low (Hurrell, 1995; Hurrell and van Loon, 1997; Jones *et al*., 1997; Rogers, 1997). During the positive mode of the NAO (Figure 2.1 d), the simultaneous strengthening of the two centres of action occurs. As a result, a strong westerly flow, directed from the North Atlantic into north-western Europe and reaching as far east as central Siberia, develops and storm tracks intensify accompanied with the influx of warm and humid air into Eurasia (Hurrell, 1995). Thus, an increase in air temperature and precipitation is observed between southern Greenland and northern Russia (Trigo *et al*., 2002). During the negative phase, both centres of action are either weak or, on rare occasions, a reversal is observed between the Azores high and Icelandic low. The westerly flow is weakened and displaced towards southern Europe and the Mediterranean resulting in colder and drier winters in northern Europe and wetter winters in southern Europe (Hurrell, 1995). Figure 2.2 b shows a time series of the NAO index for December-February (DJF), and Figure 2.3 displays the index for the December-March (DJFM) period revealing pronounced decadal variability (Hurrell, 1995; Hurrell *et al*., 2003). The most notable feature of the time series is strongly positive values during winter in the 1920s-1930s and the late 1980s-1990s, which corresponded to periods of warmer and wetter winters in northern Europe. Although the future climate projections suggest that the NAO may remain in a strongly positive mode in the future (e.g. Hartmann *et al*., 2000; Hoerling *et al*., 2001; Visbeck *et al*., 2001), the NAO index has declined since the mid-1990s (Figure 2.3; Cohen and Barlow, 2005).

A reconstructed NAO winter (DJF) index extended to 1500 (Figure 2.4; Luterbacher *et al*., 2001) allows to place the oscillations observed during the 20th century into historical context. The quality of these data and correlation with the CPC indices are discussed in section 3.3.3.

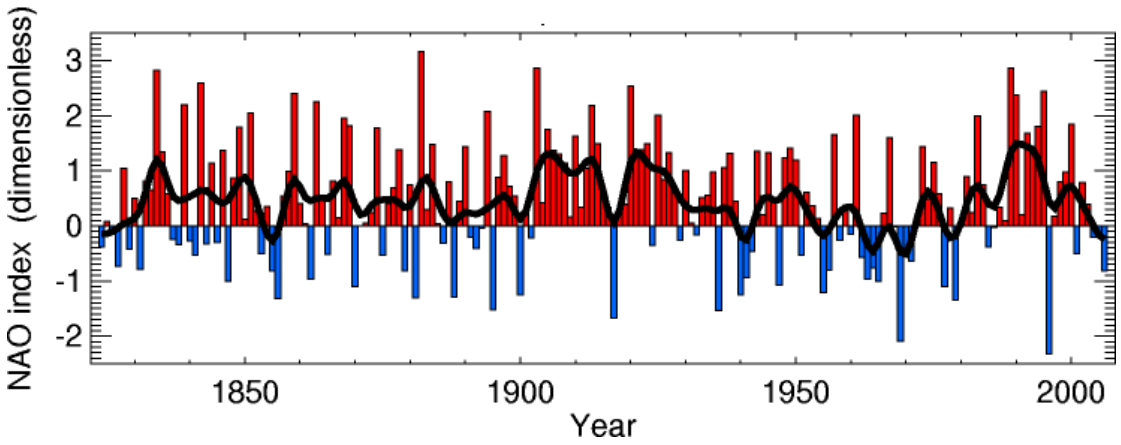

Figure 2.3. Time series of the December-March (DJFM) NAO index calculated as the difference between the normalised sea level pressure over Gibraltar and the normalised sea level pressure over southwest Iceland (Jones *et al.*, 1997; www.cru.uea.ac.uk/~timo/projpages/nao_update.htm). Columns represent actual index values; the black line is a running mean.

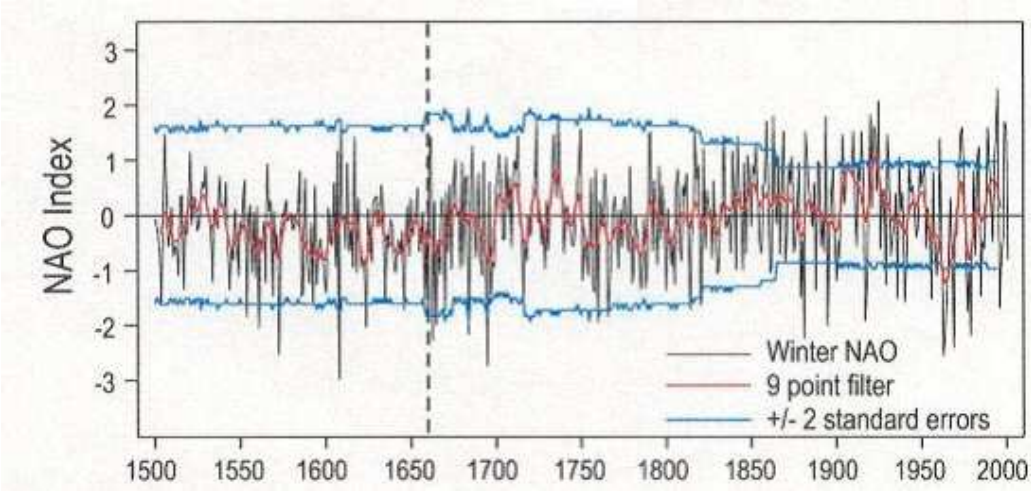

Figure 2.4. Reconstructed time series of December-February (DJF) NAO index (Luterbacher *et al.*, 2001).

However, two points should be briefly mentioned here: Firstly, reliability of the reconstructed time series increases over time: the post-1659 period is more reliable than the pre-1659 reconstruction (Luterbacher *et al.*, 2001). Secondly, there is a strong correlation between the CPC NAO index and the reconstructed NAO index for the winter months (Table 3.4) during the overlapping period from 1950-95. Luterbacher *et al.* (2001) argue that periods of persistently high NAO index, similar to those observed at the end of the 20th century, have

occurred in historical times as well, most notably at the beginning of the 16th and 18th centuries and around 1850. Therefore, the persistently positive NAO index values observed until the early 1990s are not unusual in the context of the 500-year record.

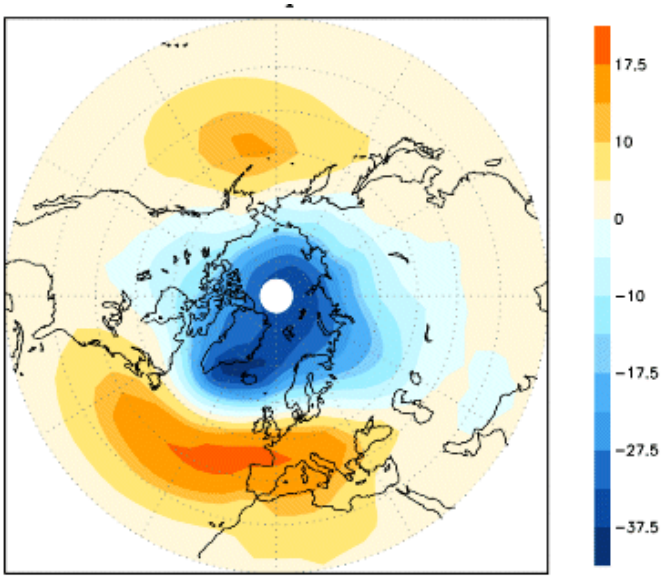

Figure 2.5. Map of the positive phase of the Arctic Oscillation (AO) pattern. The AO has been defined as the leading empirical orthogonal function (EOF) of the NH monthly mean SLP anomaly field. Units are m δ^{-1}, where δ is the standard deviation of the principal component time series (Thompson and Wallace, 2000 a).

In recent years, the identity of the NAO has become a subject of a debate (Thompson and Wallace, 1998; Wallace, 2000; Wanner *et al.*, 2001; Osborn, 2006). An alternative teleconnection pattern, termed the Arctic Oscillation (AO), has been proposed by Thompson and Wallace (1998; 2000 a, b) and its index has been calculated for the period after 1899 (Thompson and Wallace, 1998). The AO resembles the NAO, but its main centre covers most of the Arctic region (Figure 2.5), while the NAO is confined to the North Atlantic region (Figure 2.1 d). Thus, the NAO is often considered a regional manifestation of the AO (e.g. Thompson and Wallace, 1998; Wallace, 2000; Wanner *et al.*, 2001; Osborn, 2006).

The AO is best expressed during the cold season (November through April). Thompson and Wallace (2000 a, b) argue that the AO exhibits a closer link with the surface air temperatures in Eurasia than the NAO. While the NAO is an important modulator of precipitation predominantly in north-western and south-western Europe (Hurrell, 1995), the AO is highly correlated with precipitation variability across the middle latitudes (New *et al.*, 2001) as well

as in the Canadian Arctic (Déry and Wood, 2004; Déry and Wood, 2005). In fact, 90% of the precipitation variability and the decline in annual precipitation in the Canadian Arctic between the mid-1960s and mid-1990s have been attributed to the positive AO phase prevailing during the recent decades (Déry and Wood, 2004).

Strong causal links between AO/NAO and hydrological variability have been proven by many studies. Straile *et al*. (2003) provide a detailed review of the NAO impacts on freshwater ecosystems including river discharge, thermal and ice regimes of rivers and lakes, and lake level oscillations. Shorthouse and Arnell (1997) studied monthly river discharge variability at 477 drainage basins in Europe between 1961 and 1990 confirming a strong forcing of the wintertime NAO on discharge. Wilby (2001) and Wedgbrow *et al*. (2002) discussed a strong impact of the NAO on both winter and summer discharge in England and Wales. Wilby (2001) suggested that NAO provides useful skill in forecasting river discharge in England and Wales, particularly in late summer when it explains up to 40% of variance in discharge. Kiely (1999) studied trends in river discharge in Ireland and attributed an increase in discharge, observed since the mid-1970s, to the strongly positive NAO index. By contrast, a negative correlation between river discharge and NAO in southern Europe and the Middle East has been confirmed for rivers Rhone (France) and Ebro (Spain) (Lloret *et al*., 2001) and for the Euphrates and Tigris (Cullen and de Menocal, 2000). The controls of AO/NAO on river discharge in the Arctic Ocean basin will be further discussed in section 2.5.

2.3.2. Scandinavian pattern (SCA)

Particularly in northern Europe, the SCA pattern is a dominant mode of atmospheric circulation variability between August and May, which was also termed by Barnston and Livezey (1987) as ‘Eurasia 1 pattern’. The positive mode of SCA is defined by positive SLP and geopotential height anomalies over Scandinavia and north-western Russia, whereas the negative SCA mode is represented by negative anomalies over these regions (CPC, www.cpc.ncep.noaa.gov/data/teledoc/scand.shtml) (Figure 2.1 f). During the positive SCA phase these pressure anomalies frequently develop into blocking anticyclones, which break the progression of the westerly flow and make the storm track deviate from its mean path. In winter, the positive SCA phase is associated with below-average temperatures across western Europe and central Russia (Barnston and Livezey, 1987), and below-average precipitation, and reduced snow pack in northern Europe and European Russia (Clark *et al*., 1999; Qian *et*

al., 2000) where its influence extends as far south as the Caucasus Mountains (Shahgedanova *et al*., 2005). Precipitation is above average in central and southern Europe (CPC, www.cpc.ncep.noaa.gov/data/teledoc/scand.shtml) because the westerly jet is deflected south by the high-pressure anomaly centred over Scandinavia. Thus the extreme positive phase of SCA caused anomalous precipitation in western Europe and floods in the northern Alps in the autumn of 2000 (Lawrimore *et al*., 2001).

Time series of the SCA index (Figure 2.2) exhibit strong interannual variability, however, in contrast to the NAO decadal cycles are not well expressed in both the 20th century time series (Figure 2.2 d) and the reconstructed 1675-1995 time series (Luterbacher *et al*.; 1999; not shown).

2.4. Geography, climate, and hydrology of the Arctic Ocean basin.

2.4.1. Geography of the Arctic Ocean basin and importance of the Eurasian sector with emphasis on the European sector

The Arctic Ocean contains 1% of global seawater volume but receives 11% of global total river discharge (Kalinin and Shiklomanov, 1974). The Arctic Ocean basin is divided into ten large watersheds shown in Figure 2.6 together with discharge gauging stations. The Arctic Ocean basin extends as far south as 48^{o} N (R-ArcticNet, www.r-arcticnet.sr.unh.edu/v3.0/index.html), thereby significantly exceeding the Arctic region (defined as the area north of 60^{o} N, e.g. Aleksandrov *et al*., 1986; Johanessen *et al*., 2004). However, the SD catchment (as well as the whole of the European sector) does not extent that far south reaching just further south of 60^{o}N. According to different estimates, Eurasian and North American rivers deliver between 3,000 km^3 a^{-1} (Treshnikov, 1985) and 6,475 km^3 a^{-1} (Alekseev & Buzuev, 1973) of freshwater into the Arctic Ocean. Shiklomanov *et al*. (2000) estimated the total annual inflow between 1921 and 1996 at 5,249 km^3 a^{-1}. The total annual input from Eurasian rivers alone is estimated, with less spread, between 2,890 (Ivanov, 1994) and 2,960 km^3 a^{-1} (Gordeev *et al*., 1996). The differences between estimates are due to differences in geographical definitions of catchment areas (Prowse and Flegg, 2000) and different averaging periods. Densities of the monitoring networks vary across the Arctic Ocean basin contributing to uncertainties in the estimation of discharge. While river discharge

is not monitored across approximately 30% of the European Russian sector, no more than 15% of the area is unmonitored across the Asian part (Shiklomanov *et al*., 2000). The input of the Eurasian rivers constitutes the bulk of the total inflow into the Arctic Ocean. The three largest Siberian rivers alone – the Yenisei, Lena, and Ob – deliver 70% (1,554 km^3) of the annual discharge of the seven largest Arctic rivers (2,215 km^3 a^{-1}) (Table 2.2).

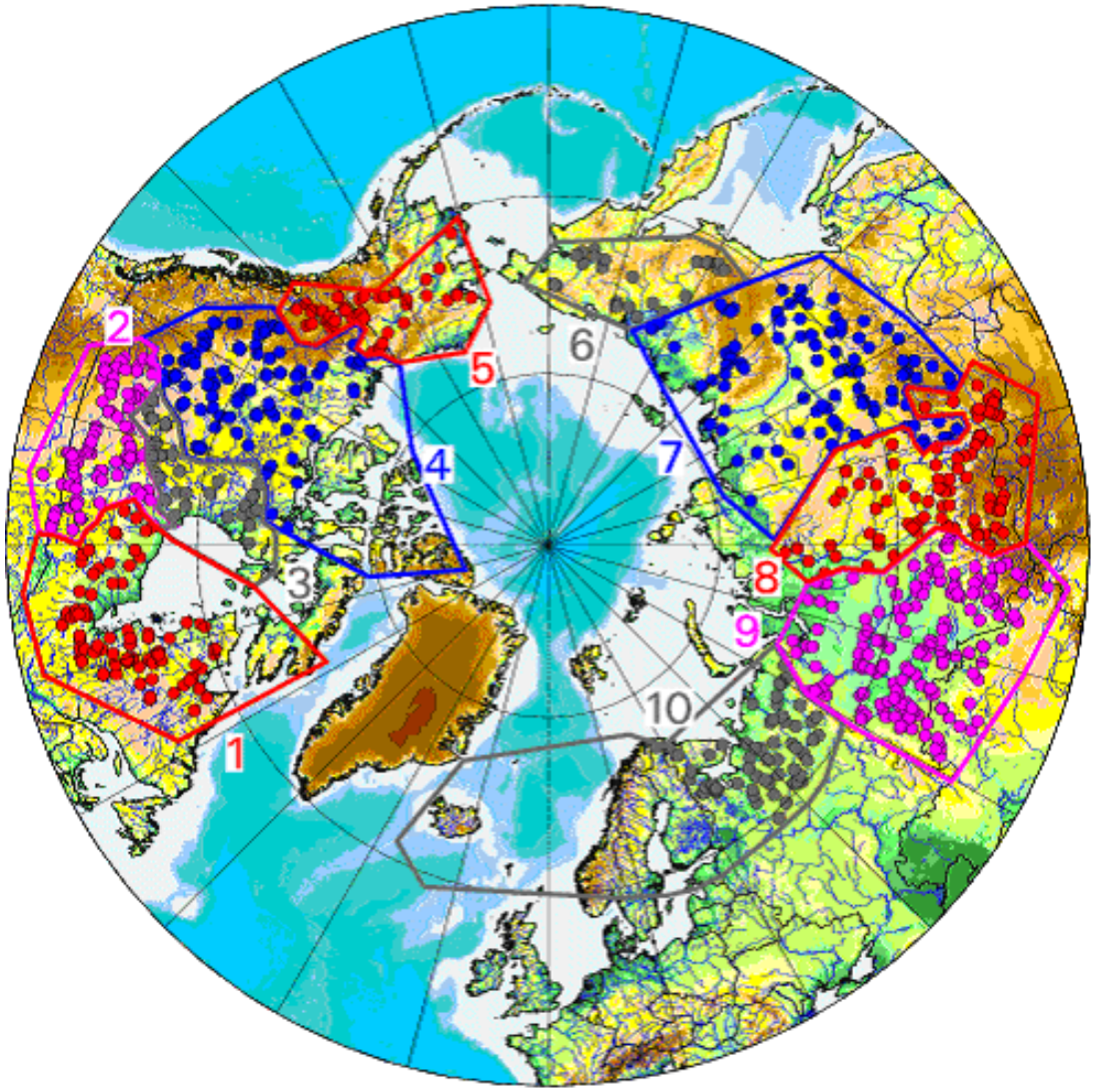

Watersheds: 1 – South and East Hudson Bay; 2 – Nelson; 3 – North-west Hudson Bay; 4 – Mackenzie; 5 – Yukon; 6 – Anadyr Kolyma; 7 – Lena; 8 – Yenisei; 9 – Ob; 10 – Barents, Norwegian Sea

Figure 2.6. The pan-Arctic watersheds (Source: R-ArcticNet, www.r-arcticnet.sr.unh.edu/v3.0/index.html). The SD catchment is located in Sector 10.

Table 2.2. Annual discharge of the seven largest rivers of the Arctic Ocean basin (Peterson *et al*., 2002; Grabs *et al*., 2000). Rivers are ordered by discharge. Data refer to the 1936-1999 (Eurasian rivers) and 1972-1992 (Mackenzie) periods.

Rank	**River**	**Catchment size** (km^2)	**Annual mean discharge** ($m^3\ s^{-1}$)	**Annual total discharge** ($km^3\ a^{-1}$)
1	Yenisei	2,440,000	19,660	620
2	Lena	2,430,000	16,806	530
3	Ob	2,950,000	12,810	404
4	Mackenzie	1,660,000	8,974	283
5	Pechora	312,000	4,471	141
6	Kolyma	526,000	4,185	132
7	Severnaya Dvina	348,000	3,330	105
TOTAL				**2,215**

2.4.2. Climate of the European Russian sector of the Arctic Ocean basin

Lydolph (1977) and Shahgedanova (2002) discuss the climate of Northern Eurasia in detail, including the climate of north-western Russia (or northern European Russia) that is part of the Arctic Ocean basin. Serreze *et al*. (2003 a) offer a useful summary of hydro-climatology of the terrestrial Arctic drainage system, although the main focus of this publication is on the Siberian sector and the Mackenzie catchment. This section provides a brief description of climatic regimes of north-western Russia with emphasis on the aspects of climate and atmospheric circulation that are known to be important factors in the formation of hydrological regimes.

Throughout the year, processes primarily developing in the North Atlantic and over its north-easternmost extension, the Barents Sea, control atmospheric circulation over the region (Shahgedanova, 2002; section 2.3). In winter, the area is located between the Polar and the Arctic fronts (the latter is on average positioned along the northern coast of Eurasia). In summer the Polar front migrates into the area predetermining strong depression activity throughout the year but with a peak between October and February (Shahgedanova, 2002). Depressions developing either over the North Atlantic or over the Barents Sea dominate the region. Rogers (1997) argues that a centre of low pressure developing over the Barents Sea in autumn-winter is of most importance for the development of cyclones and formation of

precipitation regimes over north-western Russia, the impacts of which exceeding those of the NAO on regional climate. Another prominent feature of atmospheric circulation controlling both precipitation and temperature regimes is the formation of persistent high-pressure systems (blocking highs) over Scandinavia and north-western Russia (SCA pattern; section 2.3). As already stated in section 2.3.2, Clark *et al*. (1999) and Qian *et al*. (2000) argue that this mode of circulation mainly controls winter precipitation and snow depth in northern Europe.

2.4.2.1. Thermal climate

Sub-zero temperatures prevail over north-western Russia approximately between October-November and March-April (Shahgedanova, 2002). Seasonal variations in air temperature at two stations (Arkhangelsk, located at the SD outlet, and Kirov, located in the south-eastern part of the catchment) are shown in Figure 2.7.

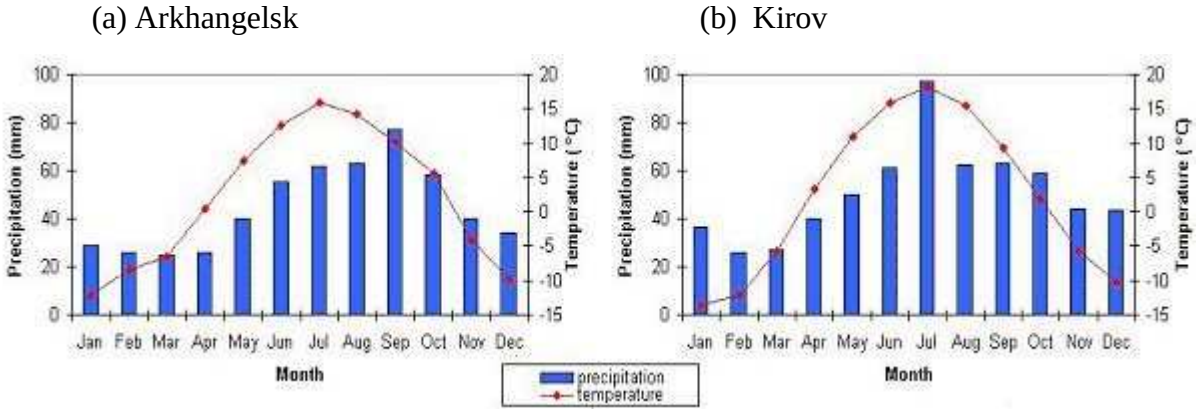

Figure 2.7. Mean monthly temperature and precipitation totals for two stations located in the SD catchment (a) Arkhangelsk (64^{o} 6’ N, 40^{o} 5’ E) and (b) Kirov (58^{o} 5’ N, 49 ^{o} 7’ E).

In winter, the temperature gradient is directed from west to east. Thus, the severity of the winter thermal climate increasing eastwards alongside the declining effect of warmer air masses advected into the region by the Atlantic or Barents Sea depressions (Figure 2.8).

These characteristics of the regional thermal winter climate have two important implications with regard to the formation of river discharge regimes:

(i) Rivers remain frozen between approximately mid-November and mid-April (section 3.2.2; Vuglinsky, 2000);

(ii) Winter precipitation occurs as snow and the amount of snow accumulated during the cold season predetermines river discharge in the subsequent seasons (Figure 2.13; section 2.5).

In addition, the comparatively (to Siberia) high winter temperatures and the fact that the area was repeatedly glaciated in the Quaternary (Velichko and Spasskaya, 2002) predetermine the absence of continuous permafrost in northern European Russia with island (or sporadic) permafrost developing along the Barents Sea coast and in the north-east of the region (Tumel, 2002). Therefore, unlike in Siberia and the North American Arctic, permafrost does not affect river discharge and its observed and projected melt in the western part of the region (SD catchment), while it affects discharge only to a very limited extent in the east (Pechora catchment). The lack of permafrost in northern European Russia suggests that, in contrast to the watersheds located in northern Siberia, (a) precipitation can infiltrate deep downwards into the soils and thus is not available for surface runoff; (b) in contrast to Siberia, where permafrost is dominant, increasing soil temperatures cannot generate additional (future) runoff in case of future warming, as is often suggested for the 21st century in recent literature (e.g. IPCC, 2001).

Cold-season air temperatures at the high latitudes of Northern Eurasia have risen between 1961 and 1990 (Rawlins and Willmott, 2003). Thompson *et al*. (2000 b) attribute the warming observed between 1968-1997 across Northern Eurasia to variability in atmospheric circulation. During that time, annual mean temperatures have risen by 1.1^{o} C over the Eurasian landmass (40-70^{o} N, 0-140^{o} E). An increase in winter (JFM) temperature of 3.0^{o} C is even stronger, but of this 1.6^{o} C is related to the positive AO mode (Thompson *et al*., 2000 b). Thus, 53% of the observed warming in winter (in the area including the SD basin) is attributed to the positive phase of the AO. Thompson and Wallace (1998) have established that a very close correlation exists between the AO and NAO indices and air temperature in Eurasia with correlation coefficients in excess of 0.65 for the November-April period of 1900-1995. These results have been confirmed by two other studies. Kryjov (2002) used air temperature data from a number of stations located along the White Sea coast and showed that variability in the AO index has a strong impact on winter (January-March) temperatures and a moderate effect on spring (April-June) temperatures. Popova (2005) obtained similar results showing that the positive NAO index leads to higher air temperatures (1-2^{o}C above average) over the high latitudes of European Russia.

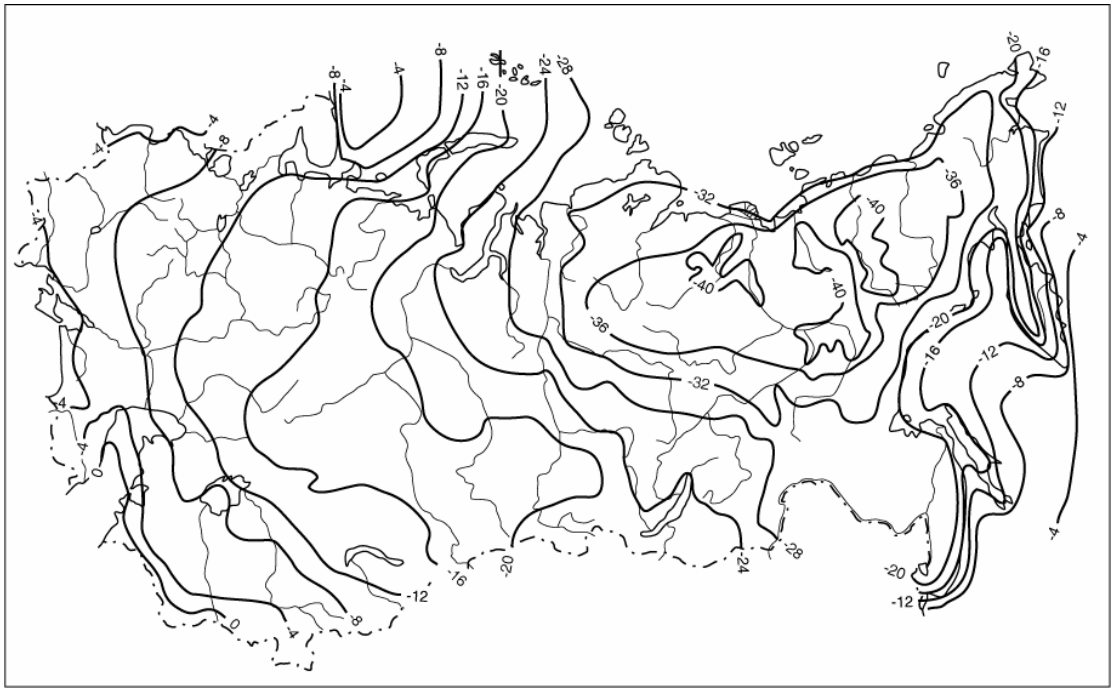

Figure 2.8. Mean January surface air temperature (^{o} C) in Northern Eurasia (Shahgedanova, 2002: 79)

In summer, depression activity over north-western Russia remains relatively strong in comparison to other regions of Northern Eurasia although its intensity is not as high as in the autumn-winter months (Shahgedanova, 2002). This predetermines comparatively low insolation of 13-14 kcal cm^{-2} (Myachkova, 1983) and comparatively low air temperatures declining from south to north (Figure 2.9). The role of distant forcing is reduced and teleconnections, such as AO/NAO patterns defining winter temperature, do not exhibit significant correlations with the summer temperatures (www.cpc.ncep.noaa.gov/data/teledoc/telecontents.shtml). In contrast to winter and spring, no strong increase in summer temperatures has been observed over north-western Russia (Rigor *et al*., 2000; Serreze *et al*., 2001).

Temperature changes and trends between the late 19th and late 20th century have been well documented in the literature. Two phases of climatic warming have occurred during the 20th century: between approximately 1920 and 1940, and since the 1970s/80s.

The first warming of the 20th century occurred during the 1920s and 1940s and has been termed the 'early 20th century warming' (Bengtsson *et al*., 2004). Major studies documenting this phenomenon include Polyakov *et al*. (2002 a), Polyakov *et al*. (2002 b), Bengtsson *et al*. (2004), and Johanessen *et al*. (2004). This was an important regional phenomenon as the strong climatic warming was observed in the Arctic and the northern part of the Arctic Ocean basin (e.g. Bengtsson *et al*., 2004; Johanessen *et al*., 2004). During this period, the highest air temperatures in the Arctic and sub-Arctic regions (defined as 60-90^{o} N; Aleksandrov *et al*., 1986; Johanessen *et al*., 2004) occurred with a maximum over northern European Russia. The warming was particularly strong over the area stretching from the White Sea and Barents Sea to the Kara Sea and the adjoining coastal Arctic land area (Bengtsson *et al*., 2004). In 1935-1944, regional mean annual air temperatures were 1.7^{o} C above the long-term mean, winter air temperature were 2.2^{o} C above the long-term mean, and summer temperatures were about 0.9^{o} C above the 1892-1998 long-term mean (Bengtsson *et al*., 2004). Bengtsson *et al*. (2004) attribute this phenomenon to changes in regional atmospheric circulation (increasing oceanic and atmospheric heat transport into the Barents Sea, which led to a reduced sea ice coverage and increasing surface temperatures).

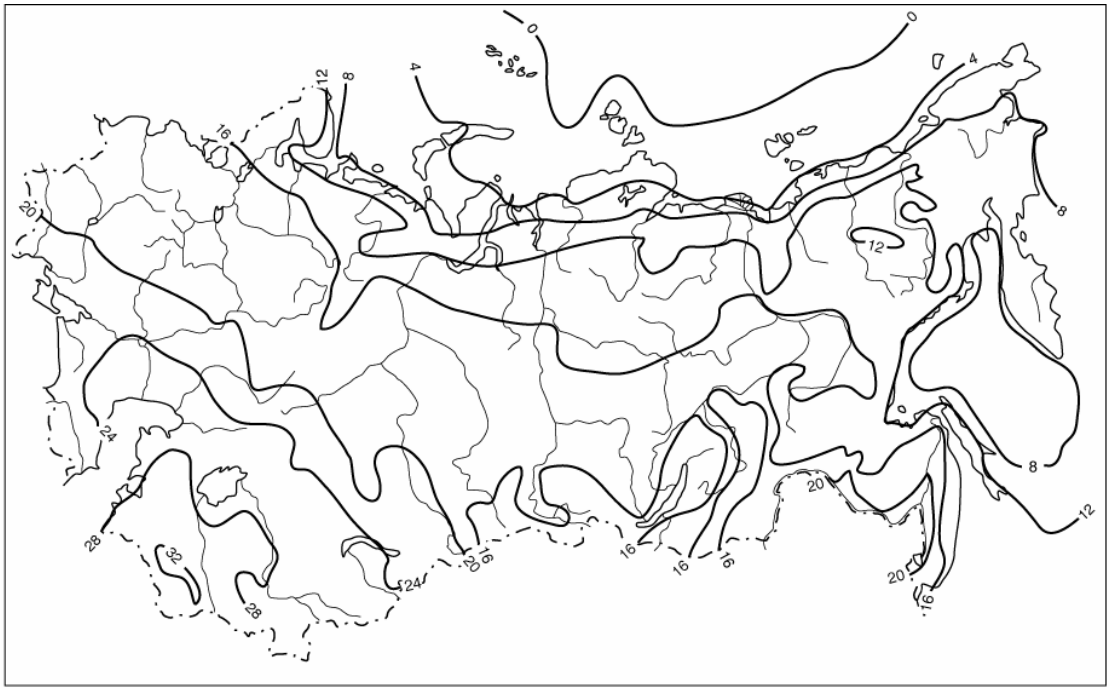

Figure 2.9. Mean July surface air temperature (^{o} C) in Northern Eurasia (Shahgedanova, 2002: 83)

The second strong warming in the Arctic and sub-Arctic land areas occurred since the early 1970s/80s (depending on study region), when annual mean surface air temperatures (SAT) started to increase strongly. The increases have been calculated from station data (e.g. Chapman and Walsh, 1993; Alekseev *et al*., 1999; Jones *et al*., 1999; Przybylak, 2000; Polyakov *et al*., 2002 a, b) and satellite observations (e.g. Rigor *et al*., 2000). Strong warming occurred in the high latitudes of the Northern Hemisphere between 1970 and the present (e.g. Serreze and Francis, 2006) and particularly between 1985 and 2001 in the region north of 62^{o} N, where annual mean temperature increased by 0.7^{o} C per decade (Polyakov *et al*., 2002 b). Focusing on seasonal scales, Johanessen *et al*. (2004) analyzed a station data set (Alekseev *et al*., 1999) and concluded that the strongest increases occurred during winter in the high Arctic between 1980 and 1999. For a more detailed summary on recent trends in the Arctic, the reader is referred to the reviews by Johanessen *et al*. (2004) and Serreze and Francis (2006).

Serreze and Francis (2006) have analyzed mean annual temperature trends based on a data set by Jones and Moberg (2005) in order to document mean annual SAT anomalies differentiated by latitudinal bands between the 1930s and 2000. The highest mean annual air temperatures on record were found in the band from 70-75^{o} N during the late 1930s, being higher than during the late 1990s. In contrast, the latitudinal bands of 65-70^{o} N and 60-65^{o} N are also characterised by positive thermal anomalies in the 1930s, however the 1990s feature higher annual temperatures (Serreze and Francis, 2006). On a seasonal basis, the 65-75^{o} N zone was warmest in winter (DJF) and autumn (SON) during the late 1930s, while the springtime (MAM) and summer (JJA) mean annual temperatures were higher during the 1990s (Serreze and Francis, 2006). Some authors attribute the observed recent warming to changes in atmospheric circulation (e.g. Thompson *et al*., 2000 a, b) while others argue that this may constitute an emerging signal of changing climate (e.g. Serreze and Francis, 2006).

Most authors agree that the nature of the two warm periods is not the same. The major difference between the early 20th century warming and the warming during the late 20th century concerns its spatial extent across the Northern Hemisphere. While the exceptional warmth of the 1920-40s has been confined only to high latitudes, the recent warming has affected most of the Northern Hemisphere (e.g. Alley *et al*., 2003; Johanessen *et al*., 2004). Serreze *et al*. (2000), Johanessen *et al*. (2004), or Serreze and Francis (2006) provide further analyses of temperature changes in the high latitudes of the Northern Hemisphere in the 19th and 20th centuries.

2.4.2.2. Precipitation and snow cover

North-western Russia receives abundant precipitation originating from both frontal and convective activity and ranging between 600 and 800 mm a^{-1} (Figure 2.10). Precipitation maximum occurs between June and October peaking in early autumn (Figure 2.7). In contrast to Siberia, which receives little precipitation in winter, precipitation in the European north remains relatively high throughout the winter months (Figure 2.7 and Table 2.3). Between October-November and March-April precipitation occurs as snow. The duration of snow cover ranges from 160 days in the south to 200 days in the north of the SD catchment (Figure 2.11). These values are in line with the values calculated for the meteorological stations of Arkhangelsk and Kotlas (Figure 1.1) where the average duration of snow cover was 196 and 194 days per year respectively. Snow depth peaks in March decreasing rapidly in April (Figure 2.12), resulting in maximum discharge and spring floods (section 2.4.3).

Table 2.3. Seasonal total rainfall (mm) at various locations across the SD catchment. Stations are ordered from north-west to south-east. Source: ROSHYDROMET (http://meteo.ru/data_temperat_precipitation/) and DSS UCAR (http://dss.ucar.edu/data sets/ds570.0/).

Station	***Location***	***Winter (DJF)***	***Spring (MAM)***	***Summer (JJA)***	***Autumn (SON)***
Arkhangelsk	64° 6’ N, 40° 5’ E	99	97	228	171
Kotlas	61° 2’ N, 46° 6’ E	82	98	191	142
Kirov	58° 5’ N, 49° 7’E	105	117	220	166

As it has already been mentioned, precipitation and snow depth are strongly controlled by variability in atmospheric circulation. Particularly important controls are variability in SLP in the Barents Sea (Rogers, 1997) and the occurrence of blocking highs over Scandinavia, which form a barrier to the moisture-bearing westerly air flow (Clark *et al*., 1999; Qian *et al*., 2000). Frequent and prolonged blocking events result in low precipitation and low snow accumulation. For example, the snow pack in European Russia has been low between 1983-1985 due to the frequent blocking over Scandinavia (Shahgedanova *et al*., 2005). It should be noted that the strong negative anomalies in precipitation have been observed in the Arctic and sub-Arctic regions in the 1930s at the time of the strong regional warming (Paeth *et al*., 2001; Polyakov *et al*., 2002 a; Bengtsson *et al*., 2004). These anomalies are confirmed by both

station precipitation data and gridded data sets used in this study (section 5.1.1). In the context of this thesis, this time period is important because many discharge records, such as those of Siberian rivers used by Peterson *et al*. (2002) in their analysis of trends in freshwater discharge in the Arctic Ocean, started in the 1930s (section 2.5). However, the period centred on the 1930s contained the warmest (Polyakov *et al*., 2002 a) and, with regard to annual total precipitation, driest years (e.g. Paeth *et al*., 2001) on record in the high latitudes of the Northern Hemisphere. Although no data are available on evaporation, it may be suggested that evaporation from the Eurasian watersheds was also at its highest because of the unusually high summer temperatures (Bengtsson *et al*., 2004). A combination of these factors should have affected discharge of the rivers of the Arctic Ocean basin reducing discharge below the long-term means.

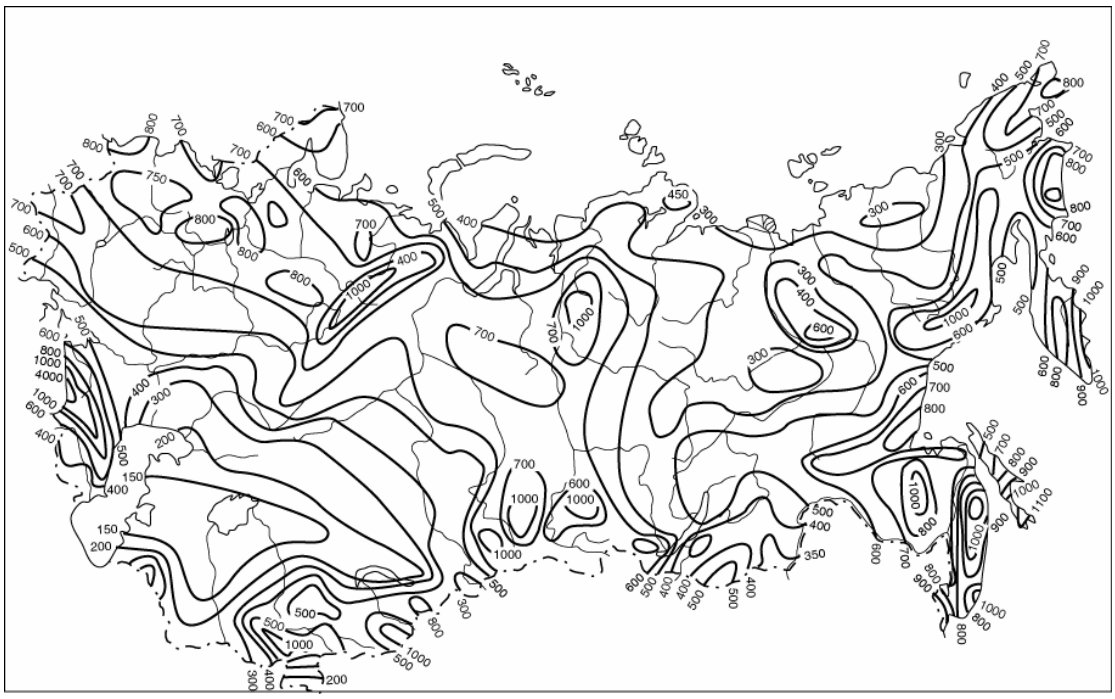

Figure 2.10. Mean annual precipitation totals (mm) in Northern Eurasia (Shahgedanova, 2002: 84).

Three main publications assess annual precipitation trends over the large Northern Eurasian watersheds for the periods after 1881 (Groisman and Rankova, 2001) and after 1936 (Berezovskaya *et al*., 2004; Rawlins *et al*., 2006). These studies use different data sets and there is no agreement between the authors as to which of the employed data set is the most reliable (for further discussion see section 3.3.2).

Groisman and Rankova (2001) examined changes in annual precipitation in the Russian permafrost-free zone between 1881 and 1998 using an archive collated by Gruza *et al*. (1999) and Groisman *et al*. (1991) and concluded that annual precipitation has increased by approximately 5% over the whole period and across the whole region. This study does not provide any analysis of spatial variations (e.g. trends are not analyzed specifically for north-western Russia or any other region) treating the vast region as a whole. Studying a 63-year (1936-98) regional record of annual precipitation, Berezovskaya *et al*. (2004) have found declining precipitation over the Yenisei basin (- 16 mm) and a weaker increase (+ 4 mm) over the Lena basin over the duration of record. No significant precipitation change has been detected in the Ob basin. This study was based on New *et al*. (2000) precipitation data set which is a fine-resolution gridded data set extending most back in time but employing a varying number of meteorological stations with implications for trend analysis (section 3.3.2). Recently, Rawlins *et al*. (2006) assessed annual precipitation trends over the six large Northern Eurasian watersheds between 1936 and 1999. According to their results, total annual rainfall has decreased over time. With regard to the SD catchment, little change has been uncovered in winter precipitation and a small increase has been registered in summer (Rawlins *et al*., 2006).

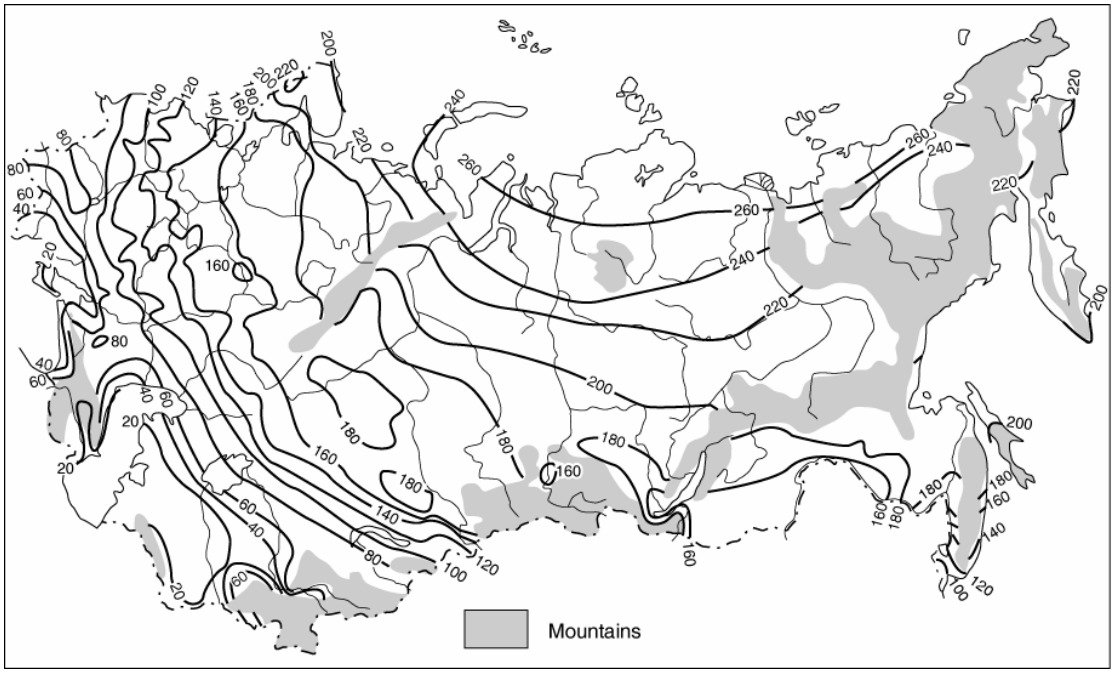

Figure 2.11. Snow cover (in days) in Northern Eurasia (modified from Rikhter, 1960, in Shahgedanova, 2002: 90).

Importantly, the authors urge caution regarding the early years of the records when the uneven spatial distribution of meteorological stations resulted in overrepresentation of rainfall in annual precipitation. This problem affects all data sets used in the study by Rawlins *et al*. (2006).

Fallot *et al*. (1997), Ye *et al*. (1998), Brown (2000), Ye and Ellison (2003) and Rawlins *et al*. (2006) have documented changes in the extent and duration of snow cover in the Arctic Ocean basin for various regions and time periods. The obtained results differ between different sectors and time periods.

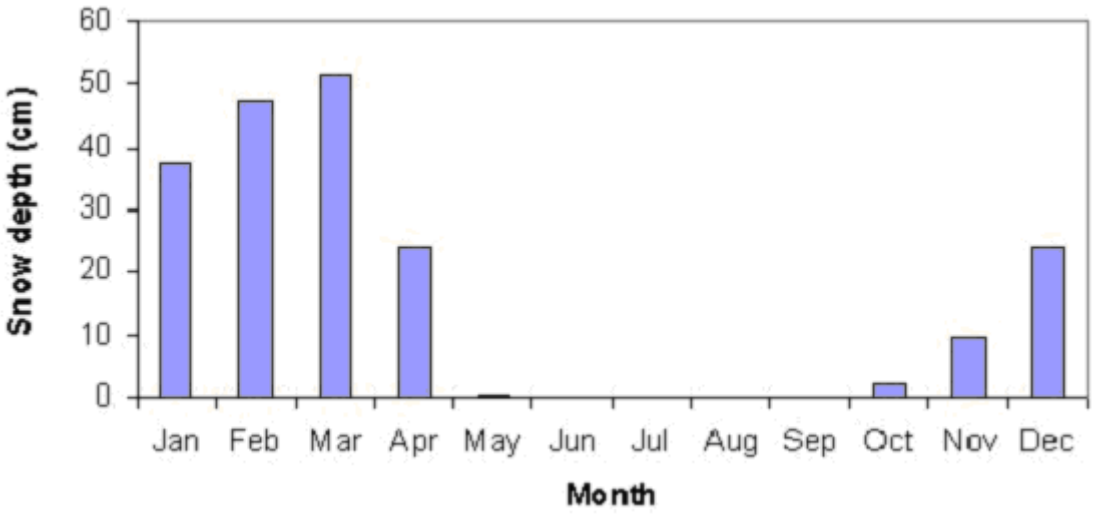

Figure 2.12. Mean monthly snow depth at Arkhangelsk (based on data by Breiling *et al*., 2006).

Ye *et al*. (1998) have found that between 1936 and 1983 snow depth has increased by 4.7% per decade in the 60-70^{o} N latitudinal zone of Russia and decreased by 0.8% per decade in the 50-60^{o} N latitudinal zone. These results agree with Fallot *et al*. (1997) who concluded that snow depth during winter has increased over European Russia, north of 63^{o} N, between 1945-1950 and the early 1980s. Overall, the snow water equivalent over the 50-70^{o} N zone has increased over the past decades (Ye *et al*., 1998).

Brown (2000), Ye and Ellison (2003), and Rawlins *et al*. (2006) have evaluated changes in the spatial extent of snow cover. Brown (2000) has found that in the region of 40-60^{o} N and 20-90^{o} E, no long-term change in the extent of snow cover occurred between 1922 and 1997

at the beginning of the snow cover season (October). In contrast, in March and April significant decline in the spatial extent of snow cove has occurred. The earlier melt of snow has been attributed by Brown (2000) to a pronounced warming trend of 2.5^{o} C per 100 years observed in the region in March-April (Brown, 1997). Brown (2000) has estimated that the April extent of snow cover was declining by 740,000 km^{2} per 1^{o}C warming. This trend has been partly attributed to the positive snow-albedo feedback whereby an earlier disappearance of snow pack results in faster and stronger warming of the Eurasian landmass (Groisman *et al*., 1994 a). Changes in duration of snow cover in northern European Russia (43-73^{o} N) have been evaluated by Ye and Ellison (2003) who found that the length of snow cover season has increased in this latitudinal zone between 1937 and 1994. The observed increase has been attributed to an earlier onset of snow cover (two days per decade) over northern European Russia in the early 1990s in comparison to 1936. The authors have found that snow melt was occurring earlier in the recent decades in line with the observed climatic warming and with the results by Brown (2000). Changes in snow depth and duration of snow cover in the SD catchment are analyzed in section 5.2.3. The uncovered trends do not entirely agree with those discussed in literature.

2.4.2.3. P-E (effective precipitation) and droughts

Of most importance for regional water balance and river discharge regimes is effective precipitation (P-E or P-ET; Serreze *et al*., 2003 a). Information on effective precipitation is limited in comparison with that on precipitation. Importantly, long-term data on evaporation in the region is to the author's knowledge not available. Nevertheless, references to station data are available from traditional literature (e.g. Borisov, 1965; Myachkova, 1983), while Serreze *et al*. (2003 a) discuss spatial and temporal distributions of effective precipitation derived from the gridded NCEP/NCAR data on vertically integrated monthly zonal and meridional vapour fluxes and precipitable water. The main implication of relatively low temperatures and high precipitation observed in north-western Russia is that although in this area (a large part of which is characterised as wetlands and most as taiga forest) evaporation is not limited by moisture availability and occurs at near potential rate, P-E remains mostly positive throughout the year. According to the station data, actual evaporation in the region ranges from 150-300 mm a^{-1} (Borisov, 1965; Myachkova, 1983). This is lower than annual precipitation (Figure 2.5) and close to summer precipitation totals (Table 2.3). Serreze *et al*. (2003 a) have estimated monthly totals of both evaporation and effective precipitation for the 1960-1999 period. In July, which is the warmest month in the SD catchment, evaporation is

highest and ranges between 70 and 90 mm that is close to the monthly precipitation totals (Figure 2.7) and P-E remains positive (at approximately 10 mm) in the northern pat of the catchment and slightly negative (at approximately -15 mm) in the southern part.

Soil moisture deficits (droughts) are infrequent in north-western Russia and occur on no more than 5% of all summer seasons (Shahgedanova, 2002) although notable exceptions occur such as the prolonged summer drought of 1972 (Buchinsky, 1976). Soil moisture trends, which depend on precipitation and evaporation and affect water availability for discharge, have been investigated by Vinnikov and Yeserkepova (1991) using a short-term data set for 1972-1995. During this time period, in the 55-60^{o} N latitudinal zone, a small increase in soil moisture occurred in the upper 1 m levels of soil moisture layer during all months in line with an increase in precipitation.

2.4.3. Peculiarities of river regimes in the Arctic Ocean basin

In this section, the main features of hydrological regimes of the rivers of the Arctic Ocean basin are highlighted together with the unique factors shaping these regimes. The links between atmospheric circulation, climatic forcings, and hydrological responses will be discussed in section 2.5. Lewis *et al*. (2000) provide a detailed discussion of the peculiarities of the Arctic Ocean basin hydrology. Koronkevich (2002) provides a brief discussion of hydrological regimes in the Eurasian sector of the Arctic Ocean basin.

The main natural factors shaping river regime of the Arctic Ocean basin include:

- Low annual mean air temperature and sub-zero air temperatures lasting for more than half year;
- Snow pack persisting for more than half year and providing water storage;
- Ice cover persisting for about half year or more;
- Mostly positive effective precipitation and low (or zero) soil moisture deficit;
- Permafrost (an insignificant factor within the SD catchment);
- Large meridional (north-south) extent of the rivers with different climatic conditions affecting the upper and lower river basin area.

As a result of the features of the Arctic Ocean basin summarised above, river discharge across the Arctic Ocean basin (including the SD catchment) is unevenly distributed throughout the year. During the winter season (when rivers are frozen), discharge is low across the Eurasia being especially low in eastern Siberia relatively relatively high in Scandinavia (Figure 2.13). In contrast to low winter discharge, the spring flood is well expressed across the Arctic Ocean basin and accounts for 50-70% of annual discharge (Koronkevich, 2002). The timing of both high-flow season during spring and periods when rivers are frozen varies from west to east with increasing degree of continentality. The north-south variations are less well expressed because of the large north-south extent of the rivers and the influence of the upstream regions on the downstream regions.

The main regularities of ice cover extent and the timing of the spring high-flow season are as follows:

(i) Ice breaks up and snowmelt begins in April and the high-flow season occurs in April-May in the westernmost regions of Eurasia (e.g. Scandinavia);

(ii) Ice breaks up and snowmelt begins in April and the high-flow season occurs between April and June in European Russia (e.g. SD and Pechora basins);

(iii) Siberia (especially its eastern part) is characterised by a longer period of snow accumulation and ice break up and snowmelt are delayed until June.

Hydrological seasons in the Arctic Ocean basin are not spatially homogeneous and are different from standard seasons. Therefore, it is important to define ‘internally homogeneous’ seasons for each studied river basin (e.g. Ahrens, 2000). Hydrological seasons for SD are defined in section 4.2.

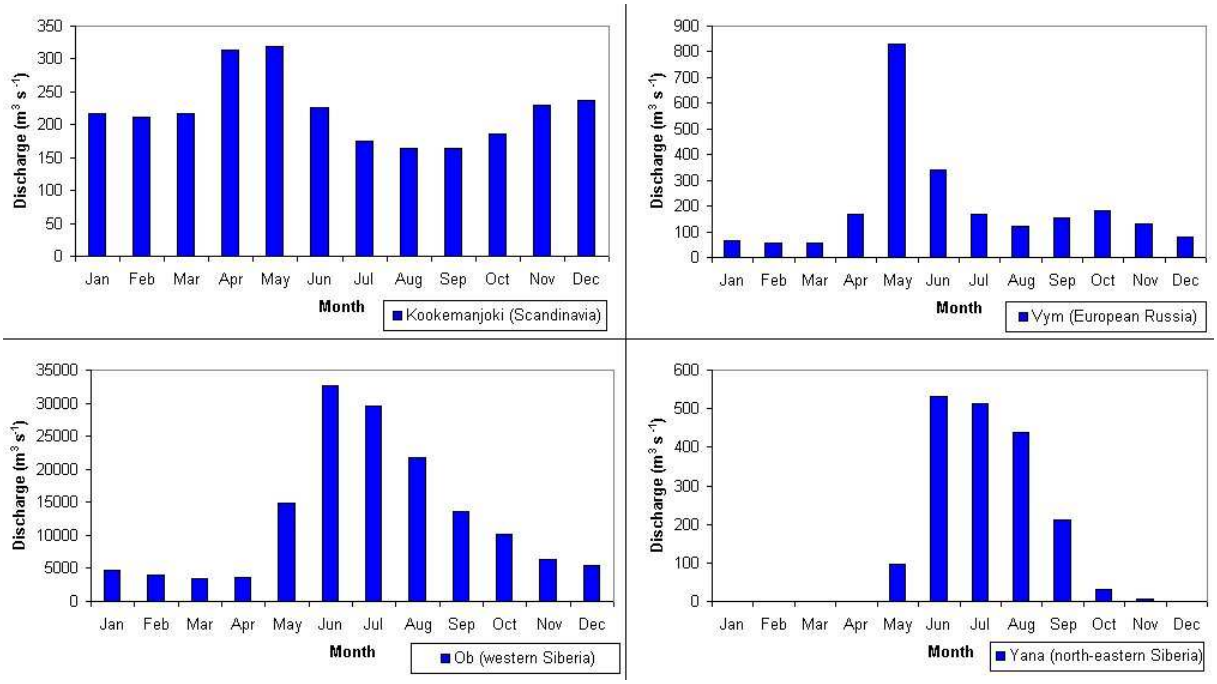

Figure 2.13. Hydrographs showing average monthly discharge (m^3 s^{-1}) at four selected gauging stations across the Eurasian sector of the Arctic from west (Scandinavia) to east (north-eastern Siberia). Hydrographs are based on data from R-ArcticNet (www.r-arcticnet.sr.unh.edu/v3.0/index.html).

Permafrost is another factor affecting discharge (Serreze *et al*., 2003 a; McClelland *et al*., 2004). Its main effect is to act as a water-impermeable barrier, which channels rainfall and snowmelt rapidly into streams and rivers. Unlike considerable parts of the Siberian watersheds, the SD catchment is not affected by permafrost (Tumel, 2002).

2.5. Trends in and atmospheric controls over river discharge in different sector of the Arctic Ocean basin.

In recent years, terrestrial hydrology of the Arctic Ocean basin, and particularly trends in river discharge and climatic controls over these trends, have received much attention. The need for understanding the observed and projected changes in regional water balance has arisen from the pronounced changes occurring recently in the natural environment of the Arctic Ocean basin. This includes rising cold-season air temperatures (Rawlins and Willmott, 2003), changes in snow cover (Groisman *et al*., 1994 a; Fallot *et al*., 1997; Ye *et al*., 1998; Brown, 2000; Ye and Ellison; 2003; Rawlins *et al*., 2006), warming of soils and permafrost

(Osterkamp and Romanovsky, 1999), and from the importance of the potential impacts of hydrological changes on oceanic circulation (e.g. Broecker *et al*., 1999; Clark *et al*., 2002; Rahmstorf, 2000, 2006). This section reviews the main publications investigating trends in discharge of the rivers of the Eurasian sector of the Arctic Ocean basin and the main controls over the detected changes.

The debate on trends in river discharge into the Arctic Ocean and links between climatic oscillations and the discharge trends has been initiated a study by Peterson *et al*. (2002) investigating changes in annual total inflow of the six largest Eurasian rivers into the Arctic Ocean between 1936 and 1999 and reporting a 7% (128 km^3) increase in the freshwater inflow. A strong correlation between the observed rise in air temperature and increasing discharge has also been reported. Controversially, an earlier study of trends in annual river discharge during the 1921-1996 period for the Arctic Ocean basin as a whole (Shiklomanov *et al*., 2000) has not uncovered any continuous change. Instead of linear changes, pronounced interdecadal fluctuations have been detected as shown in Figure 2.14. Note that although Shiklomanov *et al*. (2000) extend their records to1921 (Figure 2.14), they warn that the hydrological network in the early years in the study area was very sparse and suggest that reliability of Database is highest between 1960 and 1990. The authors point out that a peak in discharge has been reached in the 1970s and values of discharge observed at the end of the 20^{th} century are not unprecedented in the context of the whole record. The authors, however, emphasize that a strong warming has occurred in the 44-64^o latitudinal zone, where the highest air temperatures on record (since 1866) were observed leading to a 10-12 % increase in river discharge since the 1980s in most of the European territory of Russia. Differences between the two studies may be due to the fact that 1936, the starting year of the record used by Peterson *et al*. (2002), was marked by exceptionally low precipitation (e.g. Paeth *et al*., 2001) and extremely low annual river flow (Figure 4.4).

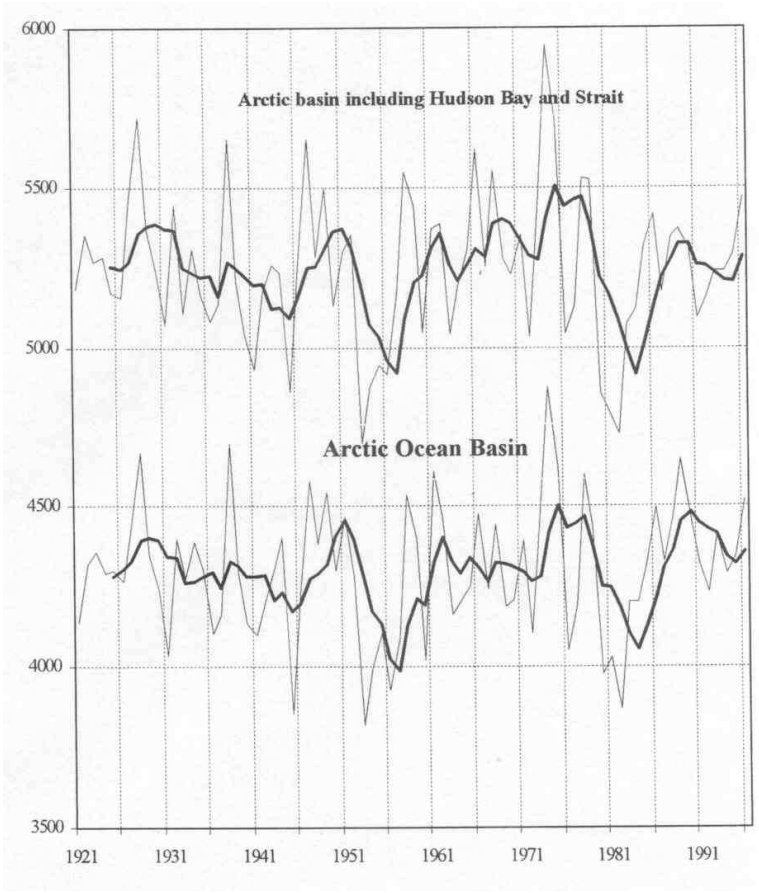

Figure 2.14. Annual river discharge (km^3 a^{-1}) into the Arctic Ocean between 1921 and 1996 (Shiklomanov *et al*., 2000: 287). A line in bold shows the 5-year moving average. The 'Arctic basin' includes the Hudson Bay basin while the 'Arctic Ocean basin' discharge is calculated without inflow into the Hudson Bay.

In addition to these two studies encompassing the Arctic Ocean basin, a number of publications investigating trends in regional river discharge and climatic and atmospheric forcings of these changes have been presented (e.g. Shiklomanov *et al*., 2000; Lammers *et al*., 2001; Semiletov *et al*., 2000; Yang *et al*., 2002; 2004 a, b; Ye *et al*., 2003; Berezovskaya *et al*., 2004; Koster *et al*., 2005; Déry *et al*., 2005; Déry and Wood, 2005). The main difficulty faced by the researchers is a relatively short length of discharge records available from the Arctic Ocean basin. The Eurasian sector compares positively to the North American sector, however, even in the Eurasian sector the continuous discharge records date back mostly to than the mid-1930s (Prowse and Flegg, 2000). The SD discharge record, dating back to 1882, stands out from the discharge database available for the Arctic Ocean basin. Another important historical discharge record is that for the SU (1882-1998 for summer, 1915-1998 for other months).

Semiletov *et al*. (2000) have investigated changes in annual river discharge of ten Siberian rivers (Figure 2.15). The longest discharge records started in 1936, however, observations on some rivers started about a decade later. Several rivers across the territory (the Yenisei, the Anabar, the Olenek, the Yana, and the Kolyma) exhibit positive linear trends in discharge while the discharge of River Amguema (Chukchi Peninsula, Russian Far East) is declining. The authors point out that the observed increase in discharge is related to rising air temperatures. By contrast, a declining river flow in the Chukchi Peninsula is linked to climatic cooling observed in the region during the investigated period. The largest changes are observed in discharge of smaller rivers exhibiting a stronger and faster response to the warming of climate and changing water balance.

Analysis of discharge trends across Siberia has been further elaborated by Serreze *at al*. (2003 a) and Berezovskaya *et al.* (2004), who investigated trends in and associations between annual precipitation and discharge over the largest Siberian watersheds (Yenisei, Lena, and Ob). Serreze *at al*. (2003 a) investigated trends in the components of water balance (precipitation, evaporation, and discharge) across the Siberian watersheds between 1960 and 1999. Berezovskaya *et al.* (2004) compared changes in discharge during two time periods of 1950-98 and 1936-98 linking these to changes in regional climate. In their analysis, Berezovskaya *et al*. (2004) employed three precipitation data sets, compiled by New *et al*. (2000; CRU data set), Kistler *et al*. (2001; NCEP data set) and by Willmott and Matsuura, (2001; University of Delaware, USA, data set). An important conclusion from the study by Berezovskaya *et al.* (2004), highlighting the importance of data quality in the investigation of long-term trends, is a lack of agreement between the precipitation data sets, and resulting inconsistency in the estimated trends. Another important finding is the difference between the results obtained for the two study periods used by the authors (Table 2.4).

In contrast to most other studies (reporting changes in km^3 or $m^3\ s^{-1}$), Berezovskaya *et al.* (2004) report discharge and precipitation trends in mm to aid comparison between precipitation and discharge. According to their estimates, Yenisei's annual discharge has increased by 21 mm between 1950 and 1998 (statistically significant at 0.10), whereas basin precipitation has declined ranging between 10 mm (Willmott and Matsuura, 2001 data set) to 65 mm (Kistler *et al*., 2001 data set) over the time period.

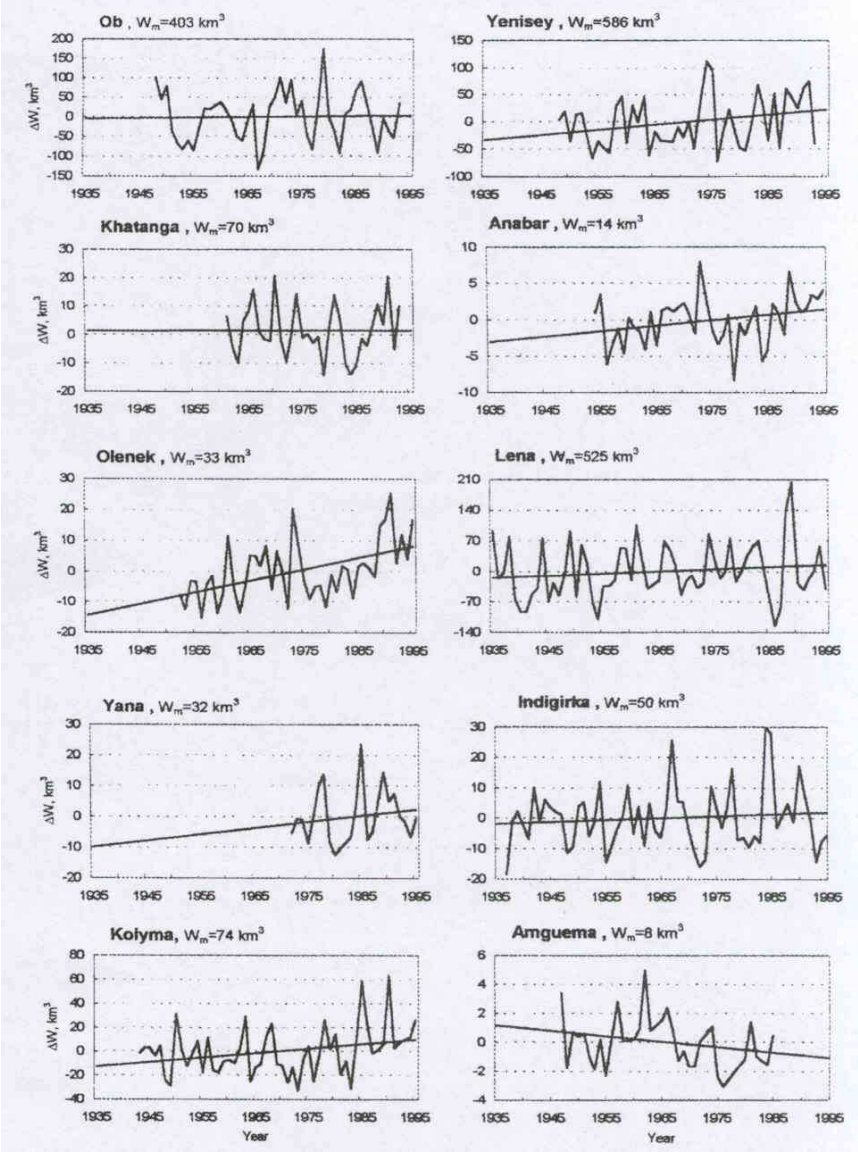

Figure 2.15. Trends in annual river discharge anomalies at ten Siberian rivers (Semiletov *et al*., 2000: 335).

Over the 1936-1998 time period, the Yenisei's annual discharge increased by 9 mm (not significant at 0.10), while precipitation has declined by 16 mm (New *et al*., 2000 data set; significant at 0.10). River Lena's discharge has increased more substantially than that of the Yenisei (20 mm; significant at 0.10), while precipitation shows an upward trend of merely 4 mm (not significant at 0.10) over the 1936-1998 time period (Berezovskaya *et al.*, 2004). These estimations disagree with the results for the 1950-1998 period showing that annual precipitation over the Lena's watershed has declined by 10-84 mm (depending on the precipitation data set) and also with the results by Yang *et al*. (2004 b), who reported a slight

decline in annual precipitation of 5 mm over the Lena for the 1936-1998 time period. Berezovskaya *et al*. (2004) suggested that the identified inconsistencies between trends in precipitation and discharge in the Ob, Yenisei, and Lena Rivers raise the question of uncertainties in the quality of the employed data sets. According to Serreze *et al*. (2003 a), and based on earlier estimates by Korzoun *et al*. (1974), a much larger increase in annual precipitation of 43–49 mm over the 49-year period (1950-98) would be required to support the observed positive changes in discharge and a positive precipitation trend of 30 mm is necessary to explain the observed discharge increase (+ 14 mm) over the 64-year period (1936-99) (Holmes *et al*., 2003).

Table 2.4. Changes in annual precipitation (P; mm per 49-year and 63-year period) and discharge (D; mm per 49-year and 63-year period) across the three Siberian watersheds between 1950-98 versus 1936-98 (after Berezovskaya *et al*., 2004).

Period	**Ob**		**Yenisei**		**Lena**	
	P	*D*	*P*	*D*	*P*	*D*
1950-1998	0	0	-10 to -65	+21	-10 to -84	+15
1936-1998	0	0	-16	+9	+4	+20

Apart from the already highlighted issue of data quality (discussed further in section 3.2) and sampling time periods, results obtained in these studies highlight the potential importance of other factors such as change in evaporation and permafrost melt. These issues have been addressed by Serreze *et al*. (2003 a), whose study confirmed positive trends in winter and spring discharge, significant at 0.05, for the Yenisei and Lena basins for the 1960-1999 time period. Changes in precipitation, nevertheless, have not been found sufficient to be a sole factor explaining the observed increase in discharge and links with thawing permafrost have been suggested. Similarly to Berezovskaya *et al*. (2004), Serreze *et al*. (2003 a) have not detected changes in discharge from the Ob basin. This lack of response from the Ob system has been attributed to a strong contribution of evaporation into the water balance of the area. In comparison to other Eurasian basins, a very large proportion of the Ob basin is covered by wetlands. Thus, evaporation, not being limited by soil moisture, occurs at or near its potential rate accounting for over 70% of precipitation (Serreze *et al*., 2003 b). The observed climatic

warming in the Ob basin, therefore, results in an increase in evaporation, which, in turn, limits the impact on discharge.

A number of detailed investigations of changes in the water balance of the individual Siberian basins have been undertaken. Yang *et al*. (2002) have analyzed trends in monthly discharge of River Lena between 1935–1999 linking these to the observed changes in air temperature, precipitation, river ice and permafrost regimes. This study has identified a significant increase in discharge during the cold season (October-April) with changes ranging between 25 to 90% in different months. The observed pronounced warming during the spring season, leading to an earlier snowmelt and ice break up (May) resulted in lower maximum discharge in June. Although this analysis has not accounted for flow modification by dams and reservoirs, which can distort the signal of natural change contained in these data (McClelland *et al*., 2004). These findings are in line with seasonal discharge trends uncovered by Serreze *et al*. (2003 a). Little change has been found in summer discharge with a small increase in July-August and a decrease in September. The authors have concluded that changes in discharge volume and shifts in hydrological regime are strongly linked to the observed changes in regional air temperature and precipitation.

Ye *et al*. (2003) have produced a more detailed study of hydrological changes in the Lena basin distinguishing between the sub-basins, which have and have not been affected by dam and reservoir construction. Results for the sub-basins that have not affected by human activities to a significant extent have confirmed an increase in winter and spring discharge and earlier summer melt. However, a greater increase in summer discharge than suggested by the previous study has been found. This has been related to a stronger thawing of permafrost, which dominates the Lena watershed and an increase in the active layer. Different results (a strong reduction in summer flow and increase in winter flow of nearly 90% between 1936 and 1999) have been uncovered in the regions affected by the dam construction. An adjustment for the anthropogenic impact (the authors term it ‘naturalisation’ of time series) has resulted in much smaller trends and different seasonal distribution of changes. Flow regulation has resulted in a strong increase in the cold season (November-April) flow and strong decline during the warm season. The adjusted time series show a weak increase in discharge between January and March and between August and October and a decline in discharge between April and July.

Yang *et al*. (2004 a) have investigated trends in monthly and annual discharge of the rivers of the Ob basin in the 1936-1990 period aiming at determining spatial variations between the sub-basins. An increase was detected during the cold season discharge across the basin. Similarly to Serreze *et al*. (2003 a), the authors have noted a decline in summer discharge in the upper Ob regions and an increase in discharge in the lower reaches of the river. The study highlights that different sub-basins may experience different and sometimes opposite hydrological trends. In contrast to the conclusions by Serreze *et al*. (2003 a), the observed changes have been attributed to the impacts of reservoirs on the hydrological regime of the region rather than changes in regional climate and other components of water balance, as proposed by Serreze *et al*. (2003 a).

Hydrological changes observed between 1935 and 1999 in the Yenisei basin have been investigated by Yang *et al*. (2004 b). Pronounced changes in monthly discharge have been detected. Due to the construction of four large dams and reservoirs on the Yenisei, the seasonal discharge patterns have changed in the watershed: Summer discharge has increased, while winter discharge has decreased over time in different parts of the basin. To remove artificially inserted linear trends, Yang *et al*. (2004 b) have adopted a similar approach as Ye *et al*. (2003) by generating naturalised time series. After this process, the naturalised time series show only weak changes. In particular, the changes during November and December are close to zero. Therefore, the authors relate the changes found in the observed data to reservoir regulation rather than climate change, suggesting that the measured discharge records from the basin outlet do not completely reflect natural changes and variations.

These papers, discussing changes in discharge of the Siberian rivers, highlight yet another problem of detecting climatic signals in changing hydrological regimes: Regional human activities are often more important in altering regional hydrological regimes than the influence of changing climate. Lammers *et al*. (2001) recommended that out of 813 Arctic Ocean basin discharge gauging sites, data from 30 sites should not be used due to strong human modification of river flow. In particular, this applies to the Siberian rivers, which accommodate a number of large dams. McClelland *et al*. (2004) have attempted to quantify the effects of mechanical modifications on river discharge in the Ob, Yenisei, Lena, and Kolyma basins. They show that dam construction has pronouncedly changed the seasonality of Siberian river discharge between 1936 and 1998. The strongest modification occurred in the Yenisei basin, while the effects on Ob and Lena Rivers were less pronounced. In all

regions, however, human modifications did not fully explain discharge trends and only the combination of natural and anthropogenic factors provided a full explanation.

Atmospheric circulation is recognised as an important driver of climatic (e.g. Alekseev *et al*., 1991; Przybylak, 2002) and hydrological changes (e.g. Fukutomi *et al*., 2003; Semiletov *et al*., 2000; Walsh, 2000; Proshutinsky *et al*., 1999) in Northern Eurasia. All the studies discussed in this section highlight the strong relationships between regional warming, changes in precipitation, and snow cover extent and duration in Siberia.

Serreze *et al*. (2003 a), Peterson *et al*. (2002), Fukutomi *et al*. (2003), and Ye *et al*. (2004) adopt a more complex approach connecting regional hydrological and climatic changes with the variability in atmospheric circulation. Their conclusions are conflicting. Peterson *et al*. (2002) concluded that NAO is an important predictor of hydrological behavior in Eurasia without quantifying the importance of this factor. Semiletov *et al*. (2000) analyzed the impacts of regional circulation anomalies, AO, and NAO on discharge of four Siberian rivers (the Ob, Yenisei, Lena, and Kolyma) concluding that winter and spring AO is an important control of the spring and summer discharge. The positive winter and spring AO mode results in an enhanced spring discharge; by contrast, the positive AO mode in spring leads to a reduction in summer discharge. Serreze *et al*. (2003 a) described the impacts of the AO and various Euro–Atlantic and Pacific teleconnections patterns on discharge variations in Siberia as weak. Although statistically significant correlations were obtained for some months, little month-to-month persistence has been found. By contrast, Ye *et al*. (2004) described AO as one of the important controls over the discharge of the Siberian rivers in autumn. Fukutomi *et al*. (2003) studied changes in the components of the summer (June-August) hydrological budget across the three main Siberian watersheds between 1979 and 1995 and concluded that both regional and Northern Hemisphere (NH) circulation anomalies, some of which originate over the North Atlantic, exert an impact on both surface climate and hydrological regimes of the Siberian watersheds. However, this study as well as the works by Rogers *et al*. (2001) and Serreze *et al*. (2003 a) showed that indices of the established teleconnection patterns exhibit no significant correlation with the summer water balance across Siberia.

2.6. Research questions to be addressed.

Many studies have now been published concerning changes in river discharge into the Arctic Ocean and connections between climatic variability and discharge. However, as the literature review shows, many of these studies are not consistent with each other. Conflicting findings have been reported on trends in discharge and both climatic and non-climatic factors affecting discharge. Most of the literature focuses on the Siberian sector of the Arctic Ocean basin and studies of the North American sector are available too (e.g. Zhang *et al*., 2001; Déry and Wood, 2004; Déry *et al*., 2005). The focus on the Siberian sector can be explained by the large contribution of the Siberian rivers delivering freshwater discharge into the Arctic Ocean.

Two major problems exist with regard to analysis of Siberian and North American discharge:

(i) A short length of discharge and climatic records dating back to the mid-1930s;

(ii) Regulation of river discharge by dams and reservoirs.

The former issue can potentially compromise the reliability of the detected linear trends, which strongly depend on the selected sampling period. Thus, selecting starting points for linear trends investigation in river discharge in the 1930s, which was one of the warmest and the driest decade on record, may produce spurious results whereby the 'noise of natural climatic variability' (such as the pronounced warming during the 1920/30s) may conceal impacts of a true climatic change signal on river discharge. The latter issue introduces additional uncertainty into analyses of interactions between climatic fluctuations and river discharge.

Changes in river discharge from the European Russian sector of the Arctic Ocean basin have received little attention. The studies by Shiklomanov *et al*. (2000) and Peterson *et al*. (2002) consider European rivers but contain little specific information regarding trends in the individual discharge trends of these rivers. Almost nothing has been published on links between climatic and discharge fluctuations in the region. Meanwhile, two rivers draining the region – the Pechora and SD – rank as 5th and 7th largest contributors of freshwater influx into the Arctic Ocean basin (Table 2.2). Regular and uninterrupted measurements of discharge were established on the SD in 1882 and are ongoing making this discharge time series the longest in the Arctic Ocean basin along with that for SU (1882-1998 for June to September, 1915-98 for the remaining months), as already mentioned. The length of these records allows one to place shorter-term trends as discussed in literature into the longer historical context. In

contrast to Siberia, no dams and reservoirs have been constructed on SD making it easier to detect climatic signals in hydrological time series. There is no permafrost in the area and water released by melting permafrost does not affect water balance in the catchment.

The lack of knowledge about hydrological trends in the European Russian sector of the Arctic Ocean and the importance of its contribution to the total freshwater discharge demonstrates the need for research in this area. Also, lack of knowledge on those factors that influence discharge on both a regional/local and larger scale invites a more detailed investigation. Large-scale forcing includes Euro-Atlantic teleconnection patterns dominating vast land and ocean areas with impacts on the SD catchment, regional factors include temperature, precipitation, and SLP characteristics averaged across the SD basin, and local factors refer to climatic conditions at individual points within the basin (Arkhangelsk, Kotlas, and Koynas mainly).

Interactions between ocean-atmosphere and atmosphere-hydrosphere, finally translating into river discharge, can be thought of as a causal chain. This study considers atmosphere-hydrosphere links (shown on right side). Figure 2.16 shows a scheme linking large-scale atmospheric circulation (teleconnections) to regional circulation (SLP affecting temperature and precipitation patterns), of which finally discharge is the result of these main processes.

The literature review has helped in planning this thesis and in the formulation of the research questions to be addressed. These are as follows:

1. What are the trends in annual, seasonal, and monthly discharge of the SD and SU for the duration of the record?
2. What are the trends in annual, seasonal, and monthly discharge of the SD and SU during the last two decades in which, as stated by many authors, a signal of climate change is emerging from the noise of climatic variability (IPCC, 2001)?
3. To what extent do changes in regional climate affect and control trends in discharge of SD?
4. To what extent do distant atmospheric forcings (major Euro-Atlantic teleconnection patterns) explain trends and variability in discharge of SD?
5. Can a combination of regional climatic characteristics and teleconnection indices be used to explain a significant proportion of variance in SD discharge with the view of developing a simple method of possibly predicting future discharge?

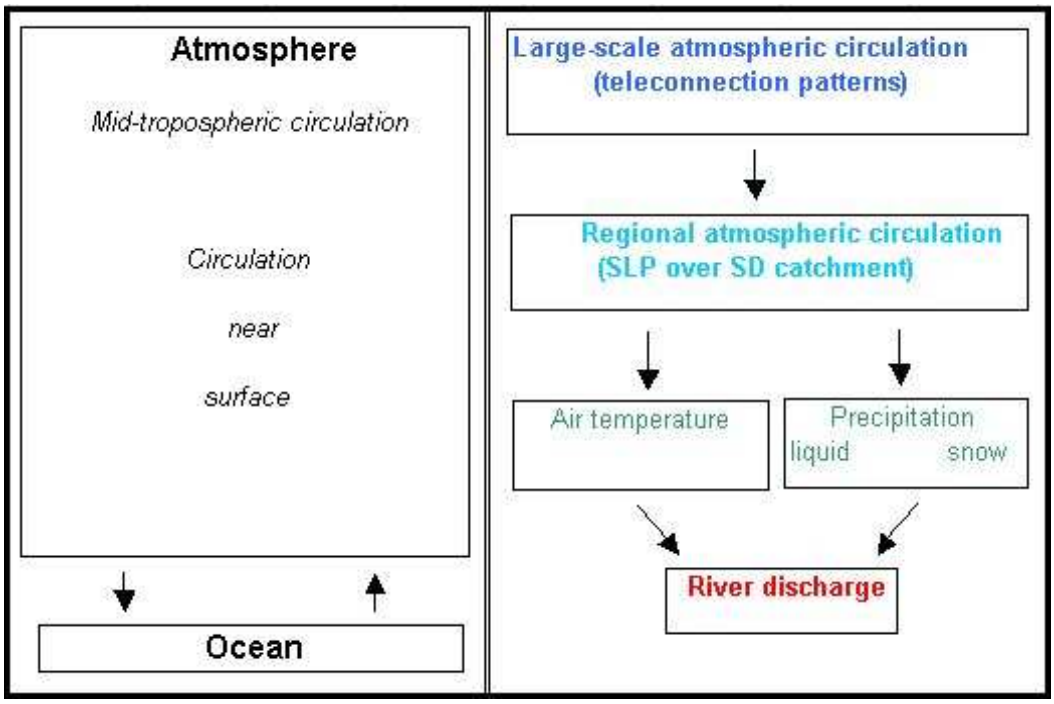

Figure 2.16. Schematic sketch of the interactions between (left side) atmosphere and ocean; (right side) teleconnection patterns, regional circulation over the SD catchment, and SD discharge.

These research questions will be addressed using statistical analysis. The long-term discharge records for SD and SU will be used together with climatic station data and gridded climatic data sets. These are discussed in Chapter 3.

Chapter 3. Data and Methods.

3.1. Introduction.

This chapter discusses the hydrological and climate data sets used in this study as well as statistical techniques. Monthly discharge data for two rivers, the Severnaya Dvina (SD) and the Sukhona (SU), have been used and methods, used to compile the hydrological data set, and data quality are discussed. Meteorological data include

(i) Standard meteorological and snow depth station data;

(ii) Gridded meteorological data sets;

(iii) Two sets of teleconnection indices.

Section 3.2 is devoted to hydrological data sets; section 3.3 focuses on climatic data sets; section 3.4 discusses statistical techniques employed in this study.

3.2. Hydrological data sets.

3.2.1. Sources of hydrological data

Two monthly discharge data sets have been used for the rivers of

(i) SD measured at the outlet Ust Pinega site (64^{o} 13’ N; 41 ^{o} 92’ E) since 1882;

(ii) SU measured at the Kalykino site (60^{o} 67’ N; 45^{o} 87’ E) between 1882 and 1998.

As stated before, the rivers Severnaya Dvina and its southwestern tributary, Sukhona, have mainly been selected with regard to (i) the length of the monthly discharge time series available for both rivers and (b) the under-representation of northern European Russia in the literature so far (Chapter 2). Discharge on SD has also been measured at two other sites (Abramkovo and Zvoz) but both stations are located upstream (thus not integrating basin-wide changes) and have been read only until 1988. Other rivers drain northern European Russia as well, and data from two other gauging stations are available, too: for (i) the SD’s southeastern tributary, Yug (measured at the station of Gavrino between 1936 and 1988), and (b) Pechora (measured at Ust Tsilma from 1932 to 1998). In summary, the main advantage of the two gauges analyzed in this study (Ust Pinega and Kalykino) is their downstream location (Figure 1.1) integrating hydrological changes across the catchment, and their exceptional temporal coverage being far more extensive than those of all other sites available.

This thesis focuses mainly on the SD discharge record and uses the SU time series to corroborate results obtained for SD. This approach – using a tributary in order to corroborate findings for the main channel – has been selected due to the facts that

(i) The SU catchment is characterized by even lower population density and less industry suggesting even less human impact than in the SD watershed (section 3.2),

(ii) Correlation coefficients between monthly discharge of SD and SU are high for most of the year suggesting discharge consistency between both rivers (Table 4.1),

(iii) Both time series possess equal length.

As a whole, the author suggests that the results obtained in this study are regionally representative for a large area of north-western Russia (i.e. the SD basin), although not necessarily for the whole of northern European Russia. An evaluation for the whole northernmost part of north-western Russia bordering the Arctic Ocean coastline (incorporating both the SD and neighbouring Pechora catchments) is, to date, possible only for the overlap period (1932-1998) of the rivers Severnaya Dvina, Sukhona, Yug, and Pechora.

The location of the Ust Pinega site at the outlet of the river (Figure 1.1.) is an advantage as these data reflect integrated hydrological changes over the whole of the SD basin. Measurements at Ust Pinega began in 1882 and are ongoing. The SU gauge at Kalykino operated between 1882 and 1998. At this site, readings were taken continuously during the summer months (June to September) since 1882, whereas continuous measurements in all months (January through December) began only in 1915.

For both rivers, discharge is expressed in $m^3 s^{-1}$. Daily observations have been obtained in the course of regular hydrological measurements conducted by the Hydrometorological Service of Russia (ROSHYDROMET), which have been subsequently transformed into monthly averages by ROSHYDROMET. The monthly data have been obtained from two archives, R-ArcticNet, Version 3.0 (www.r-arcticnet.sr.unh.edu/v3.0/index.html; Lammers *et al*., 2001) and Arctic RIMS (http://rims.unh.edu/data.shtml). Both archives provide monthly data while Arctic RIMS also provides daily data for SD for the post-1978 period.

An obvious advantage of the monthly data sets is a very low percentage of missing values. The SD time series lack merely 0.75 % (11 out of 1,476 entries) of all monthly values for the 1882-2004 period. These are: (i) October-December 1982, (ii) January-July 2000, and (iii)

February 2001. The SU time series lack 3.57 % for the 1915-1998 period. These are: (i) all months in 1936 and 1937; (ii) April 1943; (iii) April, May, and December 1996; (iv) June, July, and October-December 1997; (v) August and November-December 1998. The identified missing monthly values have been replaced with the long-term arithmetic means for the respective months. The daily data are a blend of measured and estimated discharge values. Quality of the daily data, methods of discharge measurements and estimation, and the ratio between measured and estimated values are also discussed in section 3.2.2.

3.2.2. Methods of discharge estimation and associated uncertainties

River discharge is measured directly only in small rivers or streams. In contrast, discharge of larger rivers is approximated taking into account various river characteristics such as water stage (water level) and flow velocity (Shaw, 1999).

River discharge in open channels is estimated as

$$Q = V*A \qquad (3.1)$$

where Q (m^3 s^{-1}) is discharge, V is stream velocity in m s^{-1}, and A is the wetted area in m^2 . The necessary procedure includes both the estimation of velocity and area of an open channel either directly or indirectly (Herschy, 1999).

The method of discharge estimation (at a velocity-area current meter station) and subsequent computation of discharge is in detail given by Herschy (1999). Firstly, the cross-section of the channel is divided into segments, whereby verticals are spaced at intervals across the channel with the aim of accounting for velocity at different points and the bed profile. Herschy (1995) recommends that segments containing no more than 5-10% of the total flow are most suitable to obtain the most reliable measurements. Secondly, discharge is being estimated as the product of velocity, depth, and distance between the verticals. The spacing of the verticals depends largely on the configuration of the riverbed's geometry, flow conditions, and the channel width. In general, as channel depth and width increase, intervals between the verticals become smaller, given that the uncertainty associated with the number of verticals is the largest single source of error in discharge estimation (Herschy, 1999).

Besides this important source of error, other factors introduce uncertainties as well. Dickinson (1967) discusses 16 possible sources of systematic and random errors related to discharge measurements in general. The most significant are:

- Differences between assumed and real velocity distribution in the vertical and horizontal of the channel;
- Accuracy of current meter calibration;
- Pulsation in the flow regime related to distribution of point velocity over time;
- Real and assumed riverbed configuration.

While the above-discussed factors affect the accuracy of river discharge in general, major uncertainties in discharge estimates and measurements arise particularly during winter time under ice-cover conditions when measurements can be complicated by severe weather, dangerous conditions in the field, and ill-adapted sampling methodologies (instruments and methods). Pelletier (1990) discusses these in detail with relation to the Canadian Arctic but with significance for the rivers draining cold regions in general.

The major outcome – following the discharge estimation in the area-velocity current meter station – is the subsequent generation of the river's stage-discharge curve, which is calculated after a sufficient number of velocity readings have been obtained. This curve is constructed by plotting discharge (expressed as $m^3\ s^{-1}$) on the x-axis versus stage (in m) on the y-axis (Herschy, 1999). The established correspondence between stage and discharge is convenient for future discharge determination, because subsequently, only stage needs to be read on the gauge in order to learn the related discharge value. These relationships between stage and discharge are available in graphic form on arithmetic graph paper and in tabular form, the latter of the two containing information on discharge (Q), water stage (h), constants (c and n) as well as the value of stage at zero flow (a), known as datum correction (Herschy, 1999). On the graph, all discharge measurements are plotted and a median line is drawn through the scatter, typically resulting in a curved line (Herschy, 1999). Nevertheless, the stage-discharge curve is not necessarily correct for all times once established (Dickinson, 1967; Herschy, 1999). Herschy (1999) argues that the relation will often change slowly over time or sometimes abruptly, with reasons including aquatic growth near the meter, erosion, deposition of sediments, or following the occurrence of ice and flooding.

Shiklomanov *et al*. (2006) argue that earlier studies so far (e.g. Dickinson, 1967; Herschy, 1985) considered merely uncertainties of discharge estimates computed from open channel conditions. Therefore, Shiklomanov *et al*. (2006) provide a detailed discussion of methods of river discharge measurements and estimation as well as possible error sources specifically for

the cold season of the large Northern Eurasian rivers including SD. To assess stability of Equation (3.1) for SD, Shiklomanov *et al*. (2006) created a rating curve based on daily measurements discharge and water stage conducted between 1955 and 2000 (Figure 3.1). The authors have listed and examined possible sources of error in the monthly discharge data sets including:

(a) Changing measuring techniques and instrumentation;

(b) Changing frequency of measurements;

(c) Errors introduced by ice cover and flooding of the flood plain.

To assess stability of the rating curve, Shiklomanov *et al*. (2006) plotted all available daily discharge measurements against water stage (Figure 3.1), without testing for probable faults. The authors provide no equation for the rating curve. Although potential errors have not been eliminated, the stage-discharge relationship appears stable over time. The observed deviations from the otherwise stable relationship refer to the periods of ice cover and high flow in spring when water spreads across the flood plain.

According to Shiklomanov *et al*. (2006), the instrumentation and measurement techniques, used on SD, have not changed over the past 60-70 years (personal communication with Dr Shiklomanov), which means until the 1930s/40s. No information exists about possible changes in the earlier period. This is not the case regarding frequency of daily observations (used to derive monthly averages), which has changed. This can potentially introduce uncertainty into the estimation of monthly discharge values. Figure 3.2 shows frequency of measurements conducted per year at the Ust Pinega site used to estimate monthly discharge. The frequency of daily measurements peaked in the mid-1950s and around the mid-1980s (exceeding 40 per year) being lower during the 1960s and 1970s. The number of observations declined again during the 1990s (about 15 per year) implying even stronger reliance on rating curves. By contrast, the number of observations during the ice-cover season has remained relatively stable over time. [2] Yet again, no information is available about frequency of daily measurements in the pre-1950s time period.

[2] An analysis of a data set for river ice cover, 1978 – 1988 (Vuglinsky, 2000; http://nsidc.org/data/g01187.html) has shown that SD has stable ice cover between mid-November and mid-April.

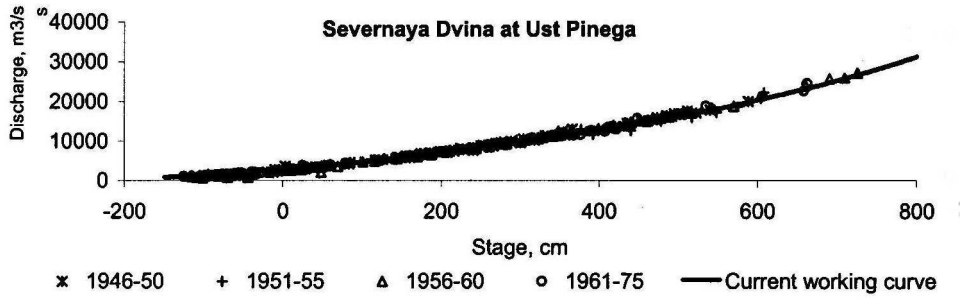

Figure 3.1. Rating curve for SD daily discharge. The rating curve relates daily discharge to water stage (Shiklomanov *et al*., 2006).

According to Shiklomanov *et al*. (2006) the sufficient number of stage and discharge measurements is 15 – 20 for the duration of the ice cover season extending from November through April. This represents readings every 9 – 12 days. More frequent measurements do not improve monthly data quality. However, the number of measurements on SD does not exceed 10. Therefore, it remains below the recommended guideline. More importantly, the rating curves have not been specifically developed for the ice-cover period. This leads to additional uncertainty in winter discharge data (Shiklomanov *et al*., 2006). To minimise possible errors that prevail during the ice-cover season, two types of corrections are applied:

(i) Winter correction coefficient;

(ii) Interpolation between discharge measurements.

These corrections are generally applied across northern countries during the winter season (Pelletier, 1990). While the interpolation technique is self-explanatory (e.g. interpolation between two consecutive measurements), the corrections coefficient is estimated as:

$$C_{ice} = \frac{Q_{ice}}{Q'} \tag{3.2}$$

where Q_{ice} is discharge measured under the conditions of ice cover and Q' is discharge at the same gauge calculated from an open-water stable stage-discharge relationship. Discharge values for the time periods when SD is frozen are calculated by multiplying discharge values derived from the standard rating curves by the winter correction coefficient C_{ice}. Figure 3.3 illustrates the use of these two corrections in 2001. Between November and April, measurements were taken ten times per 180-day period (November-April), thus on average every 18 days. Linear interpolation between consecutive measurements has been applied to

derive daily data for the November-March period, and the correction coefficient technique has been applied to derive daily values for April. Subsequently, open channel measurements have been used.

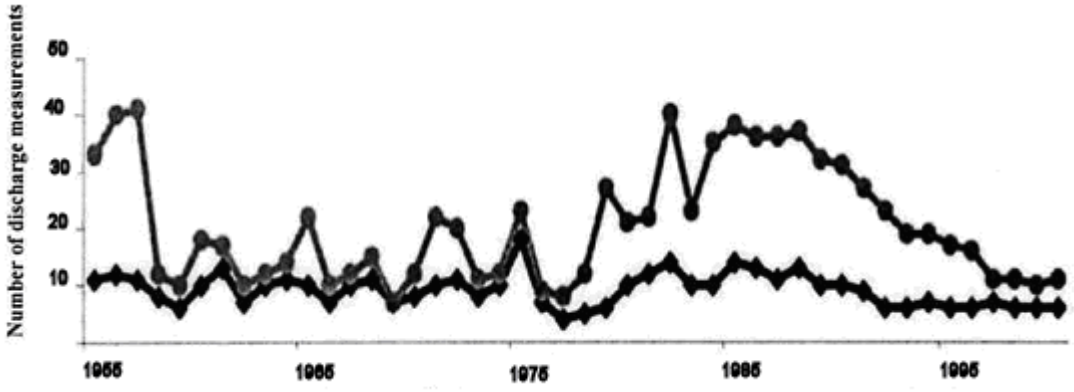

Figure 3.2. Number of discharge measurements per year for the 1955-2000 period. The upper line shows total number of measurements throughout the year. The lower line shows the number of measurements during the ice-cover period (Shiklomanov *et al*., 2006).

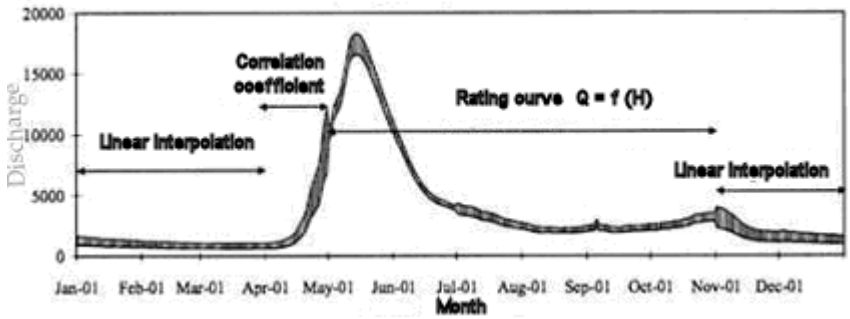

Figure 3.3. Correction techniques used to estimate daily SD discharge between November and April in 2001 (Shiklomanov *et al*., 2006).

Shiklomanov *et al*. (2006) have analyzed the overall errors (probably expressed as % of measured daily, monthly, and annual discharge, as the authors don't refer to it more specifically) in SD daily, monthly, and annual discharge values for the 1955-2000 period, resulting from the above-discussed problems. The authors admit that the division between the annual and long-term relationship is subjectively defined, based upon the long-term mean number of discharge measurements used to confirm the rating curve. The errors are shown in Table 3.1. The largest errors occur during the ice-cover season (November-April) and decline in May with regard to monthly discharge values and June with regard to daily discharge

values. Summer discharge is characterised by the lowest daily and monthly errors. Errors in the daily discharge values range from ~6% (summer) to 17 % (winter), whereas monthly discharge errors range between ~4% and 13 % (Table 3.1). Errors in daily winter discharge compare well with the large Siberian rivers whereby January error ranges between 25 and 28% (Shiklomanov *et al.*, 2006). In contrast, the long-term error in annual SD discharge measurements is reduced to about 4%.

Table 3.1. Long-term mean errors in SD discharge (%) for 1955-2000 (Shiklomanov *et al.*, 2006).

	Jan	**Feb**	**Mar**	**Apr**	**May**	**Jun**	**Jul**	**Aug**	**Sep**	**Oct**	**Nov**	**Dec**
Daily	17.4	17.4	17.4	17.4	15.4	5.8	5.8	5.8	9.4	12.2	17.4	17.4
Monthly	12.8	12.8	12.8	12.8	8.6	4.1	4.1	4.1	6.7	7.5	12.8	12.8
Annual	**4.3**											

Figure 3.4 illustrates the relationships between the estimated errors and daily discharge values. It shows that the largest errors in the estimated daily discharge occur when the river flow is at its lowest (i.e. February-March). The lowest errors are confined to river flow between 6,000 and 16,000 m^3 s^{-1}, which are observed in the few weeks following the ice break-up encompassing circa late April to mid-June (as inferred from daily observations 1978-2005 available from ArcticRIMS).

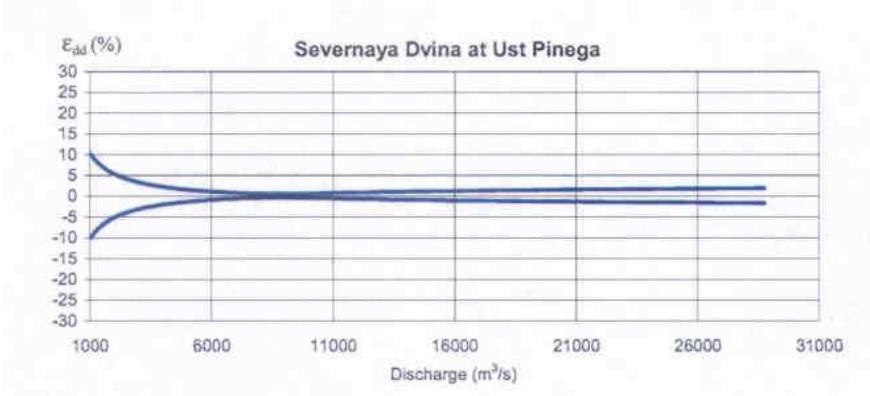

Figure 3.4. Relative error (ε_{dd}; %) in daily discharge estimates computed using the best-fit polynomial for approximation of long-term stable rating curve from the daily discharge values (Shiklomanov *et al.*, 2006).

3.2.3. Non-climatic factors affecting quality of the discharge data sets

A number of non-climatic factors can affect river discharge introducing uncertainty into discharge data sets and obscuring climatic signals contained in data (section 2.2). The influence of anthropogenic factors, especially construction of dams and reservoirs, river alterations and diversions, and changes in water abstraction, produce the strongest impact. In contrast to the large Siberian rivers, there are no dams or reservoirs on SD and SU (McClelland *et al*., 2004) and the projects to divert water from the rivers draining northern European Russia to the Volga, planned to start in the 1980s, have not been carried out (Koronkevich, 2002). Therefore, these important factors do not introduce uncertainties into the discharge data sets used in this study making them particularly suitable for detecting climatic signals.

Data on water abstraction from SD and its tributaries are sparse. The region accommodates several medium-size urban areas, for example within Kholmogorskii, Vinogradovskii, Kotlasskii, and Velsky Raion (Table 3.2). The administrative region through which SD mainly flows, Arkhangelskaya Oblast (Arkhangelsk region of Russia), comprises a vast territory of 587,400 km^2 with a total population of 1,318,000 (Administraciya Arkhangelskoi Oblasti; www.dvinaland.ru/region/info.asp?part=2), indicating a low population density of 2.24 people km^{-2} on average. Data on population density for selected administrative districts within Arkhangelskaya Oblast are sparse, however, statistics for those districts within Arkhangelskaya Oblast, for which data is available, are displayed in Table 3.1. The region's capital is Arkhangelsk, an industrial city with a population of 356,000. There is no large-scale arable agriculture, given that only a negligible part of Arkhangelskaya Oblast (1.3%) comprises of arable lands (*ibid*.). Regional precipitation is high and evaporation is low (section 2.3.2), therefore, the need to abstract river water for irrigation is very low. Water is mainly abstracted for municipal and industrial use in the Kholmogory region, a small district in the lower reaches of SD just south of Arkhangelsk (*ibid*.). Annual total water abstraction and returned water rates have been kindly provided by Mr V. Shevchenko (Meteorological Division of the Russian Hydrometeorological Service for the North (Sevmeteo UGMS), Arkhangelsk, Russia; pers. com.). In 2000-2002, about 0.90 km^3 have been abstracted annually, of which 0.85 km^3 (94%) have been returned into the river (in the form of waste, mine and drainage waters). Thus, only a minimal fraction of 0.05 km^3 (6%) is lost, representing 0.05% of annual total SD discharge. In contrast to SD, no large cities or industrial centres are situated near SU, thus water abstraction is even lower.

Table 3.2. Population statistics of selected administrative districts within Arkhangelskaya Oblast from north to south (Administraciya Arkhangelskoi Oblasti; www.dvinaland.ru/region/info.asp?part=2)

Raion (District)	Area (km^2)	Population	Population density
Kholmogorskii	16,800	29,290	1.8
Vinogradovskii	12,560	20,440	1.65
Kotlasskii	6,300	27,000	3.81
Velsky	10,060	61,800	6.1

3.3. Climatic data sets.

Climatic data sets (abbreviated names are given in full in section 3.3.1) are ordered from large-scale to regional to local scales including:

- Gridded NCEP/NCAR 500-hPa and 850-hPa monthly geopotential height data (Kalnay *et al*., 1996; Kistler *et al*., 2001) averaged over the SD catchment (1948-2004).
- Monthly teleconnection indices (1950-2004) from CPC
- Monthly teleconnection indices (1660-1995) reconstructed by Luterbacher *et al.* (1999)
- Gridded SLP monthly data set (Trenberth and Paolino, 1981) averaged over the SD catchment (1899-2004).
- Gridded monthly and seasonal temperature data from New *et al*. (2000) from which time series have been averaged over the SD catchment (1901-2000)
- Gridded monthly and seasonal precipitation data from New *et al*. (2000) from which time series have been averaged over the SD catchment (1901-2000)
- Monthly and seasonal temperature time series for the stations of Arkhangelsk (1881-2003) (DSS UCAR) and Kotlas (1936-94) (ROSHYDROMET)
- Monthly and seasonal precipitation time series for the stations of Arkhangelsk (1881-2003) (DSS UCAR) and Kotlas (1936-94) (ROSHYDROMET)
- Snow depth station data for Arkhangelsk (1900-2001), Kotlas (1936-2001), and Koynas (1924-2001) (Breiling *et al*., 2006)

- Dates of the onset and end of snow cover at Arkhangelsk (1900-94) and Kotlas (1936-94) (HSDSD; Armstrong, 2001).

In the following, firstly the station data sets are discussed, which is followed by the gridded data sets and teleconnection indices. The fact that the data sets have different lengths (Table 3.3. and 3.4) is typical of the high latitudes of Northern Eurasia and unavoidable, where only few observations span a full century or longer. During the 1880s, the station network across the Russian Empire expanded rapidly from 121 stations towards more than 500 stations a decade later, but only by the middle of the 20th century had the network grown to about 9,000 station overall (Groisman *et al*., 1991). This emphasizes again that only few stations, such as Arkhangelsk, measure air temperature and precipitation (snow depth) since the 1880s (1900), which makes such station data extremely valuable regarding long-term climatic oscillations. Many more data sets start only in the 1930s, a period of political and administrative reorganisations in Russia.

3.3.1. Station data

The long-term time series (from 1881 onwards) of temperature and precipitation data for Arkhangelsk have been obtained from the Research Data Archive held at Data Support Section (DSS) by the University Cooperation for Atmospheric Research (UCAR) (DSS UCAR: http://dss.ucar.edu/data sets/ds570.0/data/). A shorter time series (1936-1994) for Kotlas has been obtained from the Russian Hydrometeorological Service (ROSHYDROMET, sometimes RIHMI-WDC) website (http://meteo.ru/data_temperat_precipitation). Details of Data sets and station coordinates are given in Table 3.3.

Arkhangelsk is located ca. 100 km north-west of the river gauging site of Ust Pinega (Figure 1.1) and is representative of the climate of the northern part (lower course) of SD. Additional information on the location, its surroundings and changes in location of the meteorological station has been kindly provided upon request by Mr V. Shevchenko (Sevmeteo UGMS, Arkhangelsk, Russia; pers. com.). The station of Arkhangelsk is located within administrative city boundaries, but on the city outskirts. Located in woodland, it is described as a station affected little, if at all, by urbanisation processes. The station has moved its location twice throughout the 20th century: for the first time, in May 1958 by 500 m to the north-west of its original location, and for the second time in November 1967 by 1.7 km to the east, where it has remained since. No recent ongoing construction works are reported in the surroundings.

Kotlas is located ca. 50 km north-east to the gauging site of Kalykino at SU at the confluence of the Yug and the Sukhona. This site is representative of the climatic conditions of the southern part of the SD catchment. The station is located at the airport and has changed its position in 1969 by 4 km. Nevertheless, regional meteorologists ascertain that the station's relocation has not affected homogeneity (NCDC, 2003). Having analyzed impacts of stations relocation on data homogeneity, Groisman *et al*. (1991) ascertain that slight relocations affect homogeneity in station measurements only to a small extent. Observations at Arkhangelsk and Kotlas continued without significant interruptions. Station coordinates and details of Data are given in Table 3.3.

Almost no long-term precipitation measurements are homogeneous over time (Groisman *et al*., 1991). Changes in gauge type and wind-induced errors such as undercatch of winter precipitation or capture of drifting snow (Groisman *et al*., 1991) are known to be significant in introducing errors in the detection of the true trends in precipitation data (Forland and Hanssen-Bauer, 2000). However, the possible errors over the Former Soviet Union (FSU) are to a large degree correctable (Groisman and Rankova, 2001), as documented in detail for historical station time series of precipitation between 1891 and 1990 (Groisman *et al*., 1991). Biases affect especially the cold season's (solid) precipitation and less the summer seasons (liquid) precipitation, as measurements of solid precipitation are particularly sensitive to instrumental design. Possible sources of inhomogeneity across the FSU involve

(i) Mainly changing measurement techniques, which introduces the most significant uncertainties,

(ii) To a lesser degree, changing frequency of readings and

(iii) Changing locations of stations and gauges.

Groisman *et al*. (1991) have adjusted the original data ('PMEASURED') to create corrected values ('PTRUE') for the FSU area they investigated (500 stations located between 37-70^{o} N, 25-140^{o} E). Two major changes in precipitation measurements took place:

1. Between 1948 and 1953, the *Tretyakov* gauges have replaced the previously used Nipher gauges. This improvement has specifically aided the accuracy of snowfall measurements. During winter, the new gauges have captured from 5 - 40% more solid rainfall than previously. In contrast, liquid precipitation measurements have not been affected by this technical change (Groisman *et al*., 1991). The gradual replacement of Nipher by Tretyakov gauges over these years and a better performance of the new gauges in comparison with the ones previously employed was closely monitored.

Thus, in order to compare agreement between the two gauge types, simultaneous readings have been taken side by side. These simultaneous measurements led to establishment of a correction formula (Hydrometeorological Service of the USSR, 1964) that has been applied to the measurements.

2. Around 1966/67, another significant change occurred due to the introduction of a second correction factor (the 'wetting factor') aimed at improving precipitation measurements further (Groisman *et al*., 1991). At the same time, the frequency of daily readings was changed from two to four. Due to these changes, measured solid precipitation recordings increased by 5 – 40%, whereas liquid precipitation recordings have risen less pronouncedly by 5 – 15% (Groisman *et al*., 1991).

Groisman *et al*. (1991) discuss possible inhomogeneities and their sources for the overall FSU area rather than for individual stations. Visual inspection of monthly time series of both stations for unusual and 'sudden' changes – with particular focus on the two identified periods when instrumental changes took place – has revealed that there is no indication of dramatic precipitation changes around or after 1948-1953 and in 1966/67. Two precipitation events at Arkhangelsk (March 1953 and December 1957) had remarkably high monthly rainfall totals (four to five standard deviations above their long-term mean), being in accord with monthly SLP data (Trenberth and Paolino, 1981; not shown) averaged across the SD catchment area confirming that SLP was very low during those months (more than one standard deviation below the long-term mean) providing a sound explanation for these extreme precipitation events.

Two data sets characterising snow cover over the study area have been used. Firstly, daily values of snow depth collected at three sites located within the SD catchment – Arkhangelsk, Koynas, and Kotlas – have been used (Breiling *et al*., 2006). Snow depth (cm) was measured daily using the traditional stake method at one location at each station (Breiling *et al*., 2006). The overall majority of the months had less than ten missing daily entries per month and the missing daily data have been replaced by an average value for the month in which the missing day occurred. The years of 1920-24 at Arkhangelsk are the only sequence of years, during which no measurements have been taken. For the purpose of statistical analysis in this thesis, missing monthly values have been replaced by the long-term arithmetic means. Information on missing monthly values is given in Table 3.3. Monthly snow depth data have been further amalgamated into seasonal averages (snow cover season lasts from October to May in the

catchment; Figure 2.12). As a whole, the centennial time series for the station Arkhangelsk is a noteworthy rarity of regular snow depth measurements in the Arctic Ocean basin.

Table 3.3. Information on the station data sets used in this study.

Station	Variable	Period	Averaging period	Missing data (%)
Arkhangelsk [a] 64° 60' N / 40° 50' E	Temperature	1881-2003	Monthly	1.19
Kotlas [b] 61° 20' N / 46° 60' E	Temperature	1936-1993	Monthly	0
Arkhangelsk [a] 64° 60' N / 40° 50' E	Precipitation	1881-2003	Monthly	1.34
Kotlas [b] 61° 20' N / 46° 60' E	Precipitation	1936-1993	Monthly	0
Arkhangelsk [c] 64° 60' N / 40° 50' E	Snow depth (cm)	1900-2001	Snow season	9.82
Kotlas [c] 61° 20' N / 46° 60' E	Snow depth (cm)	1936-2001	Snow season	4.92
Koynas [c] 64° 80' N / 47° 70' E	Snow depth (cm)	1924-2001	Snow season	4.54
Arkhangelsk [d] 64° 60' N / 40° 50' E	Onset / complete melt of snow cover	1900-1994	Julian Day	8.51
Kotlas [d] 61° 20' N / 46° 60' E	Onset / complete melt of snow cover	1936-1994	Julian Day	0

([a]) Station t, p data for Arkhangelsk (1881-2001): DSS UCAR (http://dss.ucar.edu/data sets/ds570.0/data/)
([b]) Station t, p data for Kotlas (1936-94): Russian Hydrometeorological Service RIHMI-WDC office (http://meteo.ru/data_temperat_precipitation)
([c]) Snow data set 1 (actual station snow depth in cm): Breiling *et al*. (2006)
([d]) Snow data set 2 (onset and melt of snow cover in JD): 'Historical Soviet Daily Snow Depth' (HSDSD) digital media (CD-ROM, version 2.0) (http://arcss.colorado.edu/data/g01092.html) (Armstrong, 2001)

The second snow cover data set, compiled by Armstrong (2001), has been derived from one-point station observations described above available from the National Snow and Ice Data Center (NSIDC), University of Boulder, Colorado (USA) as the 'Historical Soviet Daily Snow Depth' (HSDSD) CD-ROM, version 2.0 (http://arcss.colorado.edu/data/g01092.html) containing information on the duration of snow cover (the first and last days of snow cover in Julian days) at Arkhangelsk and Kotlas (Table 3.3).

3.3.2. Gridded data sets

In addition to the station data sets, five gridded data sets have been used. Monthly gridded precipitation and temperature (New *et al*., 2000) data sets for 1901 to 2000 have been employed (Table 3.3) to study the relationships between regional temperature and precipitation over the SD catchment and SD discharge. Data sets have two major advantages: firstly, they have fine (0.5^{o}) resolution and secondly, by covering the whole of the 20^{th} century, most of the extent of the SD discharge record is encompassed. However, these data sets are not entirely error free as they contain biases and inhomogeneities. New *et al*. (2000) have investigated the possible sources of error in the precipitation data set and summarised as follows: "*Major sources of error in gridded data sets of this nature are instrumental (isolated errors, systematic errors, and inhomogeneity), inadequate station coverage, and interpolation errors (Groisman et al., 1991; Dai et al., 1997; Jones et al., 1999). Isolated errors and subtle inhomogeneities not detected during quality control do not have a significant effect at the regional scale. However, such errors are noticeable at grid points near the offending station, particularly if the network is sparse. Inadequate station coverage is the largest source of error, but there is little that can be done about this except to ensure that the existing data are error free and that interpolation method makes maximum use of this available data*".

The centennial precipitation data set assembled by New *et al*. (2000) has a major advantage over another important long-term precipitation database collated by Dai *et al*. (1997), which covers the period from 1900 to 1988. However, New *et al*. (2000) data set does not contain adjustments for possible biases in rainfall records, whereas Dai *et al*. (1997) have applied such corrections to their data. Possible biases in the New *et al*. (2000) data set occurred between the 1940s and early 1950s due to the change in rain gauge type (section 3.3.1) affecting the snow season particularly, and the authors accept that these changes have influenced their data set slightly. Berezovskaya *et al*. (2004) compared the agreements

between three different precipitation data sets: (i) New *et al*. (2000); (ii) Willmott and Matsuura (2001); and (iii) Kistler *et al*. (2001; NCEP data set). The authors have found that the New *et al*. (2000) data set, although not corrected for possible biases due to untercatch of solid precipitation during the cold season, agrees well with the one by the Willmott and Matsuura (2001), with correlation coefficients between records derived from the two data sets ranging between 0.85 to 0.96. Little agreement has been found between Willmott and Matsuura (2001) and New *et al*. (2000) data sets with the data set developed by Kistler *et al*. (2001). Given these considerations, New *et al*. (2000) precipitation and temperature data sets have been used in this study, while certain limitations of these data sets should be kept in mind.

An important issue, potentially affecting data quality in the New et al. (2000) precipitation and temperature data sets, is changing station coverage especially in the earlier years of the records. The number of stations used for constructing Data set has varied considerably over time, and in Russia, the number peaked in the 1970s-1980s, after which it declined continuously. Rawlins *et al*. (2006) have investigated this issue further identifying two problems:

(i) Sparse station coverage in earlier years before the 1950s;

(ii) Concentrations of stations in the south of the Arctic Ocean basin in the earlier years and their expansion further north afterwards.

Given the large north-south extent of the Arctic Ocean basin, including the SD catchment, these problems (and particularly the shift in the location of the stations northward) could have introduced two uncertainties into Data sets. Firstly, the long-term trends in both temperature and precipitation are different in the southern and northern parts of the Arctic Ocean basin. The strongest warming has occurred in the latitudinal band of 44-64^{o} N rather than to the north of 64^{o} N (Shiklomanov *et al*., 2000). Secondly, the shift in the spatial distributions of stations might have led to an underestimation of snowfall and overestimation of rainfall in the Arctic Ocean basin in the earlier years. According to Rawlins *et al*. (2006) this problem has primarily affected Siberia because those catchments have a larger north-south extent than the SD catchment, however, a potential impact on data accuracy within the SD catchment should be considered. Therefore, in this study the spatially-averaged time series have been used in correlation analyses but have been treated with caution with regard to the long-term linear trends with a preference given to the individual station data. This applies in particular to the gridded precipitation data set. Regarding their gridded air temperature data set, New *et al*.

(2000) note that it is less prone to errors and biases than the precipitation data set. This is because station density, which is required to adequately describe monthly spatial variability, should generally be higher for precipitation than for mean air temperature data as precipitation varies stronger in time and space than mean air temperature. Thus, in order to achieve statistically significant correlation between between-station distances and differences in observed annual precipitation totals, between-station separations of 400 km and 300 km are required for the 30–60^{o}N and 60–90^{o}N latitudinal zones respectively (Dai *et al*., 1997). In contrast, between-station separations of 1200 km and 2000 km are required in application to temperature measurements (Hansen and Lebedeff, 1987; Jones *et al*., 1997).

Monthly 500-hPa geopotential height data (to identify the large-scale atmospheric controls in the exceptionally high and exceptionally low discharge years), and 850-hPa P-E geopotential height data (in order to study P-E variability) for the 1948-2000 period has been derived from the NCEP/NCAR Reanalysis Project (Kalnay *et al*., 1996; Kistler *et al*., 2001) (Table 3.4). Data set has been compiled using aircraft, land surface, ship, rawinsonde, and satellite data. All data have been quality controlled and assimilated with a data assimilation system being unchanged over the reanalysis period. This process has removed recognized climate discontinuities related to changes in the operational (real-time) data assimilation system. This still does not prevent uncertainties exerted by changing observation practices, which have changed in two important ways:

(i) From 1948 to 1957, while the upper air network was established, observations were fewer and the rawinsonde releases were performed three hours later than the current main synoptic times (e.g. 0300 UTC);

(ii) In 1979, satellite sounding became globally available, the observations of which have subsequently been incorporated (Kistler *et al*., 2001).

Although temporal discontinuities in the reanalysis data inevitably occur in Data set due to the differences in amount and quality of the assimilated data, the SD catchment is not strongly affected since a relatively dense rawinsonde network covers Arctic and sub-Arctic land areas in the European sector (Serreze *et al*., 1995). Also, other factors (e.g. absence of rawinsonde network over oceans; sparse observational network over the Southern Hemisphere and some remote regions of Siberia) do not apply to the study area. Kistler *et al*. (2001) argue that the introduction of satellite observations into the NCEP/NCAR data has improved the reliability of the upper atmosphere meteorological data. For that reason, the post-1979 upper air data are assumed to be more reliable than the same data in earlier periods. The 500 hPa

geopotential height has been classified by the authors of the reanalyses data sets as one of the most reliable variables of the project. In addition, monthly values (which are used in this study) have been identified as more reliable than daily reanalysis data, which are more sensitive to the above-mentioned issues (Kistler *et al*., 2001). Note that although NCEP/NCAR reanalysis data span only the post-1948 period, the main advantage is the excellent temporal coverage with no missing monthly values.

Sea level pressure (SLP) data by Trenberth and Paolino (1981) for 1899 to 2004 (Table 3.4) has been used to study the long-term trends and variability near the surface across the SD basin. The Trenberth and Paolino data set contains the longest continuous time series of monthly gridded NH data (polewards of 15^{o} N), and is one of the most widely employed databases in atmospheric applications. Trenberth and Paolino (1981) performed detailed analysis for the period 1899 to 1977 and detected several inhomogeneities. On a temporal scale, the period of 1916 to 1921 contained the largest number of errors. Spatially, data problems occurred north of 70^{o} N in the circumpolar Arctic and further south in Siberia. Both regions are well outside the study area (58-65^{o} N).

Table 3.4. Information on gridded data sets used in this study

Variable	Period	Resolution (lat * lon)	Missing data (%)
500 hPa geopotential height [a]	1948-2000	2.5 * 2.5 ^{o}	0
Effective precipitation (P-E) [b]	1948-2000	2.5 * 2.5 ^{o}	0
Precipitation [c]	1901-2000	0.5 * 0.5 ^{o}	0
Temperature [d]	1901-2000	0.5 * 0.5 ^{o}	0
Sea level pressure (SLP) [e]	1899-2000	5 ^{o} * 5 ^{o}	0

([a, b]) NCEP/NCAR reanalyses: www.cdc.noaa.gov/cdc/reanalysis/reanalysis.shtml (Kalnay *et al*., 1996; Kistler *et al*., 2001);
([c, d]) 0.5 degree monthly climate grids from 1901-95 and 1901-2000: www.geog.ox.ac.uk/~mnew/research/data_download/index.html (New *et al*., 2000).
([e]) Monthly Northern Hemisphere Sea Level Pressure Grids: http://dss.ucar.edu/data sets/ds010.1/ (Trenberth and Paolino, 1981).

3.3.3. Teleconnection indices

Two sets of monthly indices of the major NH teleconnection patterns have been used in this thesis. The positive phases of each pattern during January are given in Figure 2.1.

The first set, covering the 1660-1995 period for the major Euro–Atlantic teleconnection patterns (Luterbacher *et al.*, 1999) and the 1500-2001 period for NAO (Luterbacher *et al.*, 2001; www.cru.uea.ac.uk/cru/data/naojurg.htm), has been constructed by the application of Empirical Orthogonal Functions (EOF) analysis to a selection of surface meteorological variables and proxy data. In the pre-instrumental period (prior to 1780) these data include few instrumental precipitation and temperature records, data on the duration of sea and river ice cover, data on duration of snow cover, and air temperature reconstructed from tree rings and phenological data. Data used for the post-1780 period include three meteorological variables (instrumental atmospheric station pressure data, precipitation, and air temperature measurements) to which EOF was applied. Gridded SLP data have been reconstructed from these predictors subsequently. The NAO index has been calculated as the average of four SLP grid points over the Azores minus the average of four grid points over Iceland. The index was then defined as the difference between the two standardised SLP time series (Luterbacher *et al.*, 1999). Subsequently, EOF was applied explaining 90% of the predictor data's variance of the regressed against the NAO index time series. The calibrated period entailed 1901-60. The reconstructed NAO winter index for 1500-01 to 2000-2001 is shown in Figure 2.4.

The second data set of monthly teleconnection indices, covering the period since 1950, has been calculated by and obtained from CPC (www.cpc.ncep.noaa.gov/data/teledoc/telecontents.shtml). The indices have been calculated by taking standardised monthly amplitudes of rotated principal components of monthly mean 700 hPa geopotential height anomalies. The wintertime time series of these indices are shown in Figure 2.2.

By correlating the monthly reconstructed with the monthly CPC time series, the consistency between the two types of teleconnection indices has been estimated for the overlap period (1950-1995). The computed correlation coefficients are shown in Table 3.5. For the majority of teleconnection patterns, there is a close agreement during the autumn, winter, and spring season with correlation coefficients equal to or exceeding 0.68. During autumn, the agreement is also lower for EA pattern in October and November. Agreement for the summer season is lower. In particular, the agreement between the two NAO indices is low in June-July and moderate in May and August-October. Note that the NAO pattern is weaker in the period from May to September period than during October-April (e.g. Hurrell, 1995; Wanner *et al.*, 2001), which may explain the disagreement.

Table 3.5. Correlation coefficients between calculated (CPC) and reconstructed (Luterbacher *et al*., 1999) monthly teleconnection indices (for the overlap period of 1950-95). The teleconnection patterns are ordered alphabetically.

T/c pattern	**Jan**	**Feb**	**Mar**	**Apr**	**May**	**Jun**	**Jul**	**Aug**	**Sep**	**Oct**	**Nov**	**Dec**
EA	0.69	0.79	0.72	0.70	-	-	-	-	0.73	0.59	0.37	0.77
EAJET	-	-	-	0.65	0.73	0.83	0.76	0.79	-	-	-	-
EA/WR	0.92	0.72	0.87	0.81	-	-	-	-	0.76	0.88	0.77	0.89
NAO	0.83	0.82	0.85	0.61	0.55	0.12	0.13	0.48	0.47	0.47	0.79	0.93
POL	0.68	0.82	-	-	-	-	-	-	-	-	-	0.63
SCA	0.82	0.87	0.78	0.68	0.68	-	-	-	0.70	0.87	0.91	0.86

3.4. Methodology.

The principal objectives of this thesis are to investigate the long-term trends and shorter-term oscillations in the discharge of SD and SU and to link the identified trends and oscillations to climatic factors. To achieve these objectives, the following steps have been taken and methods of statistical analysis have been used:

(i) The long-term trends and decadal variability in SD and SU discharge have been studied. This has been performed by application of linear trend analysis, Henderson filter, and step change analysis to the monthly, seasonal and annual time series of SD and SU discharge.

(ii) In order to understand regional climatic controls over SD discharge, monthly and seasonal time series have been correlated with meteorological records from the stations of Arkhangelsk, Kotlas, and Koynas, and the time series of temperature, precipitation, and 500 hPa pressure spatially averaged over the SD catchment (defined for the purpose of statistical analysis as 58-65^{o} N, 40-50^{o} E). To isolate interannual variation, linear trends have been removed from the time series prior to correlation analysis and the time series have been standardised by subtracting the mean of the time series and dividing by the standard deviation. This is a standard and frequently used method (Box and Jenkins, 1976) using the following equation

$$X'(t) = X(t) - (a + b * t) + \overline{X} \qquad (3.3)$$

where $X'(t)$ is the detrended data point at time t, $X(t)$ is the original data point, $\overline{X}$ is the mean of the series, a is the regression intercept, and b is the regression slope.

(iii) In order to understand remote atmospheric forcings of variations in SD and SU discharge, the discharge time series have been correlated with teleconnection indices using the same techniques as in (ii). In addition, composite anomaly analysis (Wilks, 1995) of 500 hPa geopotential height fields (derived from the NCEP/NCAR reanalysis project, as discussed above) has been used to identify the large-scale atmospheric controls in the exceptionally high and exceptionally low discharge years. Anomaly maps of the 500-hPa geopotential height fields have been constructed showing the difference between the mid-tropospheric circulation observed in the high and low discharge years (assessed seasonally). The high- and low-flow years have been defined as ± one standard deviation from the 1948-2004 mean seasonal value. Statistical significance of the identified anomalies has been assessed by comparing the value of anomalies with standard deviations of the field in the studied region.

(iv) In order to assess the combined effect of the regional and remote climatic forcings on the interannual variations in SD discharge and to identify the most important groups of factors controlling SD discharge, a combination of Rotated Principal Component Analysis (RPCA) and regression analysis has been applied (section 3.4.1).

Four methods have been used although five research questions have been formulated (section 2.6), pointing to the fact that (a) different questions can be answered by the use of several, rather than just one, methods and (b) Research Question 1 and 2 are similar, a different time period under consideration being the only difference (trends and oscillations over the full duration of record in Question 1; trends and oscillations for the past decades in Question 2).

All the methods of both univariate statistical analyses, used in this thesis, have been widely applied before. Thus linear trend analysis is a standard method routinely applied in climatic studies to assess the overall changes in the time series between the start and the end point of a record (Box and Jenkins, 1976; Wilks, 1995). The *p*-statistic has been used to assess the statistical significance of the identified linear trends and rejection level has been set at 0.05 (Wilks, 1995). Variations on a shorter time scale have been examined using Henderson filter (Henderson, 1916) providing the advantage of smoothing data retaining quadratic and cubic polynomial trends and produces smoother variations than binomial filters (Kenny and Durbin,

1982). It has been used to emphasize decadal discharge and climatic oscillations indicating above-average (high flow) and below-average (low flow) discharge events in the discharge time series and also positive and negative anomalies in climatic records.

Step changes that occur in time series stand in contrast to gradual linear changes. According to McCabe and Wollock (2002: 38-I): "*A gradual [linear] change usually is expected to continue into the future; step changes inherently are thought of as less predictable unless the cause for the abrupt change is known*". Step changes may be interpreted as regime shifts in the climate system (McCabe and Wollock, 2002). Visual inspection of time series has been used to identify a potential step change in the studied time series. Statistical significance of the noted changes has been tested using the two-sample *t*-test. It assumes normal distribution and unequal variances and tests the hypothesis that an assumed change in the time series is significant at 0.05 (Wilks, 1995). The test has been applied to pairs of samples before and after the assumed change.

Correlation analysis is, perhaps, the most common way of assessing the strength of association between two variables (Wilks, 1995). Prior to correlation analysis, data have been tested for normality of distribution in the sample using Anderson-Darling test (Stephens, 1974). Pearson product-moment correlation coefficients have been used for the normally-distributed data and Spearman's rank correlation coefficients have been used in application to the non-normally distributed data. However, differences between results for Pearson and Spearman's tests have proved to be minor.

3.4.1. Multivariate statistical techniques: Principal Component Analysis (PCA) and multiple regression

River discharge is affected by multiple factors (Chapter 2.2) and methods of univariate statistics are often not sufficient to establish the nature of climatic controls over river discharge. Multiple linear regression is a prominent statistical procedure frequently applied in atmospheric and hydrological research. It ascertains the strength and nature of relationships between a predictand (discharge) and multiple predictors (such as SLP, geopotential height, teleconnection indices, air temperature, precipitation, evaporation, etc.) (Wilks, 1995). Although frequently used, multiple linear regression has one important disadvantage in the context of hydrometeorological research: multiple predictors used in regression analysis

should be independent of each other (Wilks, 1995). Climatic variables affecting river discharge, nevertheless, are not independent of each other and some climatic variables exert strong controls over other meteorological variables. For example, evaporation is a function of air temperature (Barry and Chorley, 1998) and temperature and precipitation in Europe strongly depend on the NAO (Hurrell, 1995). In order to resolve this problem and also to reduce the number of predictors that are used in multiple regression analysis, a combination of Principal Component Analysis (PCA) and regression analysis has been applied (Figure 3.5). This approach has been successfully applied to study relationships between atmospheric and climatic variables and hydrological changes before (e.g. Ye *et al*., 1998; Phillips *et al*., 2003; Ye *et al*., 2004).

PCA is one of the methods of multiple eigenvector analysis (Yarnal, 1993). Applying the eigenvector model, the researcher investigates and interprets the underlying structure of a multidimensional data set by extracting eigenvectors (principal components in case of the PCA method of extraction) from a dispersion matrix. Each eigenvector (component) is orthogonal to or uncorrelated with other eigenvectors (components). PCA, as one of the methods of eigenvector analysis, defines and isolates distinctive modes of variation in a data set. In climate research, PCA is used to reduce large data sets containing many climatic variables to a few principal components, which explain 'true' variance contained in Data set while rejecting noise. The identified components can be subsequently used as predictors in multiple regression analysis because, in contrast to original meteorological variables, they are uncorrelated with and independent of each other. Gould (1967), Johnson (1978), Richman (1986), and Preisendorfer (1988) have discussed the general concept and details of PCA, whereas White *et al*. (1991) and Stevens (1996) provide brief descriptions of the technique.

In a PCA, two new sets of data replace the original variables: component loadings and component scores. Components loadings replace the original variables (e.g. standard meteorological variables) and quantify links between original variables and principal components. Loadings are used to interpret the meaning of principal components. A high loading value (close to 1.0) on an original variable indicates a strong link between the component and the variable, while a low value (close to 0) indicates a weak link. Component scores are basically the time series for any generated Principal Component. They quantify links between components and time series of original variables and can be interpreted as values for the day's meteorological observations based on the extracted principal component.

Values of component scores depend on magnitude of the original variables and days with similar meteorological conditions exhibit similar component scores. Scores of principal components extracted from an original (here: meteorological) data set are used as independent predictors in a combined PCA and regression analysis instead of the original variables.

Figure 3.5 illustrates the main steps of a combined PCA and regression analysis. A very important step in a combined PCA-regression analysis, which is taken prior to the analysis itself, is selection of variables to be used. Which variables are included depends on (i) the established relationships between discharge and climatic processes and (ii) the type of PCA applied. The relationships between discharge and climatic variables can be established on the basis of the literature review (see Chapter 2) and in the course of correlation and composite analysis conducted prior to PCA (see Chapter 5). In this thesis, only those meteorological variables and circulation indices showing statistically significant correlation (at 0.05) with discharge have been considered as input data. As for type of PCA, a choice between two most commonly used methods – spatial single-variable and one-point multivariable (Richman, 1986) – may predetermine the selection of meteorological variables as original data set. Spatial single variable analysis aims to establish the most common atmospheric circulation factors in a studied region patterns or spatial patterns of precipitation (or temperature) that will control discharge. This type of analysis is similar to composite or anomaly maps and usually either SLP or geopotential height is used as input data (Yarnal, 1993). One point multivariable analysis employs multiple meteorological variables that exhibit the strongest links with discharge, which can be selected as described above.

The term 'single point' analysis is frequently used in climatological studies using PCA (Yarnal, 1993). Two modes of decomposition are frequently utilised in PCA: P-mode (analysis of a suite of variables varying over time at a given location) and S-mode of decomposition (analysis of spatial patterns of a single variable) (Richman, 1986). The choice of method (mode of decomposition) depends on the purpose of study, nature of the scientific problem, and type of data available. River discharge depends on a multiplicity of factors (section 2.2) and P-mode of decomposition seems to be suitable in an analysis of relationships between climatic factors and river discharge. However, unlike many other environmental characteristics that are controlled to a large extent by local processes and for which meteorological variables measured at a single location serve as useful predictors (e.g. urban air quality; McGregor and Bamzelis, 1995; Shahgedanova *et al.*, 1998), changes that occur

across the catchment area control river discharge. One way of dealing with this problem and combining the benefits of using multiple predictors and spatial impacts is to use time series of meteorological variable averaged across the catchment area. Ye *et al*. (2003) used this approach analysing links between surface climate, atmospheric circulation, and seasonal discharge of the Siberian rivers. The same approach has been adopted in this study.

Three types of dispersion matrices are used in PCA: correlation, covariance and cross-product (Yarnal, 1993). The choice of mode of decomposition (P-mode using either regional or spatially averaged time series of multiple variables) automatically resolves the question which dispersion matrix should be used. Correlation matrices are typically used in P-mode studies because multiple variables with different orders of magnitude are used, as input data and standardisation will be otherwise required (Yarnal, 1993). The correlation matrix has been used in this study.

In PCA, the largest amount of variance is explained by the first component (PC1) while contributions by other components may be underestimated (Richman, 1986; Preisendorfer, 1988; Wilks, 1995). Rotation of principal components is used to re-distribute the amount of variance explained between components facilitating contribution and interpretation of lower-order components. As a result of rotation, the total amount of variance explained by the components remains the same reaching 100% if the maximum number of components is extracted. Two categories of rotation exist: orthogonal and oblique (Richman, 1986; Preisendorfer, 1988; Wilks, 1995). Orthogonal rotation changes the relationship between various components but retains the orthogonality constraint of the eigenvector model and rotated components remain uncorrelated. Oblique rotations allow some shared variance among the components. With regard to P-mode of PCA, orthogonal rotations are most frequently used, particularly if scores of the rotated components are subsequently used in multiple regression analysis (Yarnal, 1993). Various methods of orthogonal rotation exist. Nevertheless, Varimax (Kaiser, 1960) and Quartimax (Richman, 1986) rotations are most frequently used. The Varimax rotation is used with preference in climatic studies because it produces solutions whereby the first 4-6 components contribute to the explanation of variance and are easier to interpret. This is in contrast to the Quatrimax rotation, which frequently produces results whereby the first component still dominates similarly to an unrotated solution. Richman (1986), Preisendorfer (1988), Yarnal (1993), and Stevens (1996) recommend the use of Varimax rotation and it has been applied in this study.

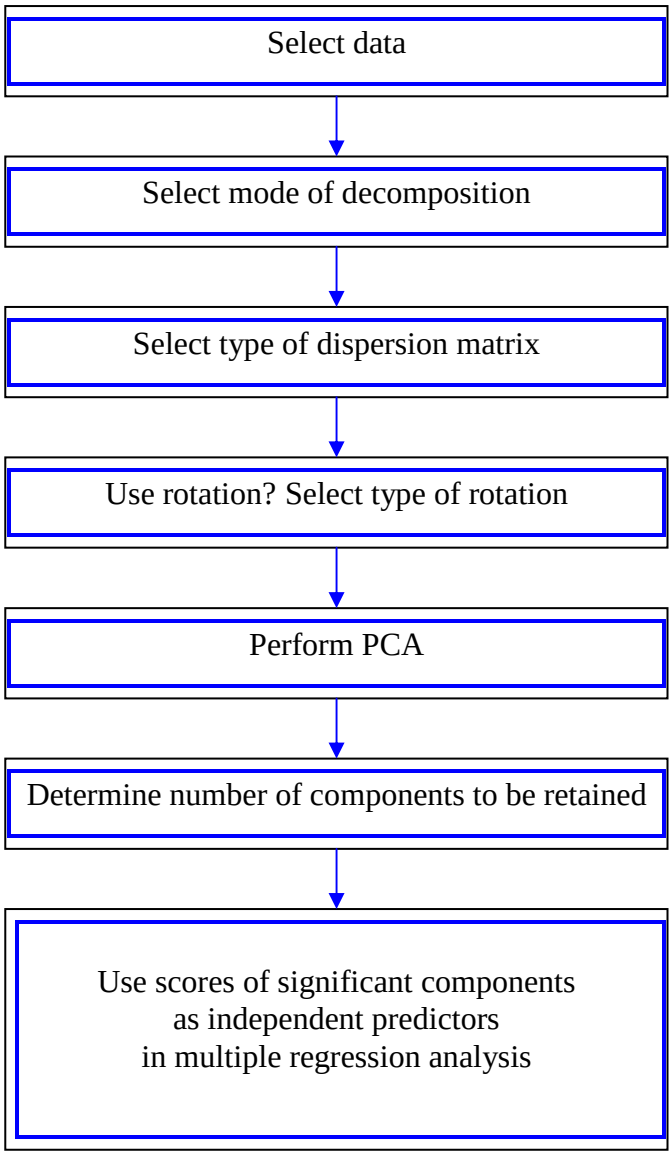

Figure 3.5. Main steps of a combined PCA and regression analysis (modified from Yarnal, 1993).

The maximum number of principal components, which can be extracted from an original data set, equals the number of original variables and explains 100% of variance in the data set. However, only a few components explain the majority (‘true’) variance in Data set while the rest represents ‘noise’ and is to be rejected. A number of approaches have been suggested to decide how many principal components are to be retained. One of the most commonly used method is the ‘eigenvalue 1.0’ rule, which states that only those components with eigenvalues larger than 1.0 are to be retained (Yarnal, 1993). Craddock and Flood (1969) have developed the so-called ‘scree plot’ test whereby a major break in a plot of eigennumber versus

eigenvalue reveals a number of components to be retained. Stevens (1996) suggested that the use of these rules may result in a loss of components, which account for a small amount of variance but represent infrequent but important events. He recommends retaining as many components as would be necessary to account for at least 70% of total variance in Data set. The downside of this approach is that frequently components with high loadings on a single variable are retained and meaningful interpretation of such components is difficult. In this study, the eigenvalue > 1.0 and scree plot test approaches have been used producing very close results.

3.5. Summary.

In this section the sources and quality of hydrological and meteorological data sets have been reviewed as well as details of statistical techniques that have been used to analyse Data. The main conclusions regarding the quality of the SD and SU discharge record are as follows:

(i) Starting in 1882 and with few gaps, the SD and SU discharge records are unique and their quality is acceptable for the analysis undertaken in this study. The obvious advantage of Data is that the river flow has not been affected by the construction of dams and reservoirs and that methods and location of discharge measurement and estimation have not changed at least since the 1950s. Also, water abstraction is low, and returned water more or less equals the abstracted amount. Uncertainties are associated with infrequent discharge measurements in some periods (particularly during the ice-cover period) and lack of information about methods of data collection prior to the 1950s.

(ii) Errors in discharge estimation have been evaluated and can be used in the subsequent result interpretation. The largest errors occur in winter, when discharge is at its lowest, and are associated with daily rather than monthly values. Errors in the estimation of monthly discharge are low.

(iii) A number of climatic data sets have been selected for analysis of relationships between climatic and hydrological variations. Advantages of the station data include the lengths of the records and unchanged position of the measuring sites. Gridded data sets cover a full century in length and are generally of good quality, provided that they have good spatial and temporal resolution. However, while

most uncertainties and errors in NCEP/NCAR reanalysis data do not affect the study area, biases occur in the New *et al*. (2000) precipitation data set and these data should be used with caution with regard to analysis of long-term linear trends.

(iv) Statistical techniques used in analysis of climate-discharge relationships have been discussed and their strengths and weaknesses have been stated leading to an informed choice of statistical techniques to be used.

Chapter 4. Trends and variability in discharge of the Severnaya Dvina (1882-2004) and the Sukhona (1882-1998).

4.1. Introduction.

One of the main objectives of this thesis is to study the long-term trends and shorter-term variability in discharge of SD and its tributary, SU. The literature review has highlighted the uncertainties in conclusions about the long-term changes in discharge of the Northern Eurasian rivers flowing into the Arctic Ocean, introduced by a short duration of the discharge records and river regulation measures. The discharge records for SD (1882-2004) and SU (1882-1998 for June-September; 1915-1998 for all months) are the longest continuous records of freshwater discharge into the Arctic Ocean. Being unaffected by extensive flow regulation and water abstraction (section 3.2.3), they are ideally suited to place the shorter-term hydrological variability into more extensive historical context. The emphasis is on SD, while the SU discharge record is used to support and verify the conclusions obtained with regard to SD. The main advantage of the SU record is the fact that there are no large cities or industrial centres abstracting water. Therefore, its discharge record should reflect almost entirely natural changes or changes due to global climate change. The discharge records have been obtained for two sites: Ust Pinega on SD (64^{o}13'N, 41^{o}92'E) and Kalykino on SU (60^{o}67'N, 45^{o}87'E). The locations of the sites are shown in Figure 1.1 and data quality is discussed in section 3.2.1.

4.2. Hydrological characteristics of the Severnaya Dvina and Sukhona.

SD is the 7th largest river of the Arctic Ocean basin with regard to its discharge and as such is considered a significant source of freshwater for the Arctic Ocean (Peterson *et al*., 2002; McClelland *et al*., 2004). Its mean annual discharge averaged over the 1882-2004 period is 3,331 $m^3 s^{-1}$ and the mean annual discharge of SU averaged over the 1915-1998 period is 449 $m^3 s^{-1}$ (Table 4.1). Table 4.1 shows discharge characteristics of both rivers and Figure 4.1 shows their hydrographs. The average date for the onset of ice cover on SD (at the Ust Pinega site) derived from a data set covering the 1978-1988 period (Vuglinsky, 2000) is 13 November, while the average date of ice melt is 16 April. The river is not completely ice-free

before the 13 of May on average. The average dates for the onset and melt of snow cover, derived from HSDSD data set (Armstrong, 2001) at Arkhangelsk are 15 October and 17 May (based on the period 1900-1994) and at Kotlas 16 October and 20 May (based on the period 1936-1994).

Table 4.1. Long-term arithmetic means ($m^3 s^{-1}$) of mean monthly discharge of SD and SU, coefficients of variation (CV; %), and correlation coefficients (*r*) between discharge time series of SD and SU. Data refer to the 1882-2004 period for SD and to the 1915-1998 period for SU. Sources: R-ArcticNet (www.r-arcticnet.sr.unh.edu/v3.0/index.html); Arctic RIMS (http://rims.unh.edu/data.shtml).

Month	SD mean	SU mean	SD CV	SU CV	r
January	1,037	130	30.1	43.0	0.71
February	830	93	29.0	45.0	0.57
March	730	75	25.1	54.9	0.69
April	2,446	868	89.5	56.6	0.79
May	13,876	1,570	23.4	36.0	0.60
June	6,965	720	40.6	36.1	0.55
July	2,974	423	36.4	47.1	0.70
August	2,172	284	48.3	45.7	0.63
September	2,321	303	51.7	61.3	0.74
October	2,898	392	47.8	58.9	0.76
November	2,324	340	59.6	61.5	0.76
December	1,399	194	42.1	47.5	0.77

There is a close correlation between the monthly discharge time series for both rivers (Table 4.1). The definition of hydrological seasons depends on hydrological characteristics and the purpose of investigation. From a purely statistical point of view, the season with lowest flow, when both rivers are frozen and discharge is low, extends from December to March (DJFM). From a point of regional importance, it is justified to consider a second low-flow season, namely July-August (JA). This is a season of high concern on a regional scale for inhabitants of the SD catchment, as particularly the SD is important for water abstraction and especially navigation in the summer months. Also, under consideration of data quality issues, discharge in the months without ice cover is estimated with higher confidence than during winter

(section 3.2.2). For both rivers, a high-flow season is defined as April-June (AMJ) as a distinct seasonal peak in discharge is observed during these months following the spring ice break-up and snowmelt (section 2.4.3). The September-November (SON) period is characterised by atmospheric processes different from those in July-August (Figure 2.7) and has been assessed separately despite similar discharge values in summer. Therefore, four seasons – AMJ, JA, SON, and DJFM – have been used in analysis of seasonal discharge records instead of the standard meteorological seasons.

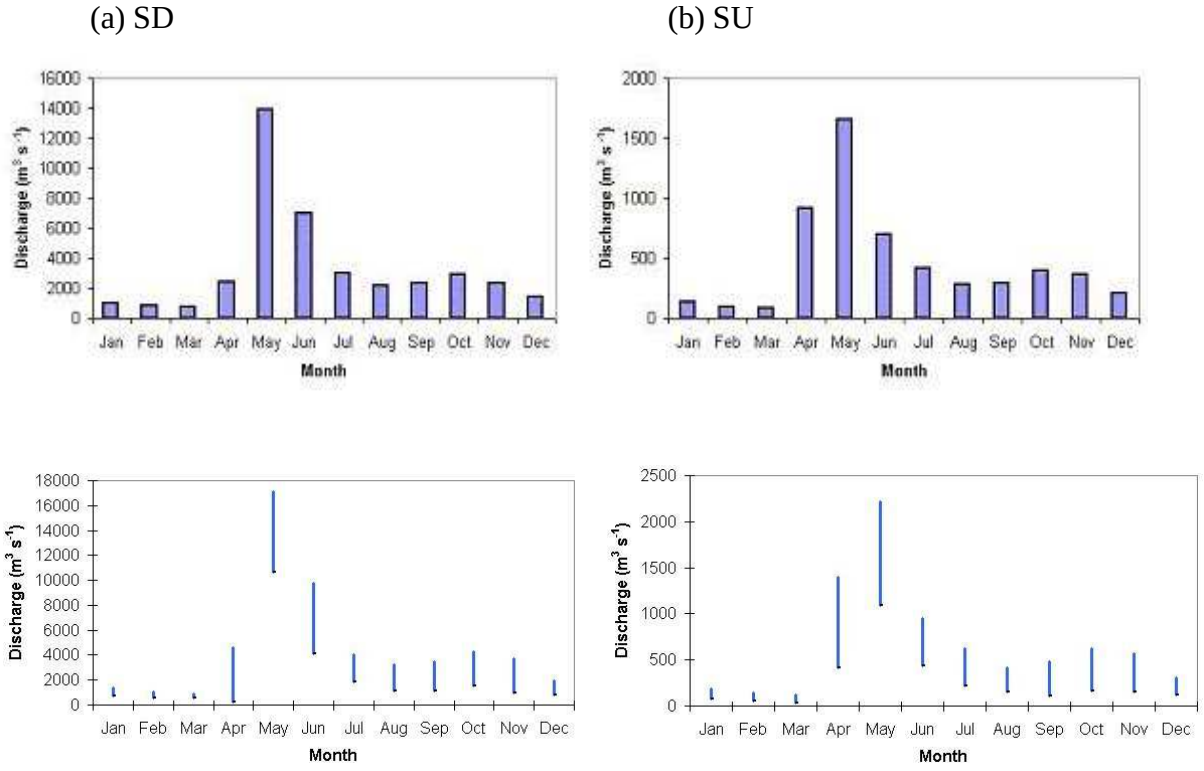

Figure 4.1. Hydrographs showing (a) average monthly discharge (m^3 s^{-1}) of SD and SU and (b) spread of monthly discharge determined by ± 1 standard deviation.

4.3. Long-term trends and variability in monthly discharge of the Severnaya Dvina and Sukhona.

In this section, monthly and seasonal discharge records of the SD and SU are analyzed. The discharge time series have been standardised by subtracting the long-term means from the time series and dividing by the standard deviation of the time series. Thereafter, time series and statistical significance tests have been carried out to identify long-term changes in

discharge. Both linear trend analysis (changes in discharge over time determined by linear regression; Wilks, 1995) and the 21-point Henderson filter (Henderson, 1916) have been used to analyse the longer-term trends and variations in the time series respectively, whereby the 21-point filter is useful in stressing anomalies that last for two to three decades. The standard *t*-test has been used to determine statistical significance of linear trends.

Figures 4.2 shows the time series of monthly discharge for SD and SU. Changes in monthly discharge of both rivers (Figure 4.2) have not been linear over the 20th century. The linear trends in the 1882-2004 discharge records are not statistically significant at 0.05 in most months and the amounts of variance explained by linear trends are low (Figures 4.2). A notable exception is a strong negative trend in SD discharge in September (explaining 5% of total variance) and SU discharge in June (explaining 12% of the total variance). The SD June record displays a similar tendency towards decrease. Nonetheless, this trend is not statistically significant at 0.05.

There were decades when significant anomalies in discharge occurred, particularly in January, March, and September. Between October and March, the highest values of discharge were observed in the 1920s – early 1930s.

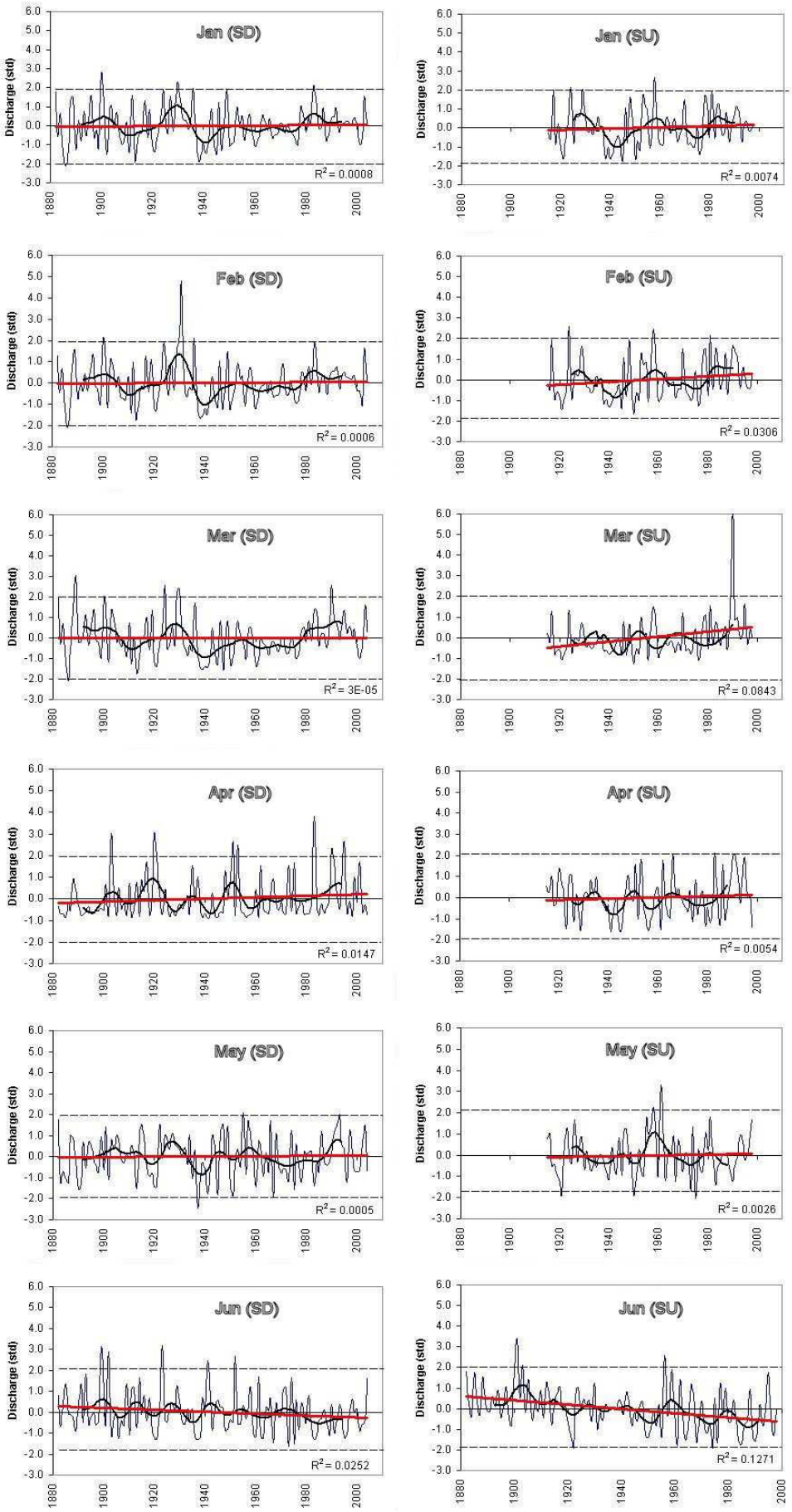
Jan (SD)
Jan (SU)
Feb (SD)
Feb (SU)
Mar (SD)
Mar (SU)
Apr (SD)
Apr (SU)
May (SD)
May (SU)
Jun (SD)
Jun (SU)
Discharge (std)
R² = 0.0008
R² = 0.0074
R² = 0.0006
R² = 0.0306
R² = 3E-05
R² = 0.0843
R² = 0.0147
R² = 0.0054
R² = 0.0005
R² = 0.0026
R² = 0.0252
R² = 0.1271

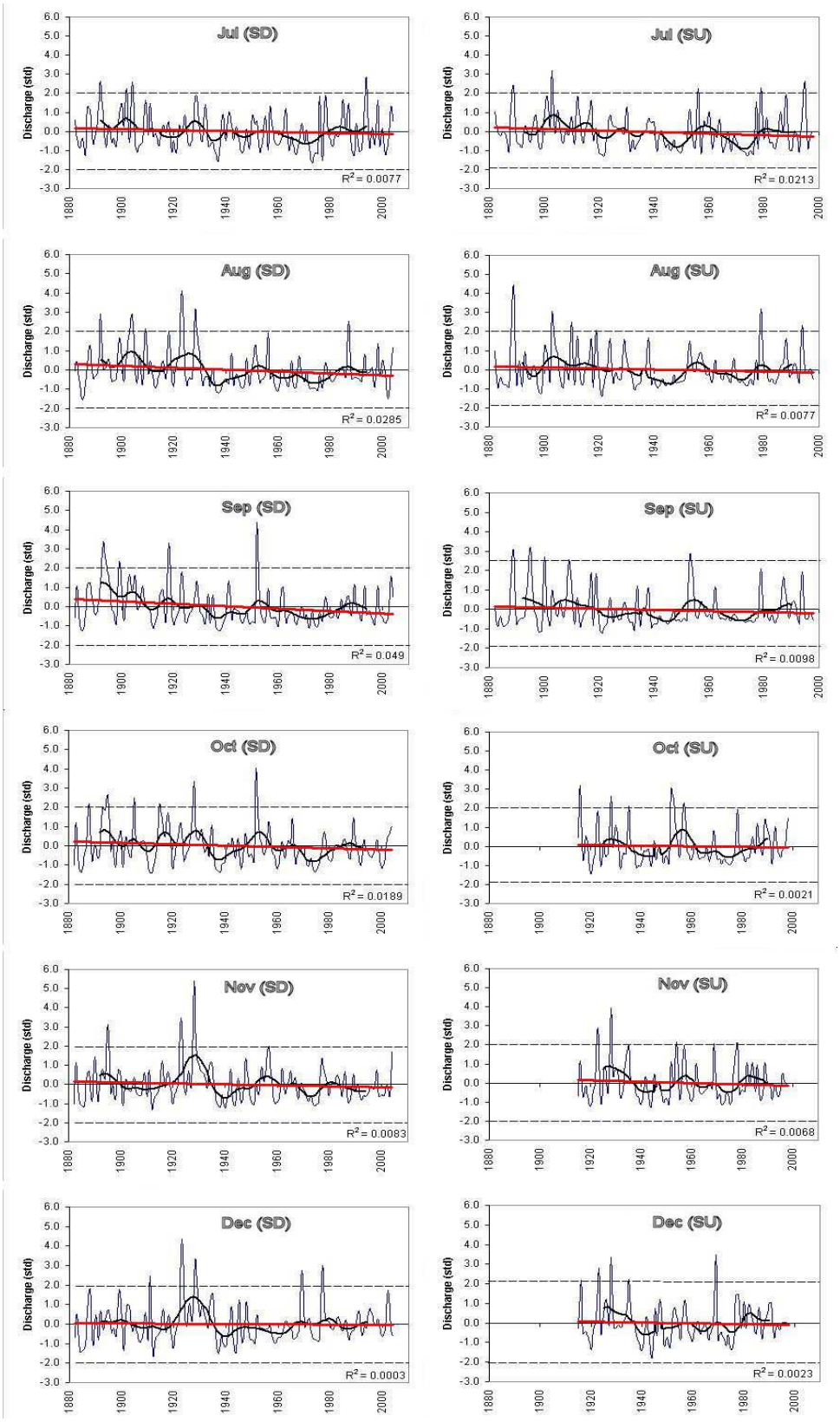

Figure 4.2. Monthly standardised discharge time series of SD and SU. The linear trends (red line) and calculated values of R^2 do not reveal any statistically significant long-term changes in the time series. The 21-term Henderson filter (black bold line) reveals low-frequency variability. ± 2 σ from mean are shown as dashed lines.

In January, March, and also between July and September high monthly discharge values were frequently observed in the 1890s. The late 1930s and 1940s were a period of very low discharge in most months. A period between the late 1930s through to the 1970s has been characterised by low discharge between December and March. The 1990s were characterised by frequent high monthly discharge values in March-May. The last two decades do not exhibit consistently high discharge values. The highest values, exceeding two standard deviations, are observed primarily in the earlier part of the record, mostly prior to the 1940s. However, these values should be treated with caution because little information exists about the quality of the earlier part of the record (section 3.2.2) in contrast to the post-1940s period. The only exception is the month of April when high values of discharge were observed frequently in recent years. This may be related to a strong increase in snow depth in some regions of the SD basin, for example at Kotlas (Figure 5.6 II b) and later melt of snow pack (Figure 5.7 b). Inspection of monthly snow depth time series (sections 5.2.3) indicates that at Kotlas, the snow depth during March has strongly increased between 1990 (6 cm) and 1998 (60 cm), whereas at Arkhangelsk, the monthly snow depth in April (not shown) has increased from 6 cm (1989) to 51 cm (1998) and declined thereafter again.

Several changes observed over the SD catchment are documented in literature as well for Northern Russia and the Arctic basin. For example, exceptionally warm and dry meteorological conditions in the 1930s and 1940s registered in north-western Russia correlate well with the period of low flow registered across the Arctic Ocean basin (e.g. Shiklomanov *et al.*, 2000). The discharge increase during spring in the 1990s may be related to positive snow depth anomalies (Serreze *et al.*, 2000). Also, annual river discharge has recently received much attention, as it increased during the past few decades across European Russia (Georgievsky, 1998) and Northern Eurasia (Peterson *et al.*, 2002),

4.4. Long-term trends and variability in seasonal discharge of the Severnaya Dvina and Sukhona.

4.4.1. Discharge trends since 1882

Figure 4.3 shows the seasonal discharge time series for SD and SU. While neither time series contains a statistically significant linear trend for the duration of record, there is pronounced

low-frequency (decadal) variability in the records. In particular, the 1920s and the early 1930s stand out as time periods when discharge was above average. By contrast, lower-than-average discharge was observed in the 1930s-1940s and this period of low discharge continued well into the 1970s (with a brief interruption in the late 1940s) in JA at both rivers. The lowest SD discharge was observed in 1937 and in 1960, followed by 1967 and 1975. In the 1970s, low flow was observed in SON at both rivers. During the low-flow period of the late 1930s, it extended into the winter months too. The last two decades were characterised by relatively high values of discharge. Nonetheless, seasonal averages have not exceeded those observed in the 1920s and at the beginning of the record. The AMJ time series for SD shows surprisingly little interannual variability in comparison to other seasons and standardised values of seasonal AMJ discharge do not exceed ±1 σ (Figure 4.3 a). A closer inspection of the individual April, May, and June time series has shown that very often the concurrent months (particularly April and May) exhibit opposite anomalies resulting in a low variability for the whole season. The AMJ discharge of Northern Eurasian rivers is driven by snowmelt (sections 2.2 and 5.2.3) and the observed pattern is consistent with snowmelt occurring mostly in April or less frequently in May. Interannual variability in individual months of the season (Figure 4.2) considerably exceeds interannual variability in the AMJ record.

4.4.2. Discharge trends since 1936

Trends in seasonal discharge for the 1936-2004 period have been estimated in addition to the trends for the whole record to facilitate a comparison with other studies which mostly used the post-1936 period. No linear trends, significant at 0.05, occurred in the post-1936 discharge of SD during AMJ, JA, and SON. However, the wintertime (DJFM) discharge has increased significantly with a positive linear trend explaining 7% of the total variance in the time series.

4.4.3. Step change in annual discharge

A visual inspection of the time series has also revealed that a number of step changes have occurred in the time series of seasonal discharge of both rivers. The SD records show that a step change occurred in the JA time series in 1931 (Table 4.2 a) and in SON time series in 1937 (Table 4.2 b). The post-1930 period in the JA discharge record can be further subdivided into the 1931-1975 period characterised by lower discharge and the 1976-2004 period

characterised by higher seasonal discharge values (Table 4.2 a). In 1972-1975 and in 1978, JA discharge was two standard deviations below the mean. High values of JA discharge were typical between 1881 and 1930 although a number of high discharge summers have been observed after 1978. Similarly to JA, in SON discharge values above two standard deviations from the mean were observed predominantly in the earlier part of the record (before 1953). Step change has occurred in 1936 and 1976 (Table 4.2 b) dividing the record into an early phase with above-average SON discharge prior to 1936, and below-average discharge afterwards. More recently, seasonal discharge values have been close to average and seasonal discharge value below two standard deviations from the mean was last measured in 1975.

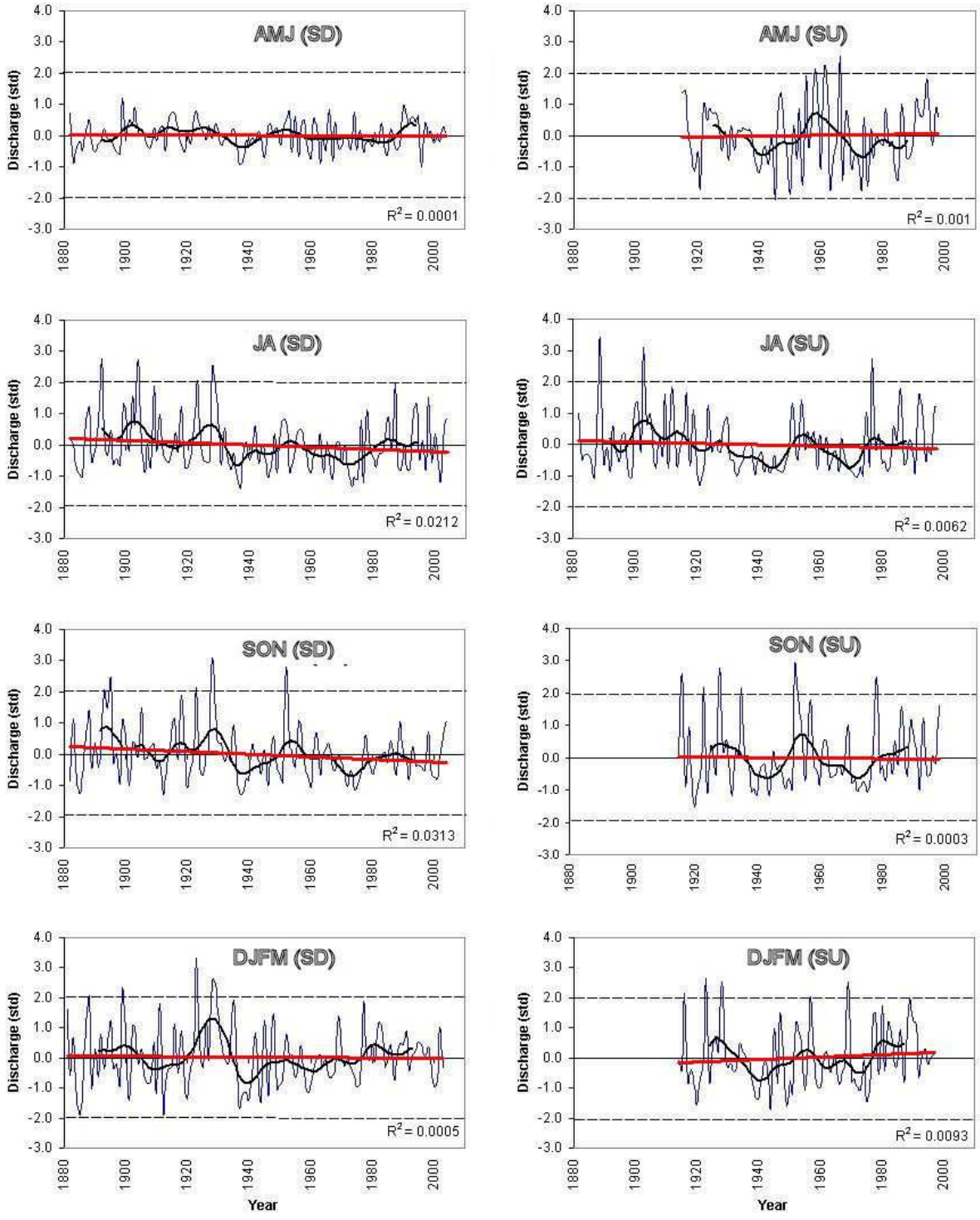

Figure 4.3. Seasonal standardised discharge time series of SD and SU. The linear trends (red line) and calculated values of R^2 do not reveal a long-term change in the time series. The 21-term Henderson filter (black bold line) reveals low-frequency variability. ± 2 σ from mean are shown as dashed lines.

The two-sample *t*-test has been used to test the hypothesis that the identified step changes in SD discharge are statistically significant. The test has been applied to the following pairs of samples:

(i) 1882-1930 and 1931-2004 as well as 1931-1975 and 1976-2000 for JA;

(ii) 1882-1936 and 1937-2004 as well as 1882-1974 and 1975-2004 for SON;

(iii) 1882-1937 and 1938-2004 as well as 1882-1923 and 1924-2004 for DJFM.

The changes in JA discharge that occurred in 1931 as well as the change in SON discharge that occurred in 1937 are significant at less than 0.01. The change that occurred between 1975 and 1976 is significant at 0.07 (Table 4.2). The AMJ discharge record does not exhibit any step changes in contrast to the JA, SON and DJFM records.

Table 4.2. Statistical significance of assumed changes in seasonal SD discharge. Means and standard deviations of the before- and after-change samples are *m* and σ; the number of years in a sample is *N*.

(a) JA

Before 'change'				After 'change'				***P***
Season/Years	***N***	***m***	σ	***Season/Years***	***N***	***m***	σ	
1882-1930	49	2.869	1.068	1931-2004	74	2.353	763	0.004
1931-1975	45	2.215	643	1976-2004	29	2.568	888	0.071

(b) SON

Before 'change'				After 'change'				***P***
Season/Years	***N***	***m***	σ	***Season/Years***	***N***	***m***	σ	
1882-1936	55	2.820	1.278	1937-2004	68	2.215	867	0.004
1882-1974	93	2.577	1.211	1975-2004	30	2.213	642	0.041

(c) DJFM

Before 'change'				After 'change'				***P***
Season/Years	***N***	***m***	σ	***Season/Years***	***N***	***m***	σ	
1882-1937	56	1.042	365	1938-2003	66	956	229	0.12
1882-1923	42	1.002	358	1924-2003	80	1.168	374	0.15

The SU records also exhibits a step change in the 1930s. Nevertheless, the length of the seasonal records does not allow to apply statistical tests with confidence to all seasons apart from summer. In JA, the decline towards the minimum of the 1930s-1940s began earlier than at SD and was less abrupt. The higher flow period of 1882-1920 and lower flow period of 1921-1998 are significantly different at 0.07 (Table 4.3).

Table 4.3. Statistical significance of assumed changes in JA discharge of SU. Means and standard deviations of the before- and after-change samples are *m* and σ; the number of years in a sample is *N*.

Before 'change'				After 'change'				***P***
Season/Years	***N***	***m***	σ	***Season/Years***	***N***	***m***	σ	
1882-1920	39	396	198	1921-1998	76	332	146	0.07
1921-1978	56	318	141	1979-1998	20	369	156	0.21

4.5. Long-term trends and variability in annual discharge of the Severnaya Dvina and Sukhona.

Figure 4.4 shows annual average discharge time series for SD and SU. Neither time series shows a statistically significant linear trend for the duration of record. However, low frequency quasi-decadal variability occurs similarly to the monthly and seasonal records. Figure 4.5 shows pentadal discharge anomalies for both rivers. The late 1930s-1940s were characterised by very low values of SD discharge. In particular, in 1937 the annual average discharge was more than two standard deviations below the long-term average. The 1960-75 period was also characterised by below-average discharge and in 1960 annual discharge was second lowest on record. An increase in annual average discharge at both rivers occurred since the mid-1970s. Nevertheless, annual discharge of the last three decades has not exceeded those values observed in the 1920s and at the beginning of the 20th century, particularly at SD.

A visual inspection of annual average SD discharge has indicated that a change in discharge occurred in 1936-37. The difference between the means of annual average discharge of SD calculated for the 1882-1936 and 1937-2004 periods is statistically significant at 0.005 (Table

4.4 a). The length of the SU record does not allow a reliable evaluation of the significance of changes that occurred in the 1940s, which were characterised by reduced discharge. However, there has been a clear change in SU discharge between 1915-1975 and 1976-1998 with a steady increase in annual average discharge (Figure 4.4 b). A positive linear trend explains ~15% of total variance in annual discharge between 1975 and 1998 (not shown) and is more pronounced than a similar trend in the annual average SD discharge (7% increase between 1975 and 2004). The long-term means for the 1915-1975 and 1976-1998 periods are significantly different at 0.06 for SU but not for SD (Table 4.4).

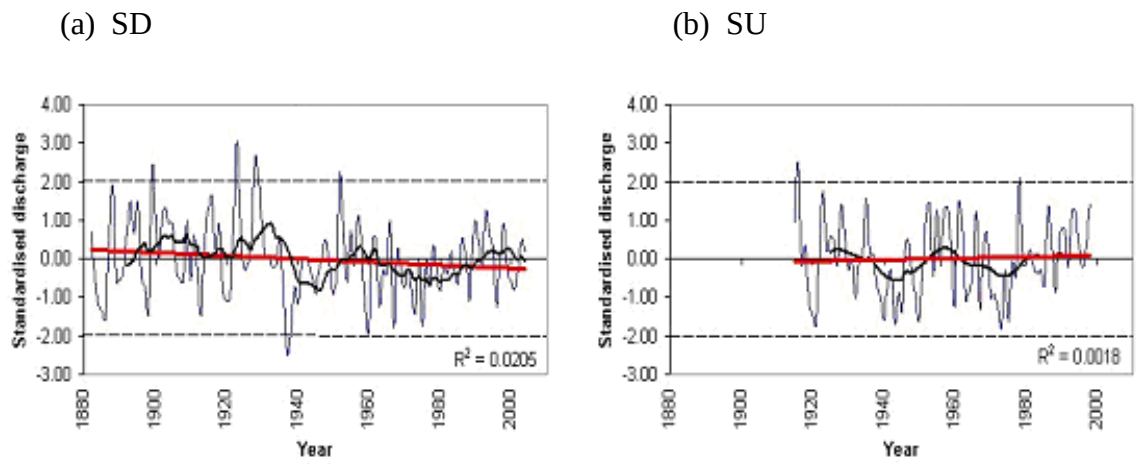

Figure 4.4. Annual average standardised discharge time series for SD and SU. The linear trends (red line) and calculated values of R^2 do not reveal a long-term change in the time series. The 21-term Henderson filter (black bold line) reveals low-frequency variability. ± 2 σ from mean are shown as dashed lines. The most notable features are the periods of low discharge values in the 1930s-1940s and in the 1970s.

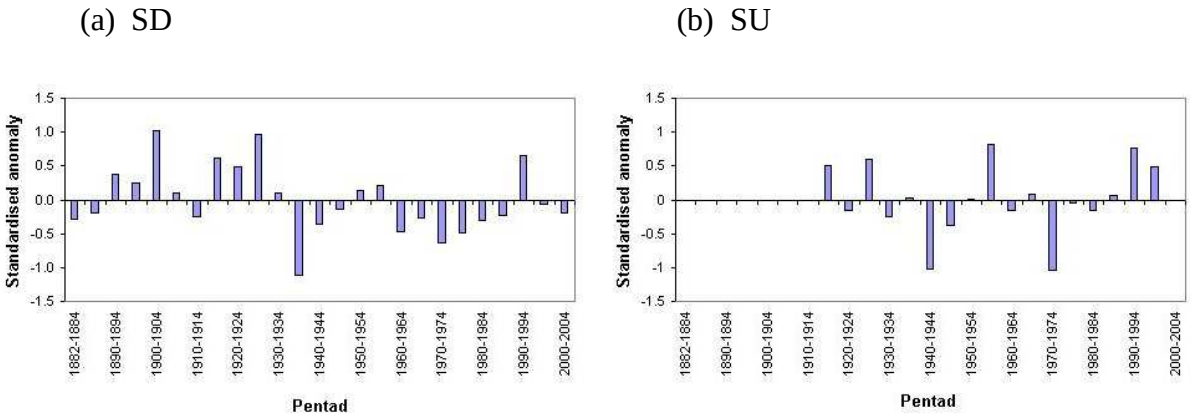

Figure 4.5. Pentadal anomalies of SD mean annual discharge (1882-2004) and SU (1915-1998). Anomalies have been calculated as the difference between long-term arithmetic means and discharge in a given pentad.

A linear trend in annual discharge of SD since 1936 (not shown) has as well been estimated to facilitate comparison with the study by Peterson *et al*. (2002). As a whole, annual discharge has increased with the positive trend explaining 4.6% of the total variance remains slightly below the level of statistical significance at 0.05 (R^2 = 5.3), constituting a larger linear change than during the post-1882 period (Figure 4.4 a).

Table 4.4. Statistical significance of assumed changes in annual discharge of SD and SU. Means and standard deviations of the before- and after-change samples are *m* and σ; the number of years in a sample is *N*.

(a) SD

Before 'change'				After 'change'				***P***
Season/Years	***N***	***M***	σ	***Season/Years***	***N***	***m***	σ	
1882-1936	55	3.502	679	1937-2004	68	3.180	526	0.005
1882-1975	94	3.333	675	1976-2004	29	3.298	388	0.727

(b) SU

Before 'change'				After 'change'				***P***
Season/Years	***N***	***m***	σ	***Season/Years***	***N***	***m***	σ	
1915-1975	61	426	113	1976-1998	23	468	83	0.062

4.6. Conclusions.

This chapter has shown results for trends in SD and SU discharge. Both discharge records span over a century and, in contrast to the discharge time series of the Siberian rivers, they are neither affected to any significant extent by river flow modification nor by water abstraction. As such, these records provide a unique source of information about climatically induced changes in the freshwater discharge into the Arctic Ocean.

In contrast to previous results obtained by Peterson *et al*. (2002) analysis of the longest records available presented does not show significant changes in seasonal and annual discharge of the 7th largest river (Table 2.2) draining the Arctic Ocean basin over a longer

study period. Peterson *et al*. (2002) estimated changes in annual discharge of the six largest rivers of the Arctic Ocean basin (including SD) relative to 1936 when most records started revealing a positive trend in discharge and relating these trends to a potential impact on the oceanic circulation. It has been shown in this study that annual discharge of SD in the 1936-37 hydrological year was one of the lowest on record and it remained exceptionally low during the 1935-39 pentad. A large duration of the SD record indicates that 1936 marked the beginning of a period of below-average discharge that continued until the 1970s. DJFM discharge of SD has increased significantly between 1936 and the present. Nevertheless, this trend does not extend to the full duration of record in any season. Discharge observed prior to 1936 exceeded the current levels. Therefore, there is no indication that freshwater influx into the Arctic Ocean from the western part of European Russia has increased during the 20th century. Studies of hydrological variability in Siberia indicate that the 1930s were a period of low flow too, similarly to SD, across the Siberian sector of the Arctic Ocean (e.g. Yang *et al*., 2002; Ye *et al*., 2003; Yang *et al*., 2004 a; Yang *et al*., 2004 b) in line with the regional climatic warming observed in the Arctic and sub-Arctic regions of Eurasia in the 1920s-1940s (Chapter 2).

The following conclusions are drawn regarding the discharge trends:

- Linear trends in the seasonal and annual time series of the SD discharge are not statistically significant at 0.05 for the duration of the records. Between 1936 and 2004, DJFM discharge increased significantly. A notable exception is a strong negative trend in SD discharge in September (explaining 4.9% of total variance).
- Linear trends in seasonal and annual SU discharge time series are not statistically significant at 0.05 for the duration of the records. A notable exception is a strong negative trend in SU discharge in June (explaining 12% of the total variance).
- The discharge records of SD and SU agree well particularly during the extremely dry conditions experienced during the 1930s and 1940s. Also, the increase in annual discharge of both rivers since the 1970s, also a phase of lower-than-average annual flow, agrees well.
- Pentadal and decadal oscillations are clearly expressed in the discharge time series.
- Pronounced step changes in the annual discharge time series occurred in 1936/37 (SD) and 1975/76 (SU). Three phases have been identified in the discharge time series of SD: (i) the 1882-1936 period was characterised by the highest annual discharge on

record; (ii) the 1937-1975 time period exhibited the lowest annual discharge; (iii) after 1976, annual discharge has been close to average.

- The lowest annual SD discharge was observed during the pentads 1935-1939 and 1970-1974. The lowest annual SU discharge was observed during 1940-1944 and 1970-1974.
- The highest annual SD discharge was observed during the pentads 1900-1904 and 1925-1929. The highest annual SU discharge was observed during 1955-1959 and 1990-1994.

The possible causes of the uncovered hydrological variability of SD and SU and its links with climatic variability are discussed in the next chapter.

Chapter 5. The links between variability in discharge of the Severnaya Dvina, regional climatic variability, and distant atmospheric forcing.

5.1. Introduction.

Regional climatic variability is the main factor affecting changes in river discharge and catchment's discharge in the absence of significant changes in basin physiography and river flow regulation (Krasovskaia, 1994). Over long periods of time, when changes in a catchment's storage tend to zero, a catchment's discharge can be approximated as the difference between precipitation and evaporation (Jones, 1997; Peel *et al*., 2001). In turn, variability in regional temperature strongly affects evaporation. Therefore, these two climatic variables (precipitation and temperature) are of primary importance to discharge. In cold regions, where precipitation accumulates as snow pack, the duration and extent of snow cover are important controls over river discharge. The impacts of changes and fluctuations in the above-listed climatic variables on discharge of the rivers of the Arctic Ocean basin have been discussed in section 2.5. It has also been shown that variability in atmospheric circulation, both regional (synoptic-scale) and large-scale (teleconnection patterns), controls changes and fluctuations in these climatic variables.

This chapter discusses links between regional and large-scale atmospheric forcings and discharge of SD. Links with SU are not discussed for two reasons: Firstly, the discharge record of SD is far longer in most months (1882-2004) than of SU (1915-1998, except for JA season; section 3.2.1). Secondly, SD is the major river in north-western Russia considered by other studies (Peterson *et al*., 2002; McClelland *et al*., 2004, 2006), whereas SU is a relatively small one (section 1.2). After a discussion of the relationships between discharge of SD with regional and local precipitation, temperature, effective precipitation, sea level pressure, and characteristics of snow cover (section 5.2), the chapter proceeds to discuss the relationship between discharge and the main NH teleconnection patterns (section 5.3) and the relationships between teleconnection patterns and climate within the SD basin (section 5.4).

5.2. Links between discharge of the Severnaya Dvina and variability in regional climate.

5.2.1. Precipitation

Two precipitation data sets, whose quality is discussed in section 3.3, have been employed to quantify the relationship between SD discharge and local and regional precipitation:

(i) Monthly and seasonal precipitation time series for Arkhangelsk (64^o 60'N, 40^{o}50E; 1881-2003) derived from DSS UCAR (http://dss.ucar.edu/datasets/ds570.0/)

(ii) Monthly and seasonal precipitation time series averaged over the SD catchment area (defined here as 58-65^o N; 40-50^o E; 1901-2000) derived from New *et al*. (2000) high-resolution data set.

Monthly and seasonal precipitation time series are shown in Figures 5.1 and 5.2. The Arkhangelsk records show that monthly precipitation totals for the individual months during the cold season (November-March) have increased over the period of observation. Linear trends, statistically significant at 0.05, explain between 7% (March) and 23% (December) of the total variance in the monthly time series. Seasonal precipitation time series (Figure 5.2) reveal positive linear trends in the spring (AMJ), autumn (SON) and winter (DJFM) explaining 12 %, 25% and 30% of the total variance respectively. In contrast, rainfall remained unchanged over the JA low flow season. The changes in the spatially-averaged (regional) monthly and seasonal regional precipitation time series (Figure 5.1 and 5.2) are not entirely consistent with changes at Arkhangelsk. There is a moderate correlation between the two time series (r = 0.51), suggesting that both records share no more than 25% of variance. The regional time series do not exhibit any statistically significant linear trends. The lack of consistency between the two time series can be explained either by different trends occurring over the SD basin as a whole and in its northern part (Arkhangelsk) or by the lack of internal consistency in the spatial data whereby the number of stations and their location have changed over time (section 3.3.1). The question arises as to the spatial agreement of trends in different areas of the SD catchment. Thus, the records of Arkhangelsk (in the northern part of the watershed) have been compared with the station records of Kotlas located in the middle part of the basin (for time series see Appendix I). The Kotlas records show that monthly precipitation totals have increased between October and April over the period of observation. Linear trends, statistically significant at 0.05, explain between 8% (April) and 32%

(December) of the total variance in the monthly time series. Both Arkhangelsk and Kotlas show their strongest linear increase during December, while the weakest significant rise is confined to March (Arkhangelsk) and April (Kotlas). Seasonal precipitation at Kotlas has not changed linearly over time with the exception of DJFM, where a strong increase occurred accounting for 32% of the observed variance (Appendix I). As a whole, agreement between the winter (DJFM) time series from the two stations is moderate ($r = 0.42$, significant at less than 0.01) whereas annual agreement is far lower ($r = 0.15$, not significant at 0.05).

Correlation coefficients, concurrent and with time lag, have been calculated to quantify the relationships between regional and local rainfall and discharge (Tables 5.1 and 5.2). There is a strong positive correlation (> 0.65) between the regional rainfall and SD discharge between July and September for the concurrent months and with one-month time lag (rainfall leading discharge) (Table 5.1 a). SD discharge and concurrent and preceding rainfall between October and December correlate moderately (r ranging between 0.3 and 0.5). A weak (but statistically significant at 0.05) and persistent correlation occurs between discharge in May (the month of highest flow) and precipitation in the previous spring and winter months. The low values of correlation coefficients are unexpected of a catchment with continuous winter-spring snow cover. Correlation coefficients between the SD discharge and the precipitation time series for Arkhangelsk display similar pattern but are weaker (Table 5.1 b). This is because Arkhangelsk is located at the outlet of SD and regional precipitation has a smaller influence on SD discharge in contrast to the catchment-averaged precipitation. There is a weak (but statistically significant at 0.05) negative correlation between winter and spring precipitation at Arkhangelsk and summer discharge of SD. This negative correlation may be explained by random chance because it is possible to obtain statistically significant association between discharge and a series of random numbers (Phillips and McGregor, 2002). Correlation of seasonal time series of the SD discharge and spatially-averaged precipitation has revealed a strong link between JA precipitation and JA discharge as well as between JA precipitation and SON discharge (Table 5.2). It should be pointed out that the lack of a long-term trend in the spatially-averaged precipitation time series is consistent with the lack of statistically significant long-term linear trend in the SD discharge time series.

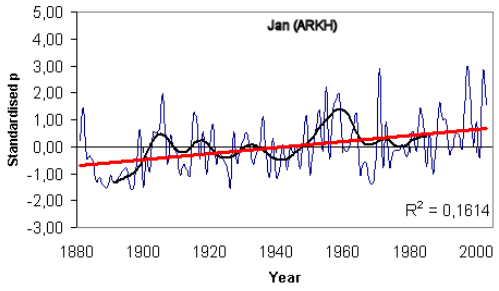
Jan (ARKH)
Standardised p
Year
R2 = 0,1614

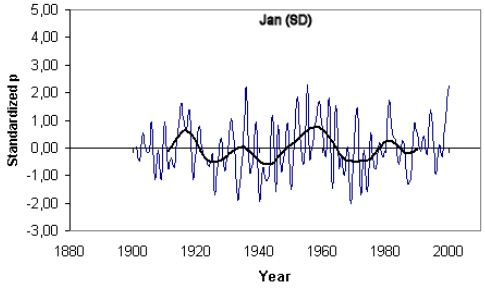
Jan (SD)
Standardized p
Year

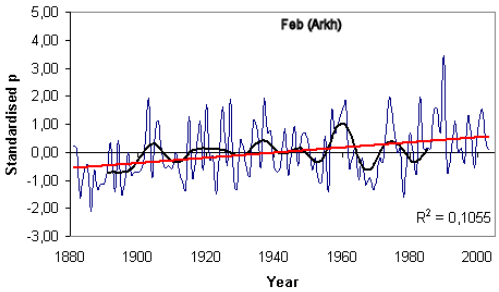
Feb (Arkh)
Standardised p
Year
R2 = 0,1055

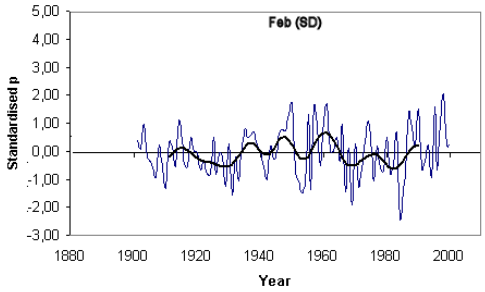
Feb (SD)
Standardised p
Year

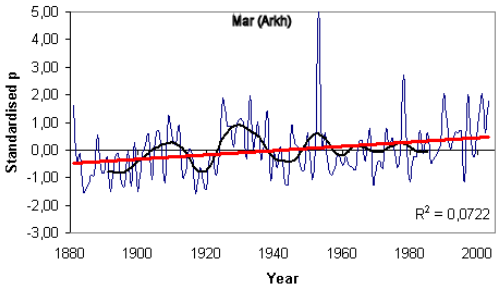
Mar (Arkh)
Standardised p
Year
R2 = 0,0722

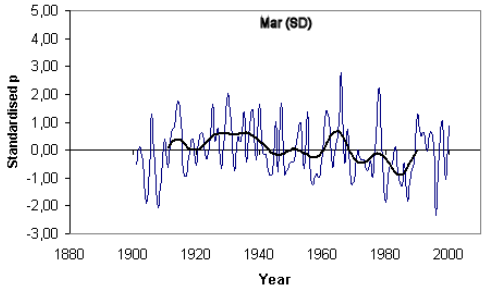
Mar (SD)
Standardised p
Year

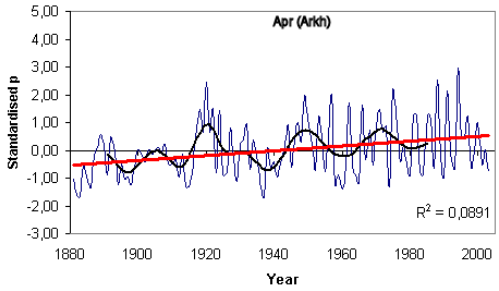
Apr (Arkh)
Standardised p
Year
R2 = 0,0891

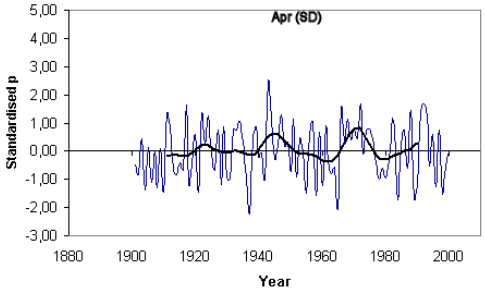
Apr (SD)
Standardised p
Year

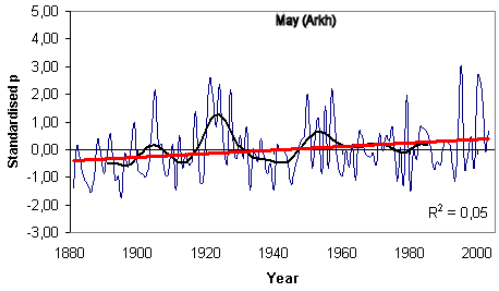
May (Arkh)
Standardised p
Year
R2 = 0,05

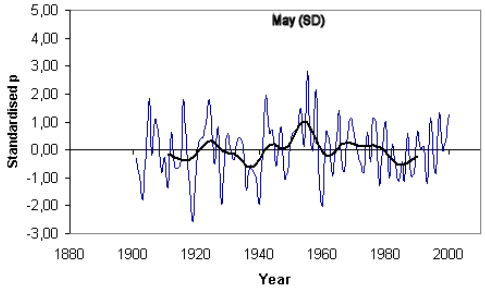
May (SD)
Standardised p
Year

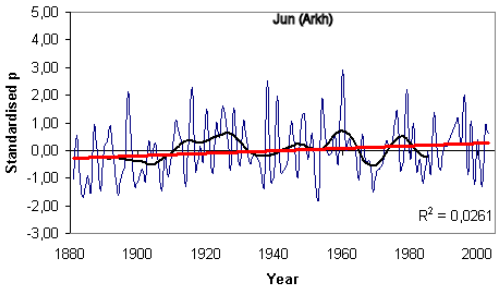
Jun (Arkh)
Standardised p
Year
R2 = 0,0261

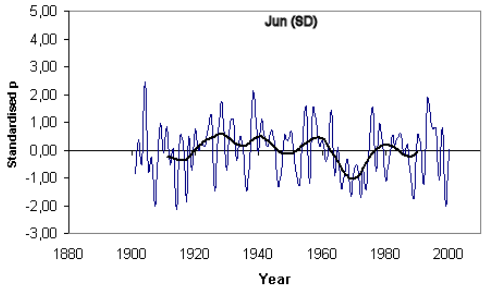
Jun (SD)
Standardised p
Year

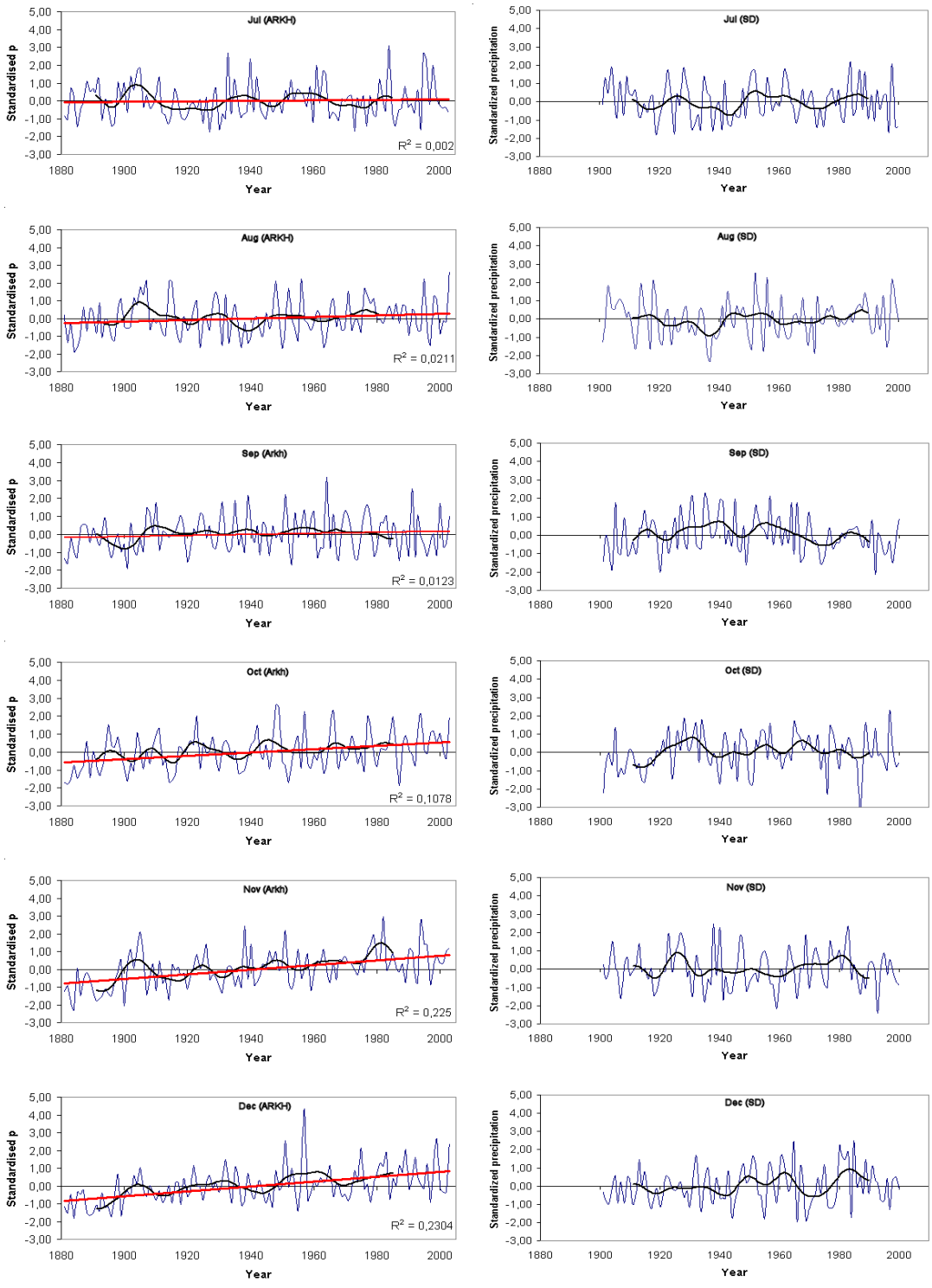

Figure 5.1. Standardised monthly precipitation at Arkhangelsk (1881-2003; 64°60'N, 40°50'E) and for the SD catchment (1901-2000). Data have been derived from New *et al*. (2000) gridded data set and averaged over the catchment of the SD (58 – 65° N, 40 – 50°E). Linear trends are shown in red (on Arkhangelsk data), Henderson filter in black.

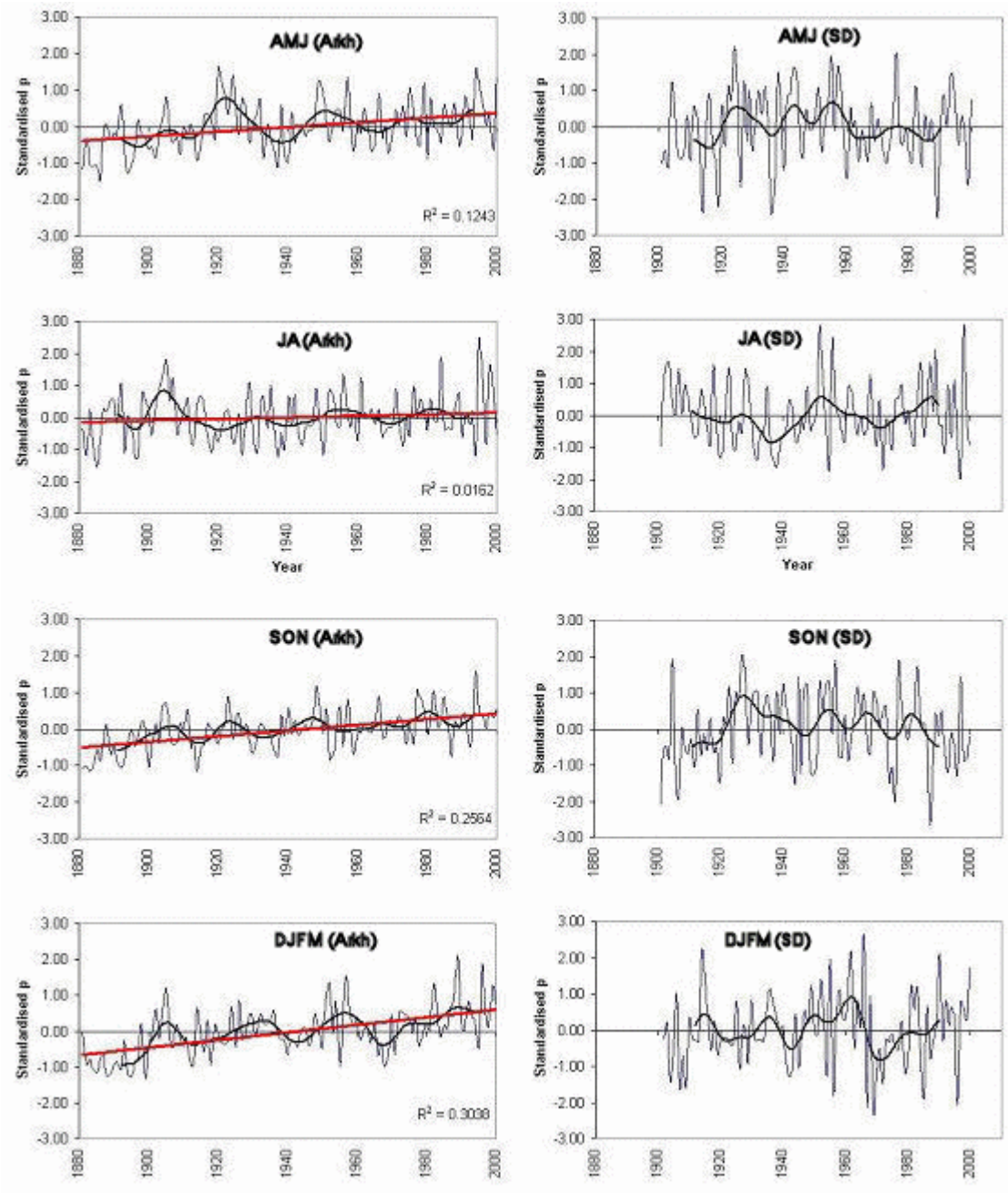

Figure 5.2. Standardised seasonal precipitation at Arkhangelsk (1881-2003; 64°60'N, 40°50'E) and for the SD catchment (1901-2000). Data have been derived from New *et al*. (2000) gridded data set and averaged over the catchment of the SD (58 – 65° N, 40 – 50°E). Linear trends are shown in red (on Arkhangelsk data), Henderson filter in black.

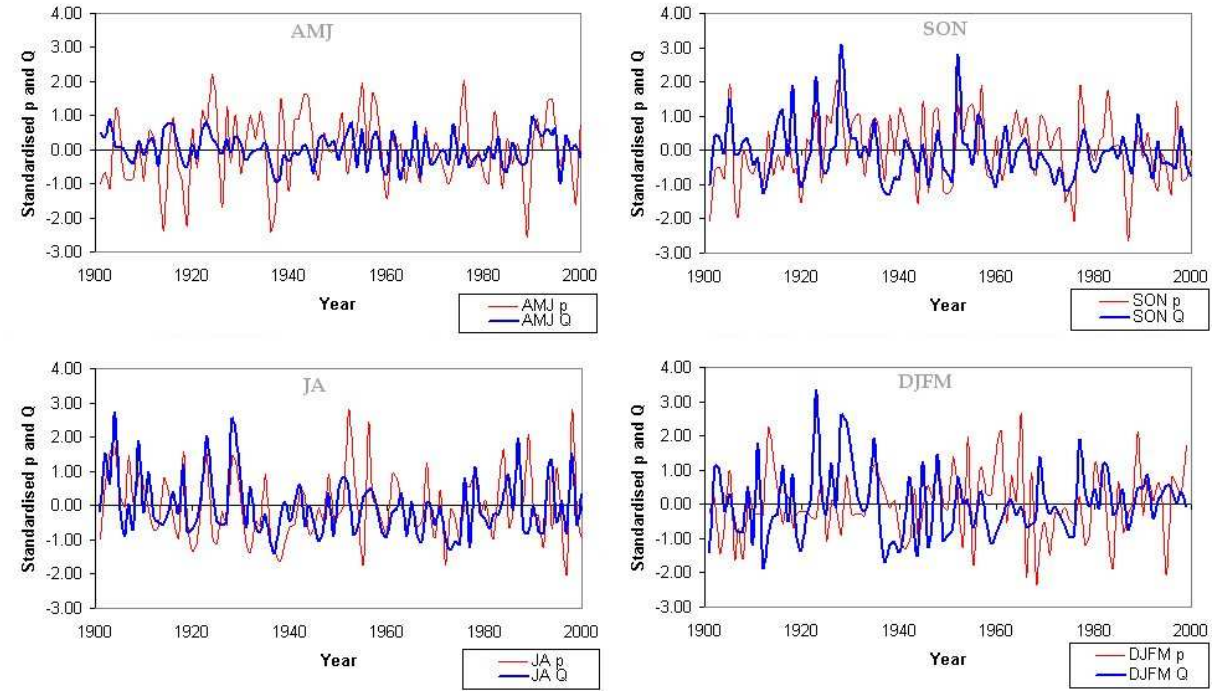

Figure 5.3. Regional seasonal air temperature versus seasonal SD discharge (1901-2000). t = temperature, Q = discharge.

Figure 5.3. shows the time series of seasonal regional precipitation against seasonal SD discharge for the overlap period (1901-1995). The association between precipitation and discharge is positive in all seasons, i.e. positive rainfall anomalies drive positive discharge anomalies, and vice versa. As it has been already shown with regard to JA temperature, the correlation between JA precipitation and JA discharge is highest of all seasons, which is in line with the positive correlation between the two variables (r = 0.52; Table 5.2). As can be seen, low (high) precipitation in JA directly translates into low (high) discharge events throughout the record, most notable during the dry 1930s and early 1970s, and also during the strong JA discharge events of 1904, 1909, 1923, 1928, 1994, and 1998. The other seasons show moderate agreement (r in AMJ: 0.30; r in SON: 0.36) and do not take into account the lagged impacts, whereby precipitation in a given season often affects the discharge in subsequent seasons.

Table 5.1. Correlation coefficients between monthly precipitation and monthly discharge of SD.

(a) Regional precipitation averaged over the SD catchment (65-58°N and 40-50°E; 1901-2000) (New *et al.*, 2000). Discharge months are shown in blue and precipitation months in red. Correlation coefficients significant at 0.05 are shown (> 0.20).

	Jan	Feb	Mar	Apr	May	Jun	Jul	Aug	Sep	Oct	Nov	Dec
Jan												
Feb	0.28											
Mar	0.24											
Apr												
May	0.22	0.21		0.28	0.28							
Jun					0.24							
Jul						0.67	0.35					
Aug						0.27	0.66	0.34				
Sep							0.41	0.65				
Oct							0.31	0.47	0.43	0.31		
Nov							0.37			0.52		
Dec							0.31			0.44	0.33	

(b) Precipitation station data for Arkhangelsk (64°60'N, 40°50'E; 1881-2003). Correlation coefficients significant at 0.05 are shown (> 0.18).

	Jan	Feb	Mar	Apr	May	Jun	Jul	Aug	Sep	Oct	Nov	Dec
Jan												
Feb												
Mar												
Apr	0.22	0.27	0.23	0.25								
May	0.20				0.19							
Jun				-0.23								
Jul		-0.19										
Aug		-0.20					0.21	0.33				
Sep												
Oct												
Nov										0.39		
Dec										0.34		

Table 5.2. Correlation coefficients between seasonal regional precipitation (65-58°N and 40-50°E; 1901-2000) (New *et al.*, 2000) and seasonal SD discharge. Only values significant at 0.05 are shown.

	AMJ precipitation	JA precipitation	SON precipitation
AMJ discharge	0.33		
JA discharge	0.35	0.52	
SON discharge		0.63	0.37

5.2.2. Air temperature

Two mean air temperature data sets have been used to quantify the relationship between SD discharge and regional and local precipitation:

1. Monthly and seasonal precipitation time series for Arkhangelsk (64^{o}60' N, 40^{o}50' E), 1881-2003, derived from DSS UCAR (http://dss.ucar.edu/datasets/ds570.0/);
2. Monthly and seasonal precipitation time series averaged over the SD catchment area (58-65^{o} N; 40-50^{o} E), 1901-2000, derived from the New *et al*. (2000) high-resolution data set.

The quality of Data sets is discussed in section 3.3. The monthly and seasonal temperature time series are shown in Figures 5.4 and 5.5. Monthly temperatures at Arkhangelsk reveal positive linear trends (significantly at 0.05) between March and June, and also in October, over the period of observations. The seasonal time series reveal a significant increase during the AMJ season since 1881.

An important feature of the temperature time series is a warming observed during the 1930-1940s. This phenomenon, known as the 'early 20th century Arctic warming' (Bengtsson *et al*., 2004; section 2.4.2.1), affected the Arctic Ocean basin (extending as far south as 55^{o} N in western Siberia) being particularly well expressed in the Barents Sea sector (which is closest to the SD catchment). With regard to the SD catchment, the warming of the 1930-1940s was particularly well expressed over the northern part of the catchment (station Arkhangelsk) between July and November (Figure 5.3). The warming correlated well with drier-than-average climate (Figure 5.1; Paeth *et al*., 2001) and low SD discharge (Figure 4.2). Following the warmer 1930s-1940s, mean air temperatures declined until the 1970s in most months (Figure 5.1). The last two decades of the 20th century and the beginning of the 21st century were characterised by increasing air temperatures. Unlike the warming of the 1930s-1940s, which predominantly affected the high latitudes of Eurasia (Bentsson *et al*., 2004; Johanessen *et al*., 2004), the recent warming trend – evident at Arkhangelsk and over the SD catchment – has been observed over most terrestrial regions (Johanessen *et al*., 2004; Serreze and Francis, 2006; section 2.4.2.1). The recent warming trend is also evident in most months with the exception of SON season, which does not exhibit a warming trend (Figure 5.5).

Correlation coefficients between air temperature and SD discharge time series, concurrent and with time lag, have been calculated to quantify the relationship between air temperature and

SD discharge (Tables 5.3 and 5.4). SD discharge between June and August correlates negatively with air temperature in the concurrent and preceding months. These correlations are driven by (i) the impact of enhanced evaporation on discharge and (ii) by the fact that in north-western Russia the warm spring and summer months are also the dry ones (blocking anticyclones forming over Scandinavia and north-western Russia lead to warm and dry conditions). The negative correlation between the SD discharge in summer and the preceding winter-spring months (in particular April) reflect the impact of air temperature on snow cover (section 5.2.3). By contrast, positive correlations between air temperature and discharge occur between October and April mostly in the concurrent months reflecting temperature control over river ice formation in November-December (Ginzburg and Soldatova, 1996) and over snowmelt between February and April (Richard and Gratton, 2001). Snowmelt in the SD basin begins on average between the 10th of April in the south-western part of the catchment and the 30th of April in the north-western catchment part (Ye and Ellison, 2003). The highest positive correlations are therefore between April discharge and April air temperature (0.75) (Table 5.3). With regard to seasonal discharge, both the concurrent JA temperature and the preceding AMJ temperature shape JA discharge, with correlation coefficients ranging between -0.36 to -0.43 (Table 5.4).

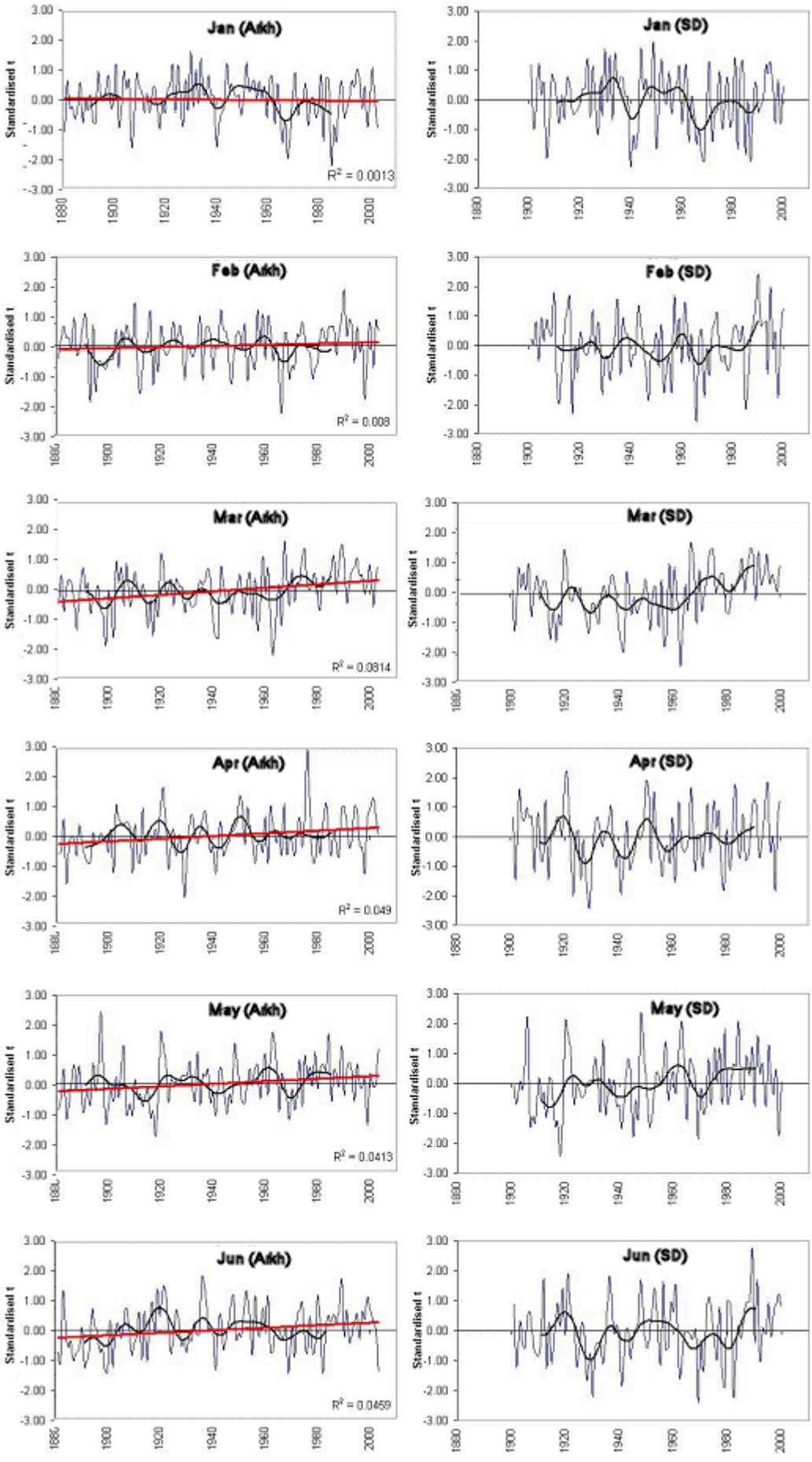
Jan (Akh)
Jan (SD)
Feb (Akh)
Feb (SD)
Mar (Akh)
Mar (SD)
Apr (Akh)
Apr (SD)
May (Akh)
May (SD)
Jun (Akh)
Jun (SD)
Standardised t
R² = 0.0013
R² = 0.008
R² = 0.0814
R² = 0.049
R² = 0.0413
R² = 0.0459

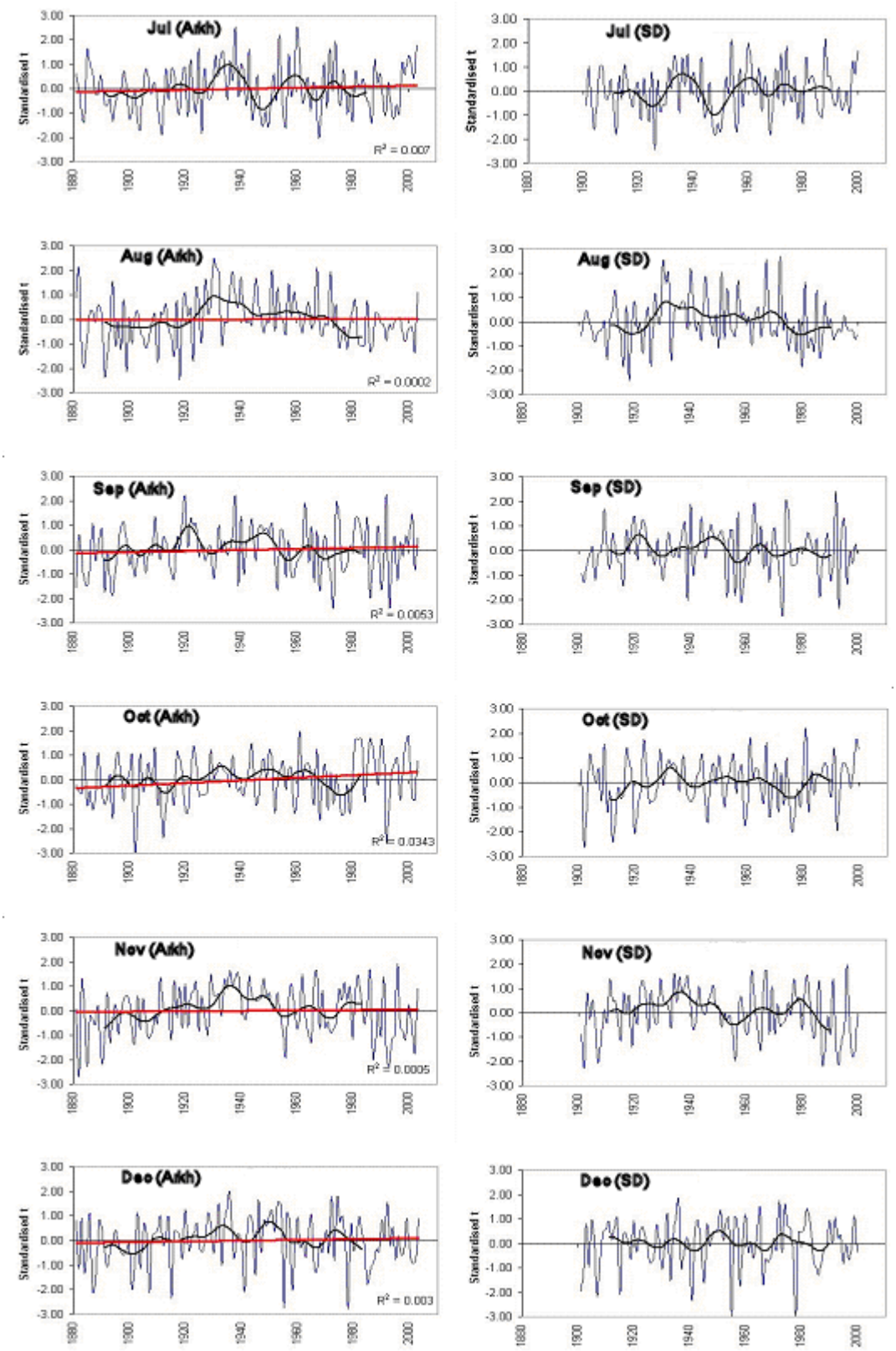

Figure 5.4. Standardised monthly mean air temperature at Arkhangelsk (1881-2003; 64°60'N, 40°50'E) and for the SD catchment (1901-2000). Data have been derived from New *et al*. (2000) gridded data set and averaged over the catchment of the SD (58 – 65° N, 40 – 50°E). Linear trends are shown in red (on Arkhangelsk data), Henderson filter in black.

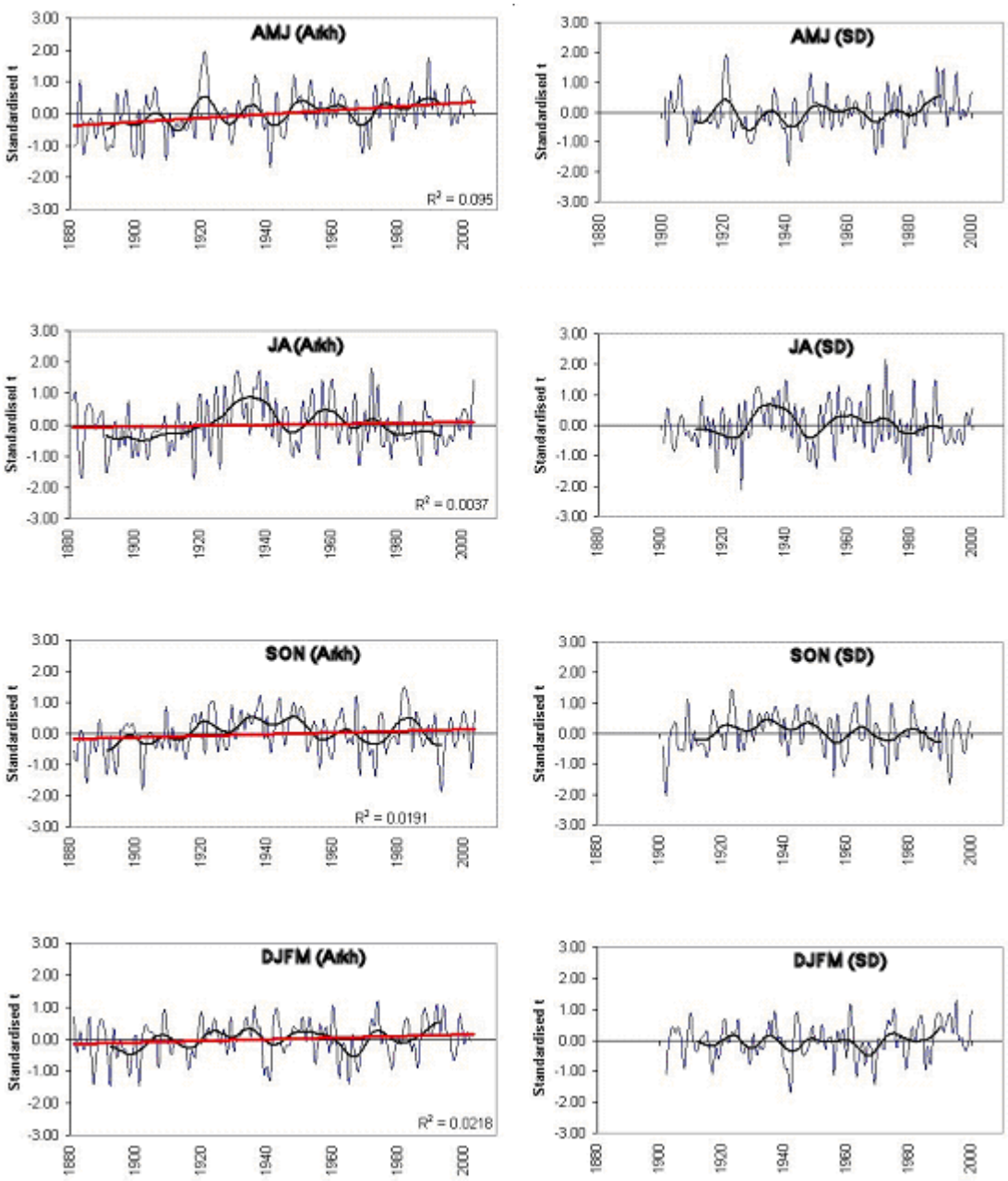

Figure 5.5. Standardised seasonal temperature at Arkhangelsk (1881-2003; 64°60'N, 40°50'E) and for the SD catchment (1901-2000). Data have been derived from New *et al*. (2000) gridded data set and averaged over the catchment of the SD (58 – 65° N, 40 – 50° E). Linear trends are shown in red (on Arkhangelsk data), Henderson filter in black.

Figure 5.6. shows the time series of seasonal regional air temperature against seasonal SD discharge for the overlap period (1901-1995). The correlation between air temperature and discharge is negative in AMJ and JA, whereby positive air temperature anomalies are associated with below-average discharge events, and vice versa.

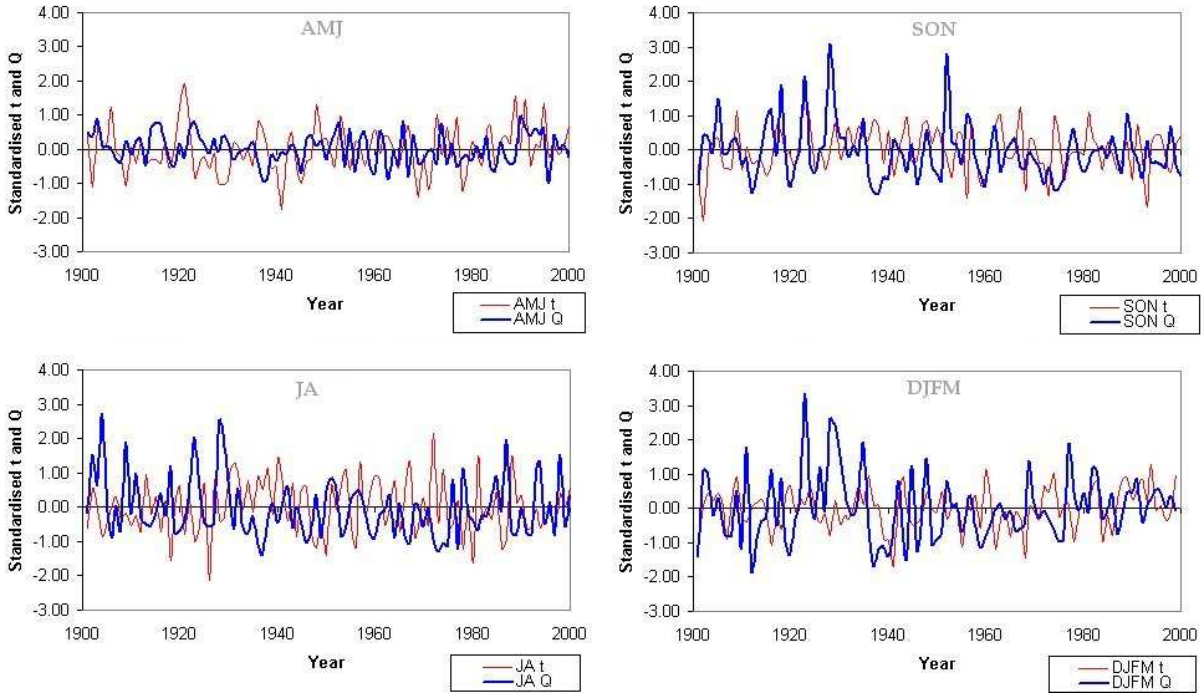

Figure 5.6. Regional seasonal air temperature versus seasonal SD discharge (1901-2000). t = temperature, Q = discharge.

Table 5.3. Correlation coefficients between monthly air temperature and monthly SD discharge.

(a) Regional temperature averaged over the SD catchment (65-58°N and 40-50°E) (1901-2000) (New *et al.*, 2000). Discharge months are shown in blue and temperature months are shown in red. Correlation coefficients significant at 0.05 are shown (>0.20).

	Jan	Feb	Mar	Apr	May	Jun	Jul	Aug	Sep	Oct	Nov	Dec
Jan												
Feb	0.26											
Mar	0.25											
Apr			0.28	0.75								
May	0.20											
Jun			-0.32	-0.67	-0.49							
Jul		-0.20	-0.27	-0.30		-0.42	-0.22					
Aug				-0.28			-0.35	-0.24				
Sep				-0.21	-0.21			-0.36				
Oct			-0.30									
Nov			-0.26							0.21	0.21	
Dec			-0.25								0.27	

(b) Temperature at Arkhangelsk (64°60'N, 40°50'E; 1881-2003). Discharge months are shown in blue and temperature months are shown in red. Correlation coefficients significant at 0.05 are shown (>0.18).

	Jan	Feb	Mar	Apr	May	Jun	Jul	Aug	Sep	Oct	Nov	Dec
Jan												
Feb	0.20											
Mar	0.18											
Apr			0.24	0.66								
May	0.21											
Jun				-0.32	-0.60	-0.28						
Jul				-0.24	-0.24	-0.49	-0.22					
Aug					-0.20		-0.39	-0.19				
Sep									-0.27			
Oct									-0.24			
Nov										0.39		
Dec										0.34		

Table 5.4. Correlation coefficients between seasonal temperatures at Arkhangelsk (64°60'N, 40°50'E; 1882-2003) and seasonal SD discharge. Only values significant at 0.05 are shown.

	AMJ temperature	JA temperature	SON temperature
AMJ discharge	-0.21		
JA discharge	-0.43	-0.36	
SON discharge		-0.24	

During SON and DJFM, the correlation turns positive. The highest correlation (r = -0.33) is found for the JA season. For example, it can be seen that in particular the 1930s show positive temperature anomalies connected with discharge far below the long-term arithmetic mean. Individual years (such as 1972 and 1973) with pronounced low flow in JA correspond well with strongly positive temperature anomalies. Again, the lack of agreement between the simultaneous temperature impact and discharge in the AMJ, SON, and DJFM hydrological seasons points towards the fact that the response of discharge often is often lagged.

5.2.3. Snow depth and duration of snow cover

Figure 5.7 shows the time series of snow depth measured at three sites located in different sectors of the SD basin: Arkhangelsk (1900-2001) representing the northernmost part of the catchment, and Koynas (1924-2001) and Kotlas (1936-2001) located in the central part of the

catchment. All three sites are on average characterised by the onset of snow cover in October and complete melt in May. Two time series of snow depth are presented for each station: October-May (O-M; termed 'snow cover season') average snow depth (Figure 5.5 I) and March (the month of maximum accumulation) snow depth (Figure 5.5 II). Duration of snow cover is also discussed. Details of the two station data sets are discussed in section 3.3.1.

As it has been shown in section 2.4.2.2, ambiguity exists about trends in snow depth and duration of snow cover in Eurasia including northern European Russia and trends at Arkhangelsk, Kotlas, and Konyas do not entirely agree with some of the published results. The long-term trends in snow depth time series for October-May (Figure 5.7 I) differ between the three sites. At Kotlas, the strongest linear increase in snow depth during the snow cover season is observed with the linear trend accounting for 28% of the total variance (Figure 5.7 I-b). Linear trend explains 21% of the total variance in the March time series (Figure 5.7 II-b). This agrees well with the conclusions by Fallot *et al*. (1997), Ye *et al*. (1998), and Popova (2005) who found that snow depth has been increasing in the second half of the 20th century in northern Russia (section 2.4.2.2). The linear increase in snow depth at Koynas has been less pronounced and accounts for about 10% in the O-M time series (Figure 5.5 I-c) and 5% in the March time series (Figure 5.7 II-c). In contrast to Kotlas and Koynas, snow depth has not changed significantly at Arkhangelsk between 1900 and 2001. The Kotlas and Koynas records indicate that the warm 1940s were characterised by low snow accumulation and the same is evident from the Arkhangelsk snow depth record for March (Figure 5.7 II-a). These trends are in line with a general reduction in precipitation observed across the SD catchment in the 1940s (Figure 5.2). Trends in snow depth in the second half of the 20th century vary across the region. At Kotlas (Figure 5.7 I-b and II-b) snow depth increased steadily towards the end of the 20th century, while at Koynas (Figure 5.7 I-c and II-c) snow depth peaked in the 1960s.

It should be note that the Arkhangelsk snow depth time series is characterised by a sharp change in the values of snow depth that occurred in 1963-64. Analysis of the snow depth data quality by Breiling *et al*. (2006) has not produced an explanation for this change. A similar change in snow depth values has been noted by Rawlins *et al*. (2006) who assessed variability in liquid and solid precipitation over the six large Northern Eurasian watersheds for the period between 1936 and 1999 (section 2.4.2.2).

(I) Snow depth averaged for the snow cover (O-M) season

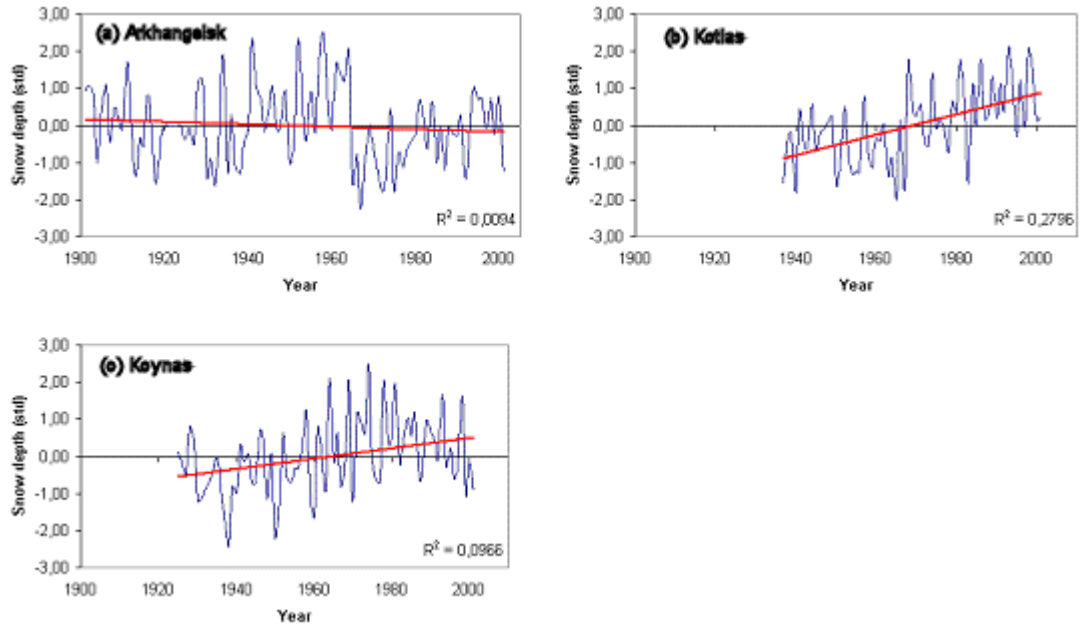

(II) Snow depth during March

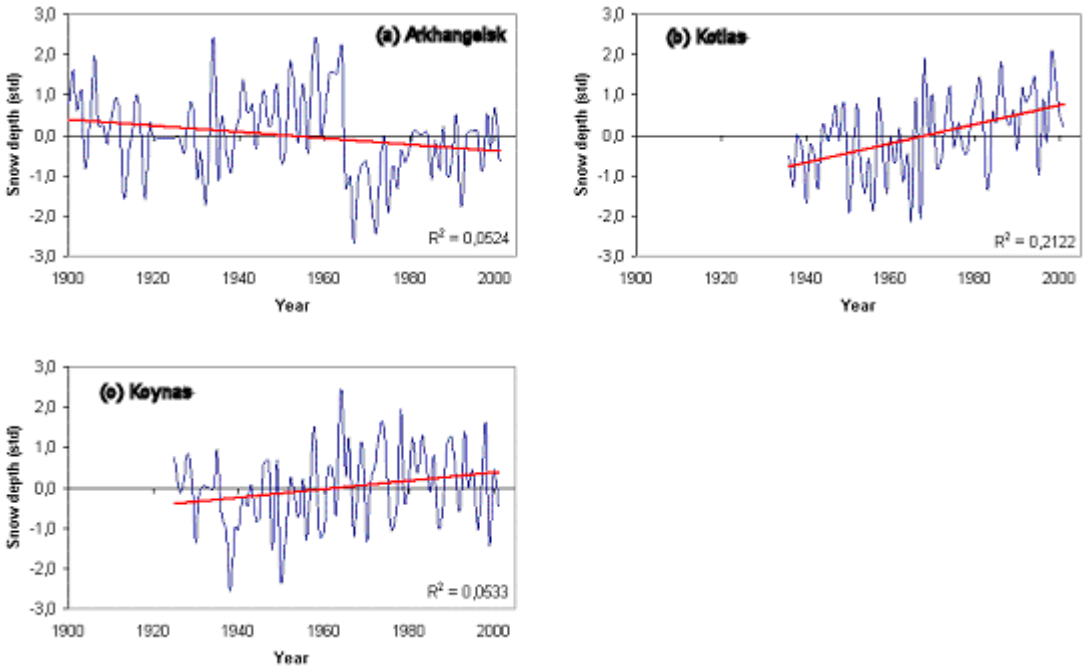

Figure 5.7. Average snow depth at Arkhangelsk, Koynas and Kotlas for (I) October-May and (II) March (based on Breiling *et al*., 2006).

Upon personal communication, Dr Rawlins (University of New Hampshire, USA) has confirmed that a sharp change in snow depth in the White Sea region during the early 1960s is evident from both the New *et al*. (2000) and Willmott and Matsuura (2001) data sets. Dr Rawlins and his co-workers investigated possible sources of error in Data sets and have not

uncovered any systematic errors in either snow depth measurements or winter precipitation measurements. Note that the application of a correction factor to precipitation data for the FSU area (37-70^{o} N, 25-140^{o} E) in 1966-67 (Groisman *et al*., 1991; section 3.3.1) has occurred *after* the observed sharp change (1963-64) in snow depth at Arkhangelsk. The two-sample *t*-test (section 3.4) has been applied to test for a possible step change around 1963-64. As a result, the sharp drop at Arkhangelsk constitutes a significant change point at 0.05. Therefore, an early phase (between 1901 and 1963) with above-average snow depth is distinguished from a later phase (1964-2001) with below-average snow depth values.

Figure 5.8 shows the time series of the onset and complete melt of snow pack, and duration of snow cover in the northern (Arkhangelsk) and central (Kotlas) areas of the SD catchment (data for Koynas are not available). It should be noted again that, although the Arkhangelsk time series is the longest of all meteorological series used in the study, it lacks data between 1920 and 1925 that have been replaced by the long-term arithmetic mean values (section 3.3.1). Therefore, the snow depth values given for the first pentad of the 1920s should not be used when linking it to discharge changes in that particular period. However, for the purpose of identifying linear changes over the centennial time span in the northernmost SD catchment, the Arkhangelsk record remains invaluable.

At both sites, the onset of snow cover occurred earlier in the 1980s-1990s in comparison with the earlier years (e.g. 1950s) although considerable inter-annual variability was evident during these two decades. This is in line with conclusions by Ye and Ellison (2003; section 2.4.2.2). Over the duration of record, the date of onset of snow cover has not changed in the northern part of the catchment (Arkhangelsk; Figure 5.8 a) but the melt of snow cover (Figure 5.8 b) started significantly later over time, with the linear trend accounting for 12% of observed variance. The opposite is true at Kotlas, where the onset of snow cover started significantly earlier (linear trend accounting for 5% of variance; Figure 5.8 a), whereas no change in the end of snow season is apparent since 1936.

Overall, the total length of the snow cover season has significantly increased since 1936 over different parts of the SD catchment either by an earlier start of snow cover formation and/or a later melt. The linear trend in the total duration of the snow cover season at both Arkhangelsk and Kotlas accounts for over 6% of the observed variance in the time series dating back to

(a) Onset of snow cover

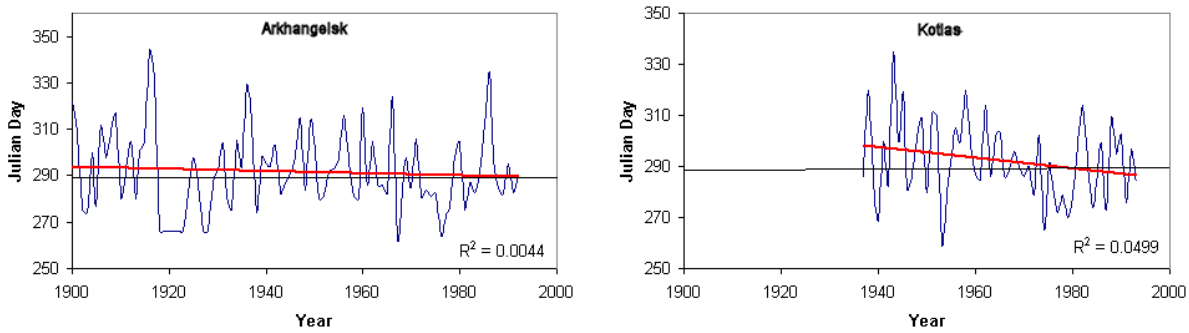

(b) Complete melt of snow cover

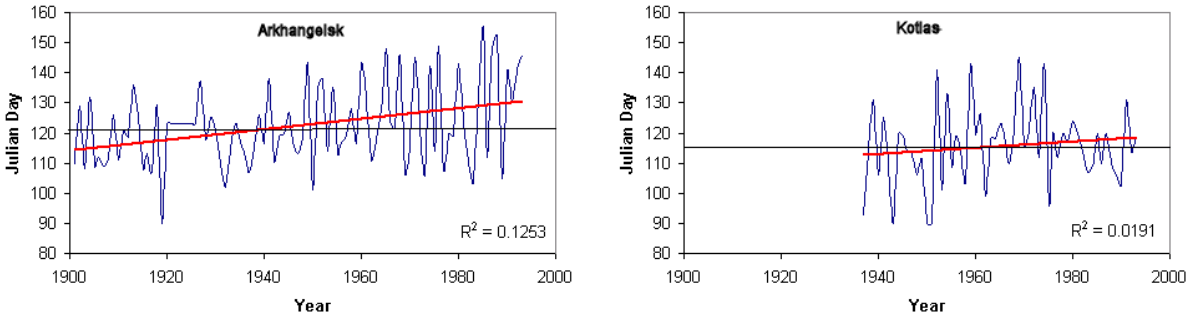

(c) Duration of snow cover season

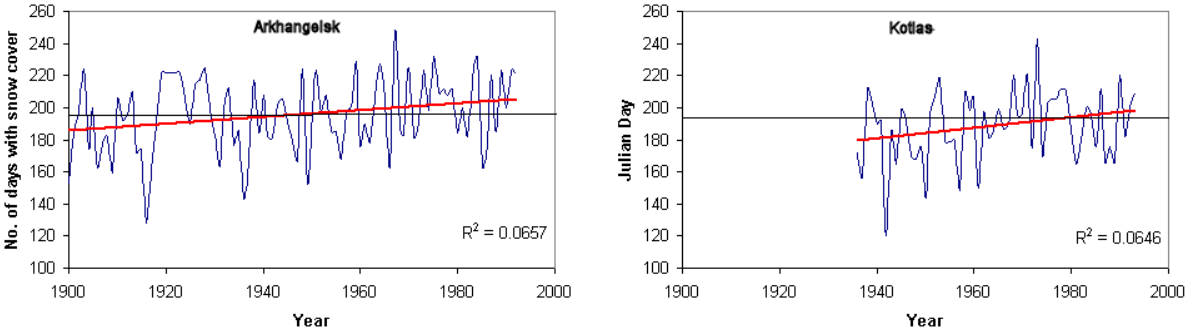

Figure 5.8. Dates (Julian day) of (a) the onset, (b) complete melt of snow pack and (c) duration of snow cover season at Arkhangelsk (1900-94) and Kotlas (1936-94

1900 and 1936 (Figure 5.8 c), whereas the linear increase at Arkhangelsk accounts for 10% of the observed variance after 1936 (not shown). These results agree with Ye and Ellison (2003) who concluded that the duration of the snow cover season in northern European Russia has shifted between 1937 and 1994 towards an earlier onset and earlier melt leading to an overall increase in the length of snow season by about four days per decade (section 2.4.2). Groisman

et al. (1994 a) suggested that a positive feedback operates between air temperature and snow pack: an earlier melt increases surface temperature over Eurasian land mass.

Table 5.5 illustrates the links between snow depth, complete melt of snow pack, and seasonal discharge since 1936. A moderate relationship is evident between snow depth at Arkhangelsk during individual winter months (December, January, February, and March) with the following AMJ high flow season and the SON season. However, snow pack depth does not affect the JA and DJFM discharge (Table 5.5 a). The end of the snow cover season in Arkhangelsk exhibits a positive relationship with the JA season (Table 5.5 c), suggesting that a later end leads to higher summer discharge.

Table 5.5. Correlation coefficients between (a) monthly snow depth at Arkhangelsk, (b) monthly snow depth at Kotlas, (c) end of snow season at Arkhangelsk, and seasonal discharge of SD (1936-2001). Only coefficients significant at 0.05 (> 0.21) are shown.

(a) Snow depth at Arkhangelsk

Discharge Season	**Oct**	**Nov**	**Dec**	**Jan**	**Feb**	**Mar**	**Apr**	**May**
AMJ			0.27	0.36	0.30	0.27		
JA								
SON				0.45	0.35	0.30	0.31	
DJFM								

(b) Snow depth at Kotlas

Discharge Season	**Oct**	**Nov**	**Dec**	**Jan**	**Feb**	**Mar**	**Apr**	**May**
AMJ				0.26	0.31	0.33		
JA							0.30	
SON							0.29	
DJFM								

(c) End of snow season at Arkhangelsk

Discharge season	**Complete melt of snow pack at Arkhangelsk**
AMJ discharge	
JA discharge	0.28
SON discharge	
DJFM discharge	

5.2.4. P-E (effective precipitation)

The question arises whether P-E is a useful concept in an environment with seasonally frozen water storage (following personal communication with Dr Hannah, University of Birmingham, UK). The author of this study argues that although solid precipitation is indeed a major component of the hydrological budget of north-western Russia – snow cover lasts from 160 to 200 days within the SD catchment (Figure 2.11) – it is significant to consider P-E as a measure of water that is effectively available for runoff and discharge generation (see, for example, Serreze *et al*. (2003 a) considering monthly P-E values over Northern Eurasia). Furthermore, even in winter, evaporation occurs (for monthly maps refer to Serreze *et al*., 2003 a). Therefore, P-E is different from raw precipitation not only during the warm half of year but also during the cold half. It is regrettable that no information is available on evaporation (monthly long-term time series), which would be another measure for studying meteorological changes in the region.

Monthly values for P-E at the 850 hPa geopotential height surface have been obtained from the NCEP/NCAR reanalysis data set (Kalnay *et al*., 1996) and averaged over the SD catchment (58-65^{o} N, 40-50^{o} E) for the 1948-2000 time period. The quality of the reanalysis data is discussed in section 3.3.2. It should be noted briefly that although temporal discontinuities in the reanalysis data inevitably occur in Data set due to the differences in amount and quality of the assimilated data, the studied region is not affected strongly because a relatively dense rawinsonde network exists in the sub-Arctic area of European Russia (Serreze *et al*., 1995).

Figures 5.9 shows climatology of the mean monthly P-E values and Figure 5.10 illustrates the variability in spatially-averaged P-E seasonal time series between 1948 and 2000. Throughout the year, P-E remains positive in the SD catchment with the exception of slightly negative values in the southern part of the catchment during July, which is consistent with the negative P-E budget over large land areas of Eurasia (Serreze *et al*., 2003 a). Monthly totals of P-E over the SD catchment (Figure 5.9) peak in September-October due to the combined effect of a stronger vapour flux convergence and a strong seasonal decrease in water vapour storage, being consistent with the other Arctic drainage basins (Serreze *et al*., 2003 a). The lowest values over the SD catchment are observed in early summer (June). This finding agrees with the study by Serreze *et al*. (2003 a), who highlight that effective precipitation is at a minimum over Eurasia in summer due to high evapotranspiration while, at the same time, the static stability is reduced after snowmelt convective heating of land surfaces resulting in high

precipitation (Serreze and Hurst, 2000). Monthly effective precipitation has been plotted along with monthly discharge for comparison. It can be seen that both factors are not moving in common. P-E decreases from October to June and increases from June to October, whereas discharge shows a rapid increase in spring, a peak in May, and a decline thereafter. The disagreement between the two factors underlines the fact that discharge often lags precipitation (Table 5.6).

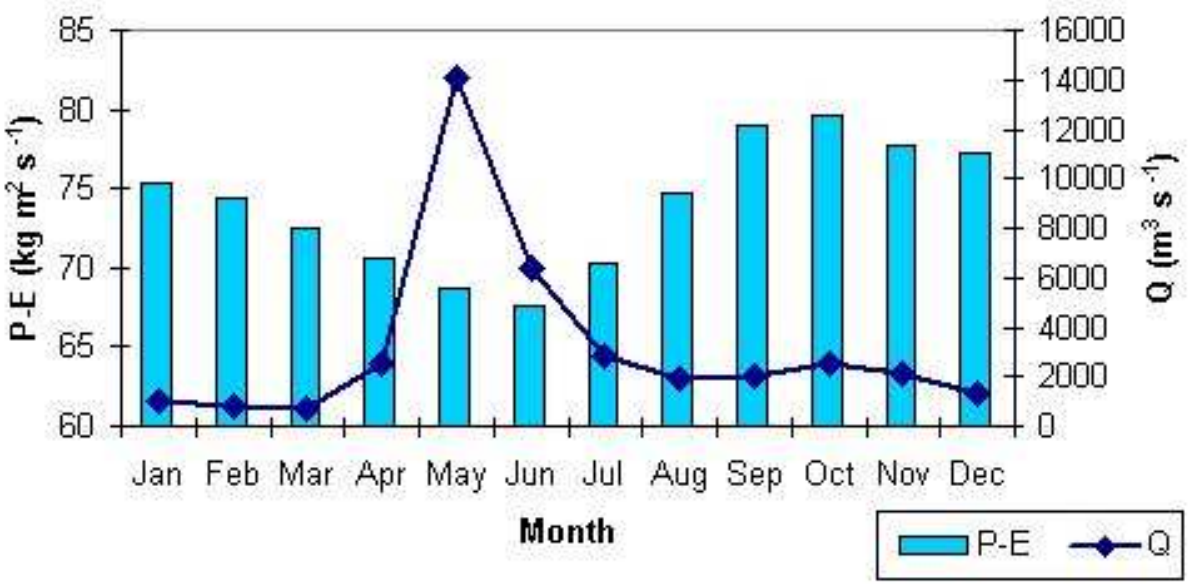

Figure 5.9. Monthly P-E (kg m^2 s^{-1}) at the 850 hPa surface averaged over the SD catchment (58-65^{o}N, 40-50^{o}E) and monthly SD discharge, shown together in order to emphasize the relationship between the two.

Two seasonal P-E time series for SON and DJFM exhibit negative trends in effective precipitation significant at 0.01 and explaining 15% and 13% of the total variance respectively. Although the negative trend in the SON P-E time series is consistent with a decrease in precipitation in the SD catchment (Figure 5.1), trends computed from both gridded precipitation data set (New *et al*., 2000) and reanalysis data should not be taken at face value as they can be influenced by the amount and quantity of the assimilated data (Kistler *et al*., 2001; Rawlins *et al*., 2006). In particular, a divergence of trends in the winter precipitation time series for Arkhangelsk and the SD catchment has been noted. Little change has been observed during the warm part of the year although the very low value of effective

precipitation should be noted in the mid-1960s and in the early 1970s when some of the hottest and driest summers on record occurred (e.g. 1973 and 1972).

The links between P-E at the 850 hPa geopotential height level and seasonal SD discharge have been established for the 1948-2000 period (Table 5.6). The monthly correlation coefficients (Table 5.8 a) are highest during summer with June and July P-E influencing the July and August discharge (r = 0.58).

Table 5.6. Correlation coefficients between monthly P-E (averaged over the SD catchment, 58-65^{o} N, 40-50^{o} E) and (a) monthly and (b) seasonal SD discharge (1948-2000). Discharge months are shown in blue and P-E months are shown in red. Coefficients significant at 0.05 (> 0.27) are shown.

(a) Monthly P-E versus monthly discharge

	Jan	Feb	Mar	Apr	May	Jun	Jul	Aug	Sep	Oct	Nov	Dec
Jan												
Feb												
Mar												
Apr												
May												
Jun					0.38							
Jul						0.58						
Aug							0.58					
Sep								0.44				
Oct									0.32			
Nov										0.44		
Dec		-0.32										

(b) Monthly P-E versus seasonal discharge

	Jan	Feb	Mar	Apr	May	Jun	Jul	Aug	Sep	Oct	Nov	Dec
AMJ		0.27			0.33							
JA						0.42	0.45					
SON	0.28							0.36	0.31			
DJFM										0.32		

Generally, effective precipitation leads discharge by one month. The correlation coefficients between P-E and discharge agree well with those between precipitation and discharge (Table 5.1 a) during the summer months (r > 0.42).

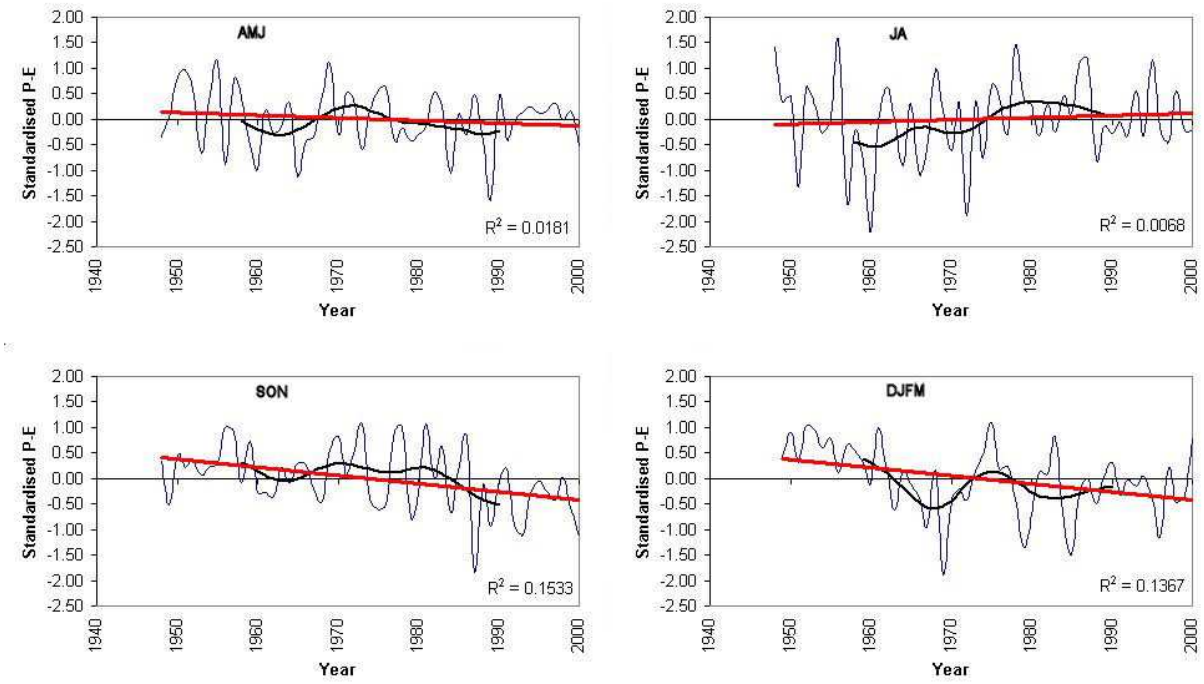

Figure 5.10. Seasonal standardised time series of P-E at the 850 hPa surface derived from the NCEP/NCAR reanalysis and averaged over the SD catchment (1948-2000).

5.2.5. Sea level pressure (SLP)

Figure 5.11 shows the seasonal time series of SLP (Trenberth and Paolino, 1981) over the SD catchment (58-65^{o} N, 40-50^{o} E). The AMJ time series does not reveal any linear changes, while JA SLP increased slightly, and SON and DJFM SLP decreased slightly. Note the high SLP values during JA in the late 1930s are associated with low discharge.

Table 5.7 quantifies the links between SLP averaged over the SD catchment and seasonal SD discharge between 1899 and 2004. The summer SLP is associated with both summer and autumn discharge with correlation coefficients ranging between -0.40 and -0.56. The underlying mechanism is straightforward: In European Russia, the warm summer months are also the dry ones (Shahgedanova, 2002). Thus, high pressure in summer leads to warm and dry conditions across the watershed, thereby reducing the JA and SON discharge of SD. This shows that during this time of year, the regional circulation over the SD catchment is more important than distant forcing. However, in the other months, regional climate is less important, given that large-scale atmospheric forcing becomes more dominant, as is discussed in the following section.

Table 5.7. Correlation coefficients between SLP over the SD basin and SD discharge (1899-2004).

(a) Monthly SLP averaged over the SD catchment (65-58°N and 40-50°E; 1901-2000) (Trenberth and Paolino, 1981). Discharge months are shown in blue and SLP months in red. Correlation coefficients significant at 0.05 are shown (> 0.20).

	Jan	Feb	Mar	Apr	May	Jun	Jul	Aug	Sep	Oct	Nov	Dec
Jan												
Feb												
Mar												
Apr		-0.21	-0.20									
May	-0.22											
Jun				-0.22	-0.27							
Jul						-0.56	-0.24					
Aug			0.20			-0.23	-0.48	-0.34				
Sep	-0.24							-0.55				
Oct								-0.41	-0.39			
Nov						-0.21	-0.27	-0.26		-0.36		
Dec						-0.19				-0.37		

(b) Seasonal SLP averaged over the SD catchment (65-58°N and 40-50°E; 1901-2000) (Trenberth and Paolino, 1981). Discharge months are shown in blue and SLP months in red. Correlation coefficients significant at 0.05 are shown (> 0.20).

	AMJ SLP	JA SLP	SON SLP
AMJ discharge			
JA discharge	-0.27	-0.40	
SON discharge		-0.50	

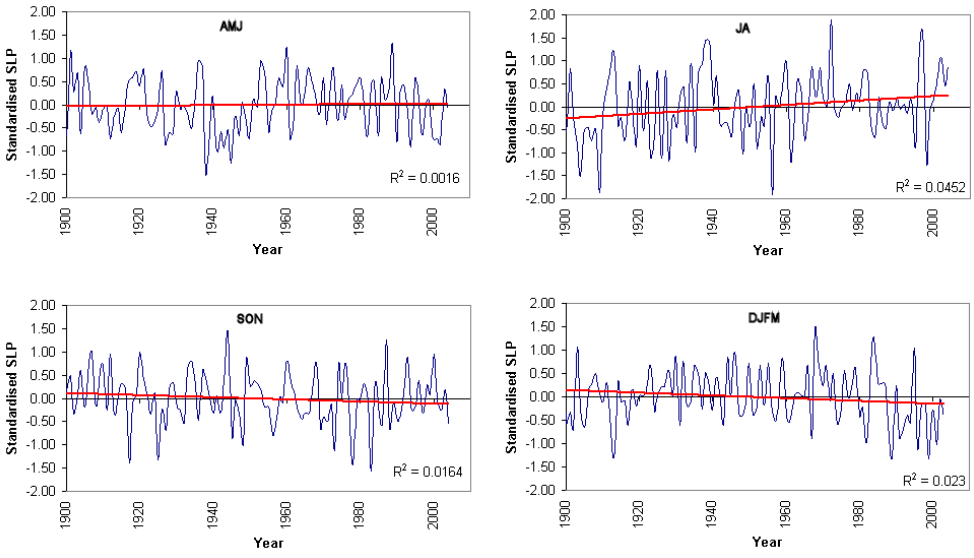

Figure 5.11. Seasonal standardised SLP time series averaged over the SD catchment (58-65° N, 40-50° E; 1900-2004).

5.2.6. Cumulative variance explained by regional climatic factors.

Table 5.8. displays the amount of variance accounted for by the various meteorological variables.

Table 5.8. Cumulative variance in the seasonal discharge of the SD explained by regional climatic factors (1882-1995). p = precipitation at Arkhangelsk, t = temperature at Arkhangelsk. Total variance explained is highlighted in bold.

(a) AMJ

Meteorological variables	Variance explained (%)	Cumulative variance (%)
p DJFM	11.36	11.36
t AMJ	7.86	19.22
t AMJ	0.97	**20.19**

(b) JA

Meteorological variables	Variance explained (%)	Cumulative variance (%)
t AMJ	17.85	17.85
t JA	8.75	26.60
p JA	6.48	33.08
p AMJ	2.04	**35.12**

(c) SON

Meteorological variables	Variance explained (%)	Cumulative variance (%)
p JA	9.21	9.21
t JA	3.07	**12.28**

(d) DJFM

Meteorological variables	Variance explained (%)	Cumulative variance (%)
p SON	20.10	20.10
p JA	18.6	38.70
t JA	2.54	41.24
t AMJ	1.96	43.20
T DJFM	3.66	46.86
t SON	1.11	**47.97**

In the previous sections the time series of regional meteorological characteristics and their links with SD discharge have been discussed, including mean air temperature (section 5.2.1), precipitation (section 5.2.2), snow cover (section 5.2.3), P-E (section 5.2.4) and SLP (section 5.2.5). Cumulative variance in SD discharge explained by temperature and precipitation has been calculated. Results are shown in Table 5.8. These two variables have been employed due to their fundamental influence on discharge and also because they are simulated by regional climate models and statistical downscaling packages (Wilby *et al*., 2004). The latter is important with regard to future projections of SD discharge.

Regional and local factors exert little influence over SON discharge explaining no more than 12% (Table 5.9 c), whereas variability in DJFM discharge is well explained with regional factors accounting for nearly half the observed variance (Table 5.8 d). Between 20% and 35% of total variance in discharge time series is explained by variability in local and regional climate in AMJ (Table 5.8 a) and JA (Table 5.8 b). Seasonal discharge is controlled by variability in meteorological conditions during both the simultaneous and preceding seasons impacted by meteorological influences during previous seasons.

5.3. Links between discharge of the Severnaya Dvina and teleconnection patterns.

It has already been shown in the literature review (Chapter 2) that teleconnections operating in the Northern Hemisphere force inter-annual and inter-decadal variability in local and regional climatic factors that, in turn, control SD discharge. Therefore, it is important to examine the relationships between the main NH teleconnection modes and SD discharge. Two methods have been used to analyse these links.

Firstly, correlation and stepwise regression analyses have been used to link seasonal averages of SD discharge with two sets of monthly teleconnection indices (concurrent and with a time lag) (section 3.3.3). The teleconnection indices used in the correlation and stepwise regression analyses include the North Atlantic Oscillation (NAO), East Atlantic pattern (EA), East Atlantic-Jet (EA-JET), East Atlantic/Western Russia pattern (EA/WR), Polar/Eurasian pattern (POL) and Scandinavian pattern (SCA). The AO index has not been used; correlations

between AO and discharge are similar or marginally lower than between NAO index and discharge. Consequently, AO has not been used. To assess the consistency of the long-term impact of the most dominant teleconnection patterns over time, a running correlation mean has been calculated. This approach is based upon Luterbacher *et al*. (1999), who performed wavelet analysis on the wintertime NAO index. They found spectral power (significant at 0.05) with different frequencies ranging from 19-23 and 50-68 years, of which a 30-year window emerges as an average. The same approach has been adopted in this study, too.

Secondly, composite analyses of the 500 hPa fields associated with low and high discharge years had been used. Data have been derived from NCEP/NCAR (section 3.3.2) referring to 1948-2004. The low and high discharge years have been defined larger than ± 1 standard deviations from the 1948-2004 seasonal averages.

5.3.1. Spring season (AMJ)

Tables 5.9 – 5.10 and Figures 5.12 – 5.13 illustrate the relationships between the AMJ discharge of SD and the main NH teleconnection patterns. For the duration of record, the links between the AMJ discharge and monthly teleconnection indices are not strong ranging between 0.19 and 0.28. AMJ discharge is negatively correlated with the SCA pattern for the winter-spring months (Table 5.11), which is consistent with negative precipitation, and snow cover anomalies in north-western Russia and Scandinavia associated with the positive phase of the SCA (Barnston and Livezey, 1987; Clark *et al*., 1999; Qian *et al*., 2000). A weak positive correlation occurs between the NAO in January and the AMJ discharge reflecting a link between positive precipitation and snow cover anomalies associated with the positive phase of the NAO (Popova, 2005) and enhanced depression activity over northern Europe in winter (Hurrell and van Loon, 1997).

Bradley and Ormerod (2001) established a similar albeit stronger connection between NAO and river discharge for central Wales and by Phillips *et al*. (2003) for Great Britain. Hänninen *et al*. (2000) and Bergström and Carlsson (1994) have shown that river discharge into the Baltic Sea increases with the positive NAO index (section 2.5). The very high values of discharge into the Baltic Sea observed in the 1990s coincide with the strongly positive NAO phase being surpassed only by high discharge in the 1920s. Above-average discharge, comparable to the beginning of the 20th century, characterised the AMJ discharge of SD in the 1990s (Figure 4.3) although in general variability in SD discharge in this season is lower than in other seasons (section 4.4).

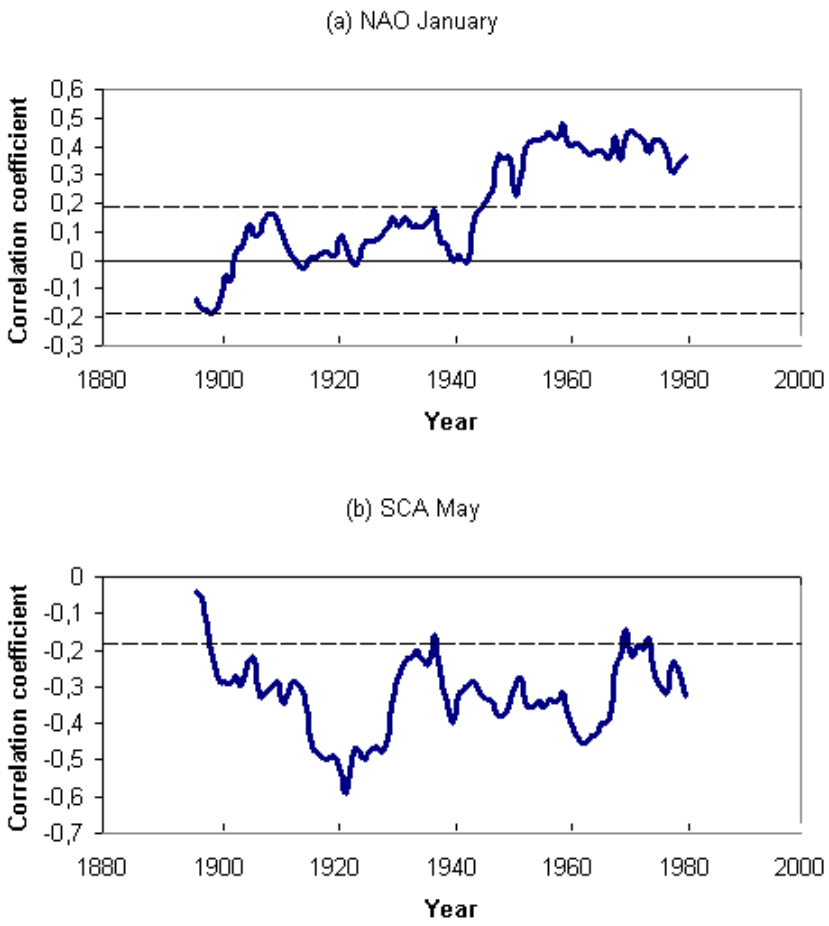

Figure 5.12. The 30-year running means of correlation coefficient between the reconstructed teleconnection indices (Luterbacher *et al.*, 1999) and AMJ discharge of SD: (a) NAO in January and (b) SCA in May. Correlation coefficients above 0.19 are statistically significant at 0.05 (shown as dashed line).

Table 5.9. Correlation coefficients between the monthly teleconnection indices and AMJ discharge of SD (1882-1995). Correlation coefficients above 0.19 are statistically significant at 0.05. Only statistically significant correlation coefficients are shown.

Teleconnection pattern	***r***
SCA_{May}	-0.28
NAO_{Jan}	0.23
NAO_{May}	-0.22
$SCA_{Feb, Mar, Apr}$	-0.19
EA/WR_{Feb}	-0.19

Table 5.10. Cumulative variance in the AMJ discharge of SD (1882-1995) explained by the main NH teleconnection patterns. Total variance explained is highlighted in bold.

Teleconnection pattern	*Cumulative variance (%)*
SCA $_{May}$	6.35
NAO $_{Jan}$	10.51
SCA $_{Feb}$	14.80
EA/WR $_{Feb}$	17.54
SCA $_{Apr}$	**19.34**

The strength of correlation between the SD discharge in AMJ and the main NH teleconnection indices varies in time (Figure 5.11). Thus correlation between the SD discharge and the January NAO index was not statistically significant prior to 1948. By contrast, a moderate correlation ($r \sim 0.4$ to 0.50) was observed in the 1948-1995 period. The change in the strength of relationship between the NAO index and SD discharge may be due to the shifts in the position of the atmospheric centres of action. Mächel *et al*. (1998) have shown that from the beginning of the 20th century to the 1930s the Icelandic low migrated north of its mean climatological position. Between 1920 and 1930, it was centred about 6^{o} west of its mean position, while the Azores high was displaced south of its climatological location between approximately 1900 and the mid-1960s. Dawson *et al*. (2002) suggested that expansion of sea ice around Greenland is one of the possible reasons for the migration of the Icelandic centre of action and displacement of the storm track. Weakening of the NAO and its influence on the climate of the Arctic and sub-Arctic regions in the 1930s-1940s, especially in the Barents Sea sector that is closest to the SD catchment, have been noted by Bengtsson *et al*. (2004). These authors suggest that warm ocean waters increasingly entered into the Barents Sea region leading to negative sea ice anomalies and higher than normal air temperatures which were not associated with the weaker-than-usual NAO observed at the time. The strength of the correlation between the SCA index in May and the springtime SD discharge increased in the 1920s and in the late 1960s – early 1970s (Figure 5.12 b).

Figure 5.13 a shows the difference in January 500-hPa geopotential heights between the years of high AMJ discharge and low AMJ discharge. The revealed pattern showing negative geopotential height anomalies over Iceland and positive over the Bay of Biscay is consistent with the NAO pattern and confirms the controlling role of the NAO over the January precipitation, accumulation of snow, and the AMJ discharge (statistical significance of the

identified anomalies has been assessed by comparing the value of anomalies with standard deviations of the field in the studied region; section 3.4).

A weak negative correlation with the NAO index in May (Table 5.9) reflects the negative precipitation anomalies in north-western Russia, which are associated with a stronger Azores high and its easterly extensions (Shahgedanova, 2002). The weak correlation between the May NAO index and SD discharge in AMJ occurs throughout the record (not shown) being marginally stronger in the late 1940s – early 1950s when the negative values of the NAO index occurred over a few consecutive years.

The anomaly map (Figure 5.13 e) visualises that of greater importance for discharge are geopotential height anomalies over north-western Russia itself and that the presence of negative geopotential height anomalies over the region translates into high AMJ discharge events. The shift from the Atlantic dipole patterns controlling the strength of westerly flow, snowfall, and AMJ discharge towards regional geopotential height anomalies controlling precipitation and discharge occurs approximately in March (Figure 5.11c).

In all, the main NH teleconnection indices explain 19% of the total variance in the AMJ discharge of SD for the duration of the discharge record (Table 5.12). In the post-1950s period (1950-1995), when the influence of the NAO on the climate of the SD catchment was stronger, its correlation coefficient with AMJ discharge approaches 0.41 explaining 16% of the total variance.

(a) January (b) February

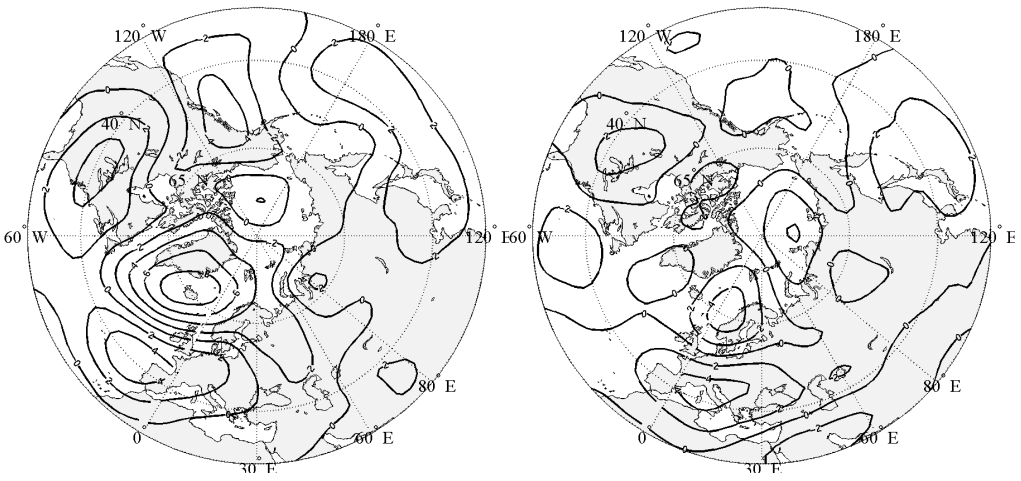

(c) March

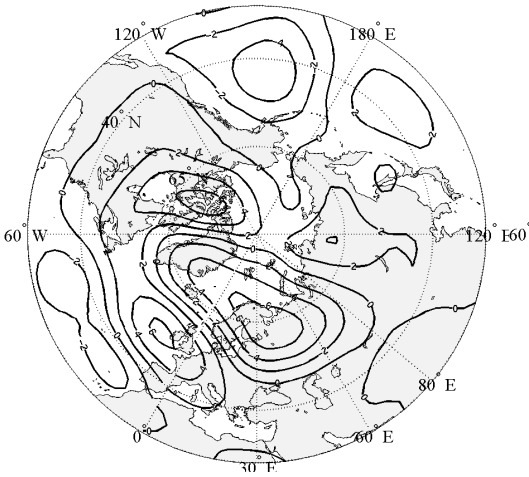

(d) April

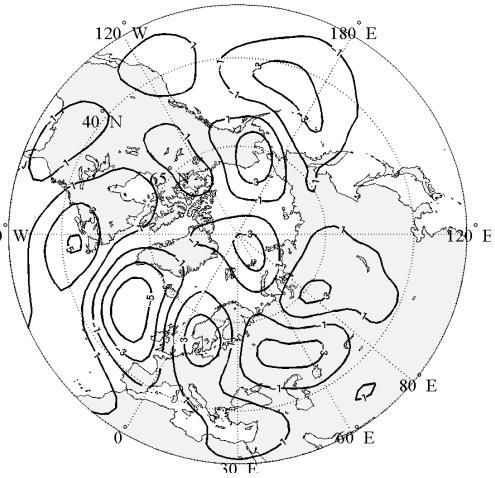

(e) May

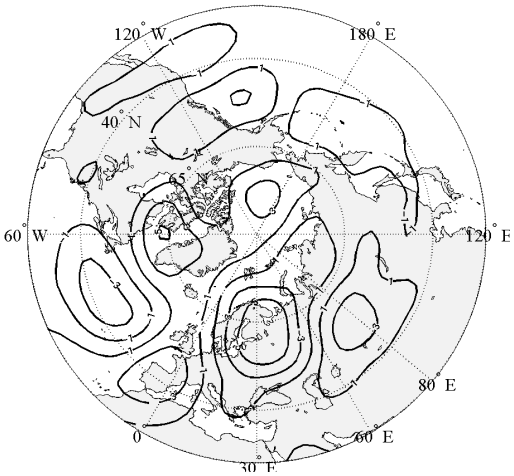

Figure 5.13. Mean 500-hPa geopotential height anomalies associated with composites of high (1952, 1955, 1958, 1961, 1966, 1968, 1974, 1990, 1991, 1993) minus low (1956, 1960, 1963, 1967, 1973, 1975, 1977, 1984, 1985, 1996) AMJ discharge years. Contour intervals are 2 dekametres (dam).

5.3.2 Summer season (JA)

Tables 5.11–5.12. and Figures 5.14-5.15 illustrate the relationships between the JA discharge of SD and teleconnection indices. For the duration of record, the links between the JA discharge and monthly teleconnection indices are weak with correlation coefficients ranging between 0.20 and 0.28. In total, the indices explain 13% of the total variance in JA discharge of SD.

Distant forcing and its influence on local and regional climate is known to be reduced in summer in comparison with other seasons (e.g. Jones and Salmon, 2005). By contrast, regional and regional factors may play a more important role controlling climatic and climate-related variables. Figure 5.14 illustrates an impact of regional anomalies in mid-tropospheric circulation on SD discharge. The low JA discharge years are associated with a strong ridge of elevated geopotential height extending from central Russia to the Barents Sea. The lowest on record JA discharge registered in 1973 (as well as 1972; not shown) was associated with a particularly strong positive geopotential height anomaly that evolved into a blocking high centred over Finland and north-western Russia. Tibaldi and Monteni (1990) identified Scandinavia and the western part of the SD catchment as an area where summer blocking events occurred more frequently than anywhere else in the NH since 1950.

Table 5.11. Correlation coefficients between the monthly teleconnection indices and JA discharge of SD (1882-1995). Correlation coefficients above 0.19 are statistically significant at 0.05. Only significant values are displayed.

Teleconnection pattern	***r***
NAO_{Jun}	-0.27
$EA\text{-}JET_{Jun}$	0.21

Table 5.12. Cumulative variance in the JA discharge of SD (1882-1995) explained by the main NH teleconnection patterns. Total variance explained is highlighted in bold.

Teleconnection pattern	***Cumulative variance (%)***
NAO_{Jun}	6.36
$EA\text{-}JET_{Jun}$	**13.37**

Similarly to AMJ, the strength of correlation between the SD discharge in JA and the main NH teleconnection indices varies in time (Figure 5.15). Thus NAO had the strongest control over SD summer discharge in the early 20th century and in the 1950s (r about –0.50) but had very little impact on the hydrology of the region in the 1970s and 1980s (Figure 5.15 a). During the latter period, a succession of dry years occurred in the SD catchment linked to the blocking events. Although statistically significant, the correlation between the JA discharge of SD and the EA-JET index (Table 5.11) was inconsistent throughout the record with moderate positive correlations observed towards the end of the record (Figure 5.15 b).

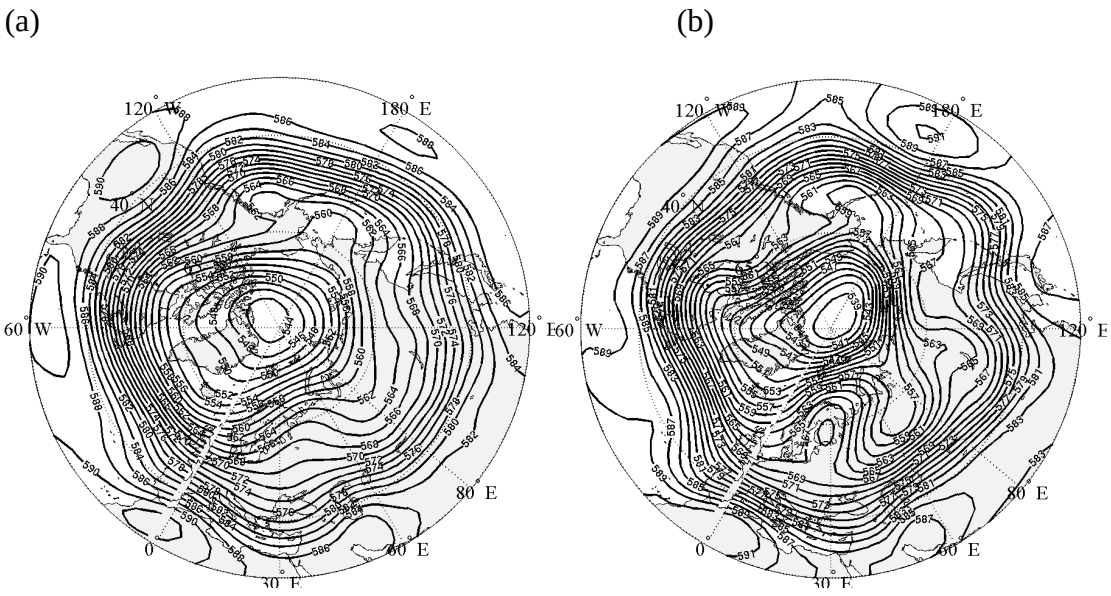

Figure 5.14. (a) July 500-hPa geopotential height anomalies for the low JA discharge years (1949, 1960, 1964, 1967, 1972, 1973, 1974, 1975, 1977) and (b) mean 500-hPa geopotential height field for July 1973. Contour intervals are 2 dekametres (dam).

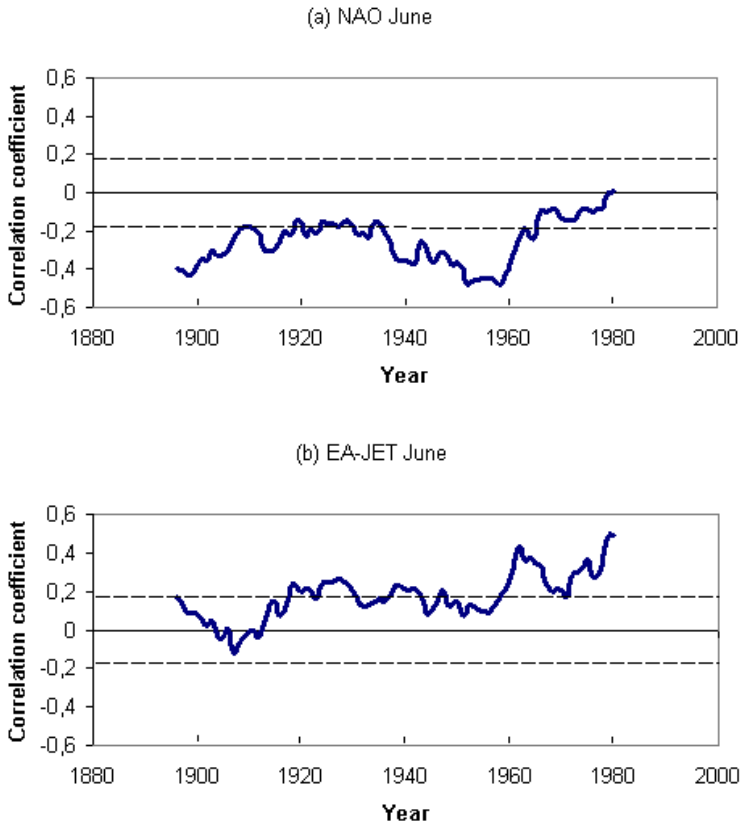

Figure 5.15. The 30-year running means of correlation coefficients between the reconstructed teleconnection indices (Luterbacher *et al.*, 1999) and JA discharge of SD: (a) NAO in June (SD) and (b) EA-JET in June. Correlation coefficients above 0.19 are statistically significant at 0.05 (shown as dashed line).

5.3.3. Autumn season (SON)

Tables 5.13-5.14. and Figures 5.16-5.17 illustrate the relationships between the SON discharge of SD and the main NH teleconnection indices. For the duration of record, the links between the SON discharge and monthly teleconnection indices are weak to moderate with correlation coefficients (statistically significant at 0.05) ranging between 0.19 and 0.33. Spring and summer patterns control SON discharge with a time lag between one and six months (teleconnection patterns leading discharge). The main patterns explain 20% of total interannual variance in the autumn discharge.

Table 5.13. Correlation coefficients between the monthly teleconnection indices and SON discharge of SD (1882-1995). Correlation coefficients above 0.19 are statistically significant at 0.05. Only statistically significant correlation coefficients are shown.

Teleconnection pattern	***r***
EA-JET $_{Jul}$	0.33
EA/WR $_{Mar}$	0.27
EA-JET $_{Aug}$	0.26
NAO $_{Jun}$	-0.19

Table 5.14. Cumulative variance in the SON discharge of SD (1882-1995) explained by the main NH teleconnection patterns. Total variance explained is highlighted in bold.

Teleconnection pattern	***Cumulative variance (%)***
EA-JET $_{Jul}$	10.05
EA/WR $_{Mar}$	16.57
NAO $_{Jun}$	18.34
EA-JET $_{Aug}$	**19.85**

The EA-JET pattern in the summer months emerges as the main control over the SON discharge of SD (Tables 5.13 and 5.14) through its connection with summer rainfall. The positive phase of the EA-JET pattern is characterised by the location of low-pressure centre over the north-eastern Atlantic and a high pressure centre over subtropical Europe and northern Africa (Figure 2.9 b). Similarly to the NAO, the positive EA-JET pattern initiates a

strong moisture flux from the north-eastern Atlantic to northern Europe and has been previously linked to floods on the river Elbe in August 2002 (Dünkeloh and Jacobeit, 2003). The impact of the EA-JET pattern on the SD discharge was strong between the 1880s-1920s with correlation coefficients of approximately 0.6 but was not significant after the 1940s (Figure 5.14 a). By contrast, the EA/WR pattern exhibits weak to moderate (r ranging between 0.30 and 0.40) but consistent correlation with the SD discharge prior to the 1970s. This association declines in the 1980s in line with the declining SLP in the north-eastern Atlantic (Hurrell and van Loon, 1997; Serreze *et al*., 2000) where one of the centres (high pressure during the positive phase) of the wintertime EA/WR pattern is located (Figure 2.9 c).

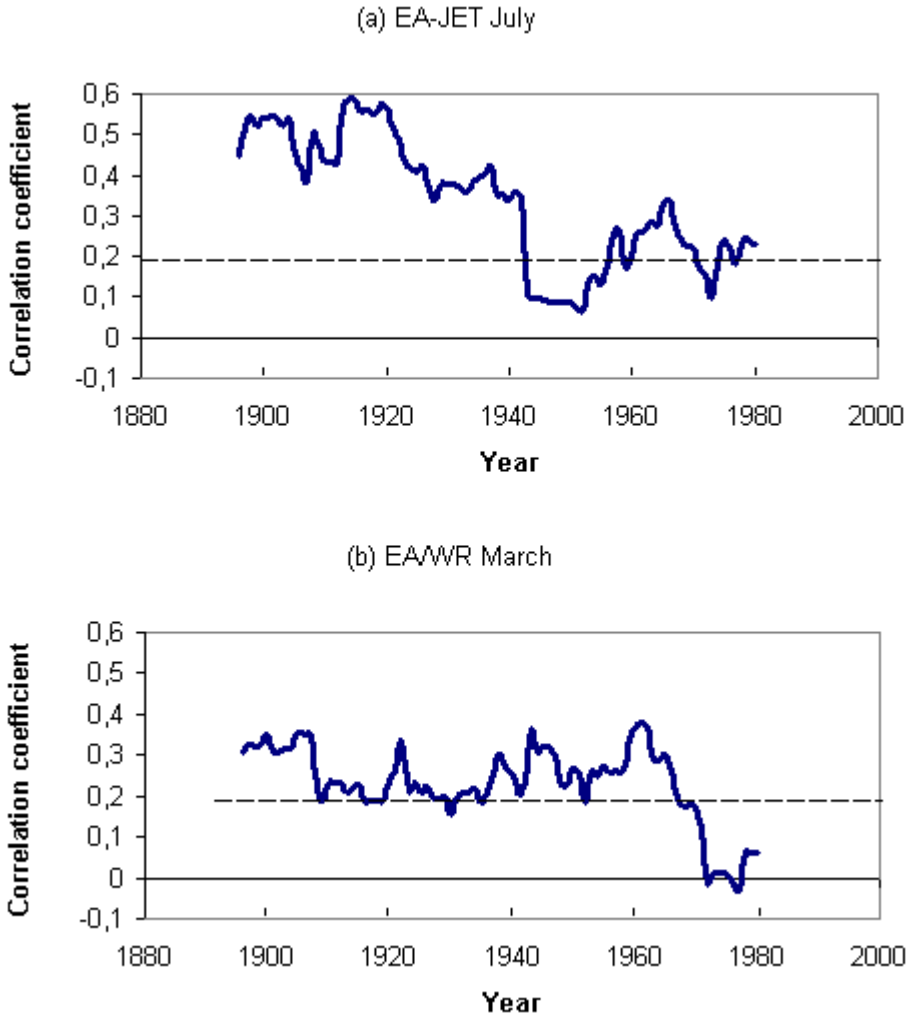

Figure 5.16. The 30-year running means of correlation coefficient between the reconstructed teleconnection indices (Luterbacher *et al*., 1999) and SON discharge of SD: (a) EA-JET in July, and (b) EA/WR in March. Correlation coefficients above 0.19 are statistically significant at 0.05 (shown as dashed line).

(a) September (b) October

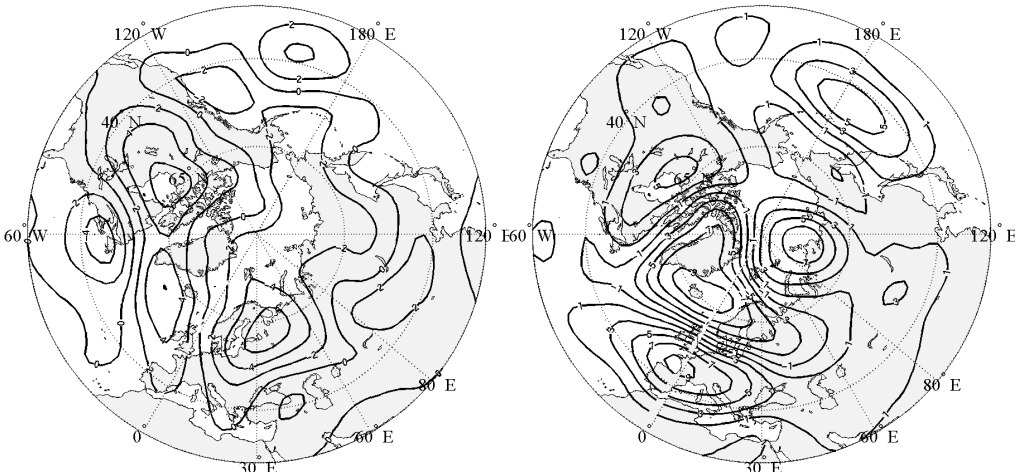

(c) November

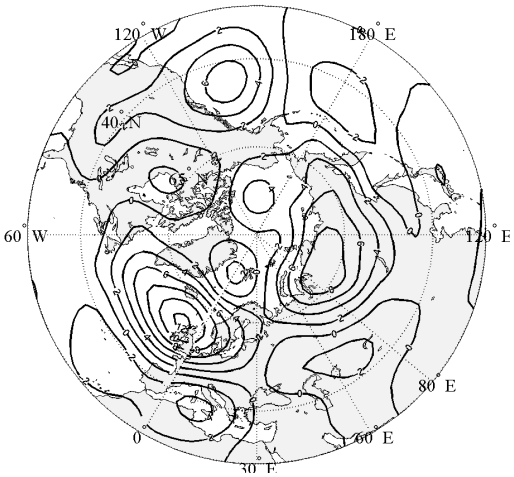

Figure 5.17. Mean 500-hPa geopotential height anomalies for the high SON discharge years (1948, 1952, 1956, 1957, 1962, 1978, 1989, 1998) minus low SON discharge years (1951, 1960, 1972, 1974, 1975, 1992). Contour intervals are 2 dekametres (dam).

Figure 5.17 shows the difference in September, October, and November 500-hPa geopotential heights between the years of high SON discharge and low SON discharge of SD. The September pattern (Figure 5.17 a) is consistent with those for July and August (not shown) suggesting that positive (negative) anomalies in mid-tropospheric circulation over north-western Russia and Scandinavia lead to negative (positive) SD discharge anomalies. Nevertheless, anomalous discharge in October and November (Figure 5.17 b, c) is coupled with a dipole pattern with centres over Iceland and the Bay of Biscay. The displacement of one of the dipole centres north-east of the Azores to the Bay of Biscay explains the lack of

significant correlations between SON discharge and the contemporaneous NAO. Geopotential height anomalies over the Bay of Biscay – rather than the NAO or the intensity of the Azores high – are known to control precipitation over European Russia (Shahgedanova *et al*., 2005).

5.3.4. Winter season (DJFM)

Tables 5.15-5.16 and Figure 5.18 illustrate the relationships between the DJFM discharge of SD and teleconnection indices. For the duration of record, the links between the winter discharge and monthly teleconnection indices are moderate with correlation coefficients ranging between 0.22 and 0.39. The SD remains frozen between mid-November and mid-April (Vuglinsky, 2000; section 3.2.2) and thus summer and autumn teleconnection patterns control the DJFM discharge (teleconnection patterns leading discharge). As the river remains frozen, the influence of the regional factors on DJFM discharge is reduced and the main NH teleconnection patterns explain about one third of total interannual variance in the DJFM discharge exhibiting the strongest influence out of all seasons. The SCA and NAO pattern emerge as the main controls over the DJFM discharge of SD (Table 5.15 and 5.16).

Table 5.15. Correlation coefficients between the monthly teleconnection indices and DJFM discharge of SD (1882-1995). Correlation coefficients above 0.19 are statistically significant at 0.05. Only statistically significant correlation coefficients are shown.

Teleconnection pattern	***r***
SCA $_{Oct}$	-0.39
EA-JET $_{Jul}$	0.30
NAO $_{Oct}$	0.23
SCA $_{Sep}$	-0.22
NAO $_{Jun}$	-0.22

The impact of the SCA pattern on the SD discharge during the DJFM season has been constantly significant over time (Figure 5.18 a). Its impact was strongest in the early part of the record as well as during the 1940s and 1950s (r between 0.40 and 0.60) while the running mean indicates a rapid decline since the 1960s. By contrast, the NAO pattern (Figure 5.18 b) has not always been a significant forcing of DJFM variability. Its greatest impact has been

Table 5.16. Cumulative variance in the DJFM discharge of SD (1882-1995) explained by the main NH teleconnection patterns. Total variance explained is highlighted in bold.

Teleconnection pattern	*Cumulative variance (%)*
SCA $_{Oct}$	14.05
NAO $_{Oct}$	25.35
EA-JET $_{Jul}$	31.49
SCA $_{Sep}$	**33.72**

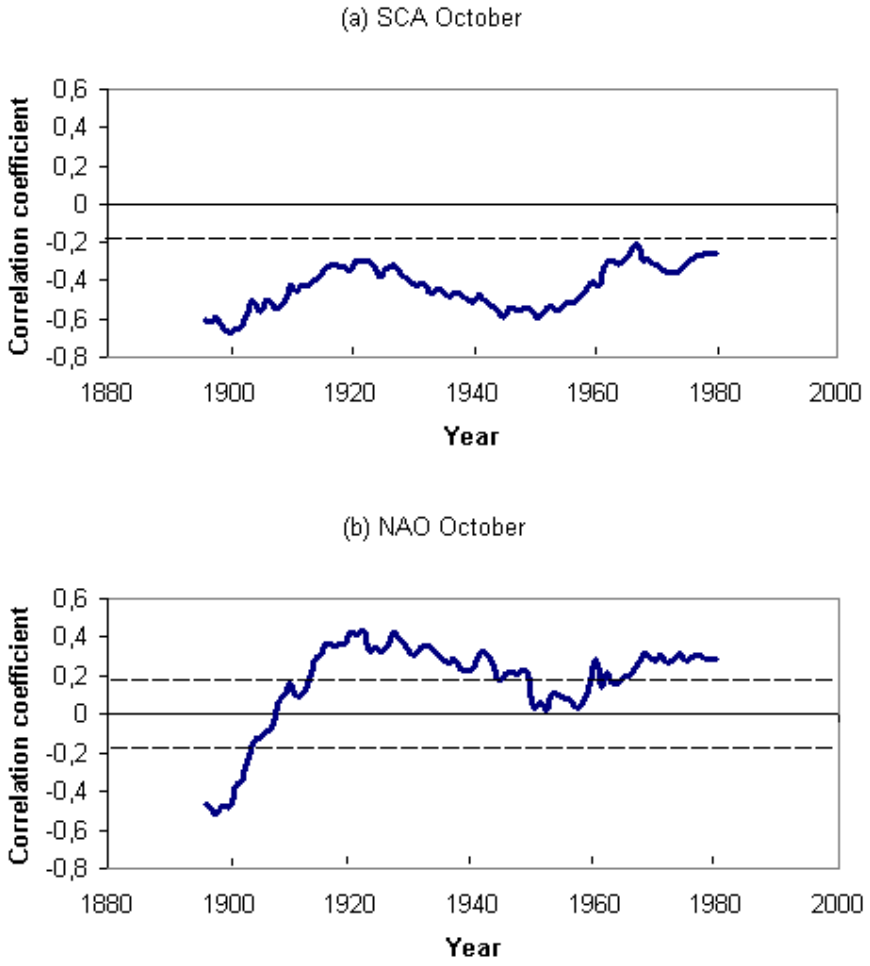

Figure 5.18. The 30-year running means of correlation coefficient between the reconstructed teleconnection indices (Luterbacher *et al*., 1999) and DJFM discharge of SD: (a) SCA in October, and (b) NAO in October. Correlation coefficients above 0.19 are statistically significant at 0.05 (shown as dashed line).

noted during the mid-1910s and 1920s and since the late 1960s, while its impact has been insignificant during certain decades in between.

5.4. Links between teleconnection patterns and regional air temperature, precipitation, and snow cover.

The influence of teleconnection patterns on precipitation over the study area has been quantified by establishing correlation coefficients between the monthly teleconnection indices of the main Euro–Atlantic teleconnection patterns and monthly rainfall, both for the Arkhangelsk station as well as for the SD basin. The results are summarised in Table 5.17. Correlation coefficients significant at 0.05 have been obtained mostly for Arkhangelsk, while significant coefficients with the spatially-averaged precipitation over the SD catchment were less frequent. The AO and NAO patterns correlate with precipitation in winter and spring (Table 5.17 a), whereas the SCA pattern emerges as the main control over precipitation in autumn and winter (Figure 5.17 d) confirming the conclusions by Clark *et al*. (1999) and Qian *et al*. (2000) (section 2.3.2). SCA exerts stronger impacts on the catchment-averaged precipitation in comparison with the Arkhangelsk station. The EA-JET pattern's influence is strongest in June (Table 5.17 b).

The AO and NAO are the strongest forcings of temperature both at Arkhangelsk and over the whole catchment area, especially during February and May (Table 5.18). These results obtained with regard to the SD catchment are in line with previous studies linking changes in air temperature in northern European Russia with changes in atmospheric circulation (as discussed in section 2.4.2.1). Kryjov (2002) has discussed the recent warming in northern Russia and in the Arctic attributing it to the impact of the AO. He estimated that mean air temperature in Arkhangelsk in JFM has increased by 3.7^{o}C between 1968 and 1997 of which 2.6^{o}C warming is related to the positive AO phase. The AMJ air temperature has increased by 1.8^{o}C of which the AO has contributed 1.1^{o}C warming. Similarly, Rigor *et al*. (2000) have calculated that more than a half of the DJF warming observed in the region between 1979 and 1997 has been caused by the positive phase of the AO. Therefore, the recent warming observed over the SD catchment (particularly between 1978-1999 in the DJFM and AMJ seasons; Figure 5.5) agrees well with the positive AO/NAO phase during that period. Another important teleconnection pattern, the SCA pattern (Table 5.18 d) exerts considerable impact on air temperature over the SD catchment in summer ($r > 0.51$ in August), but not during the other months.

Atmospheric circulation controls the interannual and interdecadal variability in snow depth and duration of snow cover although there is no consensus on the nature of these associations.

Table 5.17. Correlation coefficients between monthly teleconnection patterns and monthly rainfall at Arkhangelsk and over the SD catchment (1936-95). Precipitation months are shown in blue and teleconnection months in red. Teleconnection patterns are ordered alphabetically. Only statistically significant coefficients (at 0.05) are shown.

(a) Correlation coefficients between the AO index and the Arkhangelsk precipitation records

	Jan	Feb	Mar	Apr	May	Jun	Jul	Aug	Sep	Oct	Nov	Dec
Jan	0.28											
Feb	0.32											
Mar			0.46									
Apr												
May												
Jun												
Jul												
Aug												
Sep												
Oct												
Nov											0.32	
Dec	0.39											0.39

Correlation coefficients between the AO index and the SD catchment precipitation records

	Jan	Feb	Mar	Apr	May	Jun	Jul	Aug	Sep	Oct	Nov	Dec
Jan												
Feb												
Mar												
Apr												
May												
Jun												
Jul												
Aug												
Sep			-0.33									
Oct												
Nov												
Dec												

(b) Correlation coefficients between the EA-JET index and the SD catchment precipitation records

	Jan	Feb	Mar	Apr	May	Jun	Jul	Aug	Sep	Oct	Nov	Dec
Jan												
Feb												
Mar												
Apr												
May												
Jun						0.46						
Jul												
Aug												
Sep												
Oct												
Nov						-0.33						
Dec								0.29				

(c) Correlation coefficients between the NAO index and the Arkhangelsk precipitation records

	Jan	Feb	Mar	Apr	May	Jun	Jul	Aug	Sep	Oct	Nov	Dec
Jan												
Feb												
Mar			0.35									
Apr				-0.28								
May												
Jun												
Jul												
Aug							-0.29					
Sep												
Oct												
Nov												
Dec												

Correlation coefficients between the NAO index and the SD catchment precipitation records

	Jan	Feb	Mar	Apr	May	Jun	Jul	Aug	Sep	Oct	Nov	Dec
Jan												
Feb												
Mar												
Apr				-0.36								
May			-0.31									
Jun												
Jul												
Aug	0.34											
Sep			-0.30									
Oct												
Nov												
Dec												

(d) Correlation coefficients between the SCA index and the Arkhangelsk precipitation records

	Jan	Feb	Mar	Apr	May	Jun	Jul	Aug	Sep	Oct	Nov	Dec
Jan												
Feb												
Mar												
Apr												
May												
Jun												
Jul												
Aug												
Sep		0.29										
Oct									-0.29	-0.31		
Nov			-0.33								-0.30	
Dec												-0.47

Correlation coefficients between the SCA index and the SD catchment precipitation records

	Jan	Feb	Mar	Apr	May	Jun	Jul	Aug	Sep	Oct	Nov	Dec
Jan	-0.44											
Feb												
Mar		-0.34	-0.32									
Apr												
May		0.31			-0.36							
Jun												
Jul				0.32								
Aug												
Sep									-0.40			
Oct										-0.54		
Nov					0.31						-0.56	
Dec												-0.49

Popova (2005) has investigated the impacts from selected NH teleconnection patterns (including NAO, SCA, POL, and PNA) on snow accumulation over Northern Eurasia between 1951 and 2002. She concluded that the strongly positive NAO winters (NAO index > 1) resulted in above-averaged temperature anomalies (1 to 2^{o} C above long-term mean) and an increase in snow accumulation since the 1970s in European Russia. Correlation between the NAO index in January and the snow depth in February is particularly high for the 1975-2001 period explaining 39% of variance in the snow depth time series. Note that Popova (2005) has studied snow depth changes (for February only) in contrast to other studies (Ye *et al.*, 1998; Ye and Ellison, 2003) considering the whole snow season.

Table 5.18. Correlation coefficients between monthly teleconnection patterns and monthly temperature at Arkhangelsk over the SD catchment (1936-95). Teleconnection months are shown in red and temperature months are shown in blue. Patterns are ordered alphabetically. Only statistically significant coefficients (at 0.05) are shown.

(a) AO for Arkhangelsk

	Jan	Feb	Mar	Apr	May	Jun	Jul	Aug	Sep	Oct	Nov	Dec
Jan	0.44											
Feb												
Mar			0.58									
Apr		0.48										
May		0.49										
Jun		0.34										
Jul												
Aug												
Sep												
Oct										0.33		
Nov												
Dec												0.43

AO for SD catchment

	Jan	Feb	Mar	Apr	May	Jun	Jul	Aug	Sep	Oct	Nov	Dec
Jan	0.44											
Feb	0.59	0.55										
Mar		0.51	0.59									
Apr												
May												
Jun												
Jul												
Aug												
Sep												
Oct												
Nov												
Dec												0.45

(b) EA-JET for SD catchment

	Jan	Feb	Mar	Apr	May	Jun	Jul	Aug	Sep	Oct	Nov	Dec
Jan												
Feb												
Mar												
Apr												
May												
Jun				0.28								
Jul												
Aug												
Sep												
Oct												
Nov				-0.28								
Dec												

(c) NAO for Arkhangelsk

	Jan	Feb	Mar	Apr	May	Jun	Jul	Aug	Sep	Oct	Nov	Dec
Jan	0.31											
Feb	0.43	0.40										
Mar	0.30		0.59									
Apr		0.28										
May					0.42							
Jun	0.29	0.33										
Jul												
Aug					0.28							
Sep									0.29			
Oct		*0.34*										
Nov												
Dec												0.47

NAO for SD catchment

	Jan	Feb	Mar	Apr	May	Jun	Jul	Aug	Sep	Oct	Nov	Dec
Jan	0.35											
Feb	0.39	0.50										
Mar	0.30		0.62									
Apr		0.33										
May					0.31							
Jun		0.34										
Jul												
Aug												
Sep												
Oct		0.34										
Nov												
Dec												0.53

(d) SCA for Arkhangelsk

	Jan	Feb	Mar	Apr	May	Jun	Jul	Aug	Sep	Oct	Nov	Dec
Jan												
Feb												
Mar												
Apr												
May					0.35							
Jun												
Jul												
Aug								0.51				
Sep												
Oct												
Nov								0.37				
Dec										0.30		

SCA for SD catchment

	Jan	Feb	Mar	Apr	May	Jun	Jul	Aug	Sep	Oct	Nov	Dec
Jan												
Feb												
Mar												
Apr												
May												
Jun												
Jul												
Aug								0.56				
Sep												
Oct												
Nov								0.29				
Dec												

The snow depth time series and the time series characterising the onset and melt of snow pack (from which the duration of the snow cover season has been calculated) at Arkhangelsk, Kotlas, and Koynas have been correlated with the monthly indices of the main NH teleconnection patterns (Table 5.19). The SCA pattern has emerged as the main control over snow depth (with correlation coefficients ranging between –0.25 and –0.31), and onset and melt of snow cover in the period since 1936. The moderate negative correlation between the SCA indices in the autumn season (particularly October and November) and snow depth indicates that the positive SCA phase leads to a lower depth of snow pack. The positive SCA phase leads to an extended duration of snow season. This is consistent with the anticyclonic nature of atmospheric circulation over the SD catchment during positive SCA phases and

Table 5.19. Correlation coefficients between monthly teleconnection indices and (a, b) snow depth and (c, d) onset and melt of snow cover (for the overlap period 1936-95). Correlation coefficients significant at 0.05 are shown (> 0.21).

(a) Snow depth averaged over the 'snow season' October-May

T/c patte rn and month	*Arkhangelsk*	*Kotlas*	*Koynas*
SCA Nov	--	-0.31	--
NAO Dec	--	--	-0.25
AO Nov	--	--	0.26

(b) Snow depth during March, the month of maximum snow accumulation

T/c pattern and month	*Arkhangelsk*	*Kotlas*	*Koynas*
EA-Jet Jul	0.25	--	--
EA-Jet Aug	0.30	--	--
AO Oct	--	-0.32	--
EA/WR Nov	--	--	-0.28
SCA Oct	--	--	-0.30
SCA Nov	--	--	-0.25

(c) Onset of snow cover

T/c pattern and month	*Arkhangelsk*	*Kotlas*
NAO Dec	0.29	--
EA/WR Oct	--	0.27
SCA Nov	--	-0.33

(d) End of snow cover

T/c pattern and month	*Arkhangelsk*	*Kotlas*
EA/WR Apr	-0.34	
SCA Apr	0.34	
EA Mar	--	-0.33

associated below-average winter air temperatures and precipitation. Other Euro–Atlantic teleconnections, including the NAO and AO, exert less influence on snow depths, and dates of onset and end of snow cover season (Table 5.19 c, d). The EA/WR pattern modulates both the start and the end of the snow cover season, where its positive phase leads to a later start of snow formation at Kotlas (r = 0.27; Table 5.19 c) and an earlier melt at Arkhangelsk (r = –

0.34; Table 5.19 d), whereas the positive EA phase is associated with an earlier snow melt at Kotlas (r = – 0.33; Table 5.19 d).

5.5 Conclusions.

In this chapter, links between regional climate, distant atmospheric forcing, and interannual and interdecadal variability in SD discharge have been investigated. The following conclusions are made:

(i) A causal chain exists between large-scale atmospheric circulation and river discharge (Figure 2.16). In this specific case, the primary mechanism is that Euro-Atlantic teleconnection patterns determine geopotential height anomalies and propagate downwards to the SD catchment, where they affect sea level pressure (SLP) near the surface. SLP anomalies thereafter influence regional and local climates across the watershed by creating weather patterns. Importantly, the weather patterns (derived from mid-tropospheric and regional circulation) furthermore determine snow cover (including its lateral extent, snow depth, and its duration) and ice cover, factors that are significant in the cold environments. In summary, pressure (SLP and at higher atmospheric levels) creates certain temperature and precipitation conditions that finally translate into river discharge variability.

(ii) Air temperature, precipitation (raw and P-E), duration of snow cover and snow depth, and SLP are the main climatic factors controlling hydrological changes in SD seasonal discharge and also at Kotlas.

(iii) Seasonal precipitation has strongly increased between 1881 and 2003 at Arkhangelsk. The strongest changes in the Arkhangelsk record are found during the spring (AMJ), autumn (SON) and winter (DJFM) seasons accounting for 12 %, 25% and 30% of the total variance respectively. Linear trends have not been estimated over the SD catchment, where a changing number of stations has contributed to the observation network. However, interdecadal variability is pronounced over the catchment area between 1901 and 2000. Regional precipitation exerts the strongest effect on summer discharge (June precipitation impacting July discharge, July precipitation impacting August discharge, and August precipitation impacting September discharge) with

correlation coefficients above 0.6. On a seasonal basis, the JA precipitation strongly influences JA and SON discharge.

(iv) Seasonal air temperature has significantly increased only during the AMJ season since 1881 at Arkhangelsk, with the linear trend accounting for 9% of the observed variation. Air temperature in other seasons has not changed linearly. Linear trends have not been estimated over the SD catchment, where a changing number of stations has contributed to the observation network. However, interdecadal variability is pronounced over the catchment since 1900. April air temperature strongly affects discharge during April and June and air temperature in May strongly affects June discharge. Thus, AMJ and JA air temperatures exert strongest controls over JA discharge.

(v) Snow depth has not changed linearly at Arkhangelsk since 1900, while at Kotlas, the strongest linear increase in snow depth during the snow cover season (O–M) explains 28% of observed variance of this short-term record. During March (the month with highest snow depth accumulation), the linear trend explains 21% of the total variance. The linear increase at Koynas accounts for about 10% in the O–M snow cover time series and 5% in the March time series. The snow depth records reflect the low precipitation events observed during the 1930s. As a whole, the snow depth has significantly increased over the middle part of the SD catchment (Kotlas, Koynas) but has remained unchanged in the northernmost part (Arkhangelsk) since 1936. The onset and end dates of snow cover have been used to estimate the length of snow cover season. Both stations (Arkhangelsk and Kotlas) have experienced a significant increase between 1900 and 1994 (Arkhangelsk) and 1936 and 1994 (Kotlas), which is in line with other studies. Snow depth, measured between December and March, has the strongest effect on AMJ discharge and also on discharge in SON.

(vi) Effective precipitation (P-E), estimated for no longer than the second half of the 20th century, exhibits a significant decline during autumn (SON) and winter (DJFM) explaining 15% and 13% respectively of the total variance. Generally, the effective precipitation leads discharge by one month. Monthly correlation coefficients are highest during the summer months with June and July P-E influencing the July and August discharge. The correlations between P-E and discharge agree especially well with those between precipitation and discharge during the summer months ($r > 0.4$).

(vii) Variability in regional climatic variability (air temperature, precipitation) explains 20%, 35%, 12%, and 48% of the total variance in AMJ, JA, SON, and DJFM discharge respectively.

(viii) Teleconnection patterns explain 19% (AMJ), 13% (JA), 20% (SON) and 33% (DJFM) of the total variance in seasonal discharge. The SCA and NAO have emerged as the two strongest forcings of AMJ discharge between 1882 and 1995, and two patterns (NAO and EA-JET) are the strongest predictors of JA discharge. The two dominant drivers of SON discharge are EA-JET and EA/WR, while the SCA and NAO patterns control the DJFM discharge. Thus, the dominant teleconnection patterns influencing the SD catchment are the SCA and NAO patterns. However, calculation of the 30-year running correlation coefficients has revealed that the role of distant forcing is not always consistent over time.

Chapter 6. Statistical modelling of seasonal discharge of Severnaya Dvina (1901-95).

6.1. Introduction.

It has been shown in the previous chapter that SD discharge is controlled by regional atmospheric circulation, temperature, precipitation, and by distant forcing. The reader is again referred to Figure 2.16, where these associations have been shown in a schematic sketch. Here the combined influence of these factors is evaluated. Future projections of meteorological variables, derived from the use of regional circulation models, can be used as input into the generation of statistical models (e.g. Wilby *et al*., 2004). Certain teleconnection patterns may be predictable (Rodwell *et al*., 1999; Baldwin and Dunkerton, 2001) providing the potential to predict seasonal SD discharge up to several years in advance.

This chapter presents the results of statistical modelling of SD discharge for the four hydrological seasons (AMJ, JA, SON, and DJFM) for 1901-1995. For the purpose of statistical analyses, the SD catchment has been defined as the area 58-65^{o} N, 40-50^{o} E (section 3.3.2). To determine the dominant factors influencing seasonal discharge and to model discharge using meteorological variables as predictors, a combination of Principal Component Analysis (PCA) and regression analysis was used (Figure 3.5). The rationale for using PC scores has already been detailed in section 3.4.1 and is repeated briefly: Multiple climatic predictors of discharge should be independent of each other (Yarnal, 1993), which is often not the case. To resolve this problem, PCA has been performed providing the advantage that components independent of each other have been generated. Therefore, in terms of physical interpretation in this case, the PCs show the dominant forcing factors influencing seasonal SD discharge. The combination of PCA and regression has been used in other studies as well (e.g. Ye *et al*., 1998; Phillips *et al*., 2003; Ye *et al*., 2004) and is used here as well.

PCA was performed using monthly and seasonal regional (temperature, precipitation, SLP, and snow depth) and large-scale (teleconnection indices) predictors. In each case, meteorological variables, exhibiting close correlations with discharge (sections 5.2 and 5.3), were selected as input data for the PCA. Three to five PCs have been retained explaining around 60% of the total variance in seasonal discharge. Scores of the retained PCs were used

to model seasonal discharge by using multiple regression technique. The odd years for each season (1901-1995) were selected to derive a regression model:

Discharge = constant + a*PC1 + b*PC2 + c*PC3 + d*PC4 + e*PC5 (Equation 6.1)

The constructed models were applied using the same independent variables for the even years of the same period. The modelled seasonal discharge time series were correlated with the observed discharge data to validate the model. They have been compared graphically and by the strength of the correlation coefficient.

6.2. Modelling spring (AMJ) discharge.

6.2.1. PCA of the AMJ meteorological data

PCA has been performed on meteorological data for the spring (AMJ) season. In total 950 month-variables have been employed. These are:

- Air temperature in April averaged over the SD catchment (April regional temperature)
- Air temperature in June averaged over the SD catchment (June regional temperature)
- AMJ precipitation averaged over the SD catchment (AMJ regional precipitation)
- DJFM precipitation averaged over the SD catchment (DJFM regional precipitation)
- AMJ SLP averaged over the SD catchment (AMJ regional SLP)
- Snow depth at Arkhangelsk
- NAO index for January
- NAO index for May
- EA/WR index for February
- SCA index for FMAM

Tables 6.1 - 6.3 show results of the PCA. The 'scree plot' test (Craddock and Flood, 1969), as shown in Figure 6.1, was used in combination with the 'eigenvalue > 1.0' rule to determine the statistically significant number of components to be retained (see section 3.4.1). Five statistically significant PCs have been retained explaining 71% of the total variance (Table 6.1).

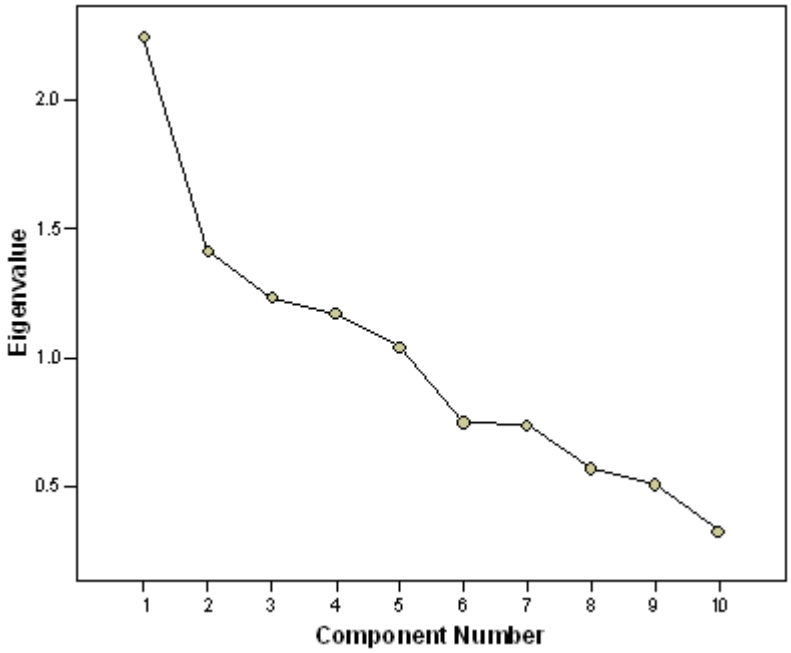

Figure 6.1. Scree plot (eigenvalues against component numbers) identifying the number of statistically significant components to be retained for the AMJ season (1901-1995).

Table 6.3 summarises the five dominant patterns of variance. PC 1 explains 20.15% of the observed variance and describes patterns of both basin-wide precipitation as well as SLP in AMJ. This component is termed “Regional circulation in spring”. It shows that regional SLP patterns control regional precipitation during AMJ and both have a strong association with the AMJ discharge. PC2 explains 13.23% of the observed variance. It exhibits high positive loadings on both NAO in May and SCA during February through to May. This component is named “Teleconnections in spring”. The positive NAO in late spring as well as the positive SCA phase impose dry conditions over the basin area thus decreasing the AMJ discharge. PC 3 (12.96%) refers to “NAO in high winter” with strong positive loadings on the NAO in January. This indicates that the January NAO and AMJ discharge are positively correlated, i.e. positive NAO phases leading to a strong zonal airflow and increased river discharge. PC 4 (12.46%) exhibits positive loadings on snow depth at Arkhangelsk during the snow season (October through May) and negative loadings on regional temperature in April and is named “Snow depth in winter”. This agrees with timing of snowmelt in the SD catchment being controlled by April air temperature (and with a response of April discharge to April mean air temperature; Table 5.3).

Table 6.1. Variance explained by the five significant components for the AMJ season (1901-1995). Explained total cumulative variance is highlighted in bold.

PC	Eigenvalue	Variance explained (%)	Cumulative variance (%)
1	2.015	20.153	20.153
2	1.323	13.229	33.382
3	1.296	12.960	46.342
4	1.246	12.458	58.800
5	1.226	12.256	**71.056**

Table 6.2. PC loadings of the five statistically significant components for the AMJ season (1901-1995). Only the highest component loadings are highlighted in bold to assist with interpretation of PCs.

Meteorological variables	Component				
	1	2	3	4	5
April regional temperature	0.211	0.034	0.599	**-0.554**	-0.082
June regional temperature	0.718	-0.181	0.201	0.077	0.245
AMJ regional precipitation	**-0.793**	-0.106	0.153	0.058	0.090
DJFM regional precipitation	0.256	-0.127	-0.112	0.066	**0.744**
January NAO	-0.088	-0.068	**0.876**	0.152	0.012
May NAO	-0.091	**0.784**	-0.205	0.049	-0.040
February EA/WR	-0.264	0.142	0.094	-0.128	**0.760**
FMAM SCA	0.292	**0.735**	0.166	-0.057	0.053
AMJ regional SLP	**0.765**	0.286	0.008	-0.255	-0.097
O-M snow depth at Arkhangelsk	-0.057	0.016	0.119	**0.903**	-0.073

The relationship between temperature and snow melt is clearly seen in the extreme years: Low temperatures below one standard deviation from the arithmetic long-term mean (e.g. 1902, 1909, 1913, 1923, 1929, 1941, 1944, 1961, 1979 and 1981) led to a late end of the snow season, while high temperatures (such as 1903, 1913, 1937, 1950, 1967, 1975, and 1983) provided for an early snowmelt. PC5 (12.26%) relates to the EA/WR index in February and regional DJFM precipitation and is termed “Moisture regime in winter”. This component

reveals the importance of the EA/WR mode of atmospheric circulation in winter for AMJ discharge but being ranked 5th shows that EA/WR pattern has a lesser impact on discharge than the concurrent NAO and SCA.

Table 6.3. Variance explained by the statistically significant PCs and correlation coefficients between the PCs and the original variables for the AMJ season.

PC	New variable name	Correlation with original variables
PC1	Regional circulation in spring	AMJ regional precipitation (-0.79) AMJ regional SLP (0.77)
PC2	Teleconnections in spring	May NAO (0.78) FMAM SCA (0.74)
PC3	NAO in high winter	Jan NAO (0.88)
PC4	Snow depth in winter	O-M snow depth (0.90) April regional temperature (-0.55)
PC5	Moisture regime in winter	Feb EA/WR (0.76) DJFM precipitation (0.74)

6.2.2. Regression model of AMJ discharge

The following multiple regression equation for AMJ discharge has been derived using independent predictors (PC scores) for the odd years:

AMJ discharge = 7,881 - 449 PC1 - 379 PC2 + 577 PC3 + 684 PC4 - 145 PC5

(Equation 6.2)

Equation 6.2 has been applied to independent predictors (PC scores) for the even years. Figure 6.2 compares the observed with and the modelled AMJ discharge revealing moderate correlation ($r = 0.36$, $R^2 = 12.96$). While some singular events (very low discharge in 1936 and 1960, as well as the high discharge in 1952, 1958 and 1990) have been quite accurately captured, the model and the observations diverge in other years (e.g. 1938, 1966, 1992).

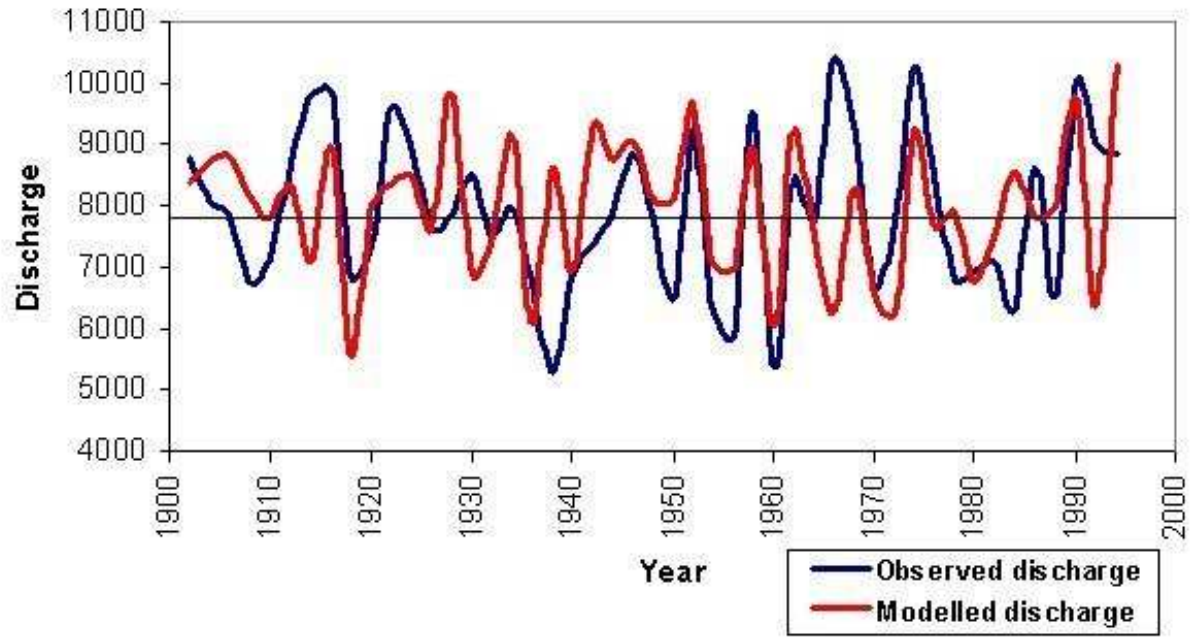

Figure 6.2. Modelled versus observed values of AMJ discharge ($m^3 s^{-1}$) of SD (1902-1994). The black line shows the long-term average of the observed AMJ discharge (7,914 $m^3 s^{-1}$).

Figure 6.3 shows the time series of the five significant PC scores. Low discharge observed during the dry years of 1936 and 1960 is reproduced well by the regression model. Both years have very strong scores on the PC1 (Figure 6.3), which describes the regional spring circulation. AMJ SLP was high in 1936, particularly during May (1020 hPa; 0.94 standard deviations above the long-term average), leading to a strong negative anomaly in AMJ precipitation over the SD catchment (93 mm, 2.4 standard deviations below the long-term average). AMJ precipitation in 1960 was only marginally higher (117 mm) than in 1936 and remained 1.4 standard deviations below the long-term mean. During this year, regional SLP was even higher than in 1936, especially during April (1023 hPa) and May (1020 hPa). At the same time, both years feature small scores of PC4 and PC5 reflecting the snow season and winter precipitation patterns. The high AMJ discharge observed in 1952 and 1958 was well reproduced by Equation 6.2. In both years, PC4 exhibited high scores suggesting that high snow depth was the main factor for high springtime discharge. In fact, snow depths at Arkhangelsk during the winter seasons of 1951/52 and 1957/58 were more than 2.3 standard deviations above the long-term average (Figure 5.6). The high discharge value observed in 1990 has been well reproduced due to the high PC2, PC3, and PC5 scores, which are related to the impact of several teleconnection patterns between January and May. The positive NAO

index in January (PC3) was 1.1 standard deviation above the long-term arithmetic average and remained consistently and strongly positive from January through April. At the same time, the SCA index (PC2) was consistently and strongly negative between February and May 1990 implying negative anomaly in SLP and geopotential height over the SD basin. The underlying pattern for the divergence between model and observations, such as in 1938 and 1966, is less obvious. It might be suggested that the poorly captured discharged values are related to those factors that have been rejected by the PCA model.

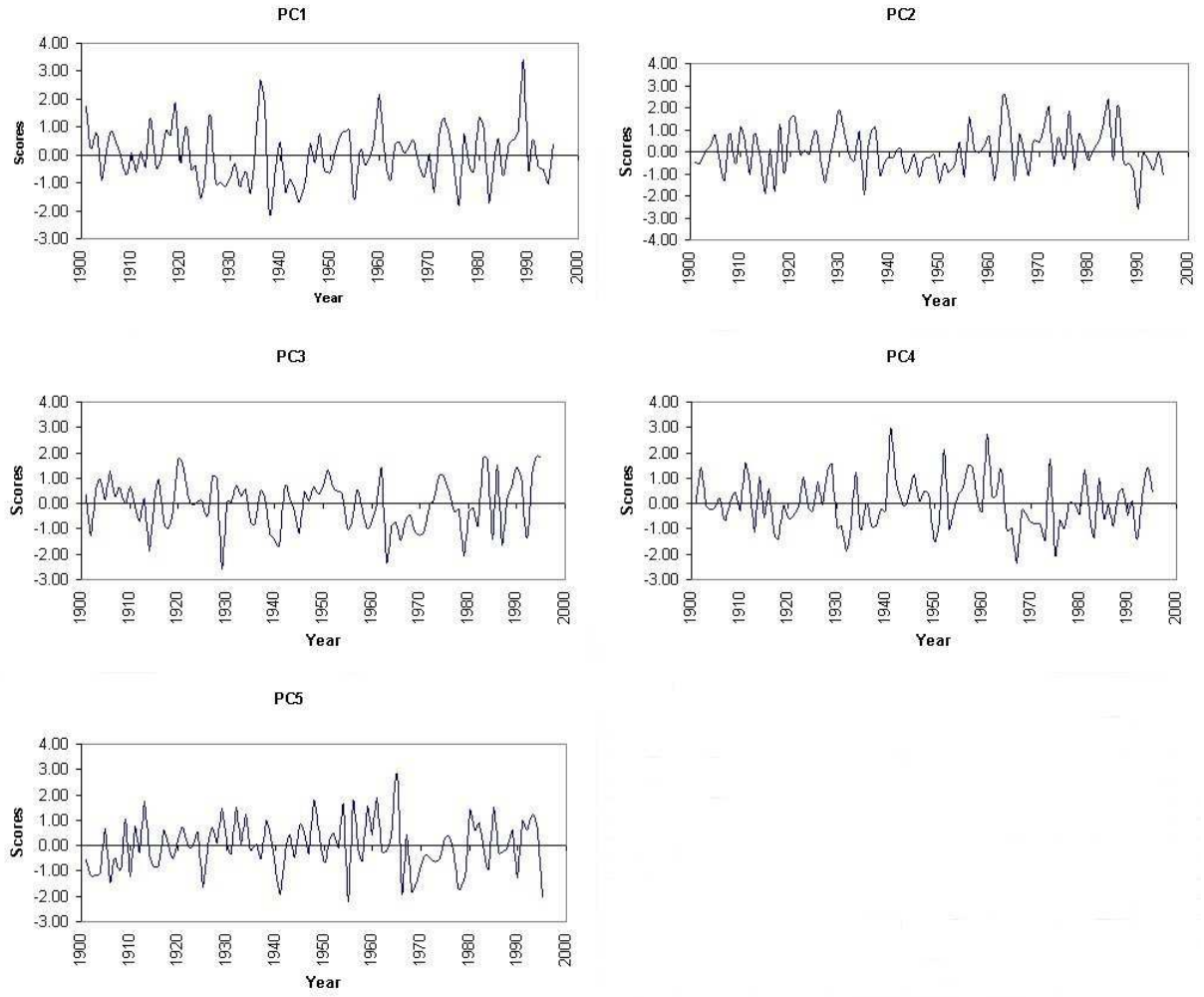

Figure 6.3. Time series of the statistically significant PC scores (AMJ 1901-1995).

6.3. Summer (JA) discharge.

6.3.1. PCA of the JA meteorological data

PCA was performed on the selected meteorological data for the summer (JA) season (1901-1995). In total 760 month-variables have been employed. These are:

- Air temperature in June averaged over the SD catchment (regional June temperature)
- June precipitation averaged over the SD catchment
- July precipitation averaged over the SD catchment
- AMJ SLP averaged over the SD catchment
- JA SLP averaged over the SD catchment
- EA-JET index for June
- NAO index for June June
- October-May snow depth at Arkhangelsk

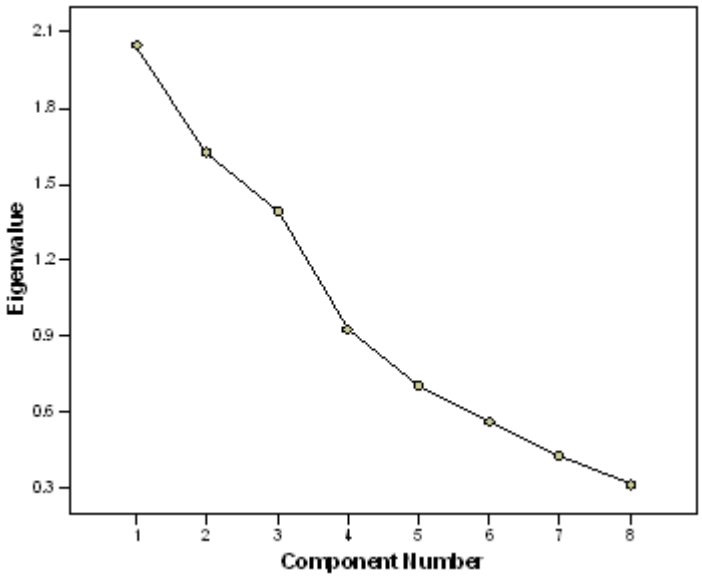

Figure 6.4. Scree plot (eigenvalues against component numbers) identifying the number of statistically significant components to be retained for the JA season (1901-1995).

Tables 6.4-6.6 show the results of the PCA conducted on the JA meteorological data. The 'scree plot' test (Craddock and Flood, 1969), as shown in Figure 6.4, was used in combination with the 'eigenvalue > 1.0' rule (Chapter 3). Three statistically significant PCs have been retained explaining 63% of the total variance (Table 6.4). Note that in contrast to other seasons, the break is less visible in the present scree plot (Figure 6.4).

PC 1 explains 25.56% of the observed variance (Table 6.4). It describes the impact of variability in regional air temperature and precipitation in June on JA discharge and was named "Regional climate in June" (Tables 6.6). These factors, clearly, are the source of the

Table 6.4. Variance explained by the five significant components for the JA season (1901-1995). Explained total cumulative variance is highlighted in bold.

PC	Eigenvalue	Variance explained (%)	Cumulative variance (%)
1	2.045	25.565	25.565
2	1.626	20.323	45.888
3	1.395	17.437	**63.325**

Table 6.5. PC loadings of the three statistically significant components for the JA season (1901-1995). Only the highest component loadings are highlighted in bold to assist with interpretation of PCs.

Meteorological variables	Component		
	1	2	3
June regional precipitation	**-0.758**	0.099	0.289
July regional precipitation	0.116	**0.778**	-0.010
June regional temperature	**0.730**	0.239	0.073
June EA-JET	-0.072	0.165	**0.880**
June NAO	0.572	-0.377	0.536
O-M snow depth at Arkhangelsk	-0.323	0.482	-0.026
AMJ regional SLP	0.582	0.059	-0.595
JA regional SLP	-0.108	**-0.750**	-0.111

Table 6.6. Variance explained by the statistically significant PCs and correlation coefficients between the PCs and the original variables for the JA season.

PC	New variable name	Correlation with original variables
PC1	Regional climate in June	June regional precipitation (-0.76) June regional temperature (0.73)
PC2	Regional environment in summer	JA regional SLP (-0.75) July regional precipitation (0.78)
PC3	EA-JET in June	June EA-JET (0.88)

most dominant atmospheric impact on JA discharge. While temperature is negatively correlated with JA discharge (Table 5.5), precipitation is linked positively to it (Table 5.1). This indicates that warmth in June and low rainfall reduce the JA discharge, whereas cool and moist conditions increase it. PC2 explains 20.32% of the observed variance (Table 6.4) and is related to the contemporaneous SLP and regional precipitation in July. This component was termed "Regional environment in summer" (Table 6.6). The relationship between this component and discharge is straightforward: negative (positive) anomalies in atmospheric pressure lead to increased (decreased) precipitation and high (low) discharge. A selection of years with strong JA SLP anomalies emphasizes this: regional atmospheric pressure below one standard deviation from the long-term average (e.g. 1904, 1909, 1923, 1928, 1948, and 1956) led to strong positive precipitation anomalies, while positive anomalies in SLP (e.g. 1913, 1938, and 1973) resulted in low rainfall (Figure 5.1). PC 3 (17.43%) reflects the impact of the EA-JET pattern in June on rainfall in SD catchment and was termed "EA-JET in June". The positive EA-JET phase refers to an increased westerly airflow over the eastern North Atlantic and into Europe, providing for higher SD discharge; in contrast, a negative EA JET phase describes blocking patterns over Greenland and Great Britain (CPC, www.cpc.ncep.noaa.gov/data/teledoc/eajet.html).

6.3.2. Regression model of JA discharge

The following multiple regression equation for JA discharge has been derived using independent predictors (PC scores) for the odd years:

JA discharge = 2,476 - 402 PC1 + 548 PC2 + 93.6 PC3 (Equation 6.3)

Equation 6.3 has been applied to the independent predictors for the even years. Figure 6.4 compares the observed JA discharge with the modelled JA discharge. The observed discharge has been well reproduced by the model ($r = 0.67$, $R^2 = 44.89$). The model reproduces the low flow events especially well in 1954, 1960, 1988 and 1992. The high-flow events as of 1916, 1928, 1942 and 1956 are also reproduced accurately. Pronounced divergence for individual years that characterised the AMJ model is not characteristic of the JA season except on three years.

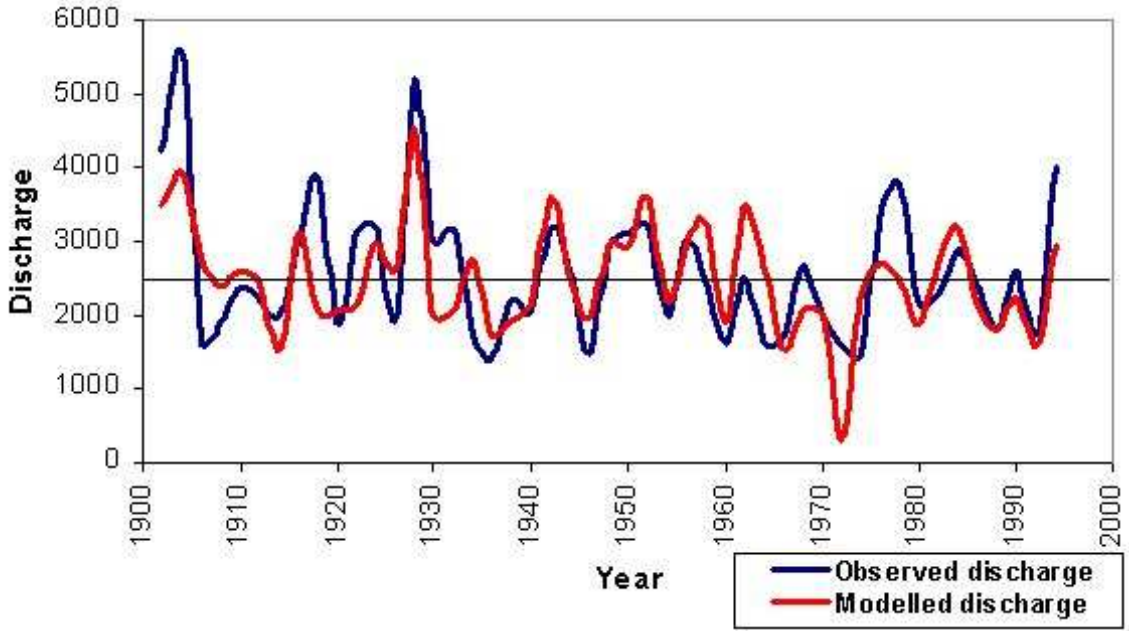

Figure 6.5. Modelled versus observed values of JA discharge (m^3 s^{-1}) of SD (1902-1994). The black line shows the long-term average of the observed discharge (2,591 m^3 s^{-1}).

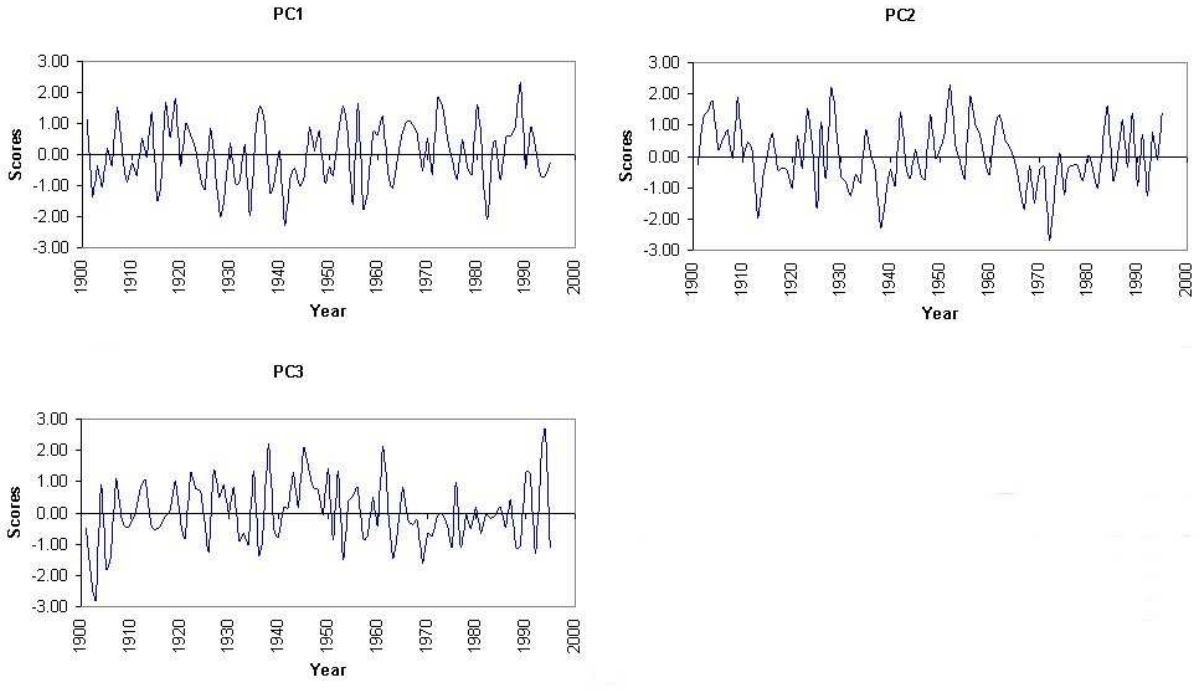

Figure 6.6. Time series of statistically significant PC scores (JA 1901-1995).

The model generally tends to slightly overestimate JA discharge in the second part of the record (1942, 1952, 1958, 1962 and 1984), and it has significantly overestimated the negative

anomaly in JA discharge observed in the extremely dry year of 1972. Inspection of the summer (JA) SLP time series has shown that in 1972 SLP was the highest on record since 1899 (1.88 standard deviations above the long-term average). The extreme duration and strength of the positive SLP anomaly and the extreme nature of the associated drought has been reflected in the very high score of PC2 (Figure 6.6) leading to the divergence between the observed and modelled discharge time series. By contrast, low discharge observed in 1948 and 1988 was simulated accurately using Equation 6.3. In 1948, high scores characterized PC2 (Regional environment in JA) while in 1988 high scores characterized PC3 (EA-JET in June), the PC3 score being more than one standard deviation below average (Figure 6.6).

6.4. Modelling autumn (SON) discharge

6.4.1. PCA of the SON meteorological data

PCA was performed on the selected meteorological data for the autumn (SON) season (1901-1995). In total 665 month-variables have been employed. These are:

- JA precipitation averaged over the the SD catchment (regional JA precipitation)
- JA air temperature averaged over the the SD catchment (regional JA temperature)
- JA SLP pressure averaged over the the SD catchment
- EA-JET index for July
- EA-JET index for August
- EA/WR index for March
- NAO index for June

Tables 6.7-6.9 show the results of the PCA of the SON meteorological data (1901-1995). The 'scree plot' test (Craddock and Flood, 1969), as shown in Figure 6.7, was used in combination with the 'eigenvalue > 1.0' rule to determine a number of the statistically significant components to be retained (section 3.4.1). Three statistically significant PCs have been retained explaining 65% of the total variance (Table 6.7).

Table 6.7 summarises the three dominant patterns of variance. PC1 explains 29.07% of the total variance in Data set. The highest loadings are on regional JA SLP and precipitation in summer and it has been termed 'Regional circulation in summer'. The loadings are of opposite signs indicating that high (low) SLP reduces (enhances) rainfall. Thus, the main

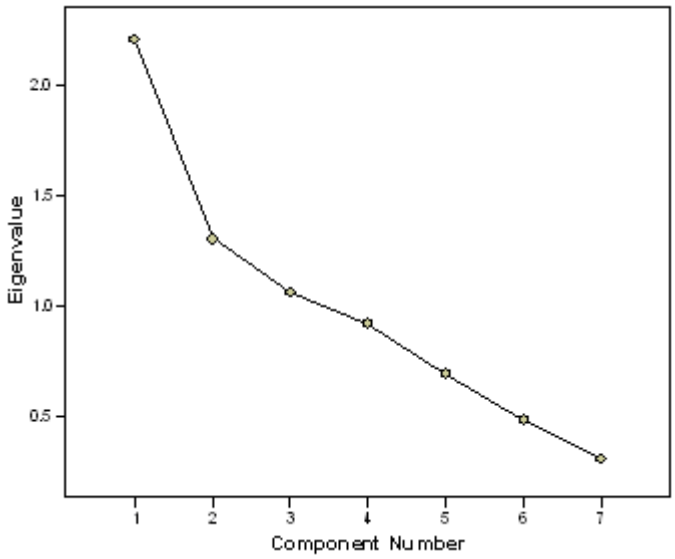

Figure 6.7. Scree plot (eigenvalues against component numbers) identifying the number of statistically significant components to be retained for the SON season (1901-1995).

Table 6.7. Variance explained by the five significant components for the SON season (1901-1995). Explained total cumulative variance is highlighted in bold.

PC	Eigenvalue	Variance explained (%)	Cumulative variance (%)
1	2.210	31.566	31.566
2	1.306	18.658	50.224
3	1.063	15.185	**65.409**

factor affecting SON discharge is regional atmospheric circulation with a time lag of 1-4 months. PC2 explains further 20.23% of the total variance with the highest loadings on the EA-JET pattern in July and the NAO pattern in June. Thus, it has been termed 'Summer Atlantic circulation'. The positive phase of the EA-JET pattern, as discussed earlier, reflects an intensified westerly circulation over the eastern North Atlantic and middle latitudes of Europe. PC 3 ('Euro–Atlantic teleconnections in March and June') explains 16.11% of the total variance, showing that the EA/WR patterns in March as well as the NAO in June are important modulators of the SD discharge in autumn. The positive EA/WR phase features low pressure north of the Caspian Sea in combination with below-averages temperatures over

western Russia (CPC, www.cpc.noaa.gov/data/teledoc/eawruss.shtml). The mechanism is straightforward: temperatures over the SD catchment during the warm-season months, particularly during JA, are negatively correlated with SON discharge (Table 5.4), whereby positive temperature anomalies provide for negative discharge anomalies, and vice versa.

Table 6.8. PC loadings of the five statistically significant components for the SON season (1901-1995). Only the highest component loadings are highlighted in bold to assist with interpretation of PCs.

Meteorological variables	Component		
	1	2	3
July EA-JET	-0.083	**0.811**	-0.078
August EA-JET	-0.321	0.538	0.422
March EA/WR	0.072	0.128	**0.723**
June NAO	0.021	**-0.426**	**0.607**
JA regional precipitation	**-0.783**	0.270	0.068
JA regional temperature	0.753	0.376	0.217
JA regional SLP	**0.860**	-0.238	-0.002

Table 6.9. Variance explained by the statistically significant PCs and correlation coefficients between the PCs and the original variables for the SON season.

PC	New variable name	Correlation with original variables
PC1	Regional circulation in summer	JA regional precipitation (-0.78) JA regional SLP (0.86)
PC2	Summer Atlantic circulation	July EA-JET (0.81) June NAO (-0.43)
PC3	Euro–Atlantic teleconnections in March and June	Mar EA/WR (0.72) Jun NAO (0.61)

6.4.2. Regression model of SON discharge

The following multiple regression equation for the SON discharge has been derived using independent predictors (PC scores) for the odd years:

SON discharge = 2,444 - 393 PC1 + 401 PC2 + 126 PC3 (Equation 6.4)

Equation 6.4 has been applied to the independent predictors for the even years. Figure 6.8 compares the observed SON discharge with the modelled SON discharge and Figure 6.9 shows the time series of the significant PC scores. The model has reproduced the observed discharge variability well (r = 0.65, R^2 = 42.25), particularly in those years when discharge was close to average. In contrast, anomalous discharge values are captured less accurately. In particular, strong underestimation of the anomalously high discharge events observed in 1918, 1928, and 1952 is evident (Figure 6.6) and it is possible that the model performance is disrupted by the occurrence of a few very strongly positive discharge anomalies in the earlier part of the record and the absence of such anomalies after the 1960s. The low-flow events of 1912, 1920, 1924, 1938, 1944, 1946, 1960, 1968, 1972, 1976, and 1980 are reproduced although values of discharge are mostly overestimated.

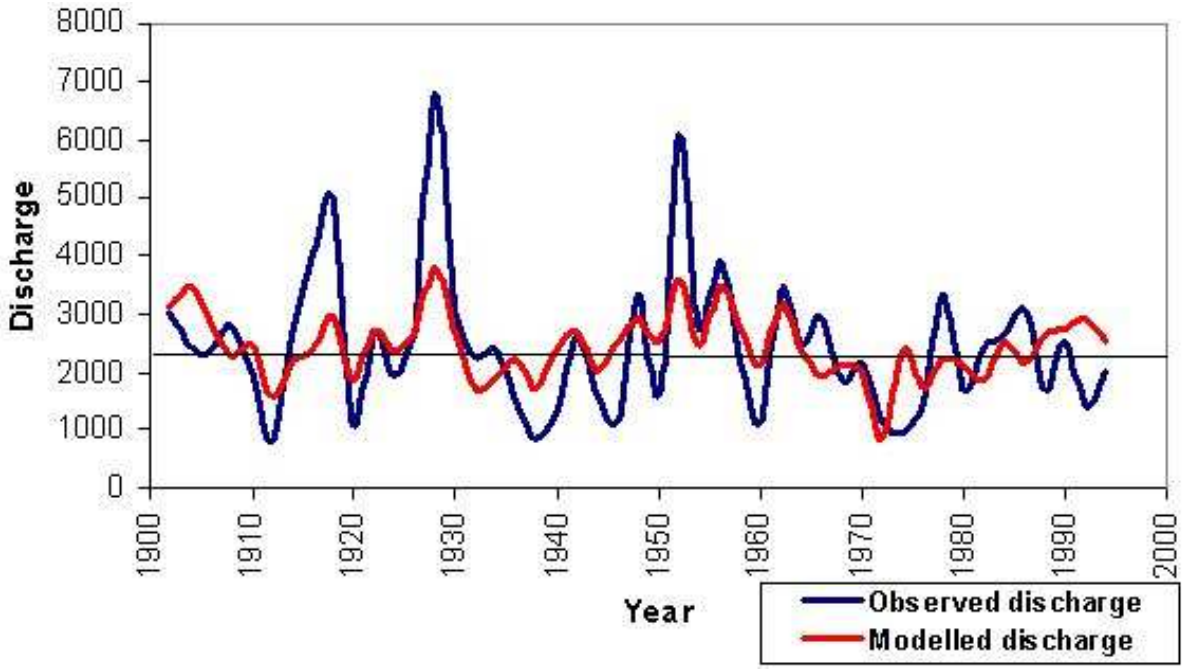

Figure 6.8. Modelled versus observed values of SON discharge (m^3 s^{-1}) of SD (1902-1994). The black line shows the long-term average of the observed discharge (2,443 m^3 s^{-1}).

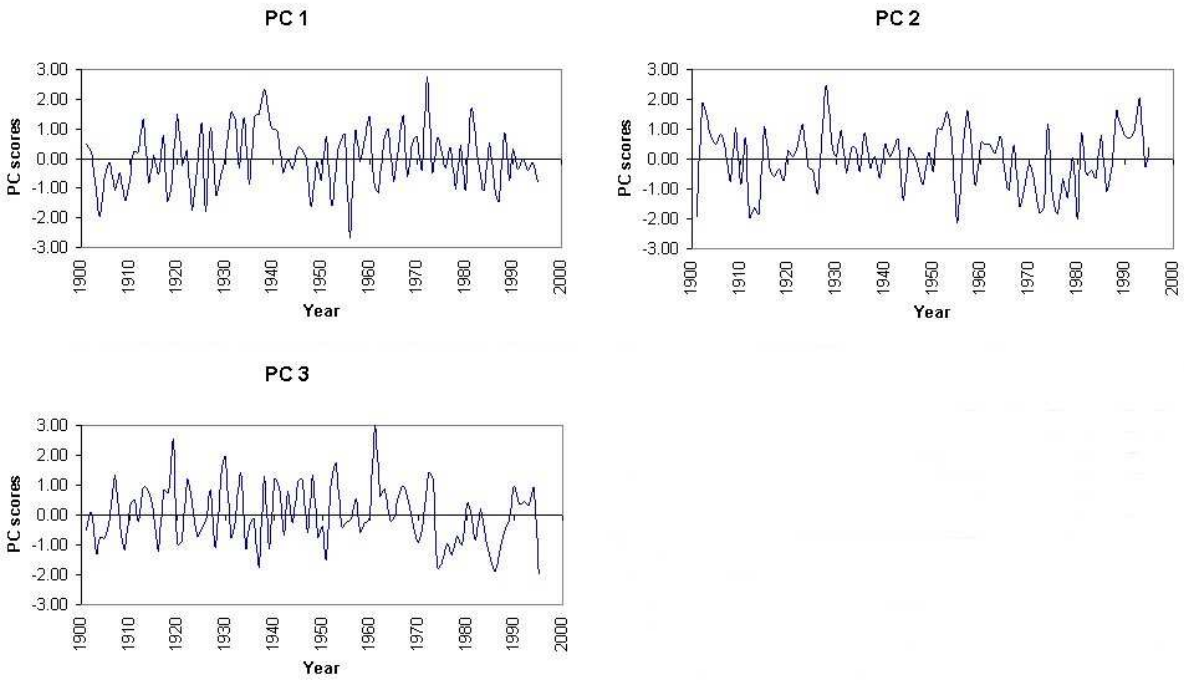

Figure 6.9. Time series of statistically significant PC scores (SON 1901-1995).

6.5. Modelling winter (DJFM) discharge.

6.5.1. PCA of the DJFM meteorological data

PCA has been performed on the selected meteorological data for the winter (DJFM) season (1901/02 – 1995/96). In total 950 month-variables have been employed. These are:

- JA precipitation averaged over the SD catchment (JA regional precipitation)
- SON precipitation averaged over the SD catchment (SON regional precipitation)
- AMJ air temperature averaged over the SD catchment (AMJ regional temperature)
- JA air temperature averaged over the SD catchment (JA regional temperature)
- SON air temperature averaged over the SD catchment (SON regional temperature)
- DJFM air temperature averaged over the SD catchment (DJFM regional temperature)
- NAO index in June
- NAO index in October
- SCA index in September
- SCA index in October

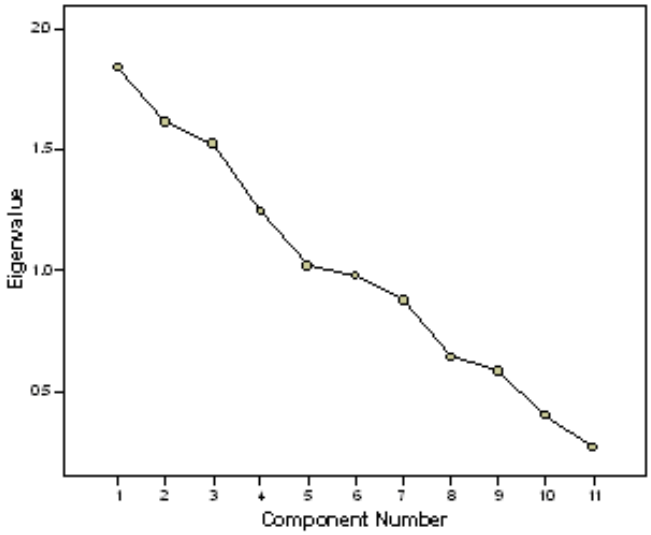

Figure 6.10. Scree plot (eigenvalues against component numbers) identifying the number of statistically significant components to be retained for the DJFM season (1901/02 - 1995/96.

Table 6.10. Variance explained by the five significant components for the DJFM season (1901/02-1995/96). Explained total cumulative variance is highlighted in bold.

PC	Eigenvalue	Variance explained (%)	Cumulative variance (%)
1	1.841	16.732	16.732
2	1.616	14.693	31.425
3	1.522	13.838	45.264
4	1.248	11.345	56.609
5	1.019	9.264	**65.873**

Tables 6.10-6.12 show the results for the PCA of the DJFM meteorological data. The 'scree plot' test (Craddock and Flood, 1969), as shown in Figure 6.10, was used in combination with the 'eigenvalue > 1.0' rule to determine a number of the statistically significant components to be retained (section 3.4.1). Five statistically significant PCs have been retained explaining 66% of the total variance (Table 6.10).

Table 6.11. PC loadings of the five statistically significant components for the DJFM season (1901/02 - 1995/96). Only the highest component loadings are highlighted in bold to assist with interpretation of PCs.

Meteorological variables	Component				
	1	**2**	**3**	**4**	**5**
September SCA	0.520	0.260	-0.128	0.113	0.208
October SCA	**0.807**	-0.003	0.221	-0.040	-0.109
July EA-JET	-0.022	0.076	0.053	0.061	**0.873**
June NAO	0.080	0.169	-0.371	-0.026	-0.330
October NAO	0.188	-0.171	**0.820**	-0.077	0.062
SON regional precipitation	0.064	**-0.704**	0.010	-0.031	0.488
JA regional precipitation	**-0.863**	0.229	0.101	-0.088	0.081
JA regional temperature	0.019	-0.118	0.016	**0.863**	-0.106
AMJ regiona temperature	-0.003	**0.805**	-0.009	0.035	0.163
SON regional temperature	-0.122	0.280	**0.733**	0.141	-0.032
DJFM regional temperature	0.102	0.224	0.048	**0.740**	0.224

Table 6.12. Variance explained by the statistically significant PCs and correlation coefficients between the PCs and the original variables for the DJFM season.

PC	New variable name	Correlation with original variables
PC1	Regional precipitation in summer	JA regional precipitation (-0.86) Oct SCA (0.81)
PC2	Regional climate in spring and autumn	AMJ regional temperature (0.81) SON regional precipitation (-0.70)
PC3	EA/WR in March and NAO in June	Oct NAO (0.82) SON regional temperature (0.73)
PC4	Regional temperatures in summer and winter	JA regional temperature (0.86) DJFM regional temperature (0.74)
PC5	EA-JET in July	July EA-JET (0.87)

The number of statistically significant components is higher than in any other season and, in contrast to other seasons, all the significant components explain approximately the same

percentage of the total variance. PC1 explains 15.8% of the variance. It is dominated by the SCA pattern in October and precipitation in JA. This suggests that negative temperature anomalies over European Russia exerted by the positive SCA phase (CPC, www.cpc.ncep.noaa.gov/data/teledoc/scand.shtml) increase the region's water budget, translating later in the year into higher DJFM discharge. The links with JA regional precipitation are less understood. PC2 (13.37%) exhibits high loadings on regional climate with temperature in AMJ and precipitation in SON. In this case, the main factor is springtime temperature that leads to higher discharge in AMJ, JA, and also DJFM (section 5.2.6). PC3 displays a high loading on the NAO index in October and on regional air temperature in SON, explaining 12.98% of the total variance. Large-scale moisture advection (NAO) and warm (regional) temperatures advected by Barents Sea depressions (Shahgedanova, 2002; section 2.3) in autumn predetermine higher DJFM discharge events. PC4 (12.25%) is linked to the concurrent regional temperature and regional temperature in the preceding summer. In particular, Barents Sea depressions during the cold half of the year (Shahgedanova, 2002; section 2.3) transport warm air masses into the study area, thereby increasing the DJFM discharge. PC5 explains another 11.48% of the total variance showing that the EA-JET pattern in July, which has been shown to control moisture advection from the north-eastern Atlantic (section 5.3.3).

In general, both regional and distant meteorological factors affect the SD discharge in DJFM and most of them lead discharge by a few months showing that DJFM discharge is largely a product of climatic conditions in the preceding spring, summer, and autumn.

6.5.2. Regression model of DJFM discharge

The following multiple regression equation for the DJFM discharge has been derived using the independent predictors for the odd years:

DJFM discharge = 979 - 152 PC1 - 130 PC2 + 96.1 PC3 - 53.1 PC4 + 156 PC5

(Equation 6.5)

Equation 6.5 has been applied to the independent predictors for the even years.

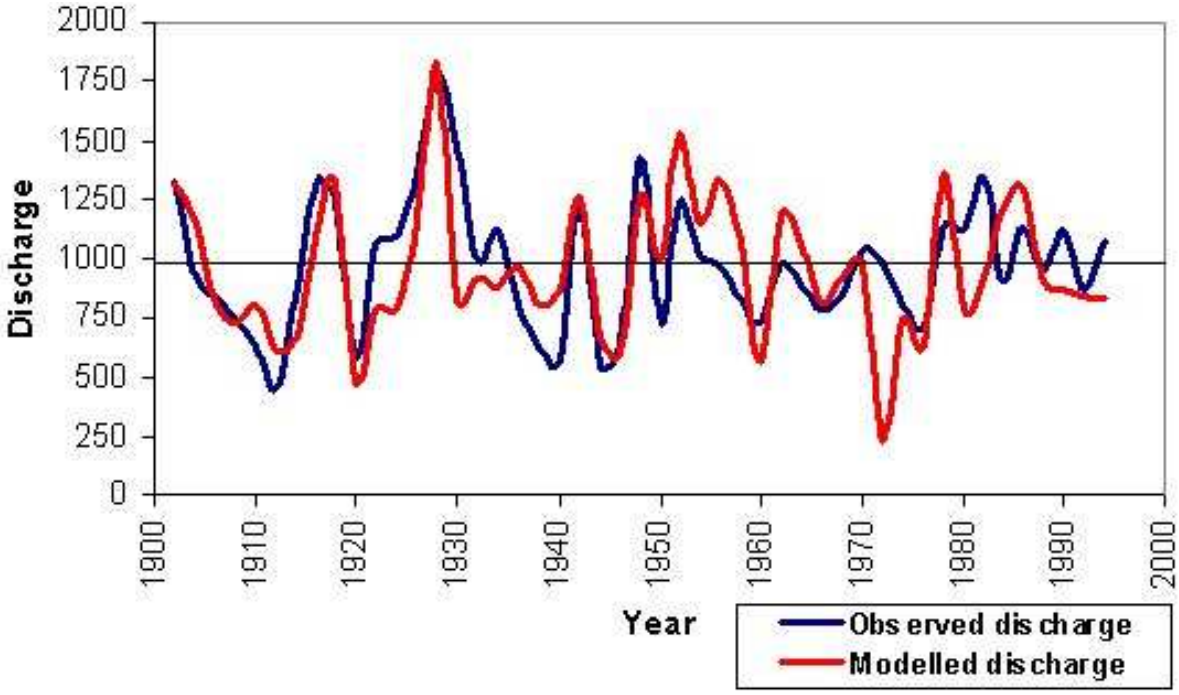

Figure 6.11. Modelled versus observed values of DJFM discharge ($m^3 s^{-1}$) of SD (1902-1994). The black line shows the long-term average of the observed discharge (975 $m^3 s^{-1}$).

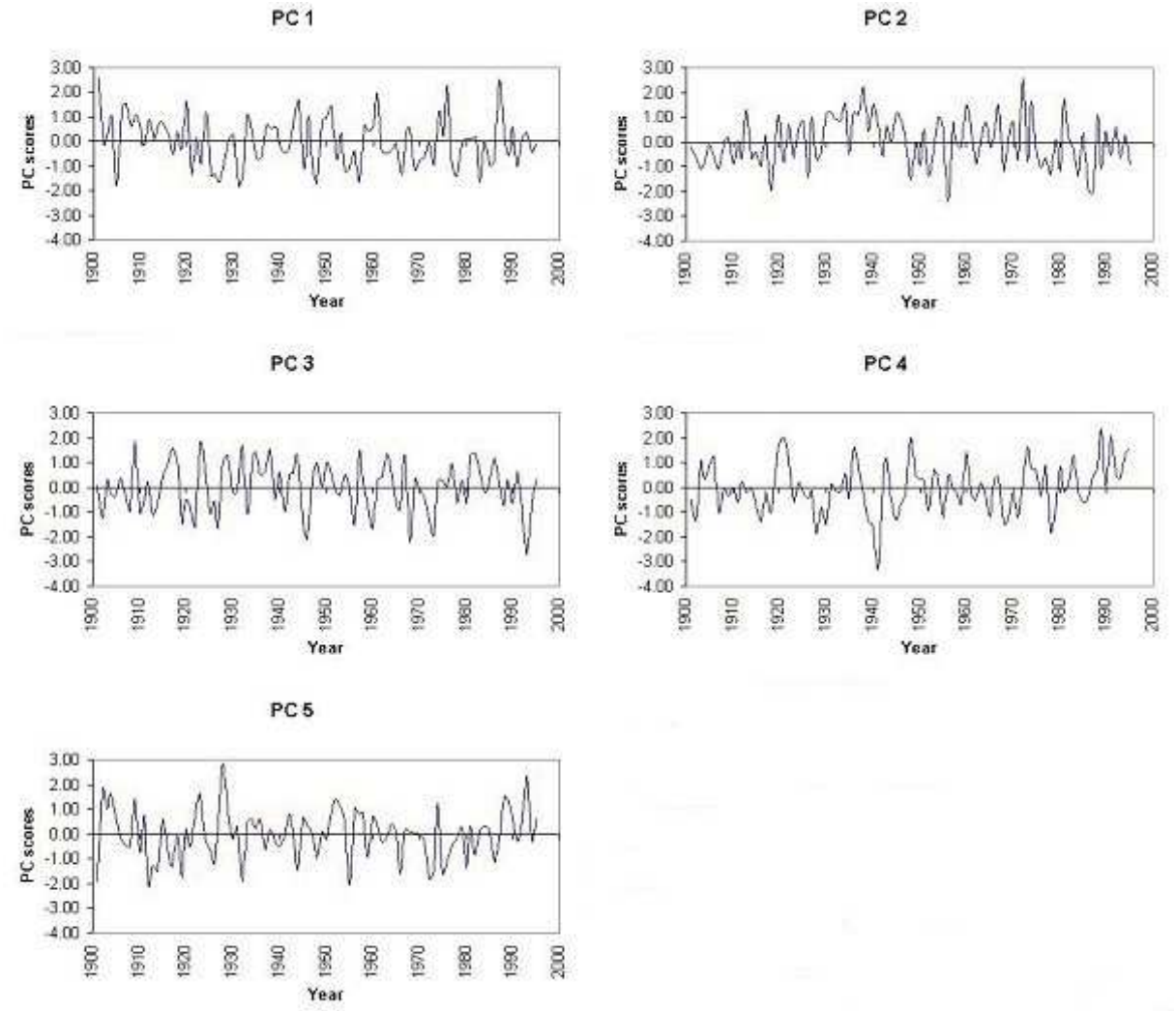

Figure 6.12. Time series of statistically significant PC scores (DJFM 1902-1994).

Figure 6.11 compares the observed DJFM discharge with the modelled DJFM discharge. The model simulates the DJFM discharge well (r= 0.65, R^2 = 42.25%) and accurately reproduces a number of high- and low-flow seasons including the low-flow of 1908, 1910, 1912, 1920, 1940, 1946, 1960, 1974, 1976, and 1992 and high-flow events of 1902, 1918, 1928, 1942, 1952, 1978, and 1986. In contrast, the predicted value in 1972 is very low, severely underestimating the true discharge in that year because of the exceptionally high absolute values of the score of PC2 associated with springtime temperature. Figure 6.12 shows the time series of the significant PC scores. The most notable aspect is the agreement of the PC 2 time series with air temperature of the SD catchment: strongly positive loadings of PC2 (referring to regional air temperature in spring) occurred during the 1920s and 1930s when the European Arctic warmed considerably (section 2.4.2.1), followed by declining loadings (and

declining air temperatures), and an increase during the 1970s in line with pronounced summer droughts during that decade.

6.6 Discussion and conclusions.

Multiple regression-based models of seasonal SD discharge have been constructed using scores of the statistically significant PCs derived from meteorological data for the odd years of the record and applied to predict seasonal SD discharge in the even years of the record.

The success of the model is estimated by visual inspection between the observed and modelled discharge time series, and by a statistical measure such as correlation coefficients for the duration of record (1902-1994). They are high in for the JA, SON, and DJFM seasons ($r = 0.65$-0.76), and much lower with regard to AMJ discharge ($r = 0.36$) over time. This obscures the fact that individual discharge events have been properly modelled, while others have been modelled wrongly in magnitude. To evaluate how well the model has performed at different periods within these 95 years of time span, a running mean for the correlation coefficients has been calculated (not shown). It has turned out that for individual decades, the correlation coefficients between the observed and the modelled seasonal discharge ranges from 0.10 to 0.90. The highest success rate has been obtained for SON and DJFM prior to the 1970s (with correlation coefficients up to 0.9), while JA discharge has not been consistently well modelled prior to the 1970s. In AMJ, the skill of the model was highest between the mid-1940s and the 1970s. The skill of the model declines sharply after the 1970s. The main reason for this is the severe underestimation of the discharge event of 1972 (exclusion of this particular year leads to higher moving-average values after the 1970s).

The question arises as to the scientific novelty of the results discussed in this chapter. Other authors (e.g. Ye *et al*., 1998; Phillips *et al*., 2003; Ye *et al*., 2004) have applied the same approach, a combination of PCA and regression, in their analyses with regard to Siberian discharge. Nevertheless, to the author's knowledge, a comprehensive study of meteorological forcing factors on seasonal long-term discharge in northern European Russia has been provided in this thesis for the first time. This has two interesting implications:

(i) It shows the links between atmospheric circulation and hydrology and thus, closes a gap by investigating the dominant forcing patterns in northern European Russia.

(ii) Certain teleconnection patterns may be predictable (Rodwell *et al*., 1999; Baldwin and Dunkerton, 2001). Thus, hydrological behaviour in the SD basin may be as well predictable ahead. This might lead to an early-warning system to be installed in the region, especially with regard to upcoming floods in spring and developing drought in summer. Regional climate may be simulated by statistical downscaling techniques (see next section). Again, their application might forecast future climatic conditions in the basin with the possibility of generating hydrological forecasts.

It is concluded that:

- The SD discharge in JA, SON, and DJFM is modelled accurately with correlation coefficients of 0.65 to 0.67 between the observed and modelled discharge. In contrast, the AMJ discharge was less accurately reproduced achieving a correlation coefficient of 0.36 between the modelled and observed discharge.
- Both regional and distant factors control SD seasonal discharge.
- Negative SLP anomalies in spring leading to higher precipitation and above-average snow depth in the SD basin are associated with positive anomalies in AMJ discharge.
- Regional circulation and the EA-JET pattern control JA discharge. Summer discharge is overestimated in the more recent part of the time series.
- Anomalies in regional atmospheric circulation during the preceding summer and the EA/WR teleconnection pattern active in March control SD discharge in SON. The low-flow values are replicated more precisely than the high-flow values, which occurred predominantly during the earlier years of the record.
- The model reproduces well both high-flow and low-flow events during DJFM. Both regional factors and distant forcing from the preceding spring, summer, and autumn season control the DJFM discharge of SD.

Chapter 7. Conclusions and prospects for future research.

7.1. An overview of research aims and context.

Research of hydrological variability and trends in Northern Eurasia, including the Russian Arctic Ocean basin, has recently received considerable attention and studies have been published addressing hydrological variability predominantly in the Siberian sector of the Arctic Ocean basin between the middle and the end of the 20th century (Grabs *et al*., 2000; Semiletov *et al*., 2000; Fukutomi *et al*., 2003; Lammers *et al*., 2001; Serreze *et al*., 2003 a; Yang *et al*., 2002; 2004 a; b; Ye *et al*., 2003). Strong scientific interest in changes in the freshwater inflow into the Arctic Ocean has been inspired by the study by Peterson *et al*. (2002), who concluded that the total annual discharge of the six largest Northern Eurasian rivers has increased by 7% into the Arctic Ocean since 1936 (section 2.5). An increase in the inflow of freshwater into the Arctic Ocean can potentially lead to a decline in salinity weakening the THC (e.g. Rahmstorff, 2006). The study by Peterson *et al* (2002) considered changes in freshwater discharge of the Siberian rivers (which provide the bulk of freshwater for the Arctic Ocean) during a relatively short period of time (1936-1999) for which discharge measurements were available. Focusing primarily on hydrological (as opposing to climatic) variability in the Eurasian sector of the Arctic Ocean basin, this work has not considered the fact that the 1930s and 1940s were a very specific period in the northern region of Eurasia characterised by unusually high air temperatures (e.g. Bengtsson *et al*., 2004; Johanessen *et al*., 2004) and largely negative anomalies in precipitation (e.g. Paeth *et al*., 2001). Therefore, the authors have chosen a period of low discharge as a baseline for the estimation of hydrological trends in the region. A potential result is the underestimation of the role of natural climatic variability (Hulme *et al*., 1999; Anderson *et al*., 2003; Esper *et al*., 2005), which explains the anomalously early-20th century warm period in the polar and sub-polar regions of Eurasia and overestimation of an impact of anthropogenic climate change on the water balance in the Eurasian sector of the Arctic Ocean.

Changes in the hydrological budget are not only important on global scales (with regard to the Thermohaline Circulation; section 1.1), but also on regional scales, where a changing seasonality might affect the vulnerability of the population living within the SD catchment. In particular, an increased frequency or magnitude of springtime floods, and/or reduced water availability for navigation and drinking water consumption during summer, should be named.

Therefore, daily data for the AMJ and JA season between 1978-2005 (ArcticRIMS, http://rims.unh.edu/data.shtml) were studied (not shown). No data are available for SU. Although slight changes in SD discharge have been noted (increase in AMJ, decrease in JA), none of these are statistically significant at 0.05: In AMJ, neither the day of occurrence of highest flow (on average mid-May), nor the discharge itself (measured as m^3 s^{-1}) has increased since 1978. In JA, neither the day of occurrence of lowest flow (on average mid-August), nor the discharge itself (m^3 s^{-1}) has decreased since 1978. As a whole, there is no statistical indication that seasonal discharge patterns have become more extreme during the past 27 years (no daily data available for the year 2000).

Many studies have also pointed out that changes in regional climate and in the larger-scale atmospheric circulation affect river discharge regimes and their variations (e.g. Sturm *et al*., 2001; Fukutomi *et al*., 2003; Jacobeit *et al*., 2004 to name but a few). Climatic variability in the European North has received much attention (section 2.6), but little has been published about the links between climatic variability in northern European Russia and river discharge in this region. Similarly, links between variability in the large-scale atmospheric circulation and river discharge have been evaluated for Siberia (e.g. Shiklomanov *et al*., 2000; Lammers *et al*., 2001; Semiletov *et al*., 2000; Yang *et al*., 2002; 2004 a, b; Ye *et al*., 2003; Berezovskaya *et al*., 2004; Koster *et al*., 2005) and North America (e.g. Déry *et al*., 2005; Déry and Wood, 2005) but have been under-reported for northern European Russia. Therefore, the second major aim of this study was to link climatic variability (including regional climatic variability and influence of distant atmospheric forcing) with river discharge, evaluate the nature of these links, and quantify them using methods of statistical analysis.

7.2. A summary of the main results.

At the end of Chapter 2, a schematic model (Figure 2.16) has been developed linking the interactions between different levels of the atmosphere (large-scale circulation and regional circulation) and their effect on river discharge of the SD watershed. These links have been explored within this research project. Clearly, distant forcing (exerted by teleconnections) affects the regional circulation (SLP) over the SD catchment with direct effects on air

temperature and precipitation (liquid and solid). The effects of the climate on discharge are often occurring simultaneously or lagged by some months or seasons, as has been shown in Chapters 5 and 6. Therefore, the model visualises a basic understanding of atmospheric-hydrological interactions and illustrates that both distant forcing and regional circulation are the predictors of SD and SU discharge.

Six main research questions have been formulated at the end of Chapter 2 (Literature Review). These questions have been addressed in Chapters 4-6. Here a brief summary is provided.

Research Question 1: *What are the trends in annual, seasonal, and monthly discharge of the SD and SU for the duration of the record?*

The long-term monthly, seasonal, and annual discharge of both SD and SU has not changed linearly since 1882 when records began (Chapter 4). The only exception is a negative trend in September discharge of SD and a negative trend in June discharge of SU. By contrast, a pronounced change in discharge values occurred in the 1930s indicating a shift from a period of higher discharge and its frequent strong positive anomalies to a period of lower discharge, which lasted until the mid-1970s. However, it should be noted that linear trends depend strongly on the choice of sampling period. Thus a linear increase in SD discharge for DJFM is registered if the sampling period starts in 1936, one of the driest years on record. Most other studies use 1936-1937 as baseline years for trend estimation because regular discharge measurements started on many Eurasian rivers at that time coinciding with the driest-ever pentad (1935-1939), a situation similar only to the early 1970s.

Research Question 2: *What are the trends in annual, seasonal, and monthly discharge of the SD and SU during the last two decades in which, as stated by many authors, a signal of climate change is emerging from the noise of climatic variability (IPCC, 2001)?*

Following the 1970s, SD and SU annual discharge was close to average. Therefore, analysis of trends and variability in the SD discharge record does not confirm the freshwater discharge from the European sector of the Arctic Ocean basin has increased with time and with the climatic warming observed at the end of the 20th century. Daily discharge data of SD, available for the period from 1978 to 2005 do not indicate that springtime floods or summer drought have significantly increased in frequency, magnitude, or timing.

Research Question 3: *To what extent do changes in regional climate affect and control trends in discharge of SD?*

Regional climate is a significant driver of historically observed seasonal variability and trends in SD discharge. The combined impact derived from precipitation and temperature at Arkhangelsk (either contemporaneous with discharge or with a time lag) explains between 12% (autumn), 20% (spring), 35% (summer), and 48% (winter) in observed discharge variation (Chapter 5). Other meteorological factors also control river discharge, such as SLP, snow cover, and P-E. Step changes in discharge of both SD and SU coincide with periods of exceptionally low precipitation over northern European Russia. High air temperatures, low precipitation, and low discharge characterising the 1930s-1940s have been attributed to natural climatic variability (section 2.4.2.1).

Research Question 4: *To what extent do distant atmospheric forcings (major Euro-Atlantic teleconnection patterns) explain trends and variability in discharge of SD?*

The main Euro-Atlantic teleconnection patterns control variability in SD discharge through the control of variability in regional climate (Chapter 5). The strongest impact is produced by the SCA teleconnection pattern. In particular, SCA in May affects spring discharge and SCA in October affects winter discharge. This conclusion is in line with a number of previous studies showing that SCA is one of the most important teleconnection patterns controlling climatic variability in European Russia (Barnston and Livezey, 1987; Clark *et al*., 1999; Qian *et al*., 2000; Shahgedanova *et al*., 2005). NAO in June is an important driver of hydrological regime in summer despite a widely accepted notion that its influence on regional climates is strongest in winter (e.g. Hurrell, 1995; Hurrell and van Loon, 1997; Hurrell *et al*., 2003). The EA-Jet in July is another pattern controlling SD discharge in autumn. The combined influence of the main Euro-Atlantic teleconnection patterns explains between 13% of summer discharge, 20% of spring and autumn discharge, and 33% of winter discharge in observed discharge variation (Chapter 5). Nevertheless, the strength of the influence of distant forcing on SD discharge varies over time.

Research Question 5: *Can a combination of regional climatic characteristics and teleconnection indices be used to explain a significant proportion of variance in SD discharge with the view of developing a simple method of possibly predicting future discharge? What proportion of variance can be explained?*

A combination of PCA and multiple regression analysis has been used to develop multiple regression models of seasonal SD discharge (Chapter 6). PCA has been conducted on the selected meteorological variables (both regional and teleconnection indices), which have shown statistically significant correlation with seasonal SD discharge. The constructed regression models reproduced the summer (JA), autumn (SON), and winter (DJFM) seasonal discharge well explaining between 42% and 45% of shared variance in the observed and modelled data. Spring (AMJ) discharge has been simulated less successfully with R^2 of 13%. The performance of regression models varied over time. Thus summer discharge has been overestimated during the more recent part of the record. The regression models have not always reproduced strong anomalies well (as it may be expected of the regression method). Thus a strong underestimation of anomalously high discharge in SON was evident in the earlier part of the record possibly because the model performance was disrupted by the occurrence of a few very strongly positive discharge anomalies in the earlier part of the record and the absence of such anomalies after the 1960s. By contrast the modelled value of JA discharge for 1972 (a year with a high SLP resulting in very dry summer conditions) was substantially lower than the observed negative anomaly in discharge. It is concluded that in general a combination of PCA and multiple regression modeling can be used as a simple method of prediction of SD discharge in summer, autumn, and winter.

7.3. Suggestions for future research.

Two major suggestions for future research are presented.

Firstly, to forecast river discharge using the simple method utilized in this study for an assessment of impacts of climate change on hydrological regime of the area, reliable projections of regional climate are required. Such projections are not available at present, however, they can be developed using methods of regional climate modeling (dynamical downscaling) or methods of statistical downscaling (Wilby *et al*., 1996; Wilby *et al*., 2004). A number of regional climate models are available at present such as, for example, PRECIS modeling system based on the regional HadRM3 climate modelled developed by the UK Met Office (www.precis.org.uk). The model simulates a variety of meteorological variables on a scale of the SD basin and its output can be used in assessments of both regional climate change and as input data for assessment of hydrological variability.

Secondly, Jones *et al*. (2006) have reconstructed river discharge for 15 rivers across England and Wales for the period 1865-2002 (available at www.cru.uea.ac.uk/cru/data/riverflow/). The same should be possible across the Eurasian Arctic Ocean basin, where currently, the employed long-term data for SD and SU (1882-2004) shed light merely onto a limited region of the European Arctic Ocean basin. Yet, comparison with the large Siberian rivers is important in order to be able to evaluate hydrological changes across Northern Eurasia over historical times, discharge of the Yenisei, Ob, Lena, Kolyma, and Pechora rivers. The centennial reconstructions should be performed in monthly resolution until at least 1882 with the main objective being comparison with the discharge of SD with the potential of obtaining a better understanding of the long-term hydrological budget and its characteristics across Northern Eurasia.

REFERENCES

Administraciya Arkhangelskoi Oblasti: Informaciya ob oblasti. Geografiya, nasseleniya (Administration of the Arkhangelsk Region. Information about the region. Geography, population). – (www.dvinaland.ru/region/info.asp?part=2) [In Russian]

Ahrens, C. D. (2000): Meteorology today: an introduction to weather, climate and the environment. – 528 pp., 6th ed.; Pacific Grove / London (Brooks-Cole).

Aleksandrov, E. I., Pietrov, L. S. and Subbotin, V. V. (1986): Structure and variability of the climate of the Northern Polar Region. – Gidromet. Ser. 37.21 Meteorol., **8**: 62 pp. [In Russian]

Alekseev, G. V. and Buzuev, A. (1973): On the evolution of the ice-surface layer of the ocean system in the region of drift of the Severnaya Polyus-16 station. – Problems of the Arctic and Antarctic, **42**: 37-43.

Alekseev, G. V., Podgornoy, I. A., Svyashchennikov, P. N. and Khrol, V. P. (1991): Features of climate formation and its variability in the polar climatic atmosphere-sea-ice-ocean system. – In: Krutskikh, B. A. [ed]: Klimaticheskii rezhim Arktiki na rubezhe XX i XI vv.: 4-29 [In Russian].

Alekseev, G. V., Aleksandrov, Ye. I., Bekriayev, R. V., Svyaschennikov, P. N: and Harlanienkova, N. Ya. (1999): Surface air temperature from meteorological data. – In: AARI [ed.]: Detection and modelling of greenhous warming in the Arctic and sub-Arctic, INTAS Grant 97-1277 Techn. Rep. On Task 1; St. Petersburg (Arctic and Antarctic Research Institute [AARI]).

Alley, R. B., Nordhaus, W. D., Overpeck, J. T., Peteet, D. M., Pielke Jr., R. A., Pierre Humbert, R. T., Rhines, P. B., Stocker, T. F., Talley, L. D. and Wallace, J. M. (2003): Abrupt climate change. – Science, **299**: 2005-10.

Anderson, L. G., Jutterstrom, S., Kaltin, S., Jones, E. P. and Bjork, G. R. (2004): Variability in river runoff distribution in the Eurasian Basin of the Arctic Ocean. – J. Geophys. Res.-Oceans, **109** (C1): art. No C01016.

Ångström, A. (1935): Teleconnections of climate changes in present time. – Geografiska Annaler, **17**: 242-58.

Arctic Climatic Impact Assessment (ACIA) (2004): Impacts of a warming Arctic. Arctic Climatic Impact Assessment. ACIA Overview report. – (www.amap.no/acia/)

ArcticRIMS (2005): A regional, integrated hydrological monitoring system for the Pan-Arctic land mass (http://rims.unh.edu/data.shtml)

Armstrong, R. (2001): Historical Soviet daily snow depth version 2 (HSDSD). - CD-ROM; National Snow and Ice Data Center (Boulder, CO) (http://arcss.colorado.edu/data/g01092.html).

Baldwin, M. P. and Dunkerton, T. J. (1999): Propagation of the Arctic Oscillation from the stratosphere to the troposphere. – J. Geophys. Res., **104** (D24): 30.937-946.

Barnston, A. G. and Livezey, R. E. (1987): Classification, seasonality and persistence of low-frequency atmospheric circulation. – Mon. Wea. Rev., **115**: 1083-1126.

Barry, R. G. and Chorley, R. J. (1998): Atmosphere, weather and climate. – 409 p.; London / New York (Routledge).

Bengtsson, L., Semenov, V. A. and Johannessen, O. M. (2004): The early twentieth-century warming – a possible mechanism. – J. Clim., **17**: 4045-57.

Berezovskaya, S., Yang, D. Q. and Kande, D. L. (2004): Compatibility analysis of precipitation and runoff trends over the large Siberian watersheds. – Geophys. Res. Letts., **31** (24): L21502, doi:10.1029/2004GL021277.

Bergström, S. and Carlsson, B. (1994): River runoff to the Baltic Sea: 1950-1990. – Ambio, **23** (4-5): 280-87.

Borisov, A. A. (1965): Climates of the USSR. – 255 pp.; London (Oliver and Boyd).

Box, G. E. P., and Jenkins, G. (1976): Time Series Analysis: Forecasting and Control. – San Francisco, CA (USA) (Holden-Day Publisher).

Bradley, D. C. & Ormerod, S. J. (2001): Community persistence among stream invertebrates tracks the North Atlantic Oscillation. – J. Anim. Ecol., **70**: 987-96.

Breiling M., Shmakin A., Sokratov S., Rubinstein K., Kostka Z., Petrov M., Phillips M. (2006): EU-INTAS project Snow and landscape. Influence of snow vertical structure on hydrothermal regime and snow-related economical aspects in Northern Eurasia. – EU-INTAS project *01-0077*, 1st NEESPI Science Team Meeting. IIASA, Laxenburg, Austria, 22-24 February 2006. Poster presentations (ftp://ftp.ncdc.noaa.gov/pub/download/NEESPI/NEESPI-posters/poster_meinhard_intas2006light.pdf)

Broecker, W.S., Sutherland, S. and Peng, T.-H. (1999): A possible 20th-century slowdown of Southern Ocean deep-water formation. – Science, **286**: 1132-1135.

Brown, R. D. (1997): Historical variability in Northern Hemisphere spring snow covered area. – Ann. Glaciol., **25**: 340-46.

Brown, R. D. (2000): Northern Hemisphere snow cover variability and change, 1915-97. – J. Clim., **13** (13): 2339-55.

Buchinsky, I. E. (1976): Zasukhi i sukhovei (*Droughts and dry winds*). – 214 pp.; St Petersburg (Gidrometeoizdat) [In Russian].

Chapman, W. L. and Walsh, J. E. (1993): Recent variations of sea ice and air temperature in high latitudes. – Bull. Am. Meteorol. Soc., **74**: 33-47.

Clark, M. P., Serreze, M. C. and Robinson, D. A. (1999): Atmospheric controls on Eurasian snow extent. – Int. J. Climatol., **19**:27–40.

Clark, P.U., Pisias, N.G., Stocker, T.F. and Weaver, A.J. (2002): The role of the thermohaline circulation in abrupt climate change. – Nature, **415**: 863-869. –

Climate Prediction Center (CPC): Northern Hemisphere teleconnection patterns. - (www.cpc.ncep.noaa.gov/data/teledoc/telecontents.shtml).

Cohen, J. and Barlow, M. (2005): The NAO, the AO, and global warming: How closely related? – J. Clim., **18**: 4498-4513.

Comiso, J. C., Zang, J. Z., Honjo, S. and Krishfield, R. A. (2003): Detection of change in the Arctic using satellite and in situ data. – J. Geophys. Res.-Oceans, **108** (C12): art. No. 3384.

Craddock, J. M. and Flood, C. R. (1969): Eigenvectors for representing the 500mb geopotential surface over the Northern Hemisphere. – Quart. J. Roy. Met. Soc., **95**: 576-93.

Cullen, H. M. and de Menocal, P. B. (2000): North Atlantic influence on Tigris-Euphrates streamflow. – Int. J. Climatol., **20**: 853-63.

Dai, A., Fung, I. Y. and Genio, A. D. del (1997): Surface observed global land precipitation variations during 1900-88. – J. Clim., **10**: 2943-62.

Dawson, A. G., Hickey, K., Holt, T., Elliott, L., Dawson, S., Foster, I. D., Wadhams, P., Jonsdottir, I., Wilkinson, J., McKenna, J., Davis. N. R. & Smith, D. E. (2002): Complex North Atlantic Oscillation (NAO) index signal of historic North Atlantic storm-track changes. – The Holocene, **12** (3): 363-9.

Déry, S. J. and Wood, E. F. (2004): Teleconnection between Arctic Oscillation and Hydson Bay river discharge. – Geophys. Res. Letts., **31** (18): L18205. –

Déry, S. J. and Wood, E. F. (2005): Decreasing river discharge in Northern Canada. – Geophys. Res. Letts., **32**: doi.10.1029/GL022845.

Déry, S. J., Stieglitz, M., McKenna, E. C. and Wood, E. F. (2005): Characteristics and trends of river discharge into Hudson, James, and Ungava Bays, 1964-2000. – J. Clim., **18** (14): 2540-57.

Dickinson, W. T. (1967): Accuracy of discharge determinations. – Hydrology Papers, **20**: 55 pp.; Fort Collins, CO (USA) (Colorado State University).

Dingman, S. L. (2001): Physical Hydrology. – 2nd edition, 575 pp.; Prentice Hall (NJ).

DSS UCAR: World Monthly Surface Station Climatology, 1738-cont. - (http://dss.ucar.edu/datasets/ds570.0/data/)

Dünkeloh, A. and Jacobeit, J. (2003): Circulation dynamics of Mediterranean precipitation variability 1948-98. – Int. J. Climatol., **23**: 1843-66.

Esbensen, S. K. (1984): A comparison of intermonthly and interannual teleconnections in the 700 mb geopotential height field during the Northern Hemisphere winter. – Mon. Wea. Rev., **112**: 2016-32.

Esper, J., Wilson, R. J., Frank, D. C., Moberg, A., Wanner, H. and Luterbacher, J. (2005): Viewpoint. Climate: past ranges and future changes. – Quat. Sci. Revs., 24: 2164-66.

Fallot, J.-M., R. G. Barry, and D. Hoogstrate (1997): Variations of mean cold season temperature precipitation and snow depths during the last 100 years in the former Soviet Union, Hydrol. Sci. J., **42**: 301– 327.

Forland, E. J. and Hanssen-Bauer, I. (2000): Increased precipitation in the Norwegian Arctic: True or false? – Clim. Chg., 46 (4): 485-509.

Fukutomi, Y., Igarashi, H. and Masuda, K. (2003): Interannual variability of summer water balance components in three major river basins of Northern Eurasia. – J. Hydromet., **4** (2): 283-296.

Georgievsky, V. Yu (1998): On global climate warming effects on water resources. – In: Water: a looming crisis? Techn. Doc. Hydrol., **18**: 3-14.

Ginzburg, B. M. and Soldatova, I. I. (1996): Long-term oscillations of river freezing and breakup dates in different geographic zones. – Russ. Meteorol. Hydrol.: 80-85.

Gordeev, V. V., Martin, J.-M., Sidorov, I. S. and Sidorova, M. V. (1996): A reassessment of the Eurasian River input of water, sediment, major elements, and nutrients to the Arctic Ocean. – Am. J. Sci., **296**: 664-91.

Gould, S. J. (1967): Evolutionary patterns in pelycosaurian reptiles: a factor analytic study. - Evolution, **21**: 385-401.

Grabs, W. E., Portmann, F. and Couet, T. de (2000): Discharge observation networks in Arctic regions: Computation of the river runoff into the Arctic Ocean, its seasonality and variability. – In: Lewis, E. L. [ed.] (2000): The freshwater budget of the Arctic Ocean: 249-67; Norwell/Dordrecht (Kluwer).

Groisman, P. Y., Koknaeva, V. V., Belokrylova, T. A. and Karl, T. R. (1991): Overcoming biases of precipitation measurement. A history of the USSR experience. – Bull. Am. Met. Soc., **72**: 1725-33.

Groisman, P. Y., Karl, T. R. and Knight, R. W. (1994 a): Observed impact of snow cover on the heat balance and the rise of continental spring temperatures. - Science, **263**: 198–200.

Groisman, P. Y. and Rankova, E. Y. (2001): Precipitation trends over the Russian permafrost-free zone: Removing the artifacts of pre-processing. – Int. J. Climatol., **21**: 657-78.

Groisman, P. Y. (2005): National Climatic Data Center Documentation for TD 9813, Daily and Sub-Daily Precipitation for the Former USSR. – 16 pp.; Asheville, NC (NCDC).

Gruza, G. V., Rankova, E. Y., Razuvaev, V. N. and Bulygina, O. A. (1999): Indicators of climatic change for the Russian Federation. – Clim. Chg., **42**: 219–242.

Hansen, J., and Lebedeff, S. (1987): Global trends of measured surface air-temperature. - J. Geophys. Res., **92:** 13 345–13 372.

Hartmann, D. L., Wallace, J. M., Limpasuvan, V., Thompson, D. W. and Holton, J. R. (2000): Can ozone depletion and global warming interact to produce rapid climate change? – Proc. Natl. Acad. Sci. USA, **97** (4): 1412-17.

Hänninen, J., Vuorinen, I. & Hjelt, P. (2000): Climatic factors in the Atlantic control the oceanographic and ecological changes in the Baltic Sea. – Limnol. Oceanogr., **45**: 703-10.

Henderson, R. (1916): Note on graduation by adjusted average. – Trans. Amer. Soc. Acturaries, **17**: 43:48.

Herschy, R. W. (1985): Chapter 14: Accuracy in streamflow measurements. – In: Herschy, R. W. [ed.]: Streamflow measurements: 474-510; Amsterdam (Elsevier).

Herschy, R. W. (1995): Streamflow Measurement. – 2nd ed.; London (E. & F. N. Spon).

Herschy, R. W. (1999): Hydrometry: principles and practice. – 2nd edition, 424 pp.; Chichester (Wiley).

Hisdal, H., Stahl, K., Tallaksen, L. M. and Demuth, S. (2001): Have stream flow droughts in Europe become more severe or frequent? – Int. J. Climatol., **21**: 317-33.

Hoerling, M. P., Hurrell, J. W. and Xu, T. (2001): Tropical Origins for Recent North Atlantic Climate Change. – Science, **292** (5514): 90-2.

Holmes, R. M., McClelland, J. W. and Peterson, B. J. (2003): Consideration of permafrost thaw as a significant contributor to increasing Eurasian Arctic river discharge. – Paper presented at SEARCH Open Science Meeting, Seattle, WA (SA), Oct 27-29, 2003.

Hulme, M., Barrow, E.M., Arnell, N.W., Harrison, P.A., Johns, T.C. and Downing, T.E. (1999): Relative impacts of human-induced climate change and natural climate variability. – Nature, **397**: 688-691.

Hurrell, J. W. (1995): Decadal trends in the North Atlantic Oscillation: Regional temperatures and precipitation. – Science, **269**: 676-9.

Hurrell, J. W. and Loon, H. van (1997): Decadal variations in climate associated with the North Atlantic Oscillation. – Clim. Chg., **36**: 301-226.

Hu, F.S., Ito, E., Brown, T.A., Curry, B.B. and Engstrom, D.R. (2001): Pronounced climatic variations in Alaska during the last two millennia. – Proc. Natl. Acad. Sci. USA, **98**: 10,552-10,556.

Hurrell, J. W., Kushmnir, Y., Ottersen, G. and Visbeck, M. (2003): An overview of the North Atlantic Oscillation. – In: Hurrell, H. W. [eds.]: The North Atlantic Oscillation: climatic significance and environmental impact: 1-35; Washington, D.C. (Am. Geophys. Un.) (= Geophys. Monogr., **134**).

Hydrometeorological Service of the USSR (1964): Deleting the inhomogeneity between the precipitation time series of the gauges with *Nipher* and *Tretyakov* windshields. – Methodological Instructions of the Hydrometeorological Service: 25 pp; Leningrad (Gidrometeoizdat). [In Russian]

IPCC (2001): Climate Change 2001: Impacts, Adaptation, and Vulnerability. Contribution of the Working Group II to the Third Assessment Report of the IPCC. – Cambridge (CUP).

Ivanov, V. V. (1994): River water inflow to the Arctic Seas. – Proc. Conf. On Arctic and Nordic Countries, Goteborg (Sweden).

Jacobeit, J., Glaser, R., Luterbacher, J. and Wanner, H. (2004): Links between flood events in central Europe since AD1500 and large-scale atmospheric circulation modes. – Geophys. Res. Letts., **30** (4): 21.1-21.4

Jevrejeva, S. (2002): Association between ice conditions in the Baltic Sea along the Estonian coast and the North Atlantic Oscillation. – Nordic Hydrol., **33** (4): 319-30.

Jevrejeva, S., Moore, J. C., Woodworth, P. L. and Grinsted, A. (2005): Influence of large-scale atmospheric circulation on European sea level: results based on the wavelet transform method. – Tellus, **57A**: 183-93.

Johanessen, O. M., Bentsson, L., Miles, M. W., Kuzmina, S. I., Semenov, V. A., Alekseev, G. V., Nagurny, A. P., Zakharov, V. F., Bobylev, L. P., Pettersson, L. H., Hasselmann, K.

and Cattle, H. P. (2004): Arctic climate change: observed and modelled temperature and sea-ice variability. - Tellus, **56A**: 328-41

Johnson, R. J. (1978): Multivariate statistical analysis in geography. – w. p. (Longman).

Jones, J. A. (1997): Global hydrology. Processes, resources and environmental management. – 399 pp.; Harlow (Addison Wesley Longman).

Jones, P. D., Jonsson, T. and Wheeler, D. (1997): Extension to the North Atlantic Oscillation using early instrumental pressure observations from Gibraltar and South-West Iceland. - Int. J. Climatol., **17**: 1433-1450.

Jones, P.D. and Salmon, M. (2005): Preliminary reconstructions of the North Atlantic Oscillation and the Southern Oscillation index from wind strength measures taken during the CLIWOC period. - Clim. Chg., **73** (1-2): 131-154.

Jones, J. A. (1997): Global hydrology. Processes, resources and environmental management. – 399 pp.; Harlow (Addison Wesley Longman).

Jones, P.D., Osborn, T. J. and Briffa, K. R. (1997): Estimating sampling errors in large-scale temperature averages. - J. Climate, **10:** 2548–2568.

Jones, P. D., New, M., Parker, D. E., Martin, S. and Rigor, I. G. (1999): Surface air temperature and its changes over the past 150 years. – Rev. Geophys., **37** (2): 173-99.

Jones, P.D. and Moberg, A. (2003): Hemispheric and large-scale surface air temperature variations: an extensive revision and an update to 2001. - J. Clim., **16**: 206-223.

Jones, P.D. and Salmon, M. (2005): Preliminary reconstructions of the North Atlantic Oscillation and the Southern Oscillation index from wind strength measures taken during the CLIWOC period. - Clim. Chg., **73** (1-2): 131-154.

Jones, P. D., Lister, d. H., Wilby, R. L. and Kostopoulou, E. (2006): Extended Riverflow reconstructions for England and Wales, 1865-2002. – Int. J. Clim., **26**: 219-31 (www.cru.uea.ac.uk/cru/data/riverflow/).

Kaiser, H. F. (1960): Review of measurements and statistics: A basic introduction. – Psychometrika, **25**: 411-13.

Kalinin, G. P. and Shiklomanov, I. A. (1974): Exploitation of the Earth's resources. – In: Gidrometeoizdat [ed.]: World Water Balance and Water Resources of the Earth: 575-606; St. Petersburg. [In Russian]

Kalnay, E., Kanamitsu, M., Kistler, R., Collins, W., Deaven, D., Gandin, L., Iredell, M., Saha, S., White, G., Woollen, J., Zhu, Y., Leetmaa, A., Reynolds, B., Chelliah, M., Ebisuzaki, W., Higgins, W., Janowiak, J., Mo, K.C., Ropelewski, C., Wang, J., Jenne,

R. and Joseph, D. (1996): The NCEP/NCAR reanalysis 40-year project. – Bull. Am. Meteorol. Soc., **77**: 437-471.

Kashparek, L. and Novicky, O. (2002): Hydrological drought studies in the wide context of climate variability. – In: Lanen, H. A. van and Demuth, S. [eds.] (2002): FRIEND 2002 – Regional Hydrology: Bridging the Gap between Research and Practice: 85-92; Wallingford (IAHS).

Kenny, P. and Durbin, J. (1982): Local trend estimation and seasonal adjustment of economic and social time series. – J. Roy. Stat. Soc., **145A**: 1-41.

Kiely, G. (1999): Climate change in Ireland from precipitation and streamflow observations. – Adv. Water Res., **23**: 141-51.

Kistler, R., Kalnay, E., Collins, W., Saha, S., White, G., Woollen, J., Chelliah, M., Ebisuzaki, W., Kanamitsu, M., Kousky, V., Dool, H van den, Jenne, R. and Fiorino, M. (2001): The NCEP-NCAR 50-year reanalysis: Monthly means CD-ROM and documentation. – Bull. Am. Met. Soc., **82** (2): 247-67.

Koronkevich, N. (2002): Chapter 5. Rivers, lakes, inland seas, and wetlands. – In: Shahgedanova, M. [ed.] (2002): Physical Geography of Northern Eurasia: 122-48; Oxford (Cambridge University Press).

Korzoun, V. I., Sokolov, A. A., Budyko, M. I., Voskresensky, K. P., Kalinin, G. P., Konoplaynsev, A. A., Korotkevich, E. S., Kuzin, P. S. and Lvovich, M. I. [Eds.] (1974): World Water Balance and Water Resources of the Earth. - St. Petersburg (Gidrometeoizdat) [In Russian].

Koster, E., Dankers, R., Linden, S. van der (2005): Water balance modelling of (Sub-) Arctic rivers and fresh water supply to the Barents Sea basin. – Permafrost and Periglac. Proc., **16** (3): 249-59.

Krasovskaia, I. (1994): Quantification of the stability of river flow regimes. – Hydrol. Sci. J., **40** (5): 587-98.

Kryjov, V. N. (2002): The influence of the winter Arctic Oscillation on the Northern Russia spring temperature. – Int. J. Climatol., **22**: 779-85.

Lammers, R. B., Shiklomanov, A. I., Vorosmarty, C. H., Fekete, B. M. and Peterson, B. J. (2001): Assessment of contemporary Arctic river runoff based on observational discharge records. – J. Geophys. Res., **106D**: 3321-34.

Lawrimore, J., and co-authors (2001): Climate Assessment for 2000. - Bull. Amer. Meteor. Soc., **82**:1-55.

Lewis, E. L., Jones, E. P., Lemke, P., Prowse, T. D. and Wadhams, P. [eds.] (2000): The freshwater budget of the Arctic Ocean. – 623 pp.; Dordrecht, Netherlands (Kluwer) (= NATO Sci. Ser., **70**).

Lindström, G. and Bergström, S. (2004): Runoff trends in Sweden: 1807-2002. – Hydrol. Sci. J., **49** (1): 69-84.

Lloret, J., Lleonart, J., Sole, I. & Fromentin, J. M. (2001): Fluctuations of landings and environmental conditions in the north-western Mediterranean Sea. – Fish. Oceanogr., **10**: 33-50.

Luterbacher, J., Schmutz, C., Gyalistras, D., Xoplaki, E. and Wanner, H. (1999): Reconstruction of monthly NAO and EU indices back to AD 1675. – Geophys. Res. Lett., **26** (17): 2745-8.

Luterbacher, J., Xoplaki, E., Dietrich, D., Jones, P. D., Davies, T. D., Portis, D., Gonzalez-Rouco, J. F., Storch, H. von, Gyalistras, D., Casty, C. and Wanner, H. (2001): Extending North Atlantic Oscillation reconstruction back to 1500. – Atm. Sci. Letts., **2**: 114-24.

Lvovich, M.I. (1971): Reki SSSR (Rivers of the USSR). – Moskva (Mysl Publishers). [In Russian]

Lydolph, P.E. (1977): Climates of the Soviet Union. – 443 pp.; Amsterdam / Oxford (Elsevier).

Manabe, S. and Stouffer, R. J. (1988): Two stable equilibria of a coupled ocean-atmosphere model. – J. Clim., **1**: 841-866.

Manabe, S. and R.J. Stouffer (1999): Are two modes of thermohaline circulation stable? - Tellus, **51A**: 400-411.

Mantua, N.J. and S.R. Hare, Y. Zhang, J.M. Wallace, and Francis, R.C. (1997): A Pacific interdecadal climate oscillation with impacts on salmon production. - Bull. Am. Met. Soc., **78**: 1069-1079.

Mächel, H., Kapala, A., and Flohn, H. (1998): Behaviour of the centres of action above the Atlantic since 1881. Part I: Characteristics of seasonal and interannual variability. - Int. J. Climatol., **18**: 1-22.

McCabe, G. J. and Wollock, D. M. (2002): A step increase in streamflow in the conterminous United States. – Geophys. Res. Letts., **29** (24): Art. No. 2185.

McClelland, J. W., Holmes, R. M. and Peterson, B. J. (2004): Increasing river discharge in the Eurasian Arctic: Consideration of dams, permafrost thaw, and fires as potential agents of change. – J. Geophys. Res., **109**: D18102.

McClelland, J. W., Dery, S. J., Peterson, B. J., Holmes, R. M. and Wood, E. F. (2006): A pan-arctic evaluation of changes in river discharge during the latter half of the 20th century. – Geophys. Res. Lett., **33**: L06715, 10.1029/2006GL025753.

McGregor, G. R. and Bamzelis, D. (1995): Synoptic typing and its application to the investigation of weather air pollution relationships, Birmingham, United Kingdom. – Theor. Appl. Climatol., **51** (4): 223-36.

Milly, P. C., Dunne, K. A. and Vecchia, A. V. (2005): Global pattern of trends in streamflow and water availability in a changing climate. – Nature, **438**: doi:10.1038/nature04312.

Moberg, A., Sonechkin, D. M., Holmgren, K., Datsenko, N. M. and Karlen, W. (2005): Highly variable Northern Hemisphere temperatures reconstructed from low- and high-resolution proxy data. – Nature, **433**: 613-7.

Myachkova, N. A. (1983): Klimat SSR (Climates of the USSR). – 191pp.; Moscow (Moscow State Univ. Press). [In Russian]

NCDC [National Climatic Data Center] (2003): Data Documentation for data set 3720 (DSI-3720), USSR Monthly Precipitation for 622 Stations, 1891-1999. – (www1.ncdc.noaa.gov/pub/data/documentlibrary/tddoc/td3720.pdf).

New, M., Hulme, M. and Jones. P. (2000): Representing Twentieth-Century Space–Time Climate Variability. Part II: Development of 1901–96 Monthly Grids of Terrestrial Surface Climate. – J. Clim., **13** (13): 2217–2238.

New, M., Todd, M., Hulme, M. and Jones, P. D. (2001): Review. Precipitation measurements and trends in the twentieth century. – Int. J. Clim., **21**: 1899-1922.

Newson, M. (1994): Hydrology and the river environment. – 221 pp.; Oxford (Clarendon Press).

Osborn, T. J. (2006): Recent trends in the winter North Atlantic Oscillation. – Weather, **61** (12): 353-55.

Osterkamp, T. E. and Romanovsky, V. E. (1999): Evidence for warming and thawing of discontinuous permafrost in Alaska. – Permafrost and Periglac. Proc., **10**: 17-37.

Paeth, H., Hense, A. and Hagenbrock, R. (2001): Comments on "Twentieth-Century trends of Arctic precipitation from observational data and a climate model simulation". – J. Clim., **15**: 800-803.

Panagiotopoulos, F., Shahgedanova, M. and Stephenson, D. (2002): A review of Northern Hemisphere wintertime teleconnections. – J. Phys. IV France, **12**: 1027-47.

Panagiotopoulos, F. (2004): Trends and teleconnections of the Siberian high. – 170 pp.; Reading (PhD thesis).

Peel, M. C., McMahon, T. A., Finlayson, B. L. and Watson, F. G. (2001): Identification and explanation of continental differences in the variability of annual runoff. – J. Hydrol., **250** (1-4): 224-40.

Pekarova, P., Miklanek, P. & Pekar, J. (2003): Spatial and temporal runoff oscillations of the main rivers of the world during the 19-20th centuries. – J. Hydrol., **274**: 62-79.

Pelletier, P. M. (1990): A Review of Techniques Used by Canada and Other Northern Countries for Measurement and Computation of Streamflow Under Ice Conditions. - Nordic Hydrology, **21**: 317-340.

Peterson, B. J., Holmes, R. M., McClelland, J. W., Vorosmarty, C. H., Lammers, R. B., Shiklomanov, A. I., Shiklomanov, I. A. and Rahmstorff, S. (2002): Increasing river discharge to the Arctic Ocean. – Science, **298**: 2171-73.

Phillips, I. D. and McGregor, G. R. (2002): The relationship between monthly and seasonal South-West England rainfall anomalies and concurrent North Atlantic Sea Surface Temperatures. – Int. J. Climatol., **22**: 197-217.

Phillips, I. D., McGregor, G. R., Wilson, C. J., Bower, D. and Hannah, D. M. (2003): Regional climate and atmospheric circulation controls on the discharge of two British rivers, 1974-97. – Theor. Appl. Climatol., **76**: 141-64.

Polyakov, I.V., Bekryaev, R.V., Alekseev, G.V., Bhatt, U.S., Colony, R.L., Johnson, M.A., Maskshtas, A.P. and Walsh, D. (2002 a): Variability and trends of air temperature and pressure in the maritime Arctic, 1875-2000. – J. Clim., **16**: 2067-2077.

Polyakov, I.V., Alekseev, G.V., Bekryaev, R.V., Bhatt, U., Colony, R.L., Johnson, M.A., Karklin, V.P., Makshtas, A.P., Walsh, D. and Yulin A.V. (2002 b): Observationally based assessment of polar amplification of global warming. – Geophys. Res. Letts., **29**: 10.1029/2001GL011111.

Popova, V. (2005): Variation of snow accumulation and annual river runoff in North Eurasia and their relation to atmospheric circulation changes in the 20th century. – INTAS project 03-51-5296 “Influence on snow vertical structure on hydrothermal regime and snow related economical aspects in Northern Eurasia”, Grant No. 00-77, Workshop from 23-26 October 2005 held at Zvenigorod, Russia, (www.landscape.tuwien.ac.at/intas/docs/workshop_zvenigorod/valeria.ppt)

PRECIS (Providing Regional Climates for Impact Studies): The PRECIS Regional Climate Modelling System. – UK Met Office / Hadley Centre (www.precis.org.uk/).

Preisendorfer, R. W. (1988): Principal Component Analysis in meteorology and oceanography. – 425 p.; Amsterdam / Oxford (Elsevier).

Proshutinsky, A.Y., I.V. Polyakov, and M.A. Johnson (1999): Climate States and Variability of Arctic Ice and Water Dynamics During 1946-1997. - Pol. Res., **18**: 1-8.

Prowse, T. D. and Flegg, P. O. (2000): Arctic river flow: a review of contributing areas. – In: Lewis, E. L. [ed.]: The freshwater budget of the Arctic Ocean: 269-80; Dordrecht (Kluwer).

Przybylak, R. (2000): Temporal and spatial variation of surface air temperature over the period of instrumental observations in the Arctic. – Int. J. Climatol., **20**: 587-614.

Przybylak, R. (2002): Variability of air temperature and atmospheric precipitation in the Arctic. – 330 p.; Dordrecht (Kluwer).

Qian, B., Corte-Real, J. and Xu, H. (2000): Nonseasonal variability of monthly mean sea level pressure and precipitation variability over Europe. – Phys. Chem. Earth, Part B, Hydrol. Oceans and Atmosph., **25** (2): 177-81.

Rahmstorf, S. (1994): Rapid climate transitions in a coupled ocean-atmosphere model. - Nature, **372**: 82-85.

Rahmstorf, S. (1995): Bifurcations of the Atlantic thermohaline circulation in response to changes in the hydrological cycle. - Nature, **378**: 145-149. –

Rahmstorf, S., J. Marotzke, and J. Willebrand (1996): Stability of the thermohaline circulation. – In: Krauss, W. [ed.]: The warm water sphere of the North Atlantic Ocean: 129-58; Stuttgart (Borntraeger).

Rahmstorf, S. (1997): Risk of sea-change in the Atlantic. - Nature, **388**: 825-826. –

Rahmstorff, S. and Ganopolski, A. (1999): Long-term global warming scenarios computed with an efficient coupled climate model. – Clim. Chg., **43** (2): 353-67.

Rahmstorf, S. (2000): The thermohaline ocean circulation - a system with dangerous thresholds? – Clim. Chg., **46**: 247-256.

Rahmstorf, S. (2003): Timing of abrupt climate change: A precise clock. – Geophys. Res. Letts., **30**: doi.

Rahmstorf, S. (2006): Thermohaline Ocean Circulation. – In: Elias, S. A. [ed.]: Encyclopedia of Quaternaty Science; Amsterdam (Elsevier).

R-ArcticNet, v3.0: A regional, electronic, hydrographic, data network for the Arctic region (www.r-arcticnet.sr.unh.edu/v3.0/index.html).

Rawlins, M. A., and C. J. Willmott (2003): Winter air-temperature change across the terrestrial Arctic, 1961 – 1990. - Arct. Antarct. Alp. Res., **35**: 530– 537.

Rawlins, M. A.; Willmott, C. J.; Shiklomanov, A.; Linder, E.; Frolking, S.;Lammers, R. B.; Vörösmarty, C. J. (2006): Evaluation of trends in derived snowfall and rainfall across

Eurasia and linkages with discharge to the Arctic Ocean. - Geophys. Res. Lett., **33** (7): L0740310.1029/2005GL025231.

Richard, C. and Gratton, D. J. (2001): The importance of the air temperature variable for the snowmelt runoff modelling using the SRM model. – 58th Eastern Snow Conference, Ottawa (www.easternsnow.org/proceedings/2001/Richard-Gratton.pdf).

Richman, M. B. (1986): Rotation of Principal Components. Review article. – J. Climatol., **6**: 293-335.

Rigor, I. G., Colony, R. L. and Martin, S. (2000): Variations in surface air temperature observations in the Arctic, 1979-1997. – J. Clim., **13**: 896-914.

Rodwell, M.J., Rowell, D.P. and Folland, C. K. (1999): Oceanic forcing of the wintertime North Atlantic Oscillation and European climate. - Nature, **398**: 320-323.

Rogers, A. N., Bromwich, D. H., Sinclair, E. N. and Cullather, R. I. (2001): The atmospheric hydrologic cycle over the Arctic Basin from reanalyses. Part II: Interannual variability. – J. Clim., **14:** 2414-2429.

Rogers, J. C. (1997): North Atlantic storm track variability and its association to the North Atlantic Oscillation and climate variability of Northern Europe. – J. Clim., **10**: 1635-47.

ROSHYDROMET (RIHMI-WDC): Hydrometeorological data. Air temperature and precipitation daily data. - (http://meteo.ru/data_temperat_precipitation)

Semiletov, I. P., Savelieva, N. I., Weller, G. E., Pipko, I. I., Pugach, S. P., Gukov, A. Yu and Vasilevskaya, L. N. (2000): The dispersion of Siberian river flows into coastal waters: Meteorological, hydrological and hydrochemical aspects. – In: Lewis, E. L. [ed.] (2000): The freshwater budget of the Arctic Ocean: 323-366; Dordrecht (Kluwer).

Serreze, M. C., Marry, R. G. and Walsh, J. E. (1995): Atmospheric water vapor characteristics at 70° N. – J. Clim., **8**: 719-31.

Serreze, M. C. and Hurst, C. M: (2000): Representation of mean Arctic precipitation from NCEP-NCAR and ERA reanalyses. – J. Clim., **13** (1): 182-201.

Serreze, M. C., Walsh, J. E., Chapin, F. S., Osterkamp, T., Dyurgerov, M., Romonovsky, V., Oechel, W. C., Morison, J., Zhang, T. and Barry, R. G. (2000): Observational evidence of recent change in the northern high-latitude environment. – Clim. Chg., **46**: 159-207.

Serreze, M. C., Lynch, A. H. and Clark, M. P. (2001): The Arctic frontal zone as seen by NCEP/NCAR reanalyses. – J. Clim., **13**: 182-201.

Serreze, M. C., D. H. Bromwich, M. P. Clark, A. J. Ertringer, T. Zhang, and R. Lammers (2003 a): Large-scale hydro-climatology of the terrestrial Arctic drainage system. - J. Geophys. Res., **107** (8160): doi:10.1029/2001JD000919.

Serreze, M. C., M. P. Clark, D. H. Bromwich, A. J. Etringer, T. Zhang, and R. Lammers (2003 b): Monitoring precipitation over the Arctic terrestrial drainage system: Data requirements, shortcomings, and applications of atmospheric reanalysis. - J. Hydrometeorol., **4**: 387– 407.

Serreze, M. C. and Francis, J. A. (2006): The Arctic amplification debate. – Clim. Chg., **76**: 241-64.

Shahgedanova, M., Burt, T. P and Davies, T. D. (1998): Synoptic Climatology of Air Pollution in Moscow. – Theor. Appl. Climatol., **61** (1-2): 85-102.

Shahgedanova, M. [ed.] (2002): The physical geography of Northern Eurasia. – 571 pp.; Oxford (Cambridge University Press).

Shahgedanova, M., Stokes, C. R., Gurney, S. D. and Popovnin, V. (2005): Interactions between mass balance, atmospheric circulation, and recent climate change on the Djankuat Glacier, Caucasus Mountains, Russia. – J. Geophys. Res. Atmosph., **110** D4: D 04148.

Shaw, E. M. (1999): Hydrology in practice. – 3rd edition, 539 pp.; New York / London (Van Nostrand Reinhold).

Shiklomanov, I. A., Shiklomanov, A. I., Lammers, R. B., Peterson, B. J. and Vorosmarty, C. J. (2000): The dynamics of river water inflow to the Arctic Ocean. – In: Lewis, E. L. [ed.] (2000): The freshwater budget of the Arctic Ocean: 281-96; Dordrecht (Kluwer).

Shiklomanov, A.I., Yakovleva, T. I., Lammers, R. B., Karasev, I. P., Vorosmarty, C. J. and Linder, E. (2006): Cold region river discharge uncertainty - estimates from large Russian rivers. – J. Hydrol., **326** (1-4): 231-56.

Shorthouse, C. & Arnell, N. (1999): The effects of climatic variability on spatial characteristics of European river flows. – Phys. Chem. Earth, **B24** (1-2): 7-13.

Semiletov, I. P., Savelieva, N. I., Weller, G. E., Pipko, I. I., Pugach, S. P., Gukov, A. Yu and Vasilevskaya, L. N. (2000): The dispersion of Siberian river flows into coastal waters: Meteorological, hydrological and hydrochemical aspects. – In: Lewis, E. L. [ed.] (2000): The freshwater budget of the Arctic Ocean: 323-366; Norwell/Dordrecht (Kluwer).

Stephens, M. A. (1974): EDF Statistics for Goodness of Fit and Some Comparisons. - J. Am. Stat. Assoc., **69**: 730-737.

Stephenson, D. B., Pavan, V. and Bojariu, R. (2000): Is the North Atlantic a random walk ? – Int. J. Climatol., **20**: 1-18.

Stevens, J. (1996): Applied Multivariate Statistics for the Social Sciences. - Malwah, NJ (Lawerence Erlbaum Associates).

Straile, D., Livingstone, D. M., Wezhenmezer, G. A. & George, D. G. (2003): The response of freshwater ecosystems to climate variability associated with the North Atlantic Oscillation. – In: Hurrell, H. W. [eds.]: The North Atlantic Oscillation: climatic significance and environmental impact: 263-79; Washington, D.C. (Am. Geophys. Un.) (= Geophys. Monogr., **134**).

Sturm, K. *et al*. (2001): Hochwaesser ins Mitteleuropa seit 1500 und ihre Beziehung zur atmosphaerischen Zirkulation. – Petermanns Geogr. Mitt., **6**: 14-23 [In German].

Thompson, D. W. and Wallace, J. M. (1998): The Arctic Oscillation signature in the wintertime geopotential height and temperature fields. – Geophys. Res. Letts., **25** (9): 1297-1300.

Thompson, D. W. and Wallace, J. M. (2000 a): Annular modes in the extratropical circulation. Part I: month-to-month variability. – J. Clim., **13**: 1000-16.

Thompson, D. W., Wallace, J. M. and Hegerl, G. C. (2000 b): Annular modes in the extratropical circulation. Part II: trends. – J. Clim., **13**: 1018-36.

Tibaldi, S., and Molteni, F. (1990): On the operational predictability of blocking. - Tellus, **42A**: 343-365.

Tishkov, A. (2002): Chapter 9. Boreal forests. – In: Shahgedanova, M. [ed.] (2002): Physical Geography of Northern Eurasia: 216-33; Oxford (Cambridge University Press).

Trenberth, K.E. and Paolino, D.A. (1981): Characteristic patterns of variability of sea level pressure in the Northern Hemisphere. – Mon. Wea. Rev., **109**:1169-1189. (http://dss.ucar.edu/datasets/ds010.1/)

Treshnikov, A. F. (1985): Main stages and prospects of study in the polar regions of the Earth. – Probl. of the Arctic and the Antarctic, Coll. of Articles, **57**: 1-19.

Trigo, R. M., Osborn, T. J. and Corte-Real, J. M. (2002): The North Atlantic Oscillation influence on Europe: climate impacts and associated physical mechanisms. – Clim. Res., **20**: 9-17.

Tumel, N. (2002): Chapter 6. Permafrost. – In: Shahgedanova, M. [ed.] (2002): The physical geography of Northern Eurasia: 149-68; Oxford (Cambridge University Press).

Velichko, A. and Spasskaya, I. (2002): Chapter 2. Climatic change and the development of landscapes. – In: Shahgedanova, M. [ed.] (2002): Physical Geography of Northern Eurasia: 36-69; Oxford (Cambridge University Press).

Vellinga, M. and R.A. Wood (2002): Global climatic impacts of a collapse of the Atlantic thermohaline circulation. – Clim. Chg., **54**: 251-267.

Vinnikov, K. and Yeserkepova, I. B. (1991): Soil moisture: Empirical data and model results. – J. Clim., **4** (1): 66-79.

Visbeck, M. H., Hurrell, J. W., Polvani, L. and Cullen, H. M. (2001): The North Atlantic Oscillation: Past, present, and future. – Proc. Natl. Acad. Sci. USA, **98** (23): 12876-77.

Vuglinsky, V. (2000): Russian river ice thickness and duration. Boulder, CO: National Snow and Ice Data Center/World Data Center for Glaciology. Digital media . – University of Boulder, USA (http://nsidc.org/data/g01187.html)

Wahl, K. L. (1977): Accuracy of channel measurements and the implications in estimating streamflow characteristics. – U.S. Geol. Surv. J. Res., **5** (6): 811-4.

Walker, G. T. Sir and Bliss, E. W. (1932): World Weather V. – Mem. Roy. Met. Soc., **4** (36): 53-83.

Wallace, J. M. and Gutzler, D. S. (1981): Teleconnections in the geopotential height field during the Northern Hemisphere winter. – Mon. Wea. Rev., **109**: 784-812.

Wallace, J. M. (2000), with notes by Weaver, E. de and Palmer, M.: On the Arctic and Antarctic Oscillations.– [http://tao.atmos.washington.edu/wallace/ncar_notes/]

Walling, D. E. & Fang, D. (2003): Recent trends in the suspended sediment loads of the world's rivers. – Glob. Planet. Chg., **39**: 111-26.

Walsh, J. E. (2000): Global atmospheric circulation patterns and relationships to Arctic freshwater fluxes. – In: Lewis, E. L. [ed.]: The Freshwater Budget of the Arctic Ocean: 21-43; Norwell/Dordrecht (Kluwer).

Wanner, H., Brönnimann, S., Casty, C., Dyalistras, D., Luterbacher, J., Schmutz, C., Stephenson, D. B. and Xoplaki, E. (2001): North Atlantic Oscillation – concepts and studies. – Surveys in Geophys., **22**: 321-81.

Wedgbrow, C. S., Wilby, R. L., Fox, H. R. & Hare, G. O.' (2002): Prospects for seasonal forecasting of summer drought and low river flow anomalies in England and Wales. – Int. J. Clim., **22**: 219-36.

White, D., Richman, M. and Yarnal, B. (1991): Climate regionalization and rotation of principal components. – Int. J. Climatol., **11**: 1-25.

Wilks, D. S. (1995): Statistical methods in the atmospheric sciences. – 467 pp.; San Diego / New York (Academic Press).

Wilby, R.L., Wigley, T.M.L., Wilks, D.S., Hewitson, B.C., Conway, D. and Jones, P.D. (1996): Statistical Downscaling of General Circulation Model Output. – 730 pp., Report prepared by the National Center for Atmospheric Research on behalf of the Electric Power Research Institute; Palo Alto, California (USA).

Wilby, R. L. (2001): Seasonal forecasting of river flows in the British Isles using North Atlantic pressure patterns. – J. Chartrd. Inst. Water and Environm. Mangmt., **15**: 56-63.

Wilby, R. L., Charles, S. P., Zorita, E., Timbal, B., Whetton, P. and Mearns, L. O. (2004): Guidelines for use of climate scenarios developed from statistical downscaling methods. – Prepared for consideration by the IPCC (www.ipcc-ddc.cru.uea.ac.uk/guidelines/dgm_no2_v1_09_2004.pdf)

Willmott, C. J. and Matsuura, K. (2001): Arctic terrestrial air temperature and precipitation: Monthly and annual time series (1930–2000). – Version 1, (http://climate.geog.udel.edu/ climate/)

Yang, D., Kane, D.. L., Hinzman, L. D., Zhang, X., Zhang, T. and Ye, H. (2002): Siberian Lena river hydrologic regime and recent change. – J. Geophys. Res., **107** (4694): doi.10.1039/2002JD002542.

Yang, D., Ye, B. and Shiklomanov, A. (2004a): Discharge characteristics and changes over the Ob River watershed in Siberia. – J. Hydrometeorol., **5** (4): 595-610.

Yang, D., Ye, B. S. and Kane, D. L. (2004b): Streamflow changes over Siberian Yenisei river basin. – J. Hydrol., **296** (1-4): 59-80.

Yarnal, B. (1993): Synoptic climatology in environmental analysis. – 195 p.; London (Belhaven).

Ye, B. S., Yang, D. Q. and Kane, D. L. (2003): Changes in Lena River streamflow hydrology: Human impacts versus natural variations. – Water Resources Res., **39** (7): art. 1200.

Ye, H., Cho, H. R. and Gustafson, P. E. (1998): The changes in Russian winter snow accumulation during 1936-83 and its spatial patterns. – J. Clim., **11** (4): 856-63.

Ye, H. and Bao, Z. (2001): Lagged teleconnections between snow depth in Northern Eurasia, rainfall in southeast Asia and sea-surface temperatures over the tropical Pacific Ocean. – Int. J. Clim., **21**: 1607-21.

Ye, H. and Ellison, M. (2003): Changes in transitional snowfall season length in northern Eurasia. – Geophys. Res. Letts., **30** (5): 561-3.

Ye, H. C., Yang, D. Q., Zhang, X. B., Zhang, T. J. (2003): Connections of Yenisei River discharge to sea surface temperatures, sea ice, and atmospheric circulation. – J. Geophys. Res.-Atmosph., **108** (D24): art 4776.

Zhang, X., Harvey, K. D., Hogg, W. D. and Yuzyk, T. R. (2001): Trends in Canadian stream flow. – Water Resources Res., **37**: 987-98.

APPENDIX.

Appendix I. Standardised precipitation at Kotlas (1936-1994; 61°2’ N, 46°6’ E). Data have been derived from Russian Hydrometeorological Service RIHMI-WDC office (http://meteo.ru/data_temperat_precipitation).

(a) Monthly precipitation

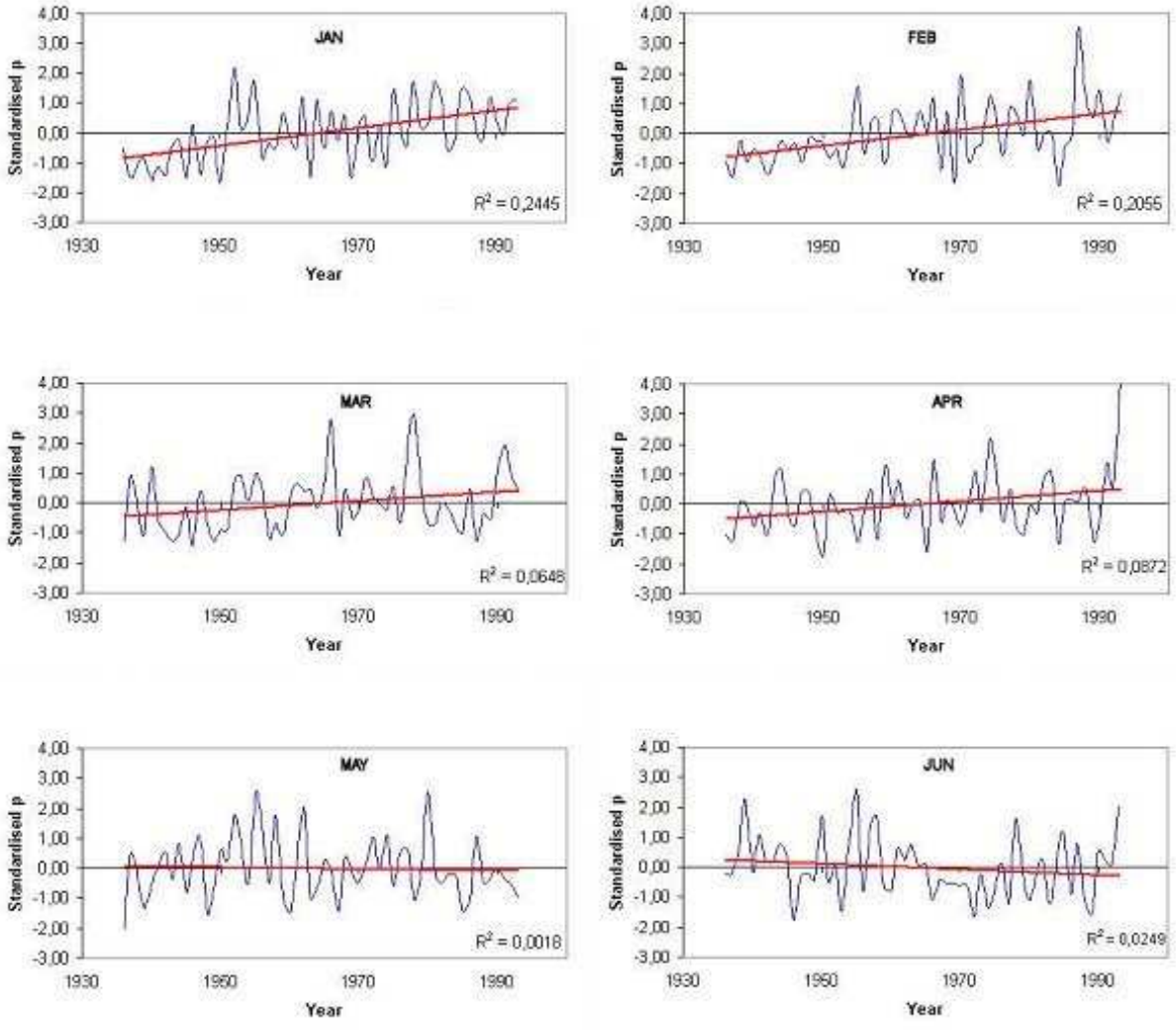

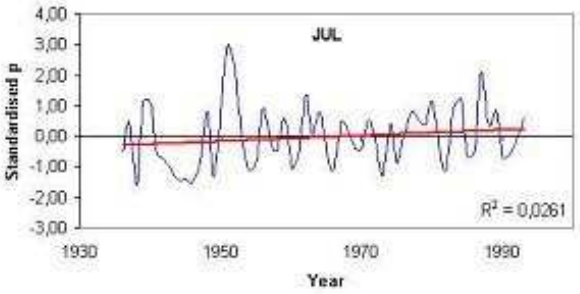
JUL
Standardised p
Year
R² = 0,0261

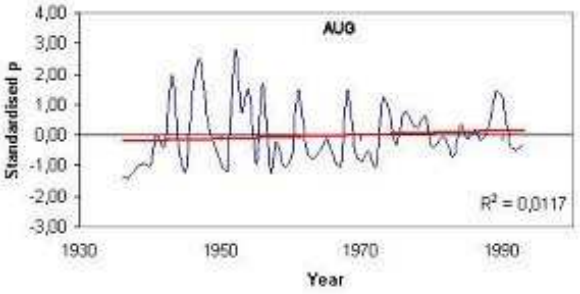
AUG
Standardised p
Year
R² = 0,0117

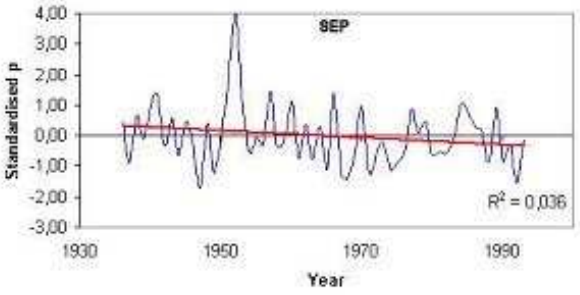
SEP
Standardised p
Year
R² = 0,036

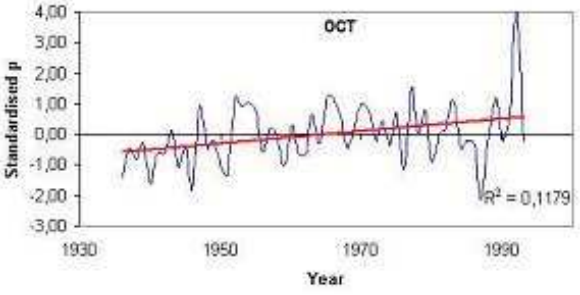
OCT
Standardised p
Year
R² = 0,1179

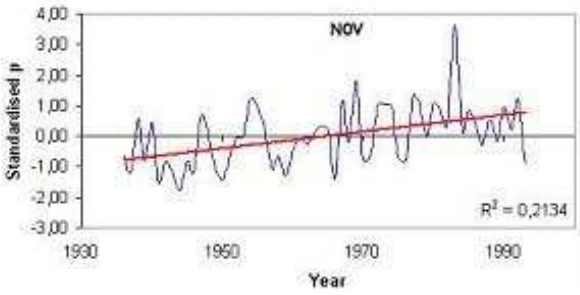
NOV
Standardised p
Year
R² = 0,2134

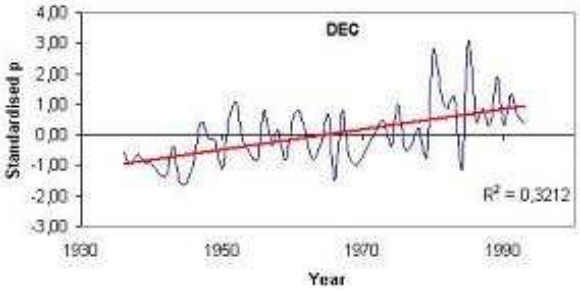
DEC
Standardised p
Year
R² = 0,3212

(b) Seasonal precipitation

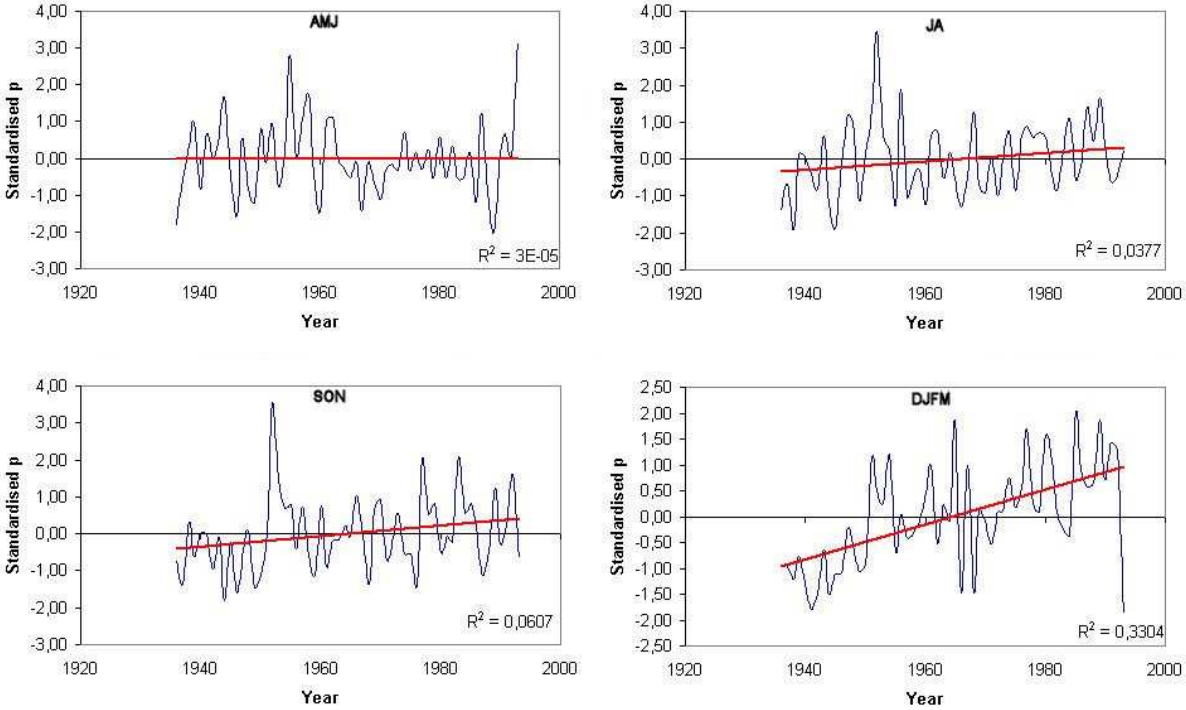

(c) Annual precipitation